TECHNISCHE UNIVERSITÄT MÜNCHEN

The function of mitochondrial dynamics, content and localization during adult hippocampal neurogenesis

Kathrin Andrea Steib

Vollständiger Abdruck der von der Fakultät Wissenschaftszentrum Weihenstephan für Ernährung, Landnutzung und Umwelt der Technischen Universität München zur Erlangung des akademischen Grades eines

Doktors der Naturwissenschaften

genehmigte Dissertation.

Vorsitzender: Univ.-Prof. Dr. Siegfried Scherer

Prüfer der Dissertation:

1. Univ.-Prof. Dr. Wolfgang Wurst
2. Univ.-Prof. Dr. Dieter-Chichung Lie

(Friedrich-Alexander Universität Erlangen-Nürnberg)

Die Dissertation wurde am 28.06.2013 bei der Technischen Universität München eingereicht und durch die Fakultät Wissenschaftszentrum Weihenstephan für Ernährung, Landnutzung und Umwelt am 05.09.2013 angenommen

.

Die vorliegende Arbeit wurde im Zeitraum von Januar 2010 bis März 2013 am Lehrstuhl für Entwicklungsgenetik, Helmholtz Zentrum München, unter Anleitung von Prof. Dr. Wolfgang Wurst angefertigt.

meinen Eltern

I. Danksagungen

An dieser Stelle möchte ich all denjenigen, die zum Gelingen dieser Doktorarbeit beigetragen haben, meinen ganz besonderen Dank aussprechen:

Prof. Dr. Wolfgang Wurst, der sich ohne zu zögern als Betreuer für diese Arbeit zur Verfügung gestellt hat.

Prof. Dr. Chichung Lie für die hervorragende Betreuung, für sein Engagment, seine Unterstützung und die vielen Anregungen und Diskussionen.

Dr. Ravi Jagasia, der das Mitochondrienprojekt ins Leben gerufen hat, und mir immer voller Enthusiasmus und mit Rat und Tat zur Seite stand.

Im Besondern auch Birgit Ebert, Iris Schäffner, Katharina Merz und Kathrin Doberauer auf deren Hilfsbereitschaft und Freundschaft ich immer zählen konnte und die zum Gelingen meiner Arbeit beigetragen haben.

Allen aktuellen und ehemaligen Mitgliedern der AG Lie die stets für Fragen jeglicher Art ein offenese Ohr hatten, für die gute Zusammenarbeit und dafür dass auch der Spaß im Labor nicht zu kurz kam.

Katrin Wassmer, Fabian Gruhn, Marija Rahm und Dr. Rosi Lederer für Ihre tatkräftige Unterstützung bei der Bewältigung alltäglicher und nicht alltäglicher Probleme.

Prof. Dr. Siegfried Scherer, der sich sofort bereiterklärt hat den Vorsitz meiner Prüfungskommission zu übernehmen.

Meinen Eltern bin ich unendlich dankbar für ihre stete Unterstützung während des Studiums und der Promotion und dass sie mir meine Entwicklung in diesem Maße ermöglicht haben.

Zuletzt gebührt mein außerordentlicher Dank meinem Freund Alexander Bochen für die Unterstützung, Verständnis und Rückhalt in allen Höhen und Tiefen die es während des Studiums und Promotionsvorhabens zu durchleben gilt.

II. Abbreviations

°C	degree Celsius
Amp	ampicillin
APS	ammonium persulfate
ATP	adenosine triphosphate
Bak	Bcl-2 homologous antagonist/killer
Bax	Bcl-2–associated X protein
Bcl2	B-cell lymphoma 2 protein
bp	basepair
BrdU	5-bromo-2'-deoxyuridine
C57Bl6J	black inbred mouse strain
CAG	cytomegalovirus immediate early enhancer-chicken *β*-actin hybrid promoter
CamK1α	Ca^{2+}/calmodulin-dependent-protein kinase 1 α
cAMP	cyclic adenosine monophosphate
cDNA	complementary DNA
cfu	colony forming unit
ChIP	chromatin-immuno-precipitation
CK	creatine kinase
cKO	conditional knock-out
Cr	creatine
CrT	creatine transporter
CREB	cAMP-response-element-binding-protein
CT	cycle threshold
ctr	control
Cy3	carbocyanin
Cy5	indodicarbocyanin
Dapi	4',6-diamidino-2-phenylindole
DBA	Dilute Brown Non-Agouti mouse
DCX	doublecortin
DG	dentate gyrus
DJ-1	parkinson protein 7
DMEM	Dulbecco's modified eagle medium
DMSO	dimethyl sulfoxide
dn	dominant negative
DNA	deoxyribonucleic acid
dNTP	deoxy nucleotide triphosphate
DOX	doxycycline
dpi	days post injection
Drp1	dynamin-related protein 1
dsDNA	double stranded DNA
DTT	dithiothreitol
E. coli	*Escherichia coli*
EBSS	Earle's Balanced Salt Solution
ECL	enhanced chemiluminescence
EDTA	ethylenediamine tetraacetic acid
EdU	5-ethynyl-2'-deoxyuridine
EF-hand	Ca^{2+} binding helix-loop-helix structural domain
EGF	endothelial growth factor

ER	endoplasmatic reticulum
EtBr	ethidium bromide
FBS	fetal bovine serum
FC	fold change
FCS	fetal calf serum
FDR	false discovery rate
FGF-2	fibroblast growth factor 2
Fis1	fission 1
FITC	fluoresceinsdothiocyanate
g	gram
GABA	*γ*-aminobutyric acid
GDAP1	ganglioside-induced differentiation associated protein 1
GED	GTPase effector domain
GFAP	glial fibrillary acidic protein
GFP	green fluorescent protein
GTP	guanosine triphosphate
h	hour
HBS	hepes buffered saline
HBSS	Hank's balanced salt solution
HC	hippocampus
HEK 293T	human embryonic kidney cells clone 293T
HeLa cells	immortalized cell line derived from cervical cancer from Henriette Lacks
HEPES	2-(4-(2-Hydroxyethyl)- 1-piperazinyl)-ethansulfonsäure
HF	hippocampal fissure
HTN-Cre	recombinant Cre-recombinase with additional N-terminal 6×His tag, a Tat peptide (GRKKRRQRRRPPAGTSVSL) and an NLS sequence (PKKKRKV) for permanent cell transduction and nuclear localization
IRES	Internal ribosome entry site
kb	kilo base
KO	knock-out
L	liter
LB	Luria-Bertani
l_i	length insert
LRRK2	leucine-rich repeat kinase 2
LTP	long-term plasticity
LTR	long terminal repeat region
l_v	length vector
M	molar
m	meter
MAP2a+b	microtubule Associated Protein 2 a+b
MARCH5	E3 ubiquitin-protein ligase
MDL	Z-Val-Phe-aldehyde (Captain Inhibitor III)
MEF	mouse embryonic fibroblasts
MEM	minimum essential medium
Mfn1	mitofusin 1
Mfn2	mitofusin 2
m_i	mass insert
min	minute

mitoDsred	red fluorescent protein from Discosoma species targeting mitochondria
ML	molecular layer
MMLV	moloney murine leukemia virus
mtDNA	mitochondrial DNA
m_v	mass vector
MW	molecular weight
NaAc	sodium acetate
NEAA	non-essential amino acids
NeuroD	neurogenic differentiation
NLS	nuclear localization sequence
NMDA	*N*-methyl-D-aspartic acid
NPC	neural precursor cells
NSC	neural stem cell
NRF1/2	nuclear regulatory factors 1 and 2
OD	optical density
oe	overexpression
Opa1	optic atrophy 1
PBS	phosphate buffered saline
PCr	phospho creatine
PDGF	platelet-derived growth factor
PFA	paraformaldehyd
PGC-1*α*	peroxisome proliferator-activated receptor-gamma coactivator 1*α*
Pink1	PTEN-induced kinase 1
PKA	cAMP-dependent protein kinase
PMSF	phenylmethanesulfonylfluoride
PolG	mitochondrial DNA polymerase-γ
Prox1	prospero homeobox 1
PSA-NCAM	polysialylated-neural cell adhesion molecule
PSF	penicillin/Streptomycin/Fungicide
PVDF	polyvinylidenfluorid
qPCR	quantitative polymerase chain reaction
rcf	relative centrifugation force
RFP	red fluorescent protein
RGL	radial glia-like cells
RIP	ribosome inactivating protein
RNA	ribonucleic acid
ROS	reactive oxygen species
rpm	rounds per minute
RT	room temperature
s	second
SDS	sodium dodecyl sulfate
SEM	standard error of the mean
Shh	sonic hedgehog
Sox11	SRY (sex determining region Y)-box11
Sox2	SRY (sex determining region Y)-box2
SUMO	small ubiquitin-like modifier
SVZ	sub ventricular zone
TAE	tris acetate buffer/EDTA

TBS	tris buffered saline
TBST	tris buffered saline + tween
TEMED	tetramethylethylendiamin
Tet	tetracycline
Tfam	mitochondrial transcription factor A
tg	transgenic
TNE	tris-HCl/NaCl/EDTA
TORC	transducer of regulated CREB-binding protein
Tris	trishydroxymethylaminomethan
TUNEL	terminal deoxynucleotidyl transferase mediated dUTP nick end labeling
U	unit
UV	ultra violet
VEGF	vascular endothelial growth factor
VSVG	vesicular stomatitis virus G-protein
Wnt	wingless
wt	wild type
λ	wavelength

III. Abstract

Mitochondria fulfill a broad range of functions including energy production, calcium homeostasis, regulation of survival and apoptosis. Neuronal homeostasis is particularly dependent on mitochondrial function. Such dependency is highlighted by the discovery that mutations affecting mitochondrial function are associated with neurodegenerative diseases. Moreover, there is emerging evidence that gene mutations associated with familial forms of Parkinson's disease affect mitochondrial function. The present study aims to elucidate the function of mitochondrial dynamics and distribution to adult hippocampal neurogenesis – the generation of neurons from stem cells in the adult hippocampal dentate gyrus. It has been demonstrated that enhancement of hippocampal neural network activity, e.g. via voluntary running, increases the rate of adult neurogenesis and promotes the synaptic integration of newborn neurons.

In the present study, I demonstrated that running-induced neuronal maturation is accompanied by increased mitochondrial mass and mitochondrial trafficking into dendrites. Moreover, I provide evidence that manipulation of mitochondrial fusion and fission, via retrovirus-mediated gain-of-function of Drp1, alters mitochondrial distribution and accelerates dendritic growth and synaptic integration during exercise-dependent neuronal development. I also found evidence that the transcription factor Sox11, which is indispensable for neuronal differentiation in the adult hippocampus, contributes to coordinating mitochondrial biogenesis and is involved in the regulation of mitochondrial trafficking by controlling the expression of microtubule associated proteins. Finally, I provided first insights about mitochondrial shape and distribution in a Parkison's disease mouse model with α-synuclein-dependent impairment of adult hippocampal neurogenesis. Taken together, these findings provide strong evidence for a central regulatory role of mitochondrial dynamics and distribution in activity-dependent generation of new functional neurons in the adult mammalian hippocampus.

These results not only promote the understanding of how mitochondria are regulated during neuronal development, but may also contribute to the development of therapeutic strategies that aim at harnessing stem cells for the treatment of neurological diseases.

IV. Zusammenfassung

Mitochondrien leisten in allen eukaryontischen Zellen eine Vielzahl von Aufgaben, wie z.B. Energieproduktion, Calcium-Homöostase und Regulation von zellulärem Überleben und programmierten Zelltod. Funktionale Mitochondrien sind für die Homöostase von Neuronen von besonderer Bedeutung. Dies wird durch den Zusammenhang von Mutationen, welche die Funktion von Mitochondrien beeinträchtigen, und dem Auftreten neurodegenerativer Krankheiten besonders verdeutlicht. Des Weiteren gibt es erste Hinweise, dass Mutationen in Genen welche mit der familiären Form von Parkinsonscher Krankheit assoziiert sind, die Funktion der Mitochondrien negativ beeinflussen. Die vorliegende Arbeit hat das Ziel, sowohl die Rolle der Mitochondriendynamik als auch ihre Verteilung während der adulten hippokampalen Neurogenese – der Neubildung von Nervenzellen aus Stammzellen im adulten Gyrus Dentatus – zu untersuchen. Bereits bekannt ist der positive Einfluss neuronaler Aktivität, z.B. durch freiwillige körperliche Betätigung, auf die adulte Neurogenese und die synaptische Integration neugeborener Nervenzellen.

In der vorliegenden Arbeit konnte ich zeigen, dass in Mäusen die durch Bewegung induzierte beschleunigte Reifung von Neuronen mit einer Erhöhung der mitochondrialer Masse und einem erhöhten Mitochondrientransport in die Dendriten einhergeht. Zudem erbringe ich den Nachweis, dass eine Manipulierung von mitochondrialer Teilung und Verschmelzung mittels retroviral induzierter Überexpression von Drp1, sowohl die Mitochondrienverteilung, als auch das dendritische Wachstum und die synaptische Integration in der aktivitätsabhängigen Neurogenese beeinflusst. Weiter habe ich festgestellt, dass der Transkriptionsfaktor Sox11, der für die neuronale Differenzierung im adulten Hippokampus unabdingbar ist, an der Koordination der mitochondrialen Biogenese mitwirkt und an der Regulation des Mitochondrientransports beteiligt ist, indem er die Expression von Microtubuli-assoziierten Proteinen steuert. Schließlich konnte ich erste Erkenntnisse über die mitochondriale Morphologie und Verteilung in einem präklinischen Mausmodel für die Parkinson’sche Krankheit gewinnen, in dem die adulte Neurogenese durch α-synuclein beinträchtig ist. Zusammenfassend zeigen diese Ergebnisse, dass

Mitochondriendynamik und –verteilung zentrale Bestandteile der aktivitätsabhängigen Neubildung funktionaler Neuronen im adulten Säugetierhippokampus sind.

Diese Erkenntnisse fördern nicht nur das Verständnis wie Mitochondrien während der neuronalen Entwicklung reguliert werden, sondern können auch zur Entwicklung stammzellbasierter therapeutischer Strategien zur Behandlung neurologischer Krankheiten beitragen.

V. Table of Contents

1. Introduction

1.1. Adult hippocampal neurogenesis

Neural stem cells continuously generate new neurons in two restricted regions of the brain of adult mammals including humans (Eriksson et al., 1998): the subventricular zone of the lateral ventricles (Altman, 1969; Lois and Alvarez-Buylla, 1994; Alvarez-Buylla and García-Verdugo, 2002) and the subgranular zone of the dentate gyrus of the hippocampal formation (Kaplan and Hinds, 1977; Cameron et al., 1993; Zhao et al., 2008). The generation of dentate granule neurons from neural stem cells is a complex process, which involves multiple developmental steps including proliferation, neuronal fate determination, selection/survival, maturation and integration into the existing hippocampal network. The hippocampal neural stem cells, which are characterized by a radial-glia-like morphology (Seri et al., 2001; Kriegstein and Alvarez-Buylla, 2009) and GFAP expression, have the capability for self-renewal and to differentiate into both neurons and astroglia (Bonaguidi et al., 2011). During neurogenesis, radial-glia-like stem cells (RGLs) give rise to fast expanding neural precursor cells (NPC), which then follow a stereotypical morphological sequence and eventually develop into mature granule neurons, which are functionally integrated, extend a complex dendritic arbor in the molecular cell layer of the dentate gyrus and project their axons towards the CA3 region of the hippocampus (Hastings and Gould, 1999; Zhao et al., 2006; Toni et al., 2007; Toni et al., 2008). In each of these developmental stages, newborn neurons can be identified by distinct morphological and electrophysiological properties, which are accompanied by the expression of stage specific proteins. Very early in development, the so called transient amplifying Type II cells are biochemically characterized by the expression of the transcription factor SRY (sex determining region Y)-box2 (Sox2). Following several rounds of proliferation and neuronal commitment, newly generated cells express neuronal transcription factors such as neurogenic differentiation (NeuroD) (Seki, 2002; Gao et al., 2009), prospero homeobox 1 (Prox1) (Kronenberg et al., 2003) and SRY (sex determining region Y)-box11 (Sox11) (Haslinger et al., 2009; Mu et al., 2012). At this stage, the cells cluster in the subgranular zone and display a bipolar morphology with horizontal processes. The cells receive sustained depolarization by GABA and display a high input resistance (Ge et al., 2006; Karten et al., 2006; Piatti et al., 2006). After exiting cell cycle, NPCs develop an apical process towards the molecular cell layer, which later on constitutes the primary dendrite of the dendritic tree. At this time newborn neurons

already express functional $GABA_A$ receptors, receive synaptic excitatory GABA inputs (Ge et al., 2006; Ge et al., 2007a), and they extend their axons towards the CA3 region (Zhao et al., 2006). Further characteristics of the cells at this developmental stage include the expression of proteins specific for immature granule neurons, such as the cytoskeleton proteins polysialylated-neural cell adhesion molecule (PSA-NCAM) (Seki and Arai, 1993) and Doublecortin (DCX) (Brown et al., 2003b; Rao and Shetty, 2004), and the Calcium binding protein Calretinin (Brandt et al., 2003). Between 2-3 weeks after birth of new neurons, with ongoing maturation, the dendritic tree continues growing and becomes increasingly complex. The onset of spine formation at this time is coinciding with the first glutamatergic excitatory inputs, while GABAergic inputs become gradually hyperpolarizing (Ge et al., 2006). Moreover, newborn neurons at this stage have already formed functional outputs on hippocampal CA3 neurons. Around day 21, the calcium binding protein Calretinin is substituted by Calbindin (Brandt et al., 2003) and the expression of specific immature neuronal proteins and transcription factors stops, (Hodge and Hevner, 2011), which indicates progression of maturation of newborn neurons. Between 4-8 weeks after birth, new neurons display further dendritic growth and maturation of mossy fiber boutons (Faulkner et al., 2008). Moreover, synaptic plasticity is enhanced, as reflected by a lower threshold for the induction of long-term-plasticity (LTP) (Schmidt-Hieber et al., 2004; Ge et al., 2007b) and continuing spine maturation which persists for up to six month after birth (Toni et al., 2007). Early transplantation studies have indicated that adult neurogenesis is tightly controlled by interaction of the newborn neuron with the dentate gyrus microenvironment (Suhonen et al., 1996; Shihabuddin et al., 2000; Lie et al., 2002). Important cellular components of this neurogenic environment include astrocytes (Song et al., 2002), the local vasculature (Palmer et al., 2000), GABAergic interneurons (Ge et al., 2006) and mature granule neurons (Ma et al., 2009).

1.1.1. The functional relevance of hippocampal neurogenesis

There is increasing evidence that neurogenesis in the adult hippocampus is functionally relevant. Studies impairing proliferation and adult neurogenesis in the dentate gyrus pharmacologically (Shors et al., 2001), genetically (Santarelli et al., 2003; Zhang et al., 2008; Jessberger et al., 2009), by irradiation (Santarelli et al., 2003; Snyder et al., 2005; David et al., 2009), and by genetic inducible ablations (Saxe et al., 2007; Dupret et al., 2008; Deng et al., 2009) demonstrated that neurogenesis contributes to hippocampus dependent learning and memory formation as well as to regulation of mood. In addition, recent findings indicated that mature adult-generated dentate granule neurons are strongly activated by experiences to which they were previously exposed during the period of synaptic integration (Kee et al., 2007; Tashiro et al., 2007), suggesting that newborn neurons are integrated into specific neural circuits. Most recently, evidence has been provided, that newborn neurons are necessary in particular for complex learning tasks. Pattern separation, which describes the ability to distinguish two pieces of information in time, by integrating new information into a previous learned representation, has been demonstrated to not only require adult neurogenesis but to be improved by an increase of neurogenesis (Clelland et al., 2009; Sahay et al., 2011; Tronel et al., 2012). Although the underlying mechanisms remain largely unsolved, a computational model has recently been proposed, that attempts to explain the role of newborn neurons in pattern separation tasks, such as contextual fear discrimination. This model suggests, that with new neurons a similarity is added to the memory formation system, which is required for pattern integration; and with the maturation, due to distinct properties of these newborn neurons with respect to their excitability, the time-dependency is added which is needed for the pattern separation (Aimone et al., 2009; Deng et al., 2010; Aimone et al., 2011). A provocative hypothesis about the functional relevance of newborn dentate gyrus granule neurons, has proposed that actually only the newborn neurons are behaviorally relevant, whereas the older neurons do not respond to environmental stimuli anymore. This hypothesis is based on expression analysis of immediate early genes and electrophysiological recordings, indicating that only a small fraction of granule neurons was active during reactivation after exposure to any environment tested. The authors concluded, that mature neurons are no longer involved in memory formations, but exclusively new populations get recruited (Alme et al., 2010).

1.1.2. Influence of physiological and pathological conditions on hippocampal neurogenesis

Various environmental stimuli have been shown to have tremendous effects on the rate of neurogenesis. One of the most potent modulators of both proliferation and survival of the newborn neurons, which additionally accelerates the onset of spine formation, is physical exercise, for instance voluntary wheel running (van Praag et al., 1999b; van Praag et al., 1999a; Zhao et al., 2006). Several studies have proven, that exposing the animals to an enriched environment (Kempermann et al., 1997, 1998; Nilsson et al., 1999; Brown et al., 2003a), as well as hippocampal-dependent learning tasks can strongly stimulate neurogenesis (Gould et al., 1999; van Praag et al., 1999b; van Praag et al., 2005; Drapeau et al., 2007; Sisti et al., 2007). In addition enhancement of neuronal activity in the brain via electroconvulsive-shock treatment (Madsen et al., 2000; Ma et al., 2009), pharmacological means (Deisseroth et al., 2004), or seizures (Mohapel et al., 2004; Jessberger et al., 2005; Walter et al., 2007), has also been demonstrated to strongly modulate proliferation, survival, cellular complexity and positioning of newborn neurons, respectively. On the other side, negative effects on the number of newly generated neurons are induced by behavioral insults, such as chronic stress (Gould et al., 1997; Gould et al., 1998; Veena et al., 2009) and sleep deprivation (Sportiche et al., 2010). Intriguingly, reduced levels of neurogenesis can be restored by antidepressant treatments, for instance fluoxetine or lithium carbonate (Malberg et al., 2000; Santarelli et al., 2003; Encinas et al., 2006; Wexler et al., 2007; Boldrini et al., 2009), suggesting a potential link between the action of these drugs and modulation of neurogenesis. Moreover, pathological conditions affecting mood, such as schizophrenia (Reif et al., 2006; Duan et al., 2007; Wolf et al., 2011), are also accompanied by a decline and impairment of hippocampal neurogenesis. Eventually, a negative correlation with the number of newborn neurons has been found for aging (Kuhn et al., 1996; Morgenstern et al., 2008; Ben Abdallah et al., 2010), as well as in preclinical neurodegenerative disease models for Parkinson’s disease (Winner et al., 2012; Marxreiter et al., 2013) Alzheimer’s disease (Mu and Gage, 2011) and Huntington’s disease (Ransome et al., 2012), raising the hypothesis that a reduction of neurogenesis could contribute to cognitive deficits in human diseases. More studies will be needed, to resolve the actual impact of adult neurogenesis on those neurological disorders.

1.1.3. Genetic programs controlling neuronal differentiation in the adult hippocampus

Considerable progress has also been made with regards to the characterization of signals involved in the regulation of stem cell maintenance and hippocampal neurogenesis: these include developmental morphogens/growth factors such as Notch-ligands (Breunig et al., 2007; Ehm et al., 2010; Lugert et al., 2010; Ables et al., 2011), Shh (Palma et al., 2005; Han et al., 2008b), Wnt (Lie et al., 2005; Kuwabara et al., 2009) and VEGF (Fabel et al., 2003; Schänzer et al., 2004) as well as neurotransmitters such as GABA (Tozuka et al., 2005; Ge et al., 2006; Jagasia et al., 2009; Kim et al., 2012) and glutamate (Cameron et al., 1995; Tashiro et al., 2006b). The underlying mechanisms how these various signals are integrated into the proliferation, differentiation and maturation processes in the adult brain are not well understood. Several transcription factors being sequentially expressed during neurogenesis have now been identified. Transcription factors that have been ascertained to coordinate genetic programs in intermediate progenitor cells are for instance the multipotency factor Sox2, which is down regulated when progenitor cells commit to the neuronal lineage (Ferri et al., 2004; Komitova and Eriksson, 2004; Steiner et al., 2006; Favaro et al., 2009; Ehm et al., 2010), and Tbr2, the expression of which stops when the neuroblasts exit cell cycle (Hodge et al., 2008). The subsequent immature neuronal stage and the following maturation require the function of NeuroD and Prox1, as well as the timely regulation of CREB activity, which has been investigated in several loss and gain of function studies (Nakagawa et al., 2002; Fujioka et al., 2004; Steiner et al., 2006; Lavado and Oliver, 2007; Steiner et al., 2008; Gao et al., 2009; Jagasia et al., 2009; Lavado et al., 2010). Another transcription factor family that has recently been shown to be indispensable for the commitment to neuronal fate and the regulation of the neuronal differentiation is the SoxC family (Mu et al., 2012). This protein family consists of the high-mobility groupbox proteins Sox4, Sox11 and Sox12. All members have been shown to have redundant functions during neuronal development, although Sox4 and Sox11 are more potent regulators whereas the presence of Sox12 was not essential (Hoser et al., 2008; Bhattaram et al., 2010; Thein et al., 2010). During adult hippocampal neurogenesis Sox4 and Sox11 have been found to be highly co-localizing, and their expression is restricted to immature newborn neurons (Haslinger et al., 2009; Mu et al., 2012), indicating a role of SoxC transcription factors during neuronal differentiation. *In vitro* experiments demonstrated that overexpression of Sox11 is sufficient to enhance the generation of

immature neurons from NSCs (Haslinger et al., 2009; Mu et al., 2012). In consistency, ablation of Sox4 and Sox11 in conditional double knock-out mice resulted in an impairment of adult neurogenesis both *in vitro* and *in vivo* (Mu et al., 2012). Even more intriguing, reprogramming from astroglia into neurons is also depended on Sox11 function (Mu et al., 2012). Eventually, there is evidence that in addition the timely shutdown of Sox11 is essential, since prolonged Sox11 expression delayed the maturation and caused miss-positioning of newborn neurons (Doberauer, 2013). The actual downstream targets of SoxC proteins during the differentiation of newborn neurons still need to be unraveled. However findings from a genome-wide binding study in embryonic stem cell-derived neurons disclosed an enrichment of Sox11 on neuron-specific genes (Bergsland et al., 2011), and the data from chromatin immuno-precipitation (ChIP) assays indicate that Sox11 directly targets the promoter of DCX, which is involved in neuronal differentiation (Mu et al., 2012).

1.2. Mitochondria function and dynamics

Mitochondria are not only the primary subcellular compartment for ATP production, which is an important contributor to cellular growth and function in general, but also subserve crucial functions in Ca^{2+} buffering, synthesis of certain hem compounds and steroids, ß-oxidation of lipid acids and they also regulate programmed cell death [reviewed in (McBride et al., 2006)]. Mitochondria contain their own mitochondrial DNA (mtDNA) which encodes 22 tRNAs, 2 rRNAs and 13 polypeptides, that are all essential subunits of the respiratory chain complexes (Bibb et al., 1981). The expression of these genes is regulated by the mitochondrial transcription factor A (Tfam), which is additionally also required for the initiation of the mtDNA replication, conducted by the mitochondrial DNA polymerase PolG (Taanman, 1999; Larsson, 2010; Schmidt et al., 2010; Clayton, 2013). The vast majority of the mitochondrial proteins, however, is nuclear encoded, synthesized in the cytoplasm and is subsequently transported into the mitochondria. The process of transcription of nuclear encoded mitochondrial proteins is coordinated by the transcriptional master co-activator PGC-1α (Wu et al., 1999; Lehman et al., 2000). Mitochondria are the main source of ROS production, which leads in turn to mitochondrial dysfunction, known to contribute to neuronal death in neurodegenerative diseases, such as Parkinson's disease and Alzheimer's disease (Lin and Beal, 2006; Exner et al., 2012; Leuner et al., 2012). Thus, quality control of mitochondria is of utmost importance. The first line of defense that ensures mitochondrial integrity is composed of the proteolytic system, which is responsible for protein quality surveillance. However, if mtDNA damage reaches a certain threshold, dysfunctional mitochondria get subsequently eliminated via mitophagy (Tatsuta and Langer, 2008). For this process prior mitochondrial fragmentation is required, which enables segregation of defective mtDNA (Twig et al., 2008). Mitochondrial fragmentation in turn is part of a dynamic process of ongoing mitochondrial fusion and fission which needs to be well balanced, in order to provide the basis for electrical and biochemical connectivity, mitochondrial turn over and exchange of mtDNA, proteins and metabolites (Westermann, 2002; Berman et al., 2008).

The protein machinery controlling mitochondrial dynamics consists of a group of large, conserved dynamin-related GTPases. The central components for mitochondrial fusion are the Mitofusins 1 and 2, which form hetero- and homotypic complexes. They are anchored with their GTPase domain in the mitochondrial outer membrane and their coiled-coil domain is exposed to the cytosol (Chen et al., 2003). The fusion of the inner

membrane is regulated by Optic Atrophy 1 (Opa1), which is present in 8 different mRNA splicing forms and is subject to proteolytic splicing. It is assumed that the presence of both long and short Opa1 products is essential for inner membrane fusion (Chen et al., 2005; Song et al., 2007; Ehses et al., 2009). For mitochondrial fission, Drp1 (dynamin related protein 1) is recruited to the outer mitochondrial membrane where it oligomerizes to rings and constricts the organelle in a GTP-dependent manner thereby inducing mitochondrial division (Smirnova et al., 1998; Smirnova et al., 2001; Ingerman et al., 2005).

Progress has recently been made by unraveling how the position of mitochondrial division is determined. Pioneering work from Gia Voeltz and colleagues demonstrated that mitochondrial division occurred at sites of close ER-mitochondria-contact, prior to the recruitment of Drp1 to the mitochondria. These results suggested that fission of the mitochondria requires physical wrapping around of ER tubules to constrict mitochondria to a diameter comparable to the diameter of Drp1 helices, thus facilitating mitochondrial division (Friedman et al., 2011). Although it has been believed for years that Fis1, a small tail-anchored protein located in the outer mitochondrial membrane, serves as an adapter molecule for Drp1 and is crucial for fission (Mozdy et al., 2000; James et al., 2003), there is now new evidence demonstrating that Fis1 is dispensable for the latter process. A new mitochondrial fission factor (Mff) and two mitochondrial division proteins (MiD49 and MiD51) have been identified, that directly recruit Drp1 to the mitochondrial surface and thus mediate mitochondrial fission (Otera et al., 2010; Palmer et al., 2011). The question whether all these adaptors are essential for Drp1 translocation or if they have redundant functions has recently been addressed, proving that Mff and both MiDs alone are sufficient to promote mitochondrial fission in a Drp1-dependent manner. However, it has been proposed, that there might be differences in the physiological circumstances (mitophagy, apoptosis) or in the activity status of Drp1 (post-translational modifications) in which individual factors become active (Koirala et al., 2013). Finally, another tail-anchored protein that has a crucial function in mitochondrial fission is Ganglioside-induced differentiation associated protein 1 (GDAP1). Structurally GDAP1 is related to cytosolic glutathione S-transferases (GST); yet GDAP1's precise mechanism of contributing to mitochondrial network morphology still needs to be solved (Niemann et al., 2005; Shield et al., 2006; Wagner et al., 2009). Loss of proteins of the fusion and fission machinery result in a shift of the balance of mitochondrial dynamics. Since neurons have been reported to particularly rely on the precise function of this process (Chen and Chan, 2006), it is not surprising that several mutations in the respective genes

have been linked to neurodegenerative diseases and other neuropathies. For instance mutations in Opa1 result in Optic atrophy (Delettre et al., 2000), loss of Drp1 leads to lethal infantile microcephaly (Waterham et al., 2007) and both mutations of Mfn2 and GDAP1 have been identified to cause various forms of Charcot-Marie-Tooth (CMT) (Zuchner et al., 2004; Niemann et al., 2006). The latter disorder is characterized by axonal degeneration that is linked to abnormal mitochondrial motility. Thus it has been hypothesized, that the underlying patho-mechanism includes a complex interplay between mitochondrial fusion and fission, and mitochondrial transport (Palau et al., 2009). In line with that, in models for Alzheimer's disease, defects in mitochondrial distribution have been reported that correlated to abnormal regulation of fusion and fission (Wang et al., 2008; Wang et al., 2009) .

In neurites, mitochondria get bidirectional transported along microtubule structures (Hollenbeck and Saxton, 2005; Chang et al., 2006), whereas short ranged trafficking in growth cones, spines and axon boutons also occurs along actin filaments, mediated by myosin motors (Pathak et al., 2010). The mitochondrial Rho GTPase Miro1 controls anterograde mitochondrial trafficking by binding to the microtubule associated motor protein Kinesin1 (Kif5) (Fransson et al., 2006; Saotome et al., 2008; Macaskill et al., 2009; Wang and Schwarz, 2009). Via its EF-hand domains Miro1 functions as a calcium-sensor, thus controlling mitochondrial accumulation at sites with high demands for energy and calcium buffering, such as active dendritic spines (Macaskill et al., 2009; Wang and Schwarz, 2009). In contrast, the mechanisms controlling retrograde mitochondrial transport are less well understood, yet it is assumed they rely on dynein motors (Pilling et al., 2006). Recent work suggested that Miro1 is at least indirectly also involved in the regulation of dynein-mediated retrograde trafficking (Russo et al., 2009; Wang et al., 2011). Although a lot progress has been recently made to elucidate the complex molecular machinery that drives mitochondrial trafficking, further studies are required to understand the full picture of the interplay between mitochondrial dynamics, biogenesis, distribution and mitophagy in ensuring neuronal health.

1.2.1. The emerging role of mitochondria in stem cell activity and differentiation

There is increasing evidence, that mitochondrial structure and metabolism are highly cell-type and tissue-specific. Recent studies have demonstrated that cellular metabolism exerts major influences over proliferation activity and differentiation processes, and therefore is a key contributor to control stemness and pluripotency (Lapasset et al., 2011; Mandal et al., 2011; Panopoulos et al., 2011; Ahlqvist et al., 2012). While human and mouse embryonic stem cells and many adult stem cell populations are mainly dependent on glycolytic energy production to facilitate rapid growth, the metabolic pathways are modulated during their differentiation and switch towards increased oxidative phosphorylation (St. John et al., 2005; Cho et al., 2006; Chung et al., 2007; Kondoh et al., 2007).

Thus stem cell differentiation is accompanied by alterations in the expression of mitochondria related genes, such as the glycolytic enzyme Hexokinase II, the Pyruvate Dehydrogenase and the mitochondrial uncoupling protein 2 (UCP2) (Varum et al., 2011; Zhang et al., 2011). The latter one has recently been shown to be crucial for regulating the differentiation capability of pluripotent stem cells, as its repression is indispensable for the metabolic transition and initiation of the differentiation process (Zhang et al., 2011). Intriguingly, these gene expression changes are accompanied by major structural and morphological changes of the mitochondria. During differentiation, not only mtDNA content is increased, but also the mitochondrial network structure is getting more complex (Facucho-Oliveira et al., 2007; Lonergan et al., 2007; Facucho-Oliveira and John, 2009; Chung et al., 2010). Thus, while pluripotent stem cells were found to be characterized by small, immature mitochondria, the organelles become more elongated, functionally active and dispersed in differentiated cells (Chung et al., 2010; Suhr et al., 2010).

Recently, Todd and colleagues described that knockdown of the mitochondrial protein growth factor erv1-like (Gfer) in embryonic stem cells results in loss of pluripotency and excessive mitochondrial fragmentation caused by highly elevated levels of the mitochondrial fission GTPase dynamin-related protein 1 (Drp1). Intriguingly, inhibition of Drp1 was not only sufficient to rescue mitochondrial morphology and function but also restored the expression of pluripotency markers. These data underline the importance of

mitochondrial morphology and structure and of mitochondrial fusion/fission regulators in stem cell regulation (Todd et al., 2010).

1.2.2. Drp1

The key protein for mitochondrial fission Drp1 belongs to the conserved dynamin GTPase superfamily and is primarily located in the cytosol. It consists of a *N*-terminal GTPase domain, a dynamin-like middle domain, a variable domain, called B-domain and a *C*-terminal GTPase effector domain (GED) (Smirnova et al., 1998; Howng et al., 2004). For mitochondrial division, Drp1 is translocated to the mitochondrial membrane, where it assembles to large oligomeric structures and divides mitochondria by GTP-hydrolysis (Yoon et al., 2001; Ingerman et al., 2005). Intramolecular interactions between the GTPase domain and the GED are also known to be involved in Drp1 self-assembly as well as Drp1 regulation (Zhang and Hinshaw, 2001; Zhu et al., 2004). So far, five different splice variants of Drp1 have been discovered (Yoon et al., 1998; Howng et al., 2004). The expression of the different variants seems to be dependent on the tissue, since it has been reported that brain tissue only expresses longer versions and there even exists a full length variant that is exclusively expressed in neurons, whereas in immortalized cell lines like MEFs and HEK cells in the majority variant 3 is present, which lacks part of the B-domain (Uo et al., 2009).

Different transcript variants allow for differential Drp1 activation, as the B-domain contains various sites for posttranslational modifications. During mitosis Drp1 is phosphorylated at S616 by CDK1/cyclinB. Phosphorylation at this position turned out to activate Drp1 function, resulting in mitochondrial fragmentation which facilitates the proper distribution and segregation of mitochondria during cell division (Taguchi et al., 2007). In contrast, phosphorylation at S637 by the cAMP-dependent protein kinase (PKA) has been shown to constrain mitochondrial fission by inhibition of the intramolecular interaction between GTPase domain and GED (Chang and Blackstone, 2007; Cribbs and Strack, 2007). Under nutrient starvation, this phosphorylation is induced by rising cAMP levels. The resulting inhibition of fragmentation protects mitochondria from mitophagy, thus sustaining cell viability (Gomes et al., 2011; Rambold et al., 2011). Dephosphorylation at S637 by Calcineurin promotes the translocation of Drp1 and stimulates mitochondrial fission (Cereghetti et al., 2008). Dephosphorylation at this site is also implicated in programmed necrosis in a model of Huntington's disease (Wang et al., 2012). Contrary to the findings mentioned above, phosphorylation at the same position in a different Drp1 isoform by the Ca^{2+}/calmodulin-dependent protein

kinase 1α (CamK1α) induced Drp1-dependent mitochondrial fission in cultured hippocampal neurons after Ca^{2+}-dependent depolarization (Han et al., 2008a). Therefore, depending on the cell type/tissue, the physiological circumstances (mitosis, excitation, autophagy, apoptosis) and/or the different Drp1 transcript variants the same posttranslational modification might have different impact on Drp1 activity, but the precise underlying mechanisms need to be elucidated. Besides phosphorylation, various other posttranslational modifications have been discovered that modulate Drp1 activity. S-Nitrosylation at C644 within the GED occurs upon elevated cellular NO levels, for instance caused by ß-amyloid overproduction in Alzheimer's disease (Cho et al., 2009). This leads to enhanced GTPase activity, resulting in excessive mitochondrial fission that eventually facilitates cell death. Sumoylation has been reported to stabilize Drp1 in a Bax/Bak-dependend manner at the mitochondria, induces fission and might contribute to apoptosis progression (Wasiak et al., 2007). Eventually, *O*-Gluc-*N*-Acylation at T585 and T586 has also been found to promote fragmentation (Gawlowski et al., 2012), whereas the ubiquitination of Drp1 by March5 probably plays a general role in quality control of mitochondrial proteins to degrade miss-folded or damaged proteins (Sugiura et al., 2011).

Significant progress has also been made in elucidating the functional relevance of Drp1-dependent mitochondrial fission. It is generally accepted that Drp1-dependent fission and following CytochromeC release are key processes during apoptosis (Frank et al., 2001; Jagasia et al., 2005). However, excessive mitochondrial fragmentation can occur in various conditions independently of subsequent cell death. Hence, additional signals are required that lead eventually to apoptosis, and on the other hand mitochondrial fragmentation is important for cellular integrity. While Drp1 seems to be dispensable for the viability of MEFs, two recent reports showed that Drp1 KO mice die very early in embryonic development with developmental defects particularly in the forebrain and in synapse formation. Consistently, neuron-specific KO mice die early, due to failure of synapse and neurite formation and subsequent neuronal loss (Ishihara et al., 2009; Wakabayashi et al., 2009). Primary neuronal cultures from these mice displayed defects in synaptogenesis and abnormal mitochondrial distribution with elongated, aggregated mitochondria. In another study, Drp1 deletion in postmitotic Purkinje cells in the cerebellum using the L7-Cre system, was characterized by mitochondrial dysfunction and age-dependent neurodegeneration (Kageyama et al., 2012). The latter study supports the hypothesis, that Drp1 is not only required for mitochondrial distribution, but Drp1-dependent fission is also crucial for neuronal viability. In this context, mitochondrial

fission serves for quality control via segregation of dysfunctional mitochondria followed by autosomal degradation. In line with those mouse model studies, a human case was reported with a spontaneous missense mutation in one Drp1 allele emphasizing the importance of Drp1 for brain development, since it resulted in microcephaly and early postnatal death (Waterham et al., 2007). The crucial function of Drp1 in mitochondrial distribution and synapse formation has also been reported in work from various other groups (Smirnova et al., 1998; Li et al., 2004; Verstreken et al., 2005; Wang et al., 2008; Wang et al., 2009; Dickey and Strack, 2011). Moreover, previous results from my Bachelor and Master Thesis (Steib, 2007, 2009) provided first insights about the role of Drp1 in differentiation during adult neurogenesis. *In vitro,* overexpression of wtDrp1 and dnDrp1 modulated mitochondrial morphology in NSCs. Interestingly, induction of Drp1-dependent mitochondrial fragmentation was sufficient to promote differentiation of NSCs into all three lineages, including immature neurons, astrocytes and oligodendrocytes. In contrast, proliferation was lowered after Drp1 overexpression, suggesting that transduced cells exit cell cycle. Cell death, reflected in number of TUNEL positive cells was not affected. Eventually, first *in vivo* results provided evidence for morphological defects in development after loss of Drp1 (dnDrp1) that were accompanied by an absence of the expression of the stage specific marker DCX in a high percentage of transduced cells. Moreover, there were indications of beneficial effects in wtDrp1 overexpressing cells with regard to maturation. However, further experiments were required to elucidate the precise impact of Drp1-dependent fission during adult hippocampal neurogenesis.

1.2.3. Creatine and its contribution to neuronal health

N-aminoiminomethyl-*N*-methyglycine (Creatine) is a nitrogenous organic compound synthesized from the amino acids arginine, glycine and methionine. Approximately 50% of the daily creatine demand is taken up with food (protein sources) (Peral et al., 2002), whereas it can also be endogenously synthetized, primary by the liver but to some extent also in the brain (Wyss and Kaddurah-Daouk, 2000; Braissant et al., 2001; Braissant et al., 2005). Its main function is to maintain cellular energy homeostasis (Saks et al., 1978). In cells that have high and fluctuating energy requirements, such as neurons, the creatine kinase/phosphocreatine system (CK/PCr) serves as a back-up system: it keeps intracellular ATP levels constant by transferring the *N*-phosphoryl group from PCr to ADP to regenerate ATP (Bessman and Carpenter, 1985; Wallimann et al., 1992; Dzeja and Terzic, 2003). Moreover, it conduces also as an energy shuttle, since the diffusion rate of

PCr is much faster compared to ATP, and Cr diffuses to a higher extend compared to ADP (Kaldis et al., 1997). CK is additionally found to be structurally and functionally associated with ATPases, such as ion pumps located in the plasma membrane, and can directly regenerate ATP where it is locally consumed (Sappey-Marinier et al., 1992; Wallimann et al., 1992). Therefore the CK/PCr system is not only important for assurance of constant cellular energy levels, but it also bridges sites where ATP is locally generated with sites that have high energy consumption, for instance active dendritic spines. Besides its crucial role in cellular energy metabolism, creatine fulfills various other functions that contribute to neuronal health. First, creatine has direct anti-apoptotic effects, since it has been reported that creatine delays the opening of the mitochondrial permeability transition pore (MPT). Opening of the MPT is a respond to excessive Ca^{2+} load (refered to as excitotoxicity) and causes the release of the apoptosis inducing factor (AIF) protein, hence initiating programmed cell death (Marchetti et al., 1996; O'Gorman et al., 1997; Kruman and Mattson, 1999; Dolder et al., 2003). Next, creatine has also antioxidant features: it does not only enhance faultless respiratory chain activity via efficient recycling of ADP inside the mitochondria, which in turn minimizes ROS production (Meyer et al., 2006), but it also functions instantaneously as a scavenger for intracellular ROS (Lawler et al., 2002; Sestili et al., 2006). Consequently, an increase of creatine levels, has been reported to directly prevent mtDNA mutations, thus protecting against neurodegeneration (Berneburg et al., 2005). Finally, several studies suggested, that creatine also mediates neuroprotection via enhancing the cerebral blood flow (CBF) (Prass et al., 2006), and defends cells from hypo-osmotic shocks during hypertonic stress conditions by acting as a compensatory osmolyt (Bothwell et al., 2001; Alfieri et al., 2006) [reviewed in (Andres et al., 2008)]. Considering all these beneficial effects of creatine for a healthy brain, it is not surprising that several attempts have been made to propose this compound as a neuroprotective treatment. Indeed, in several preclinical mouse models, including models for Parkinson's disease (Matthews et al., 1999; Klivenyi et al., 2003; Yang et al., 2009), Huntington's disease (Matthews et al., 1998; Ferrante et al., 2000), Amyotrophic lateral sclerosis (Klivenyi et al., 1999; Andreassen et al., 2001; Klivenyi et al., 2004) and Aging (Bender et al., 2008), creatine supplementation turned out to significantly improve neuronal health. Interestingly, in the latter mentioned study, expression profiling analysis revealed an upregulation of several neurogenesis related genes, for instance BDNF, after one year creatine supplementation. In the same context, work from others suggested that creatine enhances GABAergic-neuronal differentiation *in vitro* (Ducray et al., 2007*)*, and mimics the effects of Drp1-mediated synaptogenesis in

hippocampal cultures (Li et al., 2004). This brought the hypothesis forth, that creatine could potentially promote adult hippocampal neurogenesis, via modulating mitochondrial function and cellular energy homeostasis.

1.3. Synucleinopathies – Implications on adult hippocampal neurogenesis and mitochondrial function

Parkinson's disease (PD) is the second most common neurodegenerative disease in humans affecting 1% of the population of an age of 60 or older. It is characterized by a multifactorial etiology, and several genes have been identified whose mutations are associated to familial PD, including α-synuclein, parkin, DJ-1, PINK1, ATP13A2 and LRRK2 [reviewed in (Farrer, 2006; Coppedè, 2012)]. One of the pathological hallmarks of PD is the formation of Lewy-bodies (LB). LBs are eosinophilic intracellular inclusion bodies which are primarily composed of α-synuclein (Spillantini et al., 1997; Baba et al., 1998). Although PD is mainly characterized by motor symptoms, such as bradykinesia, rigidity and tremor, that most likely have the cause in loss of dopaminergic neurons in the substantia nigra, it is now generally accepted that PD is a multisystem disorder, that progresses continuously and affects stepwise brainstem nuclei, olfactory bulbs, midbrain and finally the cortex [reviewed in (Tolosa and Poewe, 2009)]. Indeed, neuropathological impairments in the affected brain regions are related to early-onset symptoms in PD, such as olfactory dysfunction, sleep disorder, anxiety and depression. Since the latter one correlates with a reduction of adult hippocampal neurogenesis (see chapter 1.1.2), it has been suggested that a diminished generation of newborn neurons might contribute to the pathology of PD. Studies with transgenic mouse models overexpressing wildtype or mutant α-synuclein under the control of a PDGF-promoter revealed defects in proliferation and survival of newborn neurons in the SGZ, that might be due to cell-autonomous or cell-non-autonomous effects, since α-synuclein is expressed in DCX-positive NPCs, but also in the CA3 region (Masliah et al., 2000; Rockenstein et al., 2002; Winner et al., 2004). In a more recent study the effects on morphology of newly generated neurons were investigated, revealing that with α-synuclein overexpression dendritic arborization was compromised, whereas spine density was surprisingly found to be increased (Winner et al., 2012). In contrast, α/β-synuclein KO enhanced the differentiation of new dentate gyrus granule neurons. The overexpression of wildtype α-synuclein on a single cell level using retroviruses was found to impair again dendritic outgrowth and decrease synaptic integration, reflected in the diminished number of spines, hence identifying a role of endogenous α-synuclein during the maturation of adult

newly generated neurons (Winner et al., 2012). Although the underlying mechanisms of the etiology in PD are very complex and require detailed clarification, mitochondrial dysfunction has long been implicated to contribute to the pathogenesis [reviewed in (Henchcliffe and Beal, 2008)]. Interestingly, all proteins that have been identified to be mutated in PD, including parkin, DJ-1, PINK1 and LRRK2, have been found to play a role in mitochondrial function, autophagy, dynamics and homeostasis (Whitworth and Pallanck, 2009; Mortiboys et al., 2010; Thomas et al., 2011). The physiological function of α-synuclein, which is a small acidic protein, composed of 140 amino acids is largely unknown. However, it has been discovered that it can directly interact with and accumulate in the inner mitochondrial membrane (Banerjee et al., 2010), which has been proposed to promote mitochondrial damage and dysfunction of the respiratory chain (Liu et al., 2009; Devi and Anandatheerthavarada, 2010; Zhu et al., 2011). In two recent reports it was observed that the accumulation of α-synuclein also inhibits mitochondrial fusion, hence increasing organelle fragmentation, although fusion and fission proteins were not directly affected (Kamp et al., 2010; Nakamura et al., 2011). If and how the mitochondrial compartment is altered during the maturation of newborn neurons in the α-synuclein transgenic mouse models described above, needs be elucidated.

1.4. Objective of this study

A central question in adult neurogenesis as well as in stem cell based strategies for central nervous system repair is the question of how newborn neurons are functionally integrated into existing circuits. There is strong evidence that network activity underlies information specific generation of synapses onto newly generated neurons. Yet, how these signals are transduced into the formation of specific synapses remains poorly understood. Preliminary data (Steib, 2009) and work from Sheng and colleagues (Li et al., 2004; Dickey and Strack, 2011; Bertholet et al., 2013) suggested that mitochondria may participate in the control of dendritic growth and synapse formation. In addition to their suggested role in neuronal maturation and integration, mitochondria have also been reported to regulate stem cell fate and cellular differentiation (Chung et al., 2007; Renault et al., 2009). Most intriguingly, it has also been found that mitochondrial morphology and network structure differ between stem cells and their differentiated progeny and that structural remodeling and functional adaptation of the mitochondrial compartment accompany differentiation processes (Lonergan et al., 2007; Uo et al., 2009; Chung et al., 2010; Suhr et al., 2010).

Therefore, I hypothesize that during the differentiation, maturation and integration of adult neural stem cells in the mammalian hippocampus, adaptation of the mitochondrial compartment in mitochondrial mass and morphology is necessary to meet the changing metabolic need of the developing newborn neurons. To decipher the underlying mitochondria-related cell biological mechanisms involved in the development of stem cell-derived neurons, I applied a retroviral approach to target specifically NSC/NPCs in adult hippocampus and assessed the following specific aims:

1) Determine mitochondrial distribution and localization during distinct stages of hippocampal neurogenesis
2) Unravel the consequences of accelerated maturation on the mitochondrial compartment
3) Elucidate the impact of Drp1 manipulation on mitochondrial distribution, and on neuronal maturation and integration
4) Approach creatine as a potential pharmacological treatment to stimulate neurogenesis
5) Investigate the role of Sox11 in regulating adaptations of the mitochondrial compartment during neuronal development
6) Assess the presence of mitochondrial defects in α-synuclein-dependent compromised neurogenesis

2. Results

2.1. Analysis of the mitochondrial compartment in newborn neurons in the adult dentate gyrus

In order to study mitochondria in adult hippocampal neurogenesis, I applied retroviral-mediated targeting of single cells. By combining a retrovirus coding for a fluorescent protein without a targeting sequence and a retrovirus coding for a fluorescence protein that is targeted to mitochondria, I could visualize cell morphology and mitochondria in the same cells and analyze their development at distinct stages.

2.1.1. Visualizing mitochondria using retroviral-mediated expression of mitochondrial targeted fluorescent proteins

To verify that mitochondrial targeted GFP (mitoGFP) and Dsred (mitoDsred) proteins indeed visualize mitochondria in transduced cells, immunofluorescence staining was performed. Analysis of immunoreactivity against the mitochondrial marker CytochromeC revealed a co-localization of CytochromeC staining and mitochondrial targeted fluorescent proteins, both *in vivo* in transduced cells in the adult mouse dentate gyrus, as well as *in vitro* in transfected HEK 293T cells. (Figure 2-1)

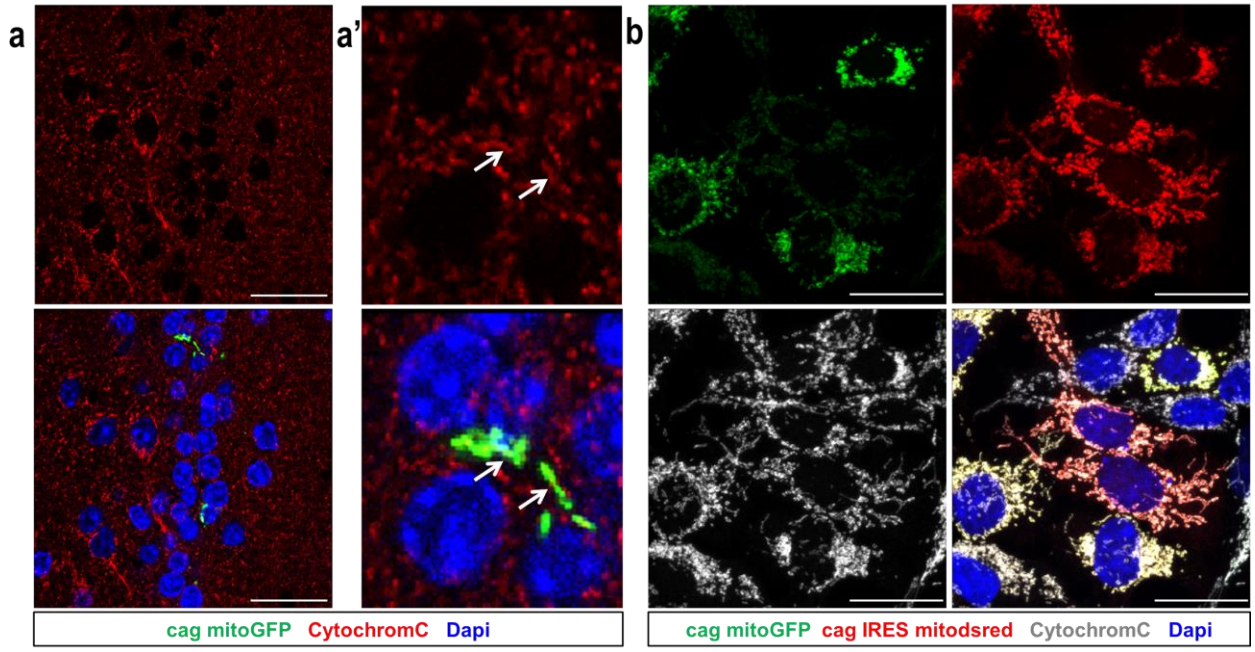

Figure 2-1 Mitochondria targeted fluorescence proteins mitoDsred and mitoGFP colocalize with CytochromeC immunoreactivity *in vivo* and *in vitro:*
a Single plane of a confocal image showing immunohistochemistry of the mitochondrial marker CytochromeC (red) in the mouse dentate gyrus. The animal was injected with a cag mitoGFP retrovirus and sacrificed at 7 dpi to visualize mitochondria (green). Dapi shows nuclear counterstain (blue). Scale bar 25 µm. ***a'*** Higher resolution of the images in a. Arrows indicate colocalization of mitoGFP protein and CytochromeC immunoreactivity. ***b*** Representative confocal images of HEK 293T cells transfected with the retroviral constructs cag mitoGFP (green) and cag IRES mitoDsred (red). CytochromeC immunocytochemistry (grey) shows overlap with both mitochondrial targeted fluorescence proteins. Dapi was used for nuclear counterstaining. Scale bar 25 µm.

2.1.2. The mitochondrial compartment during distinct stages of adult hippocampal neurogenesis

The generation of newborn hippocampal neurons is characterized by a highly stereotypical sequence of proliferation, maturation and finally integration into the pre-existing neural circuitry. As mitochondria are known to play an important role in neuronal function, it was very intriguing how the mitochondria compartment changes during the development. At early developmental stages, i.e. 3 days after retroviral labeling, mitochondria accumulated in the cell soma. When cells started to extend a primary dendrite towards the molecular layer of the hippocampus (7 dpi), mitochondria still appeared clustered, but they commenced moving out from the soma into the dendritic shaft. Analyzing later stages of differentiation of newborn hippocampal neurons, it became obvious that dendritic growth, morphological maturation and spine formation are accompanied by both mitochondrial movement into distal dendrites and increase of mitochondrial mass (16, 28, 42, 106 dpi). Indeed, quantification of mitochondrial density (number of mitochondria per µm dendrite) in dendrites in the mid third of the molecular layer (ML) showed that, from 16 dpi on (0.06 ± 0.003 mitochondria/µm) mitochondria

density constantly increased significantly to 28 dpi (0.29 ± 0.006 mitochondria/µm; p<0.001) and 106 dpi (0.35 ± 0.010 mitochondria/µm, p<0.001). (Figure 2-2)

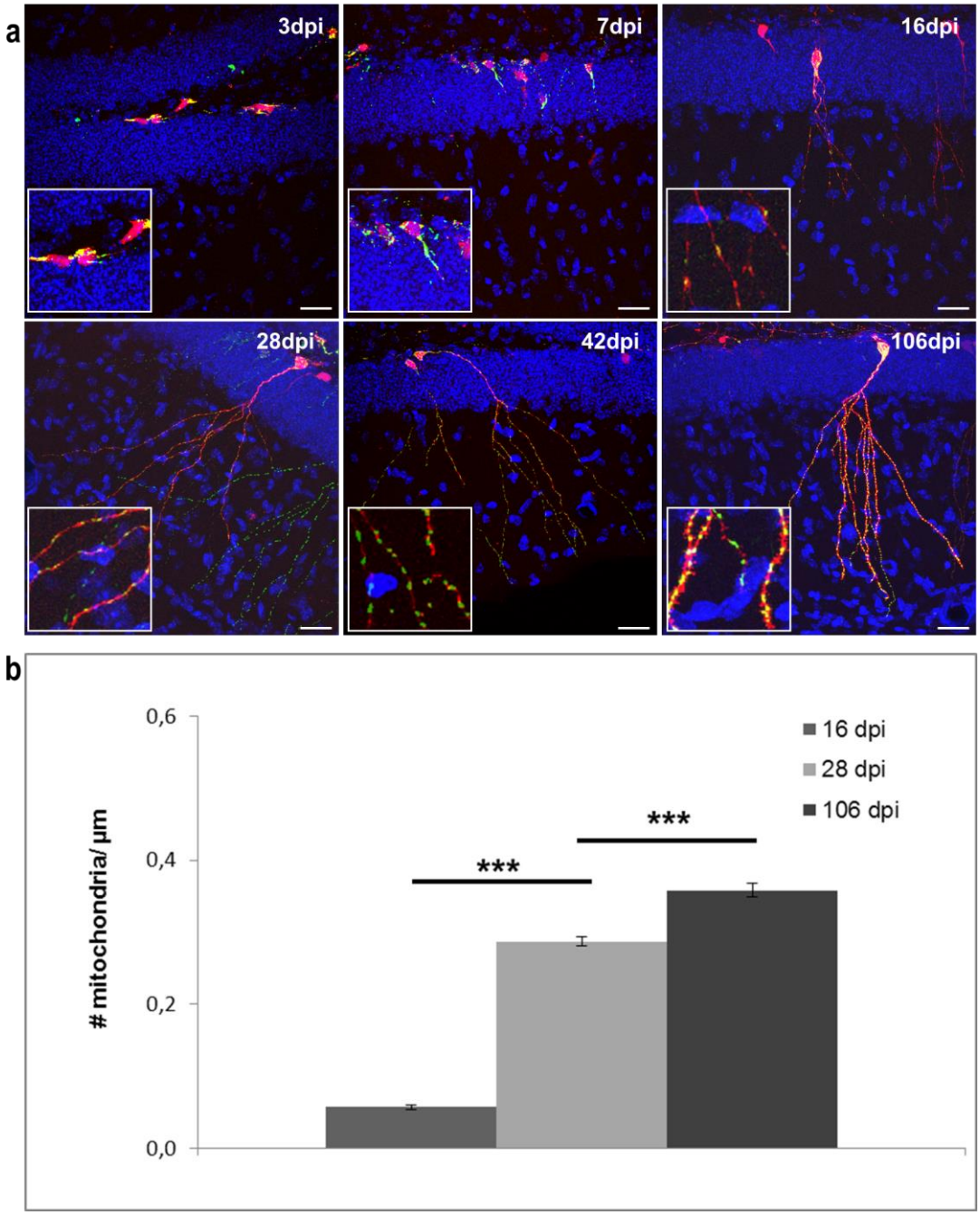

Figure 2-2 Mitochondria morphology and localization at distinct stages of adult hippocampal neurogenesis:
a Representative confocal images of RFP (red) and mitoGFP (green) transduced cells in the mouse dentate gyrus at 3 dpi, 7 dpi, 16 dpi, 28 dpi, 42 dpi and 106 dpi show that development of newborn cells is paralleled by changes in mitochondrial morphology, mass and localization. Scale bars 25 µm. White boxes show areas with higher magnification. ***b*** Quantification of mitochondria number per µm dendrite of double-transduced cells at 16 dpi, 28 dpi and 90 dpi depict significant increase of mitochondria density during cell development. n=10 dendrites from 3 animals housed in standard conditions; error bars represent ± SEM; Significance levels were assessed with Student's T-test with unpaired samples and unequal variances.

2.2. Mitochondria in the hippocampus and physical activity

Physical exercise (i.e. voluntary wheel running) has been shown to be one of the most potent stimulators of adult neurogenesis (van Praag et al., 1999b; van Praag et al., 1999a). During my Master Thesis (Steib, 2009) I could already show that housing the animals with unlimited access to running wheels does not only accelerate the morphological maturation of newborn neurons, but also increases the mitochondrial content in the soma of the cells. Hence, in this study, I aimed to elucidate whether running affects mitochondria mass in the whole cell and if it has an additional impact on the distribution of mitochondria, which was observed to change during normal development. (Figure 2-2)

2.2.1. Running accelerates the morphological maturation of newborn hippocampal neurons and changes the localization and mass of mitochondria

Mitochondria mass and distribution was analyzed in wildtype mice that were stereotactically injected with a combination of retroviruses encoding for GFP and mitoDsred and sacrificed at 16 dpi. Newborn hippocampal neurons from running animals (housed with unlimited access to running wheels) were significantly longer (971 ± 43 µm) compared to cells from control animals (404 ± 24 µm; $p<0.001$) and had more branching points (ctr 9 ± 0.8; runner 13 ± 1.0; $p<0.01$), which is consistent with the more complex overall morphology of cells from running animals that was revealed by analysis of Sholl intersections (Sholl, 1953) (see Figure 2–4). For further analysis of the mitochondrial compartment, cells were divided into three parts, 0-50 µm radius from soma, 50-100 µm radius from soma and >100 µm from soma, and mitochondrial mass and number was assessed per section and in the dendritic tree (>50 µm radius from soma) to get additional information about the localization of mitochondria. Quantification of total mitochondria mass showed an increase in the whole cell in running animals compared to control (see Table 1). Since the dendritic growth of neurons from running animals is accelerated, mitochondria content was also normalized to cell size, which revealed that mitochondrial content was still significantly increased in soma and dendritic tree, when the increase of cell size was considered. In newborn neurons under basal conditions most mitochondria were located in the soma of the cells, whereas in the more mature neurons from running animals a higher percentage of mitochondria was detected in the

peripheral parts of the cell. This is consistent with the finding that during development mitochondria move towards dendrites (see 2.1.2). To further elucidate whether mitochondria localization in newborn neurons from running animals is affected, mitochondria density in the most peripheral 50 µm from the cells was compared. The quantification revealed that the number of mitochondria per µm was significantly higher in cells from runner in contrast to those from control animals, strengthening the hypothesis that running directly affects mitochondrial distribution of newborn neurons. (Table 1, Figure 2-3 and Figure 2-4)

Table 1 Quantitative assessment of the effects after running on the mitochondrial compartment at 16 dpi:

absolute mitochondrial volume [µm^3]	**control**	**runner**	**p-value**
whole cell	80 ± 8	286 ± 39	p<0.001
dendritic tree	17 ± 3	136 ± 26	p<0.001
0-50 µm	63 ± 7	150 ± 16	p<0.001
50-100 µm	15 ± 2	70 ± 9	p<0.001
> 100 µm	1 ± 0.8	66 ± 18	p<0.01
relative mitochondrial volume [µm^3/µm length]	**control**	**runner**	**p-value**
whole cell	0.20 ± 0.02	0.30 ± 0.04	p=0.05
dendritic tree	0.05 ± 0.006	0.15 ± 0.03	p<0.01
0-50 µm	0.75 ± 0.09	1.54 ± 0.23	p<0.01
50-100 µm	0.06 ± 0.006	0.18 ± 0.03	p<0.01
> 100 µm	0.07 ± 0.05	0.13 ± 0.03	p=0.3
% of mitochondrial located per section	**control**	**runner**	**p-value**
dendritic tree	21 ± 2	46 ± 3	p<0.001
0-50 µm	79 ± 3	54 ± 3	p<0.001
50-100 µm	19 ± 2	25 ± 1	p<0.05
> 100 µm	2 ± 0.1	20 ± 3	p>0.001
mitochondrial density [mitochondria/µm length]	**control**	**runner**	**p-value**
most peripheral 50 µm dendritic length	0.08 ± 0.007	0.17 ± 0.011	p<0.001

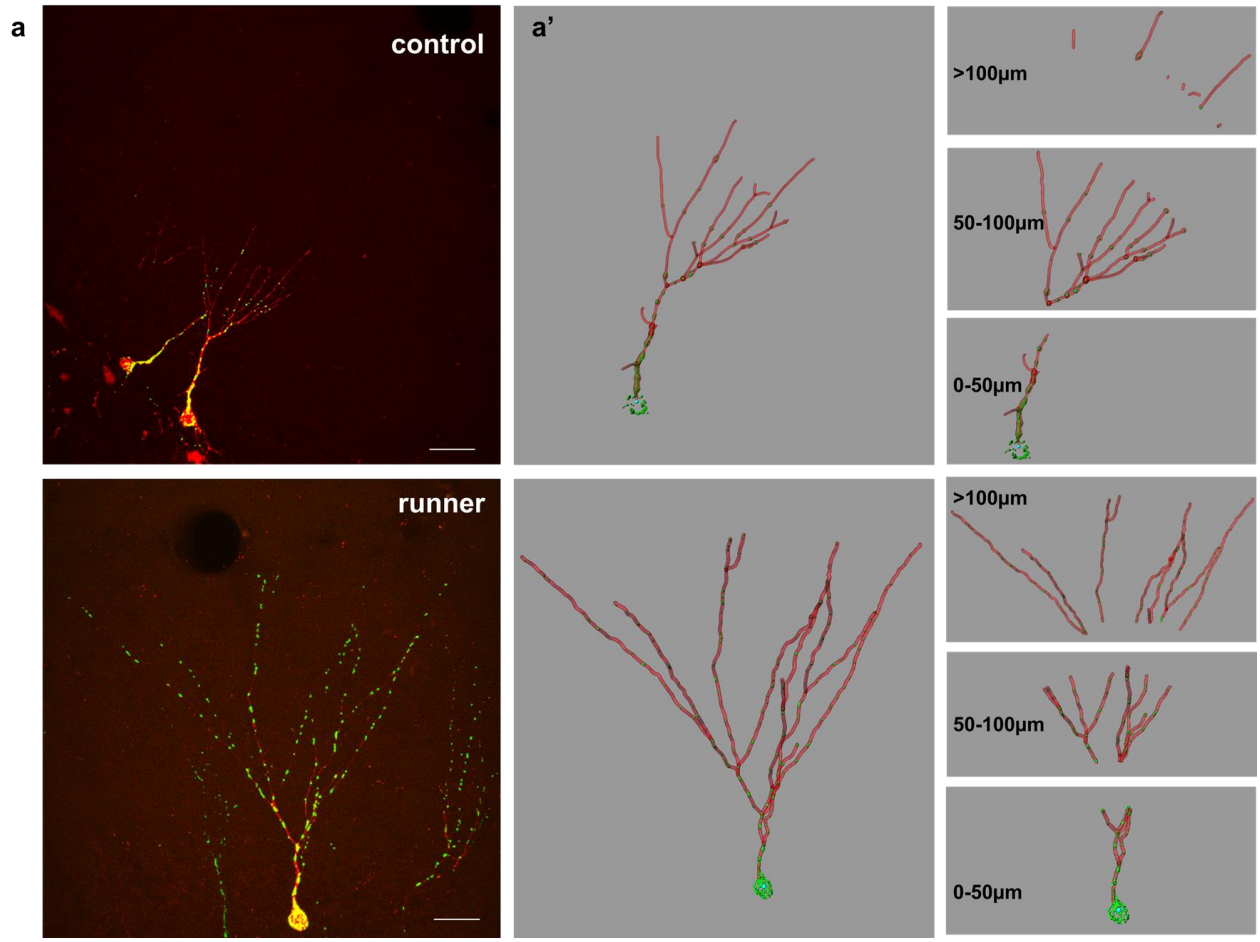

Figure 2-3 Running accelerates the maturation of newborn neurons and increases mitochondria mass and density at 16 dpi:
a Representative confocal images of a mitoDsred (red) and GFP (green) transduced cell in the mouse dentate gyrus at 16 dpi of an animal housed in standard conditions (control) and an animal housed with unlimited access to a running wheel (runner). Scale bar 25 µm. ***a'*** 3-D reconstructions of the cells depicted in a. For quantification of mitochondria localization cells were divided into the following sections: 50 µm distance from soma, 50-100 µm and more than 100 µm. Scale bars 25 µm.

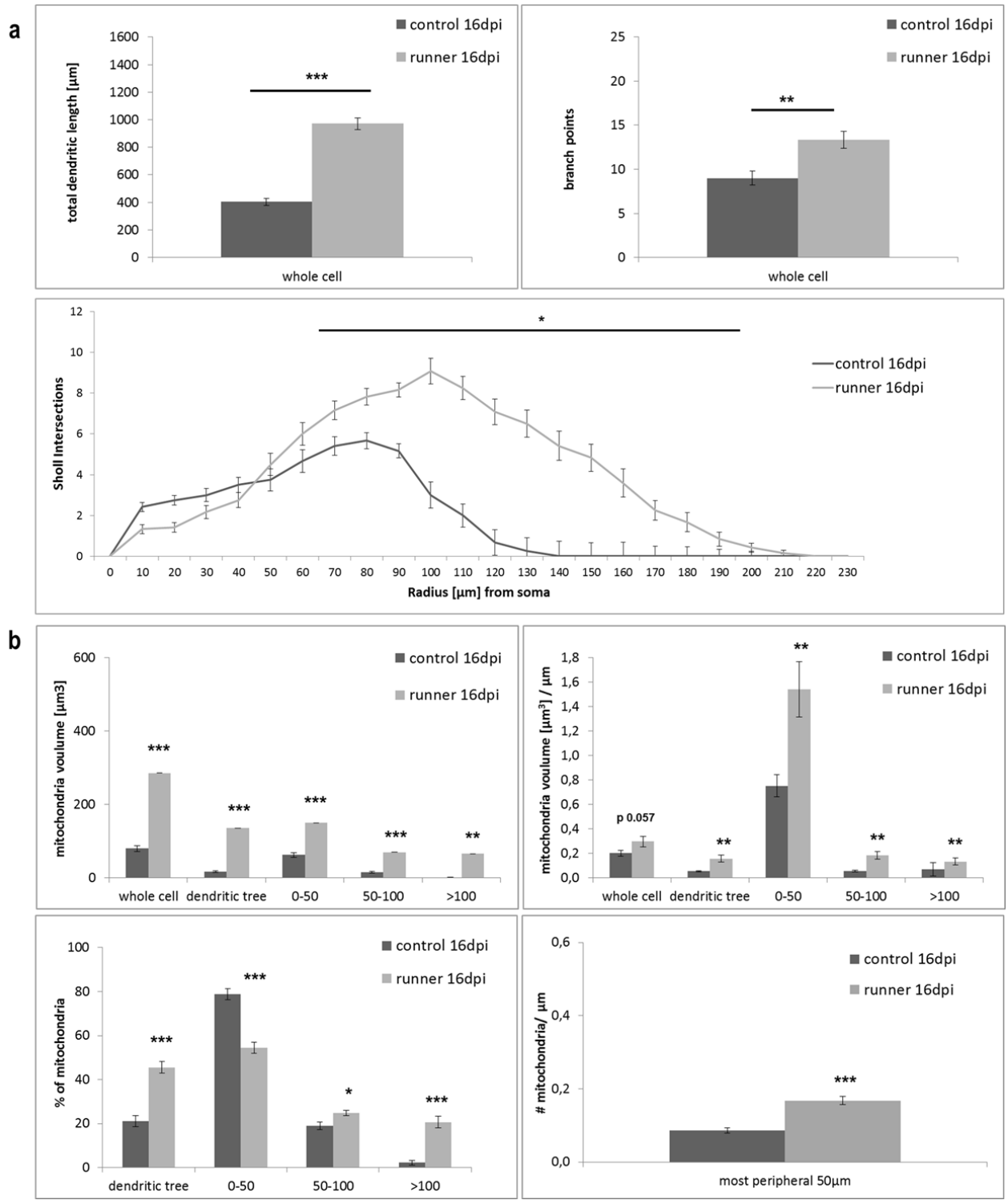

Figure 2-4 Running accelerates the maturation of newborn neurons and increases mitochondria mass and density at 16 dpi:
a Quantification of total dendritic length and number of dendritic branch points revealed an significant increase in running animals. Sholl analyses (Sholl 1953) showed a significant increase of number of intersections from 70-180 µm distance from soma. ***b*** Quantification of mitochondria mass, density and distribution demonstrated a stimulating effect on the mitochondrial compartment after running. n=12 neurons from 3 different animals; error bars represent ± SEM; Significance levels were assessed with Student's T-test with unpaired samples and unequal variances.
.

2.2.2. Effects of running are diminished at 28 dpi

The finding that running has an impact on the development of newborn neurons raises the question, whether morphological differences and alterations of the mitochondria still persist at 28 dpi, when cells are considered as mature and integrated, or if running has only an acceleration effect on the maturation process. Analyses of the morphology of GFP and mitoDsred double-transduced cells from running animals and control animals revealed that at 28 dpi, control cells catch up in the development with newborn neurons from running animals, as reflected in total dendritic length (ctr 1174 ± 45 µm, runner 1255 ± 66 µm), number of branching points (ctr 8 ± 0.3; runner 8 ± 0.7); and the number of Sholl intersections (Figure 2-6). Comparable to that result, no significant differences of mitochondrial volume, mitochondrial volume normalized to cell size and localization of mitochondria within the cells were detectable. However, quantification of only mitochondrial density, i.e. the number of mitochondria per µm irrespective of mitochondrial size, revealed, that neurons from running animals displayed a higher number of mitochondria. This suggests that mitochondrial shape is more fragmented in running animals at 28 dpi compared to control. (Table 2, Figure 2-5 and Figure 2-6)

Table 2 Quantitative assessment of the effects after running on the mitochondrial compartment at 28 dpi:

absolute mitochondrial volume [µm^3]	**control**	**runner**	**p-value**
whole cell	204 ± 15	253 ± 23	p=0.09
dendritic tree	149 ± 13	187 ± 17	p=0.1
0-50 µm	55 ± 4	66 ± 9	p=0.29
50-100 µm	44 ± 4	50 ± 5	p=0.38
> 100 µm	105 ± 10	137 ± 13	p=0.07
relative mitochondrial volume [µm^3/µm length]	**control**	**runner**	**p-value**
whole cell	0.17 ± 0.01	0.20 ± 0.02	p=0.14
dendritic tree	0.14 ± 0.01	0.16 ± 0.02	p=0.20
0-50 µm	0.60 ± 0.05	0.78 ± 0.07	p=0.06
50-100 µm	0.13 ± 0.01	0.17 ± 0.02	p=0.11
> 100 µm	0.14 ± 0.01	0.16 ± 0.02	p=0.26
% of mitochondrial located per section	**control**	**runner**	**p-value**
dendritic tree	72 ± 2	74 ± 2	p=0.6
0-50 µm	28 ± 2	26 ± 2	p=0.6
50-100 µm	21 ± 1	20 ± 1	p=0.28
> 100 µm	51 ± 2	54 ± 2	p=0.33
mitochondrial density [mitochondria/µm length]	**control**	**runner**	**p-value**
whole cell	0.31 ± 0.01	0.37 ± 0.01	p>0.001
dendritic tree	0.24 ± 0.01	0.32 ± 0.01	p>0.001
0-50 µm	1.20 ± 0.15	1.24 ± 0.10	p=0.81
50-100 µm	0.23 ± 0.01	0.30 ± 0.01	p>0.001
> 100 µm	0.25 ± 0.01	0.32 ± 0.01	p>0.001

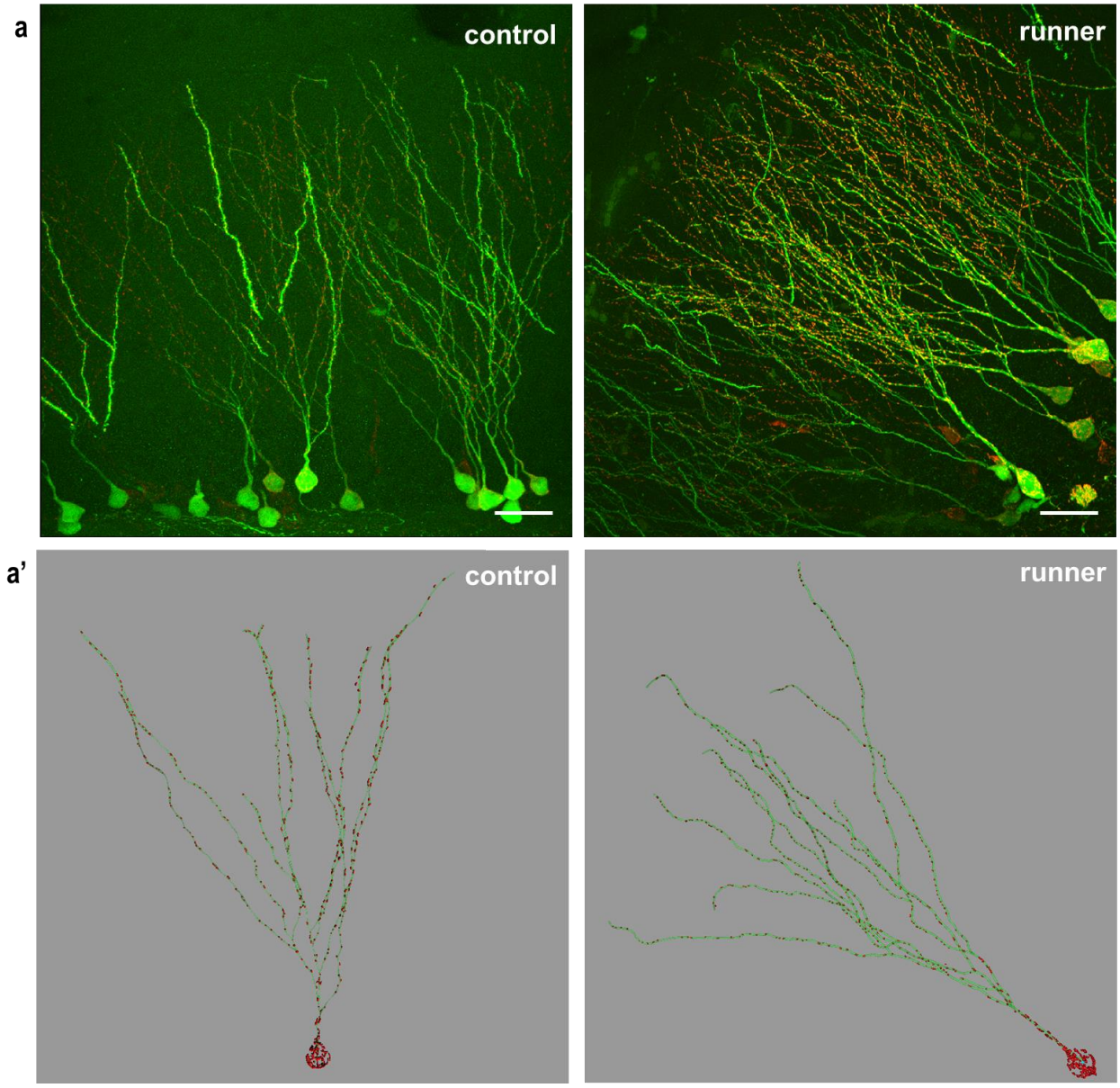

Figure 2-5 Figure Analysis of cell morphology and mitochondria after running at 28 dpi:
a Representative confocal images of a mitoDsred (red) and GFP (green) transduced cell in the mouse dentate gyrus at 28 dpi of an animal housed in standard conditions (control) and an animal housed with unlimited access to a running wheel (runner). Scale bar 25 µm. ***a'*** 3-D reconstructions of the cells depicted in **a**.

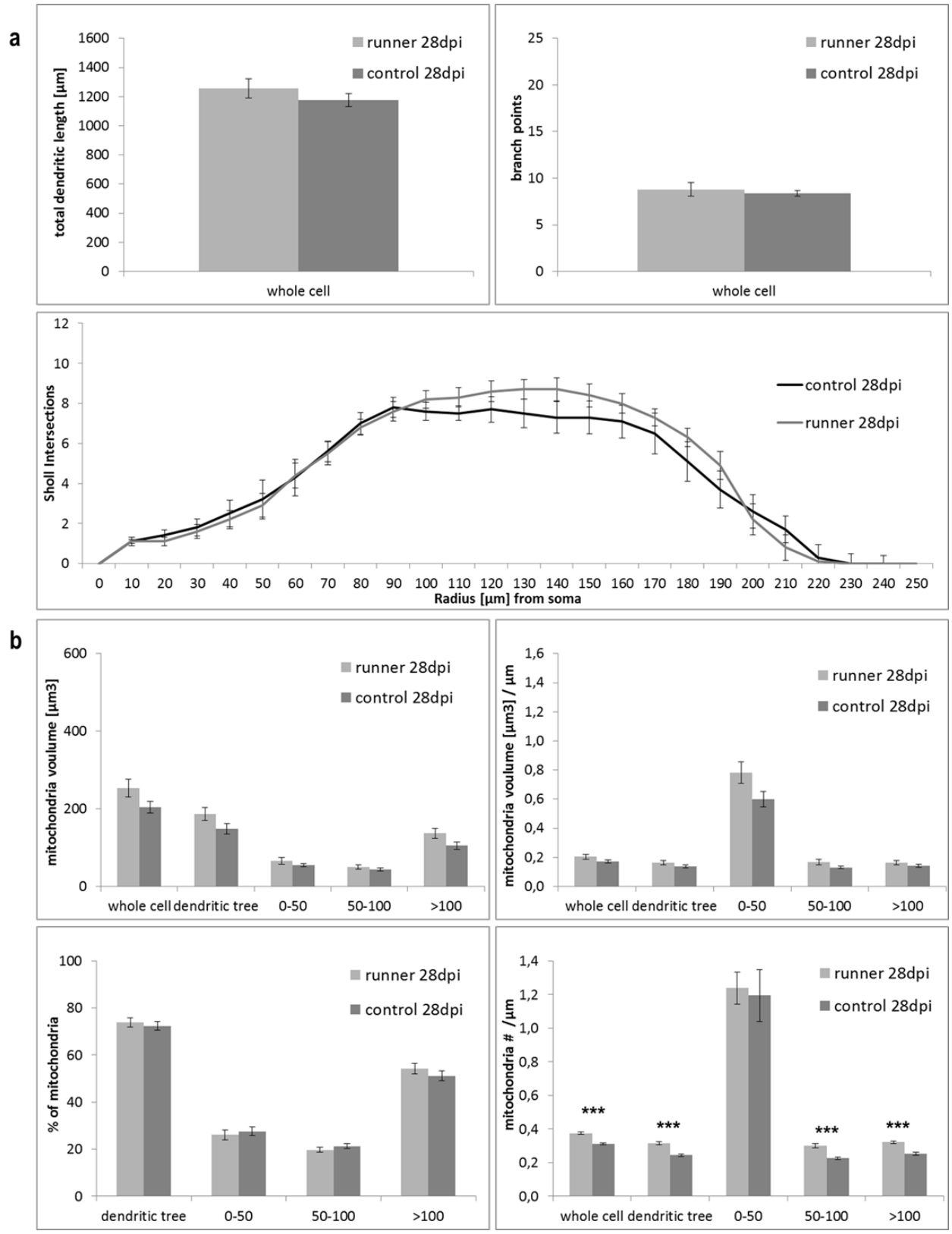

Figure 2-6 Analysis of cell morphology and mitochondria after running at 28 dpi:
a Quantification of total dendritic length and number of dendritic branch points revealed no significant differences. Sholl analyses (Sholl 1953) did not reveal significant differences in the complexity of the cells. ***b*** Quantification of mitochondria mass, volume normalized to cell size and localization showed no significant differences in runners compared to control. Only mitochondrial density was still increased after running in all sections except the first 50 µm. Scale bars 25 µm; n=12 neurons from 3 different animals; error bars represent ± SEM; Significance levels were assessed with Student's T-test with unpaired samples and unequal variances.

2.2.3. Running has no global effects in the dentate gyrus

Next, I examined whether the running-effect on the morphology and the mitochondria of the neurons is limited to developing neurons, or if it has also an impact on the mature population. To this end, animals were housed in normal conditions until newborn neurons were considered as fully mature and integrated (90 dpi). Then a running wheel was introduced into cages of running animals for 16 more days to study the effect of physical activity on moprphology and mitochondria in 90 days old neurons. In this paradigm, no siginificant effects on cell morphology were detectable, which is dipicted in total dendritic length (ctr 1309 ± 61 µm, runner 1299 ± 63 µm), number of branching (ctr 9 ± 0.7; runner 9 ± 0.7) and a comparable number of intersections revealed by Sholl analysis (Figure 2-8). Consistently, analyses of the mitochondrial compartment did also not disclose any significant differences related to running, neither in absolute mitochondrial volume, relative mitochondrial volume, localization of mitochondria within the cells, nor mitochondrial density. (Table 3, Figure 2-7 and Figure 2-8)

Table 3 Quantitative assessment of the effects after running on the mitochondrial compartment at 104 dpi:

absolute mitochondrial volume [µm^3]	**control**	**runner**	**p-value**
whole cell	353 ± 27	412 ± 35	p=0.19
dendritic tree	270 ± 23	314 ± 25	p=0.21
0-50 µm	85 ± 6	98 ± 12	p=0.33
50-100 µm	73 ± 6	67 ± 8	p=0.57
> 100 µm	197 ± 18	247 ± 25	p=0.12
relative mitochondrial volume [µm^3/µm length]	**control**	**runner**	**p-value**
whole cell	0.27 ± 0.02	0.32 ± 0.03	p=0.13
dendritic tree	0.23 ± 0.02	0.27 ± 0.02	p=0.19
0-50 µm	0.90 ± 0.13	1.22 ± 0.23	p=0.23
50-100 µm	0.21 ± 0.02	0.23 ± 0.02	p=0.47
> 100 µm	0.24 ± 0.02	0.28 ± 0.03	p=0.19
% of mitochondrial located per section	**control**	**runner**	**p-value**
dendritic tree	76 ± 2	77 ± 2	p=0.83
0-50 µm	25 ± 2	23 ± 2	p=0.52
50-100 µm	21 ± 1	17 ± 2	p=0.17
> 100 µm	55 ± 2	59 ± 3	p=0.21
mitochondrial density [mitochondria/µm length]	**control**	**runner**	**p-value**
whole cell	0.34 ± 0.01	0.36 ± 0.02	p=0.34
dendritic tree	0.30 ± 0.02	0.32 ± 0.02	p=0.31
0-50 µm	0.96 ± 0.12	1.02 ± 0.12	p=0.68
50-100 µm	0.31 ± 0.01	0.31 ± 0.01	p=0.51
> 100 µm	0.30 ± 0.01	0.33 ± 0.02	p=0.28

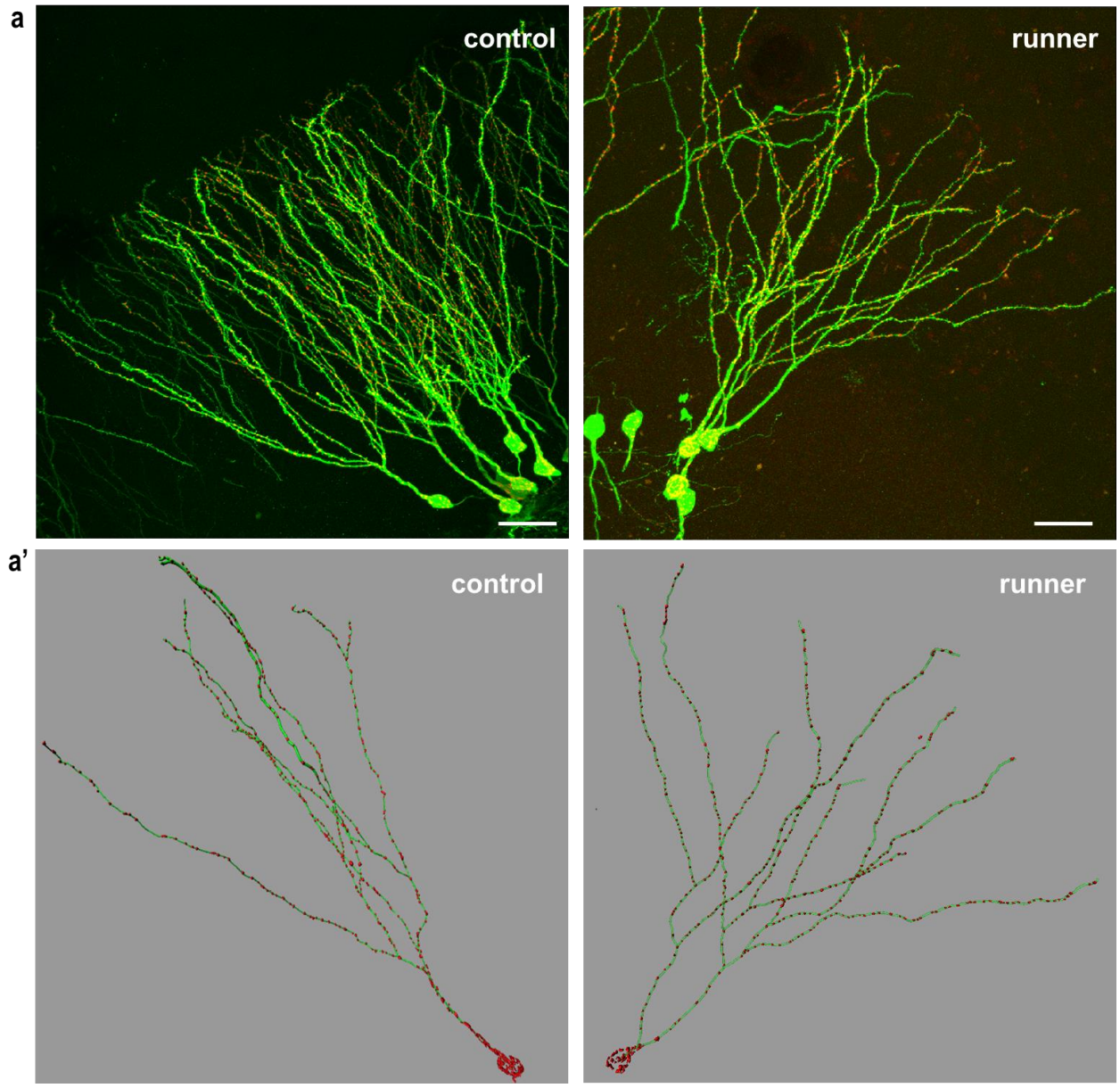

Figure 2-7 Running has no impact on cell morphology and mitochondria of mature neurons:
a Representative confocal images of a mitoDsred (red) and GFP (green) transduced cell in the mouse dentate gyrus at 106 dpi. At 90 dpi runner were housed with unlimited access to a running wheel for additional 16 days, and compared to control (housed in standard conditions for the whole experiment). Scale bar 25 µm. ***a'*** 3-D reconstructions of the cells depicted in **a**.

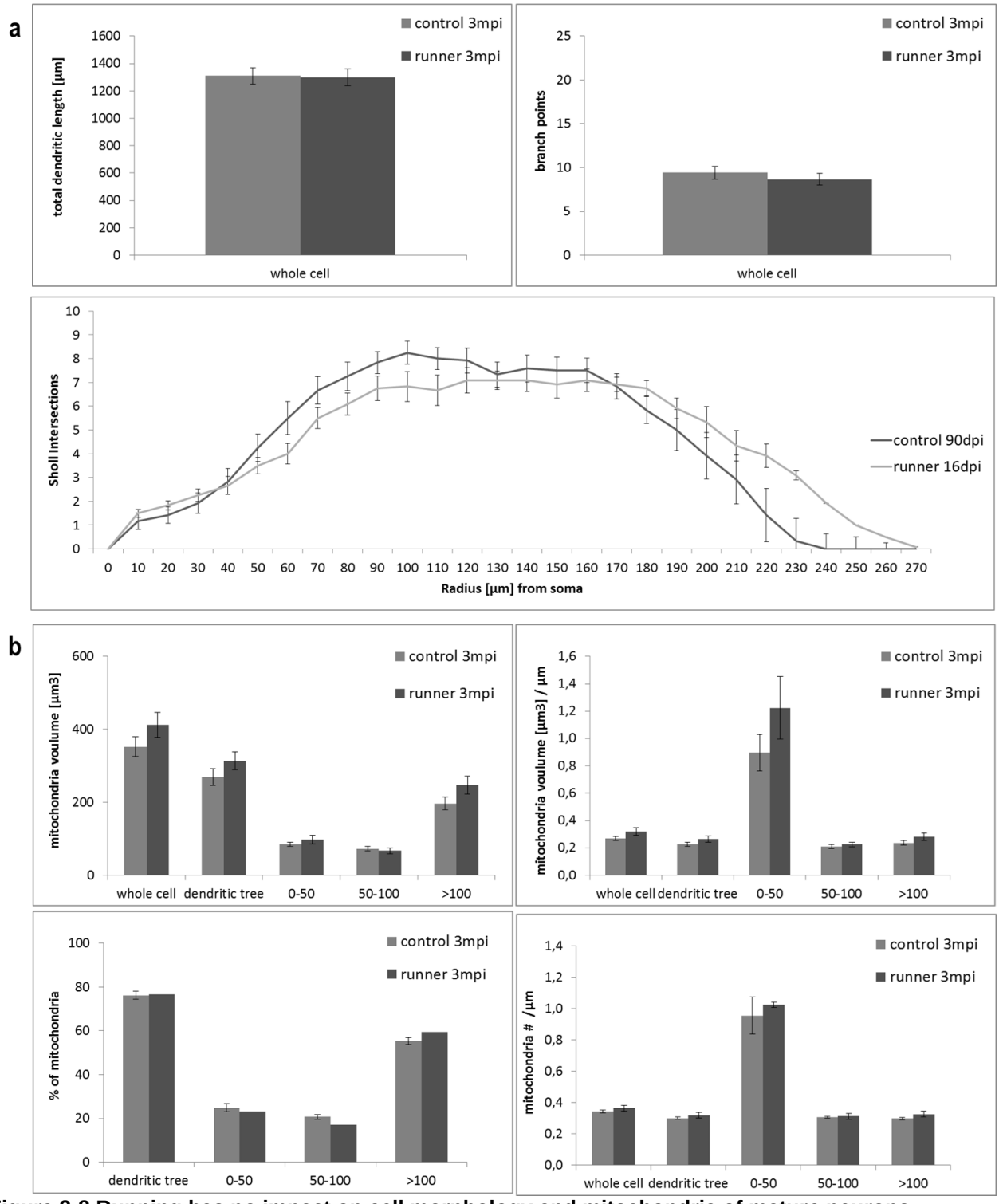

Figure 2-8 Running has no impact on cell morphology and mitochondria of mature neurons:
a Quantification of total dendritic length and number of dendritic branch points revealed no significant differences. Sholl analyses (Sholl 1953) did not reveal significant differences in the complexity of the cells. ***b*** Quantitative analysis showed no significant differences within the mitochondrial compartment; n=12 neurons from 3 different animals; error bars represent ± SEM; Significance levels were assessed with Student's T-test with unpaired samples and unequal variances.

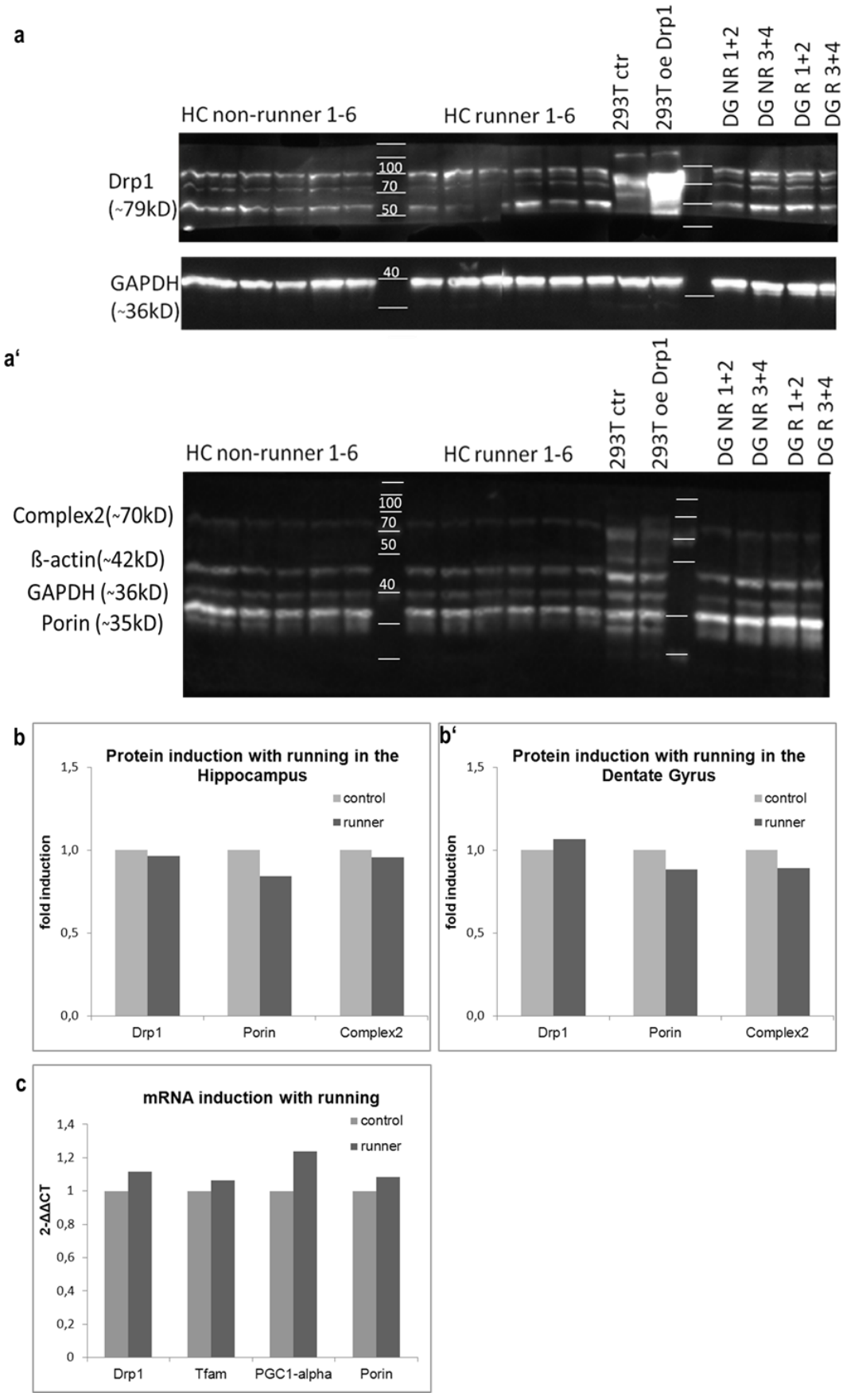

Figure 2-9 Mitochondria related mRNA and protein levels are not globally altered with running:
a Representative immunoblots from whole hippocampus (HC) tissue (samples from 6 individual animals), or microdissected dentate gyrus (DG) tissue (2 samples from 2 individual animals pooled) to determine Drp1 expression with and without running; GAPDH and ß-actin immunoreactivity were used as a loading control. Protein lysates of HEK 293T cells with and without Drp1 overexpression (oe) were used as a

positive control for the Drp1 antibody; various Drp1 bands recognized in tissue samples represent different transcript variants. ***a'*** Complex2 and Porin expression was determined by incubating immune-blots with specific antibodies raised against Porin and Complex2. ***b*** Quantification of protein induction for Drp1, Porin and Complex2 in whole hippocampus tissue after running; no significant changes were detectable. ***b'*** Quantification of protein induction for Drp1, Porin and Complex2 in microdissected dentate gyrus tissue after running; no significant changes were detectable. ***c*** Quantitative analysis of mRNA levels showed no significant increase of Drp1, Tfam, PGC-1α, and Porin levels in dentate gyrus tissue. Transcription levels were normalized to Srp14 expression.

However, it has been known for several years, that exercise stimulates mitochondrial biogenesis in skelatal muscles (Baar et al., 2002), and there is now evolving evidence, that actually a wide range of tissue, such as liver (Matiello et al., 2010), brain (Steiner et al., 2011) and adipose tissue (Sutherland et al., 2009) also react on exercise with increase of mitochondrial biogenesis to cope with higher metabolic demands (Little et al., 2011). This raised the question, whether running also affects mitochondrial content specifically in the dentate gyrus or the hippocampus, respectively. In contrast to a previous report by Steiner and colleagues (Steiner et al., 2011), western blot analysis of the expression of proteins, that are related to mitochondrial mass (Porin), mitochondrial activity (Complex2) or mitochondrial fission (Drp1) revealed that there is no significant induction of these proteins with running, neither in whole hippocampus tissue (Porin: 0.84 fold; Complex2: 0.96 fold; Drp1: 0.96 fold), nor in microdissected dentate gyrus tissue (Porin: 0.88 fold; Complex2: 0.89 fold; Drp1: 1.07 fold). Consistent with that result, quantitative analysis of mRNA induction in the dentate gyrus tissue of mice after 14 days with acces to a running wheel, showed that the relative transcription levels of the nuclear mitochondrial transcription co-activator (PGC-1α), mitochondrial transcription factor (Tfam), mitochondrial fission protein (Drp1) and mitochondrial membrane protein (Porin) are not significantly affected by exercise (PGC-1α: 1.24 fold, Tfam: 1.06 fold, Drp1: 1.11 fold, Porin: 1.08 fold) (Figure 2-9).

2.3. Manipulation of mitochondrial dynamics in hippocampal neurogenesis

Given that increase of mitochondrial mass and transport of mitochondria into dendrites are processes, which are strongly related to the development of newborn neurons, it is very intriguing how hippocampal neurogenesis is affected when the processes of biogenesis and distribution are manipulated. The question regarding the role mitochondrial biogenesis during maturation of newborn neurons was addressed in the PhD Thesis of Birgit Ebert (Ebert, 2013) by loss of function studies of the mitochondrial transcription factor Tfam. One possibility to approach the second issue about the role of mitochondrial transport is to manipulate mitochondrial dynamics. The key protein of

mitochondrial fission, Drp1, for instance has been shown to be involved in the distribution of mitochondria within cells (Smirnova et al., 1998). During my Master Thesis I could provide *in vitro* data suggesting that Drp1 plays an important role in the differentiation of neural precursor cells. In addition, first *in vivo* data from analyses of the expression of stage specific markers proposed that increased Drp1 function might be beneficial for the maturation of newborn neurons (Steib, 2009). During the present study this approach was further analyzed.

2.3.1. Drp1 overexpression changes mitochondrial density and distribution

Findings from my Master Thesis generated the assumption, that manipulation of the key protein for mitochondrial fission, Drp1, affects the mitochondrial distribution in newborn hippocampal neurons *in vivo* (Steib, 2009). To validate this hypothesis, 8 week old Bl6C57 mice were stereotactically injected, with a combination of retroviruses to visualize cell morphology (GFP) and mitochondria (mitoDsred). At the same time, via bicistronical expression of wtDrp1 or dnDrp1 with mitoDsred, respectively, mitochondrial fission was manipulated. Animals were housed with unlimited access to running wheels to increase the number of newborn neurons that can be analyzed (van Praag et al., 1999a), and were sacrificed at 16 dpi, when newborn granule neurons already have developed the characteristic apical dendritic tree and, under physiological conditions, mitochondria start to localize into the peripheral parts of the developing cells (Figure 2-2). Double transduced cells (GFP + mitoDsred, or GFP + *transgene* IRES mitoDsred, respectively) were analyzed, to evaluate differences in mitochondrial distribution. Indeed, the quantitative assessment of mitochondrial density, i.e. the number of mitochondria per µm dendritic length, in the cellular sections located in the ML, revealed that wtDrp1 overexpressing cells, are characterized by a significant increase of mitochondrial number compared to control cells (control 0.16 ± 0.02 mitochondria/µm; wtDrp1 0.22 ± 0.01 mitochondria/µm; $p>0.001$). When mitochondrial fission was inhibited by overexpression of a dominant-negative Drp1 (dnDrp1), the effects on mitochondrial distribution in newborn hippocampal neurons at 16 dpi were even more drastic. In this case, the mitochondrial number in the apical dendritic tree could not be determined, as almost the whole mitochondrial population of dnDrp1 transduced cells was located in the soma and shaft of the cells and the mitochondrial morphology appeared hyperfused and clustered. (Figure 2-10)

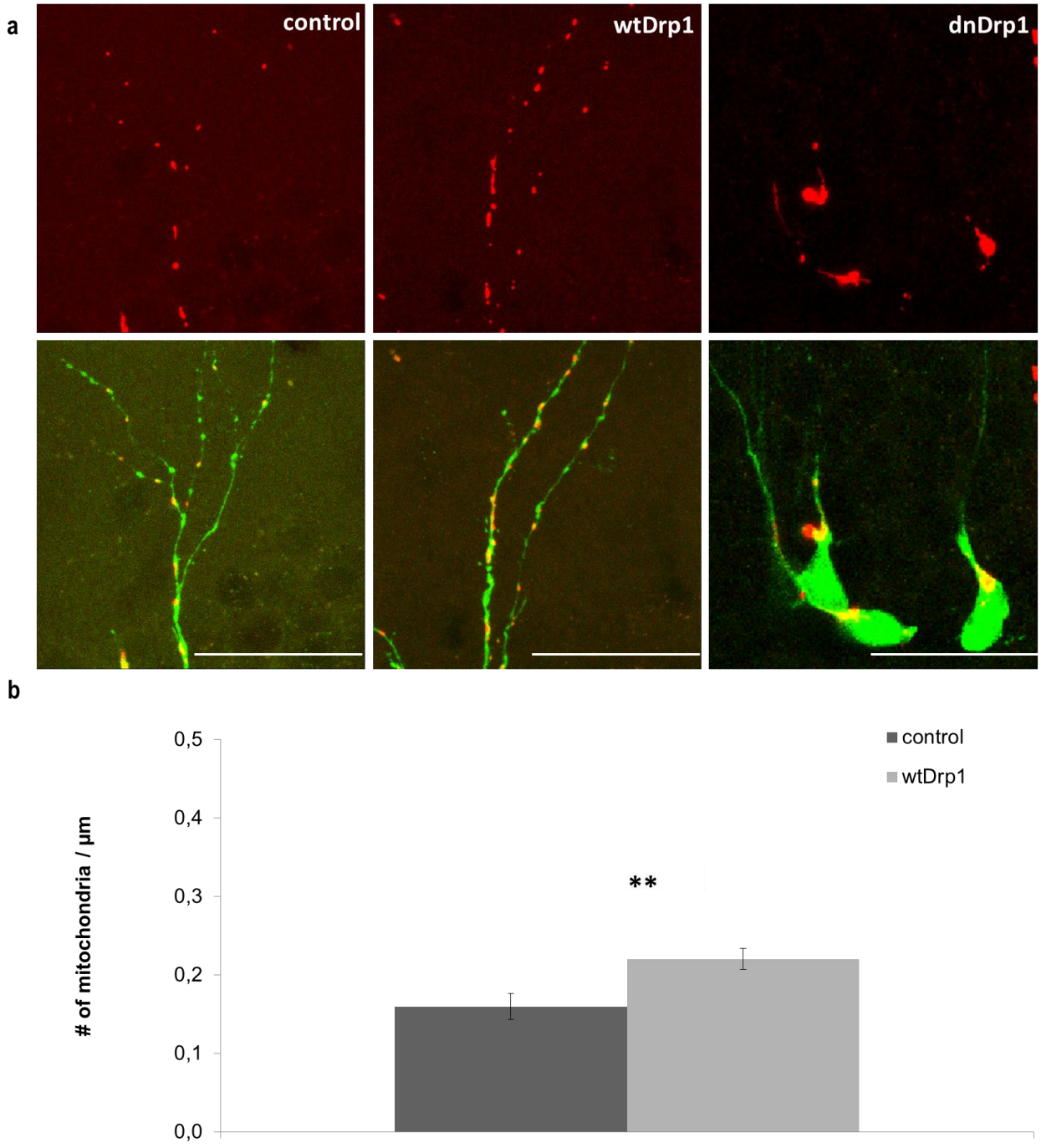

Figure 2-10 Mitochondria density is affected by overexpression of wtDrp1 and dnDrp1:
a Representative confocal images of a mitoDsred (red) and GFP (green) transduced cells in the mouse dentate gyrus at 16 dpi; transgenes wtDrp1 and dnDrp1 were bicistronically expressed with mitoDsred ***b*** Quantitative analysis of mitochondrial density in cellular sections in the ML with or without overexpression of wtDrp1. Scale bars 10 µm; n=10 dendritic areas from 3 different animals; error bars represent ± SEM; Significance level was assessed with Student's T-test with unpaired samples and unequal variances.

2.3.2. dnDrp1 overexpression impairs neuronal differentiation of neuronal precursor cells in the dentate gyrus

Consistent with the results on the impairment of mitochondrial transport into dendrites after inhibition of mitochondrial fission with dnDrp1 overexpression, affected cells showed rigorous defects in their morphological development. It has been demonstrated that a high percentage of dnDrp1 cells do not accomplish to extend an apical dendrite that spans the granular cell layer at 16 dpi, as it was observed for control cells under physiological conditions (ctr 97 ± 7%; dnDrp1 26 ± 16%; $p<0.001$) (Steib, 2009). In line with the morphological retardation, expression analysis of the stage specific marker DCX revealed a significant decrease of the proportion of DCX positive dnDrp1 transduced cells (ctr 88 ± 3%; dnDrp1 41 ± 6%; $p<0.001$) (Figure 2-12). This finding raised the question about the actual phenotype of not appropriately developed dnDrp1 positive cells. Sox2 expression was analyzed, which under physiological conditions is expressed during early stages of adult neurogenesis, i.e. in stem and uncommitted precursor cells. Quantitative evaluation of the amount of Sox2 positive cells among transduced cells, demonstrated a significant higher percentage of Sox2 expression among dnDrp1 overexpressing cells compared to control (ctr 4 ± 2%; dnDrp1 26 ± 7%; $p<0.01$) (Figure 2-13). This suggests that dnDrp1 positive cells, which do not manage to distribute mitochondria, remain in very early stages of the adult neurogenic lineage.

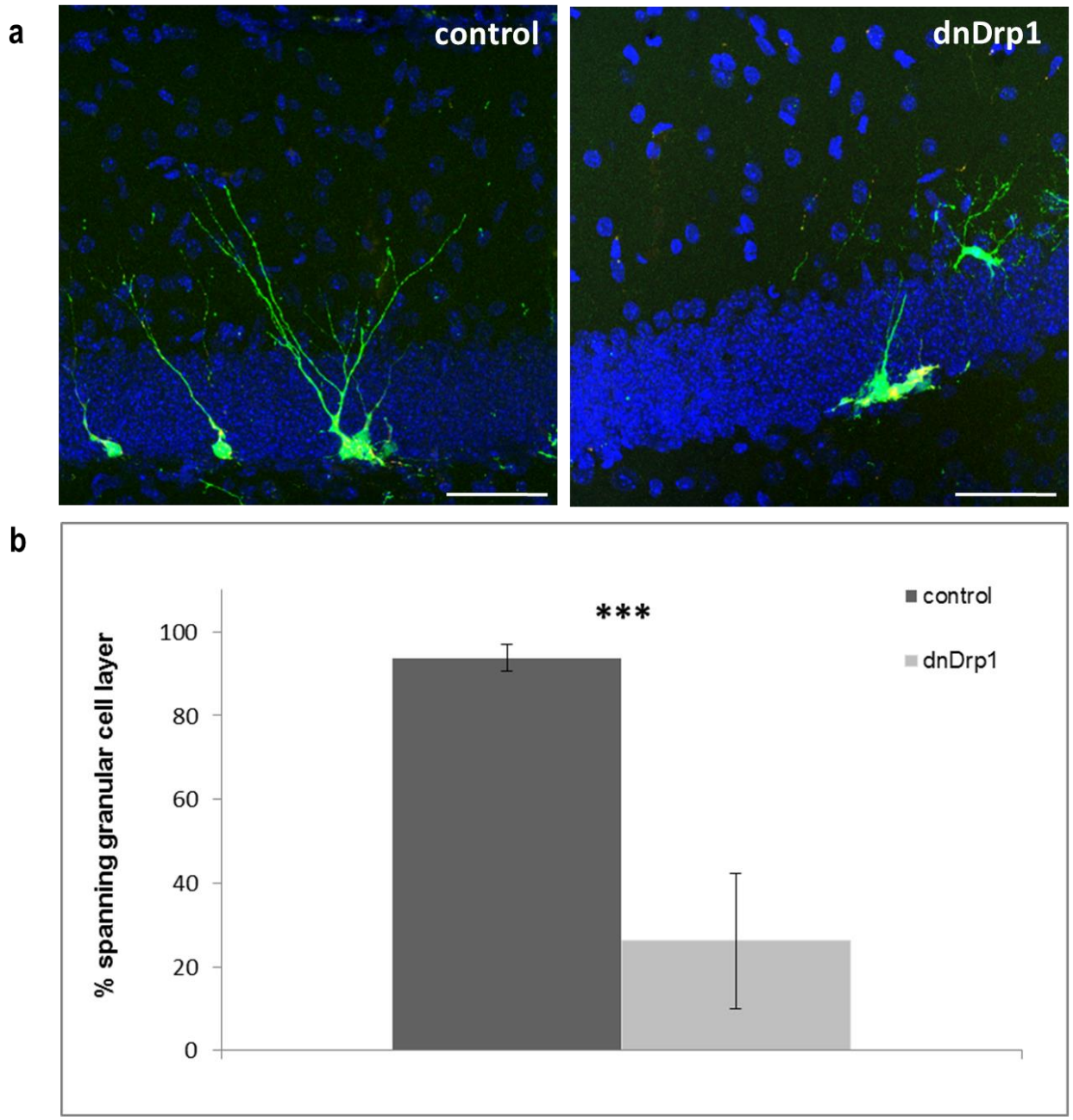

Figure 2-11 dnDrp1 overexpressing cells do not accomplish appropriate morphology:
a Representative confocal images of a mitoDsred (red) and GFP (green) transduced cells in the mouse dentate gyrus at 16 dpi, indicating that dnDrp1 do not display expected morphology at this time point; dnDrp1 was bicistronically expressed with mitoDsred ***b*** Quantification of the proportion of newborn neurons which developed an apical dendritic tree, spanning the granular cell layer. Scale bars 25 µm; error bars represent ± SEM; Significance levels were assessed with Student's T-test with unpaired samples and unequal variances.

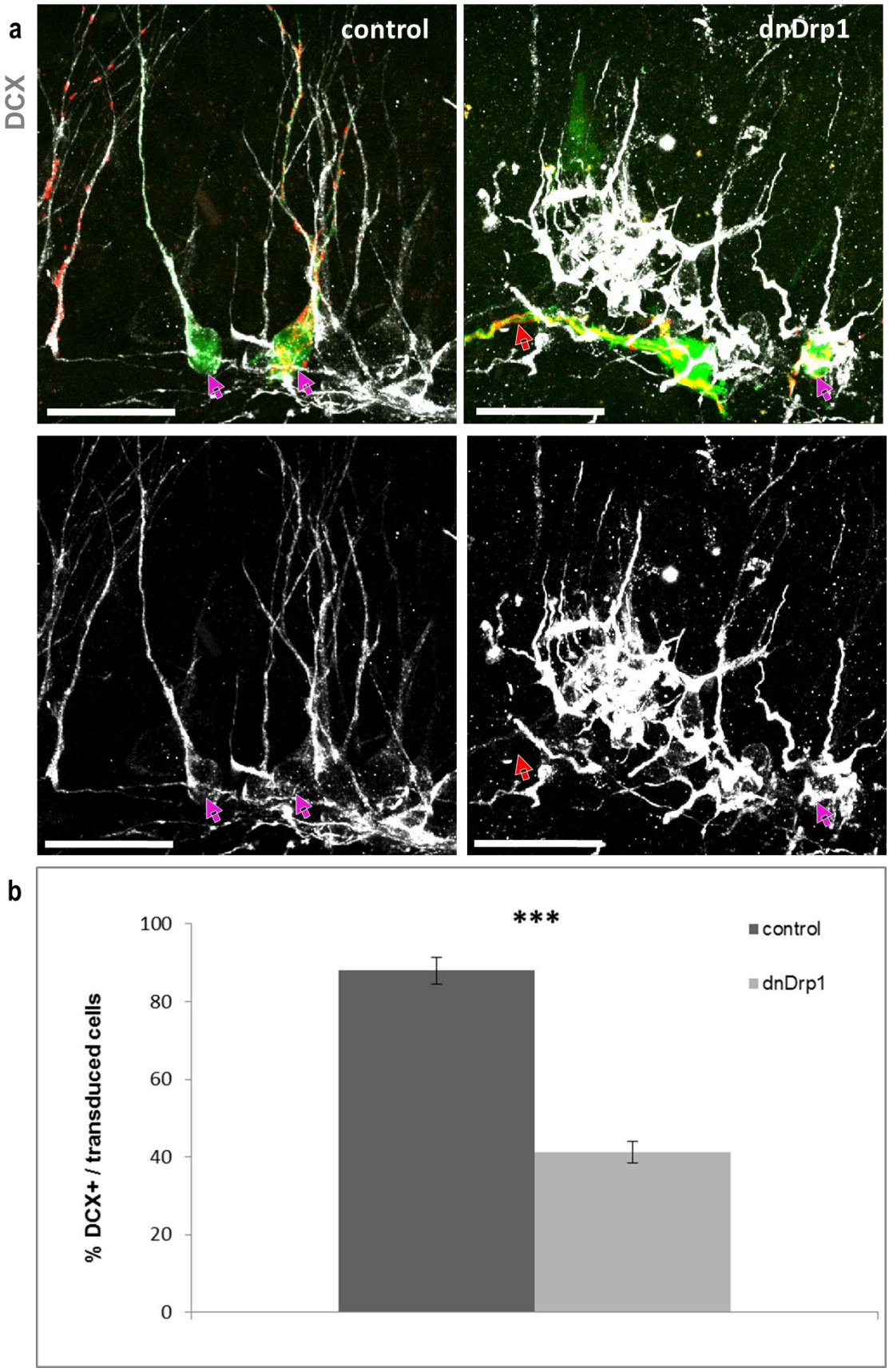

Figure 2-12 dnDrp1 overexpressing cells do not accomplish appropriate differentiation:
a Representative confocal images of immunohistochemistry of DCX in the dentate gyrus of double injected animals at 16 dpi. Purple arrows indicate DCX positive double-transduced cells, whereas the red arrow indicates a DCX negative dnDrp1 double-transduced cell ***b*** Quantification of the proportion of newborn neurons which were assessed as DCX positive. Scale bars 25 µm; error bars represent ± SEM; Significance levels were assessed with Student's T-test with unpaired samples and unequal variances.

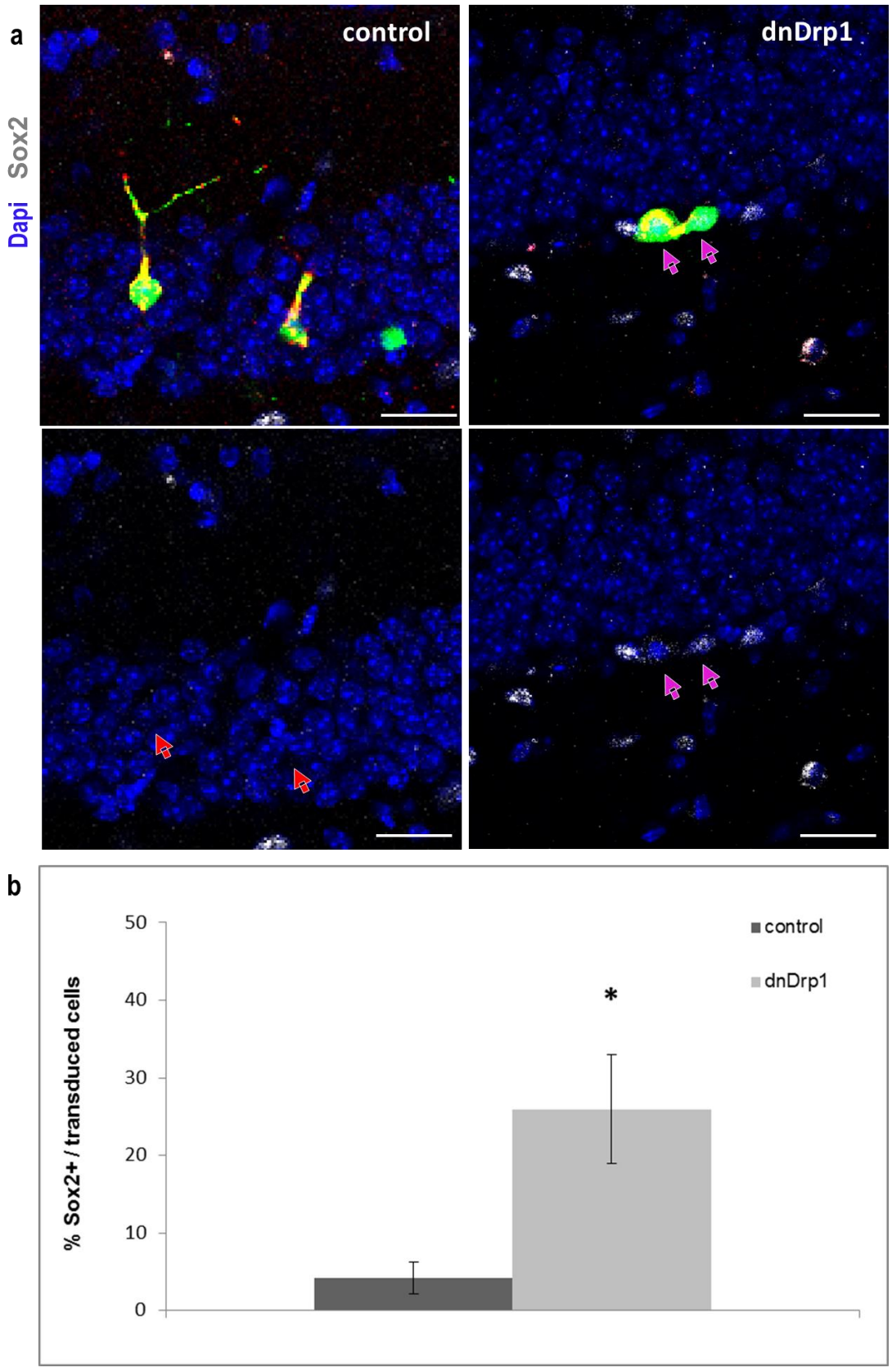

Figure 2-13 A higher percentage of dnDrp1 overexpressing cells remain Sox2 positive:
a Representative confocal images of immunohistochemistry of Sox2 in the dentate gyrus of double injected animals at 16 dpi. Purple arrows indicate Sox2 positive dnDrp1 double-transduced cells, whereas the red arrows indicate Sox2 negative double-transduced control cells ***a'*** Quantification of the proportion of newborn neurons which were evaluated as Sox2 positive. Scale bars 25 µm; error bars represent ± SEM; Significance levels were assessed with Student's T-test with unpaired samples and unequal variances.

2.3.3. wtDrp1 overexpression can accelerate maturation of newborn neurons, but requires running to stimulate this process

The investigation of the development of wtDrp1 transduced newborn neurons, was started in my Master Thesis (Steib, 2009). To determine the role of mitochondrial fission during adult hippocampal neurogenesis I performed a retroviral mediated gain-of-function of Drp1. Under basal housing conditions, analysis of total dendritic length (ctr 349 ± 19 µm, wtDrp1 404 ± 25 µm; p=0.07) and number of branching points (ctr 12 ± 1; wtDrp1 12 ± 1), revealed no significant differences in the dendritic morphology, but a trend of wtDrp1 overexpressing cells towards an accelerated morphological development. Since neurogenesis is regulated by a combination of intrinsic and extrinsic factors, I hypothesized that the effects of wtDrp1 on maturation might be more evident in the presence of running. In this housing condition, I found during my Master Thesis that wtDrp1 transduced neurons more frequently expressed the mature neuronal granule cell marker Calbindin (ctr 0 ± 0%; wtDrp1 14 ± 3%; p<0.01) (Steib, 2009), suggesting overexpression of wtDrp1 accelerated the maturation process. In addition, transgenic cells displayed an obvious more mature appearance at 16 dpi with exercise. However, analysis of total dendritic length (ctr 744 ± 65 µm, wtDrp1 875 ± 55 µm; p=0.1) and number of branching points (ctr 15 ± 2; wtDrp1 17 ± 2) in this paradigm did not disclose any significant differences (Figure 2-14). The fact that there was again a trend of wtDrp1 overexpressing cells towards maturation, suggested that there actually might be differences, but not ascertainable with evaluation of only 12 cells per group. As it is not feasible, to determine the total dendritic length of more cells, because this type of analysis requires the rare, double-transduced cells, which are additionally not pruned due to sectioning of the hippocampus, a more crude approach to assess the size of the newborn neurons was taken. The robust global morphology analysis was performed (Krzisch et al., 2013), by determining the ratio of the cell size, represented as the length from the soma to the maximal extension of the cell of double-transduced cells, to the maximal possible size of the cell in this area of the hippocampus, represented as the distance from the cell soma to the end of the ML, which is termed as hippocampal fissure (HF) and is the natural border for cellular growth. This approach allows assessment of newborn neurons in various regions of the hippocampus as the size is normalized to the position, and hence a lot more cells could be analyzed. Interestingly, quantification of the cumulative distribution of the ratios of control versus wtDrp1 transduced cells revealed,

that there are no significant differences between control and wtDrp1 overexpressing cells under basal conditions. In contrast, the evaluation of the running paradigm disclosed a significant increased percentage of newborn neurons that are longer in relation to their position (Figure 2-15; $p<0.05$), strengthening the hypothesis that the morphological maturation is accelerated among wtDrp1 transduced neurons. However, wtDrp1 overexpression could only stimulate the maturation, when adult neurogenesis was already enhanced by running as a strong environmental stimulus. (Figure 2-15)

One hallmark of the maturation of newborn neurons in the adult dentate gyrus is the integration into the existing circuitry, which is discernible by the presence of spines on the dendrites of newborn granule neurons, representing postsynaptic contact sides. Under basal conditions spine formation starts around 16 dpi (Zhao et al., 2006). Hence, the quantification of the number of spines at this time allows conclusions about the development stage of the cells. No spines were visible on dendrites of control and wtDrp1 under basal conditions at 16 dpi. Next, spine density was quantified in the set of animals that were housed with unlimited access to running wheels. This analysis revealed that spine density as represented by the number of spines per µm dendrite located in the mid ML was significantly higher in wtDrp1 transduced newborns (ctr 0.17 ± 0.01 spines/µm; wtDrp1 0.38 ± 0.05 spines/µm; $p<0.01$). The increased spine density was accompanied in the same dendrites by an increase of mitochondrial density (control 0.16 ± 0.02 mitochondria/µm; wtDrp1 0.22 ± 0.01 mitochondria/µm; $p<0.001$). This suggests a potential link between facilitated mitochondrial distribution and accelerated maturation, represented by increased size of the dendritic tree and enhanced integration at 16 dpi. (Figures 2-15 and 2-16)

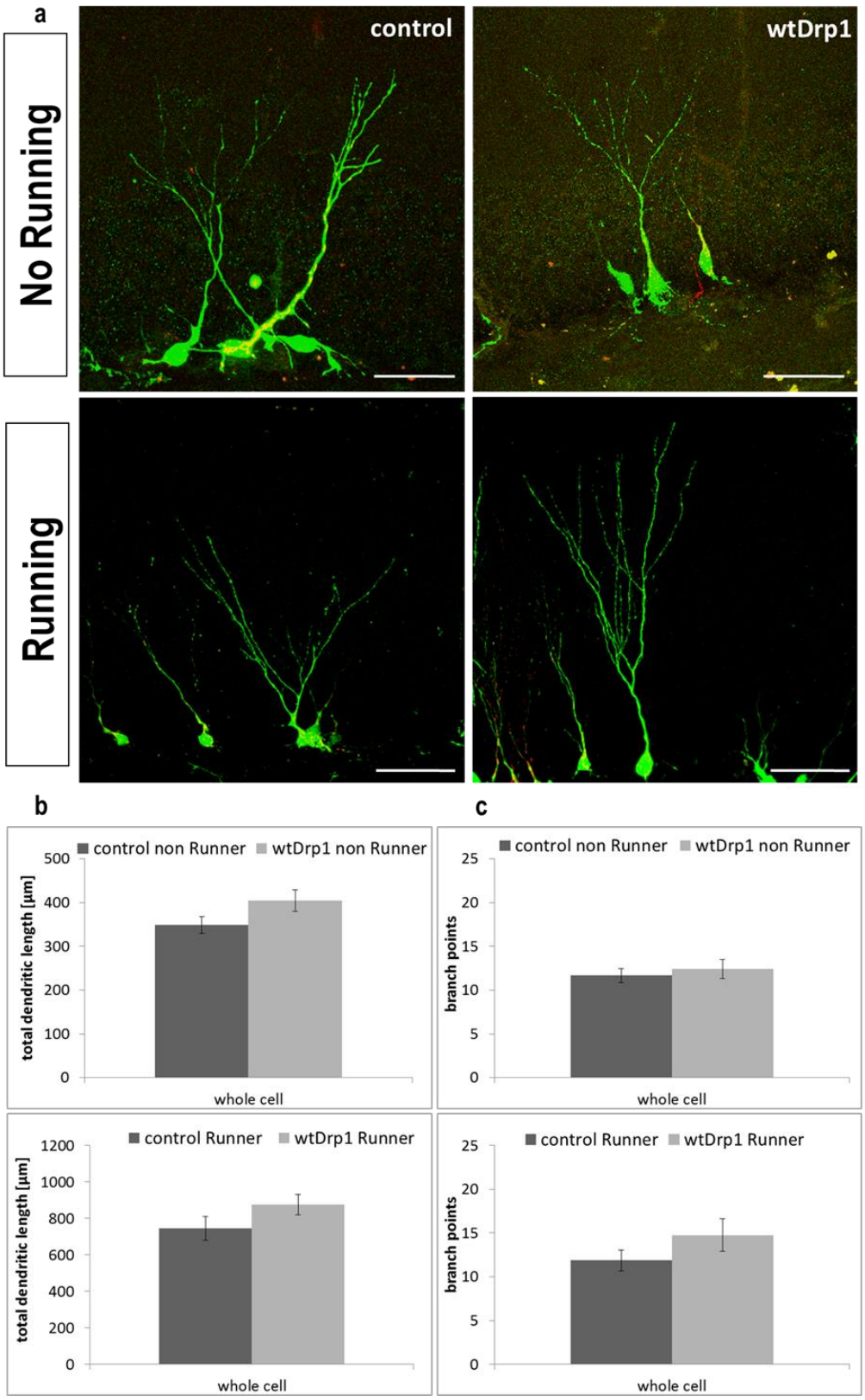

Figure 2-14 wtDrp1 overexpression stimulates maturation of newborn neurons together with running:
a Representative confocal images of mitoDsred (red) and GFP (green) transduced cells in the mouse dentate gyrus at 16 dpi, with and without running; wtDrp1 was bicistronically expressed with mitoDsred. Scale bars 25 µm. ***b*** Quantifications of the total dendritic length of ctr versus wtDrp1 cells in basal and running paradigms. ***c*** Quantifications of number of branching points of ctr versus wtDrp1 cells in basal and running paradigms. Significance levels were assessed with Student's T-test with unpaired samples and unequal variances. n=12 (running paradigm) or n=6 (basal conditions) neurons from 3 different animals, respectively. All error bars represent ± SEM.

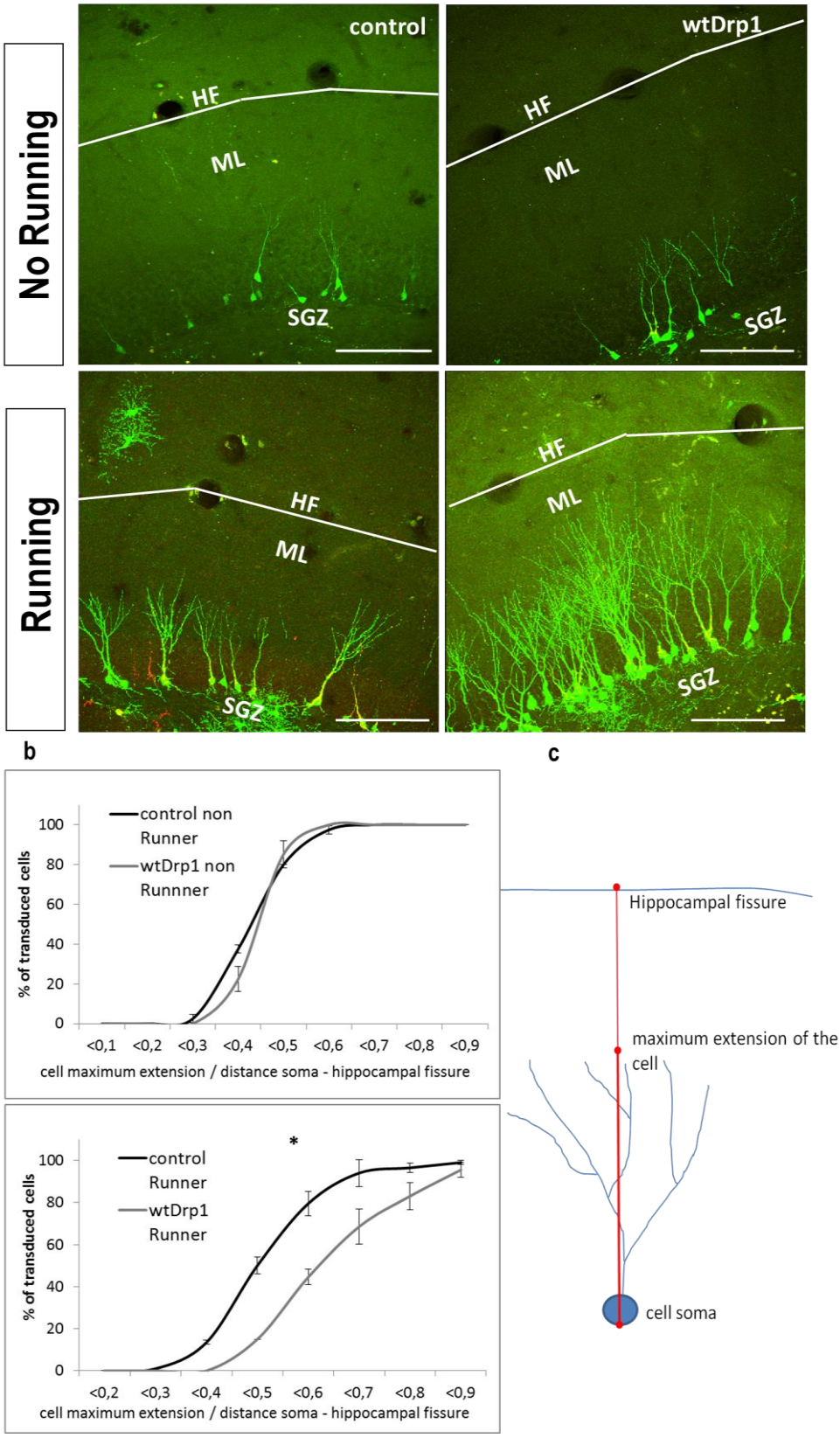

Figure 2-15 wtDrp1 overexpression stimulates maturation of newborn neurons together with running:
a Representative confocal images of mitoDsred (red) and GFP (green) transduced cells in the mouse dentate gyrus at 16 dpi, with and without running in a lower resolution, indicating also the Hippocampal Fissure, which represents the natural border for cellular growth. Scale bars 25 µm. ***b*** Cumulative distribution of ratios calculated from cell size and maximal possible cell size of ctr versus wtDrp1 cells in basal and running paradigms. Right shift of the curve of wtDrp1 cells in the running paradigm indicates an increased percentage of cells having a higher ratio. Significance levels were assessed with 2-way ANOVA. n=50 neurons per animal from 3 different animals. All error bars represent ± SEM. ***c*** Illustration explaining how ratios for cell extension were calculated.

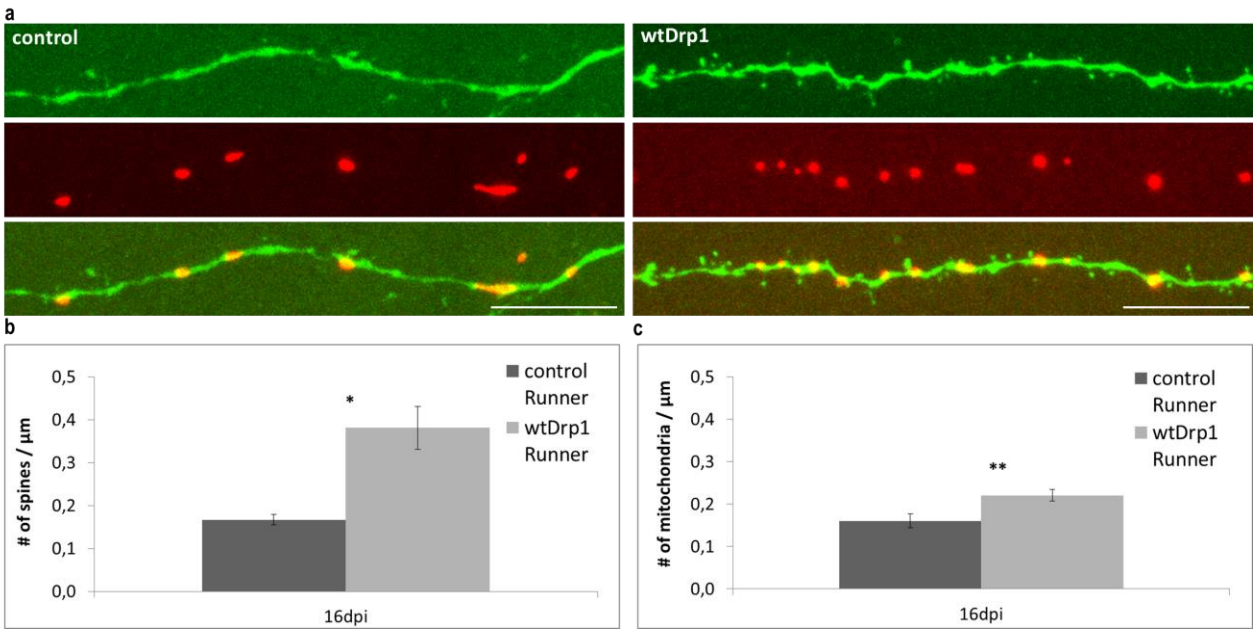

Figure 2-16 wtDrp1 overexpression stimulates maturation of newborn neurons together with running:
a Representative confocal images of dendrites in located in the ML of mitoDsred (red) and GFP (green) transduced cells in the mouse dentate gyrus at 16 dpi, with the running paradigm; wtDrp1 was bicistronically expressed with mitoDsred. Arrows indicate examples of detected spines. Scale bars 10 µm. ***b*** Quantification of spine density, i.e. number of spines per µm, of ctr versus wtDrp1 cells, after running. ***c*** Quantification of mitochondria density, i.e. number of mitochondria per µm, of ctr versus wtDrp1 cells, after running. Significance levels were assessed with Student's T-test with unpaired samples and unequal variances. n=10 dendrites from 3 different animals. All error bars represent ± SEM.

2.3.4. Improvements of morphology and synaptic integration with wtDrp1 overexpression do not persist at 28 dpi

These results raised the question of whether the improvement of cellular growth and integration persist after 28 days development, or, whether at 28 dpi control cells catch up with wtDrp1 transduced cells with maturation. At this late time point of the neurogenic process, all new neurons reach with their dendrites to the HF (Figure 2-17). Detailed analyses of the morphology of GFP and mitoDsred double-transduced control and wtDrp1 overexpressing cells revealed that at this time point, control are morphologically indistinguishable from wtDrp1 overexpressing neurons with regard to total dendritic length (ctr 1255 ± 66 µm, wtDrp1 1249 ± 68 µm), number of branching points (ctr 8 ± 0.7; wtDrp1 8 ± 0.5) and the number of Sholl intersections (Figure 2-18, a). No significant differences of absolute mitochondrial volume, relative mitochondrial volume normalized to cell size, localization of mitochondria within the cells and mitochondrial density was found (Figure 2-18, b). Quantification of the number of spines on dendrites located in the mid-third of the ML, were also comparable between control (1.61 ± 0.07 spines/µm) and wtDrp1 overexpressing (1.78 ± 0.02 spines/µm) newborn neurons. Consistent with the results of the analysis of mitochondrial density in the dendritic tree, mitochondrial density

in the dendritic segments assessed for spine density was comparable between experimental groups (control 0.32 ± 0.01 mitochondria/µm, wtDrp1 0.35 ± 0.03 mitochondria/µm). To further evaluate if wtDrp1 transduced neurons at 28 dpi are characterized by more mature synapses, the percentage of mushroom spines, which are considered as mature synaptic contact sides [reviewed in (Nimchinsky et al., 2002)] was evaluated. However, there was no significant increase detectable (control 5 ± 1%, wtDrp1 5 ± 1%) (Figure 2-19).

Table 4 Quantitative assessment of the effects after wtDrp1 overexpression on the mitochondrial compartment at 28 dpi:

absolute mitochondrial volume [µm^3]	**control**	**wtDrp1**	**p-value**
whole cell	253 ± 23	217 ± 15	p=0.21
dendritic tree	166 ± 14	187 ± 17	p=0.36
0-50 µm	51 ± 3	66 ± 9	p=0.16
50-100 µm	50 ± 5	45 ± 5	p=0.49
> 100 µm	137 ± 13	121 ± 11	p=0.38
relative mitochondrial volume [µm^3/µm length]	**control**	**wtDrp1**	**p-value**
whole cell	0.20 ± 0.02	0.17 ± 0.01	p=0.16
dendritic tree	0.16 ± 0.02	0.14 ± 0.01	p=0.28
0-50 µm	0.78 ± 0.07	0.73 ± 0.11	p=0.69
50-100 µm	0.17 ± 0.02	0.14 ± 0.01	p=0.28
> 100 µm	0.16 ± 0.02	0.14 ± 0.01	p=0.29
% of mitochondrial located per section	**control**	**wtDrp1**	**p-value**
dendritic tree	74 ± 2	76 ± 1	p=0.44
0-50 µm	26 ± 2	24 ± 1	p=0.44
50-100 µm	20 ± 1	20 ± 2	p=0.72
> 100 µm	54 ± 2	55 ± 2	p=0.69
mitochondrial density [mitochondria/µm length]	**control**	**wtDrp1**	**p-value**
whole cell	0.37 ± 0.01	0.36 ± 0.01	p=0.40
dendritic tree	0.32 ± 0.01	0.31 ± 0.01	p=0.58
0-50 µm	1.24 ± 0.10	1.27 ± 0.13	p=0.86
50-100 µm	0.30 ± 0.01	0.30 ± 0.01	p=0.96
> 100 µm	0.32 ± 0.01	0.31 ± 0.01	p=0.36

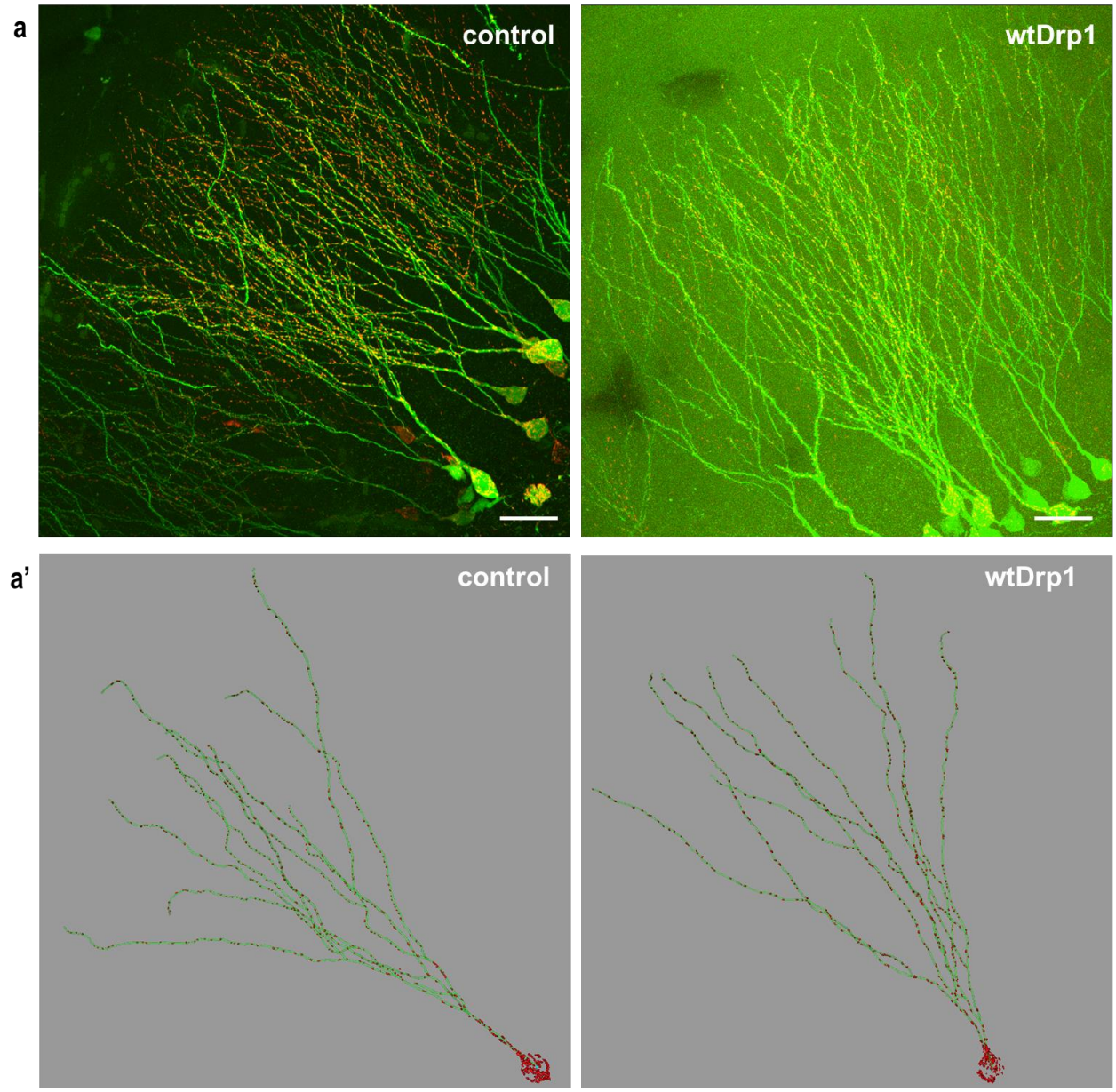

Figure 2-17 Improvements by wtDrp1 overexpression do not persist at 28 dpi
a Representative confocal images of mitoDsred (red) and GFP (green) control and wtDrp1 transduced cells in the mouse dentate gyrus at 28 dpi with the running paradigm; wtDrp1 was bicistronically expressed with mitoDsred. Scale bars 25 µm. ***a'*** 3-D reconstructions of the cells depicted in **a**.

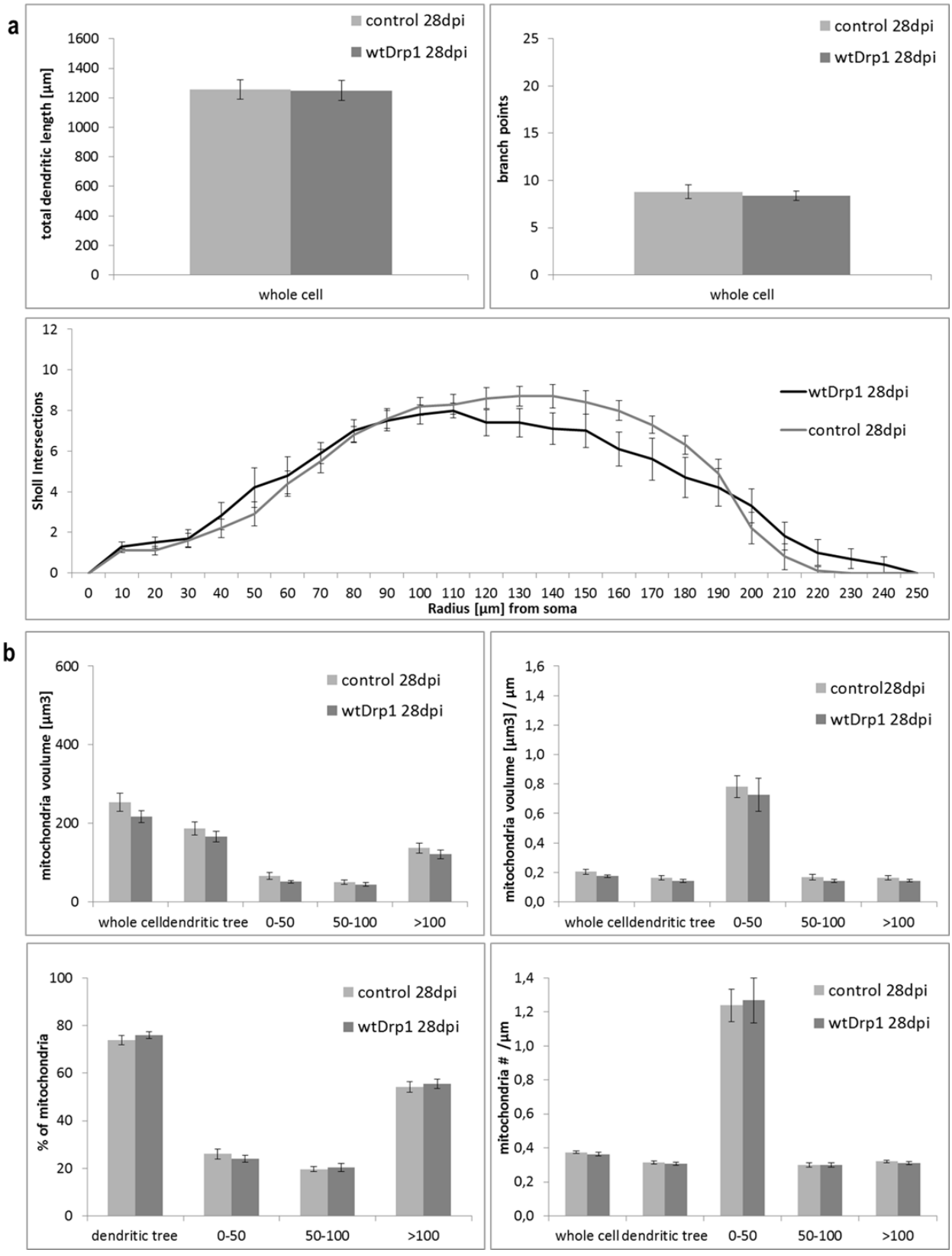

Figure 2-18 Improvements by wtDrp1 overexpression do not persist at 28 dpi
a Quantification of total dendritic length and number of dendritic branch points revealed no significant differences. Sholl analyses (Sholl 1953) did not reveal significant differences in the complexity of the cells. ***b*** Quantitative analysis showed no significant differences within the mitochondrial compartment. Scale bars 25 µm; n=12 neurons from 3 different animals; Significance levels were assessed with Student's T-test with unpaired samples and unequal variances. All error bars represent ± SEM.

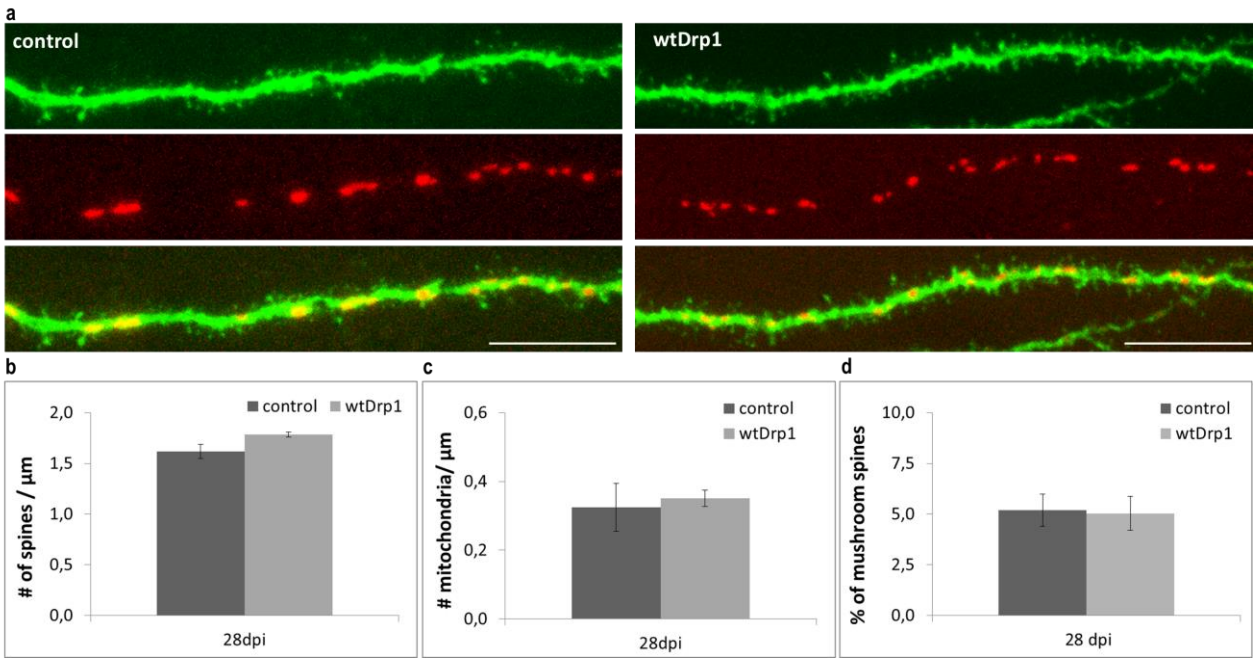

Figure 2-19 Improvements by wtDrp1 overexpression do not persist at 28 dpi
a Representative confocal images of dendrites located in the ML of mitoDsred (red) and GFP (green) transduced cells in the mouse dentate gyrus at 28 dpi, with the running paradigm; wtDrp1 was bicistronically expressed with mitoDsred. Scale bars 10 µm. ***b*** Quantification of spine density, i.e. number of spines per µm, of ctr versus wtDrp1 cells, after running. ***c*** Quantification of mitochondria density, i.e. number of mitochondria per µm, of ctr versus wtDrp1 cells, after running. ***d*** Quantification of percentage of mushroom spines, of ctr versus wtDrp1 cells, after running. Significance levels were assessed with Student's T-test with unpaired samples and unequal variances. n=10 dendrites from 3 different animals. All error bars represent ± SEM.

2.3.5. Drp1-dependent acceleration of development is independent from the transcript variant of Drp1 that is overexpressed

In 2007, when the study on Drp1 was started (Steib, 2007, 2009), most literature reporting about manipulation of wtDrp1 was referring to the human transcript variant 3 (Frank et al., 2001; Li et al., 2004). Hence, in the present study all experiments were performed by overexpression of the published human wtDrp1 variant 3. However, in 2009 it was reported (Uo et al., 2009), that Drp1 expression in neurons is restricted to the longer transcript variants (including Exons 16 and 17), and that there even exists a post-mitotic neuron-specific transcript variant which includes additionally Exon 3 (Yoon et al., 2003; Uo et al., 2009). Interestingly, the regions that are encoded by Exon 16 and 17 contain several sumo-ylation and phosphorylation sites, which allow to differentially regulate Drp1 activity via posttranslational modification (Chang and Blackstone, 2007; Taguchi et al., 2007; Wasiak et al., 2007; Han et al., 2008a). Exon 3 inserts 13 amino acids into the loop connecting the β2 and β2A sheets of the GTPase domain, and is exposed to the solvent which suggest it could be an interaction site for other proteins

(Niemann et al., 2001). This was raising the question if there might be additional benefits on the maturation of newborn neurons if not transcript variant 3, but the neuronal full length variants are overexpressed in neuronal precursor cells. Thus, I verified the expression of these variants in the mouse dentate gyrus by amplifying those regions from dentate gyrus mRNA with specific primers flanking Exon 3 and Exons 16 and 17, respectively. Indeed, two bands were detectable after amplification of the region flanking Exon 3, suggesting that the Exon 3 including variant which is expressed exclusively in post-mitotic neurons also exists in the dentate gyrus. The amplification with primers flanking Exon 16 and 17 also produced various bands, but no band with the size that is expected when neither Exon 16 nor Exon 17 is included, i.e. variant 3. This suggests that variant 3 is not expressed in dentate gyrus tissue, at all (Figure 2-20, b). Hence, I cloned the mouse full length transcript variant and full length including Exon 3 directly from the dentate gyrus, in order to investigate if differences exist regarding their impact on the maturation process. However, the analysis of the global morphology analysis at the 16 dpi did not indicate that different transcript variants evolve different effects (Figure 2-21, Figure 2-22). Consistently, quantification of neither spine density, nor mitochondrial density at 28 dpi did disclose any significant difference for any of the analyzed variants (Table 5, Figure 2-22). These results suggest that transcript variants of Drp1 do not serve differential functions in the regulation of activity-dependent maturation.

Table 5 Quantitative assessment of the effects of different Drp1 transcript variants on spine density and mitochondrial density at 28 dpi:

transcript variant	**spine density [spines/µm length]**	**mitochondrial density [mitochondria/µm length]**
ctr	1.61 ± 0.07	0.32 ± 0.01
wtDrp1 (human, variant 3)	1.78 ± 0.02	0.35 ± 0.03
wtDrp1 (mouse, full length)	1.81 ± 0.02	0.30 ± 0.01
wtDrp1 (mouse, full length, incl. Exon 3)	1.63 ± 0.02	0.33 ± 0.02

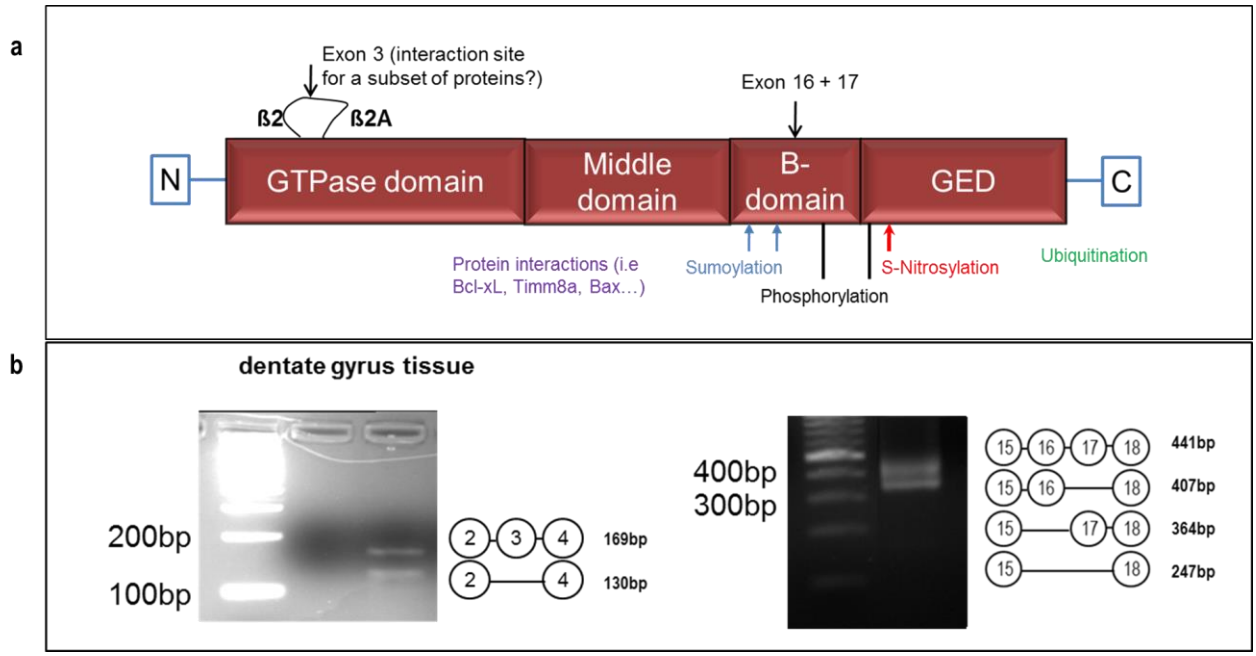

Figure 2-20 The effects of wtDrp1 overexpression on maturation are independent of the transcript variants:
a Illustration of the protein structure of Drp1: Amino Acids encoded by Exon 3 are located within the GTPase domain, are exposed to the solvent, and might be an interaction site for proteins. Exon 16 and 17 are encoding parts of the B-domain that contain post-translational modification sites. ***b*** mRNA amplifications with primers flanking the regions of Exon 3 and Exon 16 and 17, respectively, indicate that various transcript variants exist in the mouse dentate gyrus.

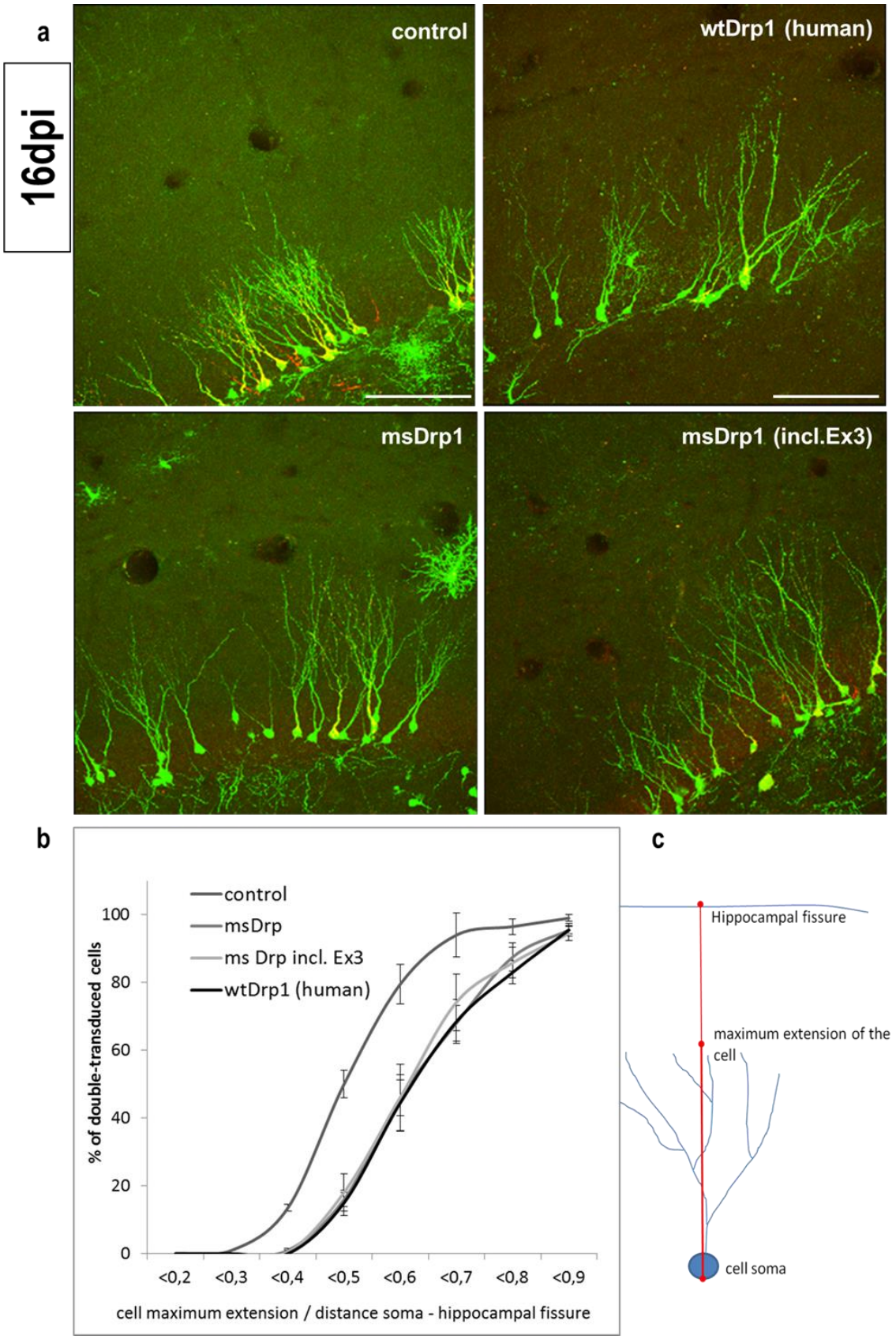

Figure 2-21 The effects of wtDrp1 overexpression on maturation are independent of the transcript variants:
a Representative confocal images of mitoDsred (red) and GFP (green) transduced cells in the mouse dentate gyrus at 16 dpi, indicating also the Hippocampal Fissure, which represents the natural border for cellular growth. Different wtDrp1 transcript variants were bicistronically expressed with mitoDsred. Scale bars 25 µm. ***b*** Cumulative distribution of ratios calculated from cell size and maximal possible cell size of ctr cells versus cells transduced with different wtDrp1 transcript variants cells. Curve progression of

different transcript variants was very similar. Significance levels were assessed with 2-way ANOVA. n=50 neurons per animal from 3 different animals. All error bars represent ± SEM. ***c*** Illustration explaining how ratios for cell extension were calculated.

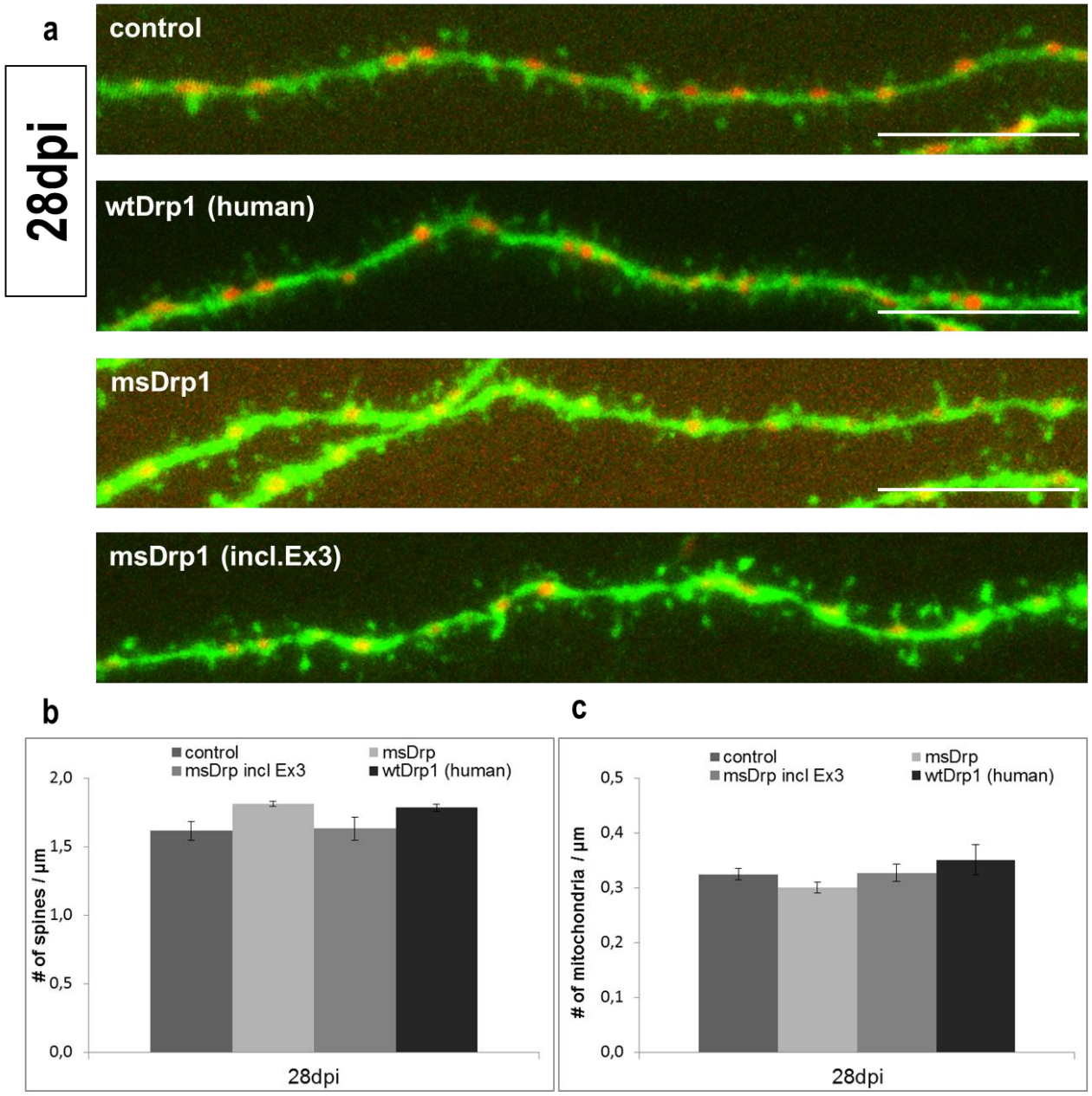

Figure 2-22 The effects of wtDrp1 overexpression on spine formation and mitochondrial distribution are independent of the transcript variants:
a Representative confocal images of dendrites in located in the ML of mitoDsred (red) and GFP (green) transduced cells in the mouse dentate gyrus at 28 dpi. Different wtDrp1 transcript variants were bicistronically expressed with mitoDsred Scale bars 10 µm. ***b*** Quantification of spine density, i.e. number of spines per µm, of ctr cells versus cells transduced with different wtDrp1 transcript variants. ***c*** Quantification of mitochondria density, i.e. number of mitochondria per µm, of ctr cells versus cells transduced with different wtDrp1 transcript variants. Significance levels were assessed with Student's T-test with unpaired samples and unequal variances. n=10 dendrites from 3 different animals. All error bars represent ± SEM.

2.4. Analysis of adult hippocampal neurogenesis after creatine-supplemented diet

Creatine has been reported to have a neuroprotective effect in mouse models for neurodegenerative diseases, due to its anti-oxidant, anti-excitotoxic and bioenergetic properties (see chapter 1.2.2), and has been shown to improve survival and health of mice (Bender et al., 2008). The next set of experiments was performed to investigate if a creatine-supplemented diet has the potential to promote adult hippocampal neurogenesis.

2.4.1. Creatine does not increase proliferation

For immunohistochemical analysis of proliferation and neurogenesis in the dentate gyrus, coronal sections from animals after 8 weeks creatine diet were evaluated for the expression of the proliferation marker Ki67p and the immature neuronal marker NeuroD. Quantitative assessment of number of Ki67p positive cells normalized to the size of the dentate gyrus did not show enhancement of proliferation with creatine, but proliferation was even slightly significantly decreased (control 9857 ± 975 cells/mm^3, creatine 8347 ± 615 cells/mm^3; $p<0.05$). In addition, no obvious increase of the number of NeuroD positive cells, which correlates to the amount of neurogenesis, was observed in creatine fed animals (data not quantified) (Figure 2-23).

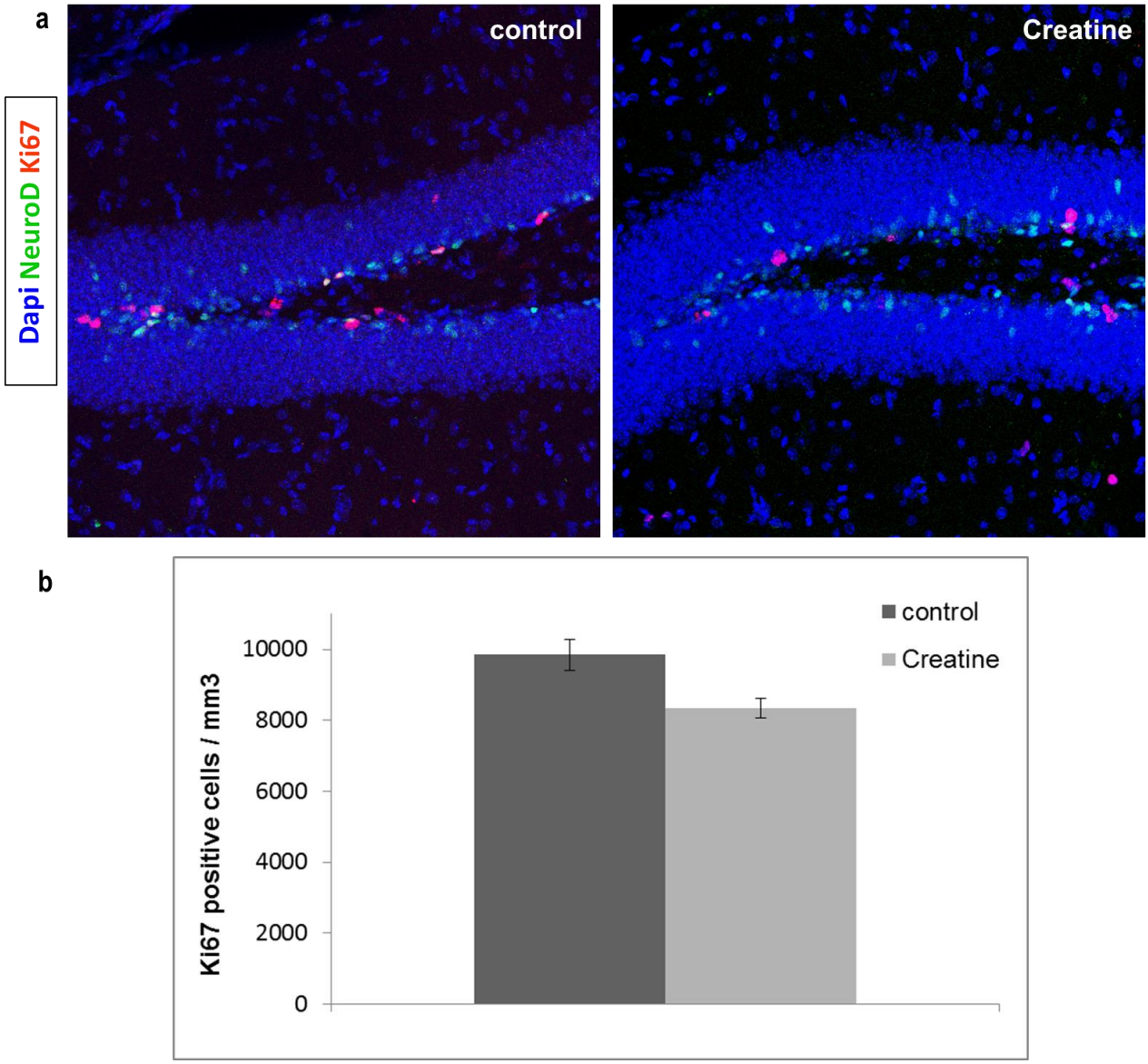

Figure 2-23 Effects of creatine supplemented diet on adult proliferation in the adult hippocampus: ***a*** Representative confocal images showing immunohistochemistry for Ki67p and NeuroD in coronal hippocampal sections from control and creatine-fed mice. Scale bar 100 µm. ***b*** Quantification of proliferation by determination of number of Ki67p positive cells. Significance levels were assessed with Student's T-test with unpaired samples and unequal variances. All error bars represent ± SEM.

2.4.2. Creatine does not upregulate the immature neuronal marker Doublecortin or mitochondrial related genes in the hippocampus

To assess whether creatine has global effects on transcription of genes related to mitochondrial function and biogenesis in the hippocampus, mRNA was isolated from the hioocampus of wildtype Bl6C57 mice that were fed with a diet containing 1% creatine between the age of four to 12 weeks on. Relative gene expression levels of mitochondria related genes, as represented by the mitochondrial transcription factor Tfam (1.09 fold), the regulator of nuclear mitochondrial gene expression PGC-1α (1.01 fold), and the mitochondrial fission protein Drp1 (1.11 fold) did not significantly change in hippocampal tissue after creatine supplementation. In consistency with the observation of NeuroD expression, analysis the of transcription level of Doublecortin (DCX), which is a marker for immature neurons and thus expression levels are correlated to the amount ongoing neurogenesis, did not increase significantly (1.26 fold), suggesting that eight weeks creatine-supplemtented diet does not strongly modulate hippocampal neurogenesis (Figure 2-24).

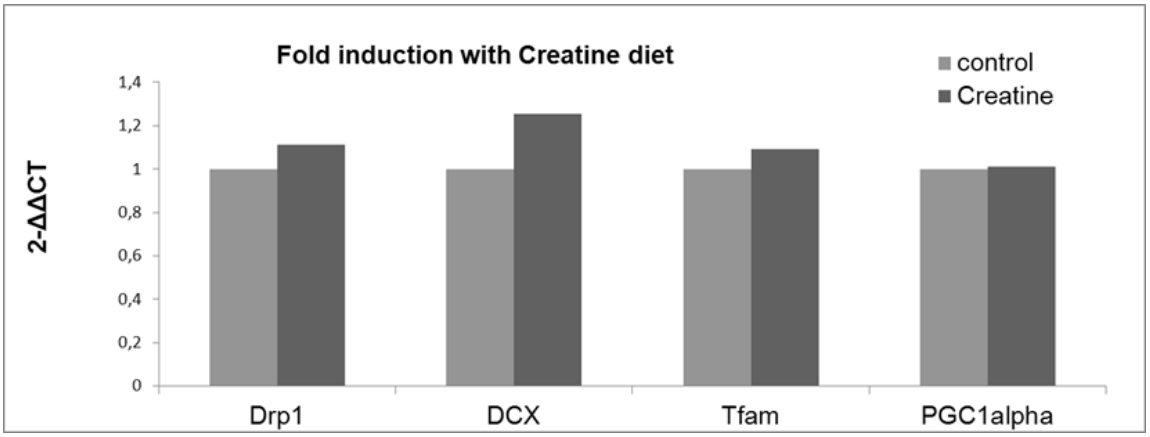

Figure 2-24 Effects of creatine supplemented diet on adult hippocampal neurogenesis realted and mitochondrial related genes:
Diagram showing detected fold induction of transcription levels in hippocampal tissue of creatine-fed animals; gene expression was normalized to srp14 levels.

2.4.3. Creatine does not improve morphological maturation, but increases the number of mitoDsred expressing cells

For further evaluation of creatine-mediated effects on neurogenesis, another set of animals was stereotactically injected with a combination of retroviruses encoding for GFP and mitoDsred 4 weeks after creatine supplementation has been started, and sacrificed at 16 dpi to assess cellular growth and mitochondria content. The global morphology analysis did not reveal a significant effect of creatine on the morphological development of newborn neurons, since evaluation of the cumulative distribution of determined relative dendritic growth did result in a similar curve progression. Comparable to the results from non-running control animals, newly generated neurons in control and creatine-fed animals did not bear spines at 16 dpi. Mitochondria content and distribution were obviously very similar between control and creatine-fed animals (data not quantified). However, it was very striking, that number of mitoDsred positive cells was dramatically increased within the creatine group (ratio yellow cells / green + yellow cells control 0.12 ± 0.03, creatine 0.76 ± 0.04; $p<0.001$), although there should be no differences, as exactly the same virus mixture was injected in both groups. This result suggests that creatine supplementation may affect mitochondrial biology in newborn granule neurons, but how exactly remains to be determined (Figure 2-25).

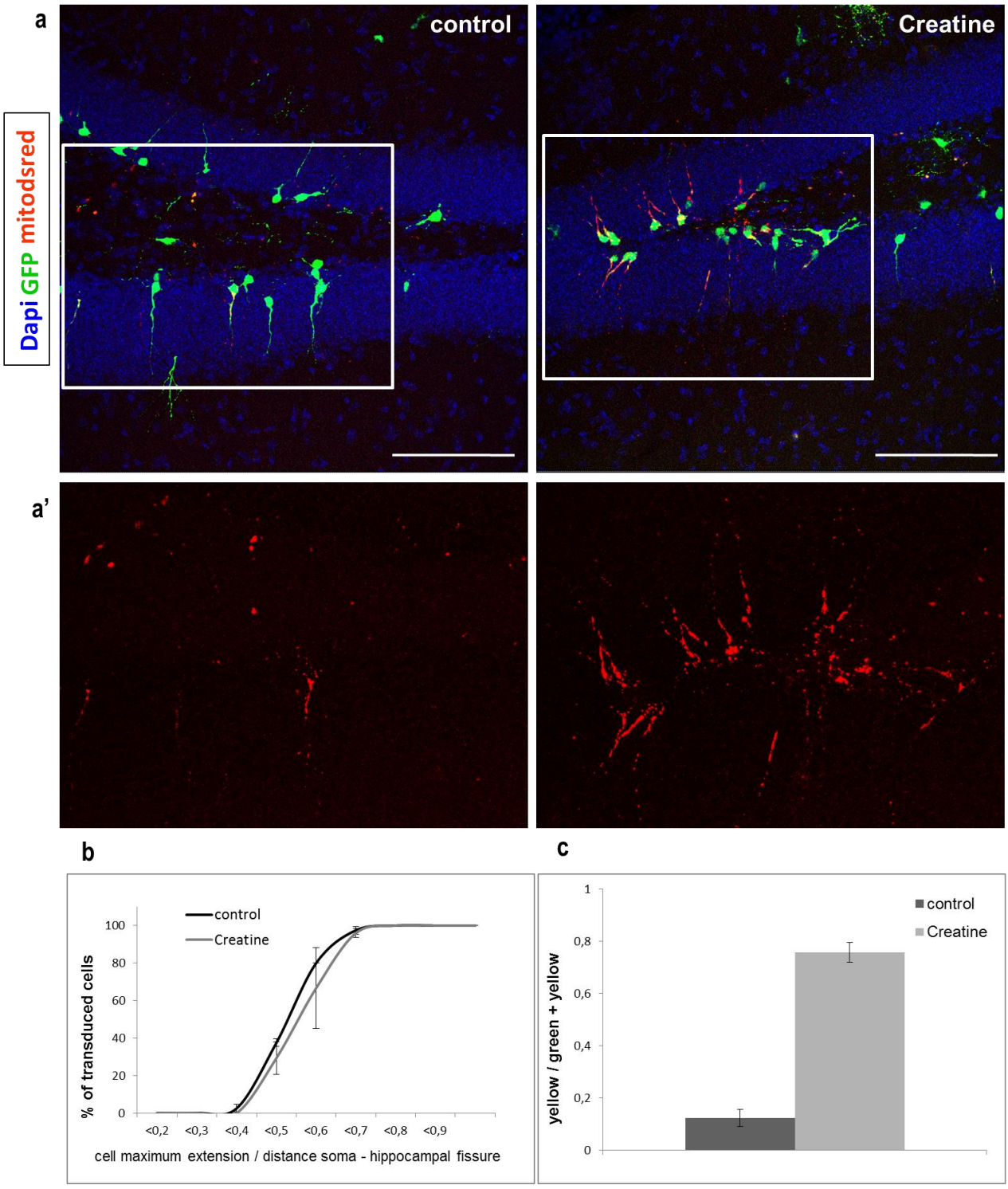

Figure 2-25 Effects of creatine supplemented diet on cellular growth and mitochondrial number: ***a*** Representative confocal images of double injections with GFP (green) and mitoDsred (red) retroviruses into the dentate gyrus at 16 dpi with and without creatine diet. Scale bar 100 µm ***a'*** Higher resolution of only the mitoDsred cells surrounded by the white boxes in a, indicating the dramatic increase of mitoDsred positive cell number in Creatine-fed animals. ***b*** Cumulative distribution of ratios calculated from cell size and maximal possible cell size of ctr cells versus cells from creatine-fed mice. Curve progression is very similar. Significance levels were assessed with 2-way ANOVA. n=50 neurons per animal from 3 different animals ***c*** Quantification of the ratios yellow / green + yellow indicating that increase of mitoDsred positive cell number, normalized to the number of green cells. Significance levels were assessed with Student's T-test with unpaired samples and unequal variances. n=50 cells from 3 different animals. All error bars represent ± SEM.

2.4.4. Creatine does not improve survival of newborn neurons or changes the phenotype

Another key step during adult hippocampal neurogenesis is the survival of newborn neurons, since most of the neuronal precursor cells die off during their development (Biebl et al., 2000). As creatine is known to have anti-apoptotic and neuro-protective characteristics, the question at hand is, if creatine supplemented diet is beneficial for the survival during adult neurogenesis. This issue was approached, by labeling proliferating neural precursor cells with the thymidine-analogue BrdU and quantification of the amount of remaining labeled cells in the dentate gyrus 28 days later. Quantitative assessment revealed that the number of BrdU positive cells was not significantly altered between creatine fed animals (8270 ± 1339 cells/mm^3) and controls (10822 ± 3284 cells/mm^3). (Figure 2-26, a-a'). Since surviving cells that incorporated BrdU do not necessarily have to be neurons, but could also be glia phenotypes, percentage of neurons among the BrdU positive cells was additionally evaluated. Expression of the neuronal marker Prox1 among BrdU labeled cells was similar between experimental groups, indicating that creatine did not alter the fate of newborn cells (ctr 86 ± 1%, creatine 86 ± 1%) (Figure 2-26, b-b').

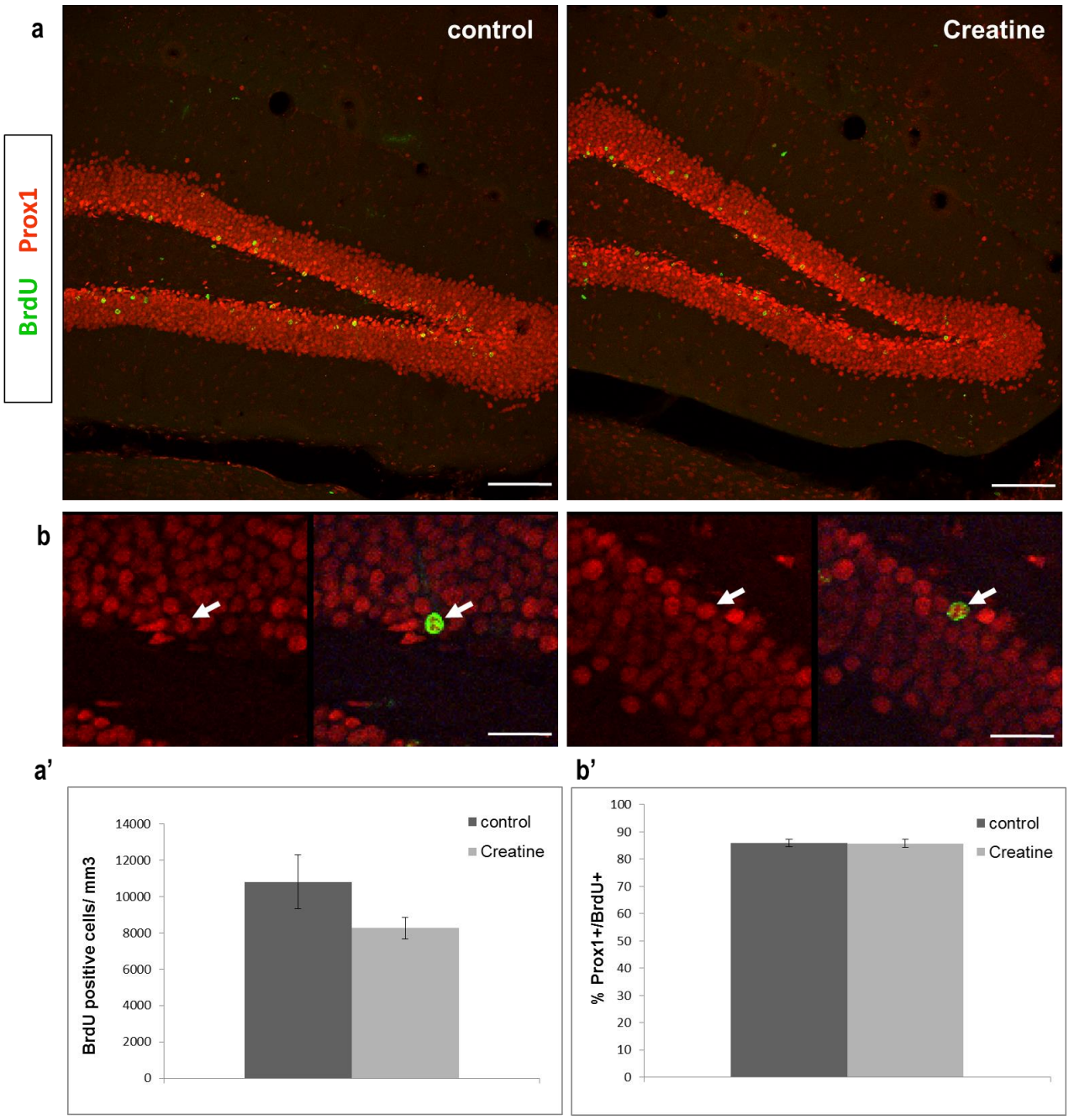

Figure 2-26 Effects of creatine supplemented diet on survival and cellular phenotype:
a Representative confocal images showing immunohistochemistry for BrdU and Prox1, at 28 dpi. Scale bar 100 µm. ***a'*** Quantification of cell survival by determination of number of BrdU positive cells at 28 dpi. ***b*** Higher resolution of representative confocal images showing immunohistochemistry for BrdU and Prox1, at 28 dpi. Arrows indicate cells that are positive for BrdU and Prox1. Scale bar 25 µm. ***b'*** Quantification of cell fate by determination of percentage of Prox1 positive among BrdU positive cells. Significance levels were assessed with Student's T-test with unpaired samples and unequal variances. n=50 cells from 3 different animals. All error bars represent ± SEM.

2.5. Sox11 as a potential regulator of mitochondrial distribution and biogenesis during adult hippocampal neurogenesis

The next question that was addressed is how increase of mitochondrial biogenesis and distribution are regulated during adult hippocampal neurogenesis. Since the transcription factor Sox11 has been shown to be expressed in precursor cells committed to the neuronal lineage, but not in mature granule neurons (Haslinger et al., 2009), and that it has been recently proven that Sox11 is indispensable for neuronal differentiation (Mu et al., 2012), I hypothesized that Sox11 could also play a role in regulation of adaptations of the mitochondrial compartment during the maturation of newborn neurons.

2.5.1. Expression profiling of neural stem cells after Sox4/11 mice loss-of-function

It has already been proven before, that loss of function of Sox4/11 in neurospheres derived from neurogenic niches in the adult mouse brain leads to an impairment of differentiation (Mu et al., 2012). However, what gene expression is directly affected by the loss of SoxC transcription factors remains unclear. In order to identify, which genes are directly regulated by SoxC transcription factors, transcription analysis of control and SoxC deficient neural stem cells was performed. Neurospheres were isolated from hippocampus and SVZ from cKO animals and expanded. To proof neural stem cell identity, differentiation assay was performed by disseminating cells on coated plates and leaving them for 4 days without proliferation factors. As depicted in Figure 2-27, isolated neurospheres are multipotent since they are capable to differentiate into both neuronal and astrocytic lineage, indicated by the expression of DCX and Map2a+b or GFAP, respectively.

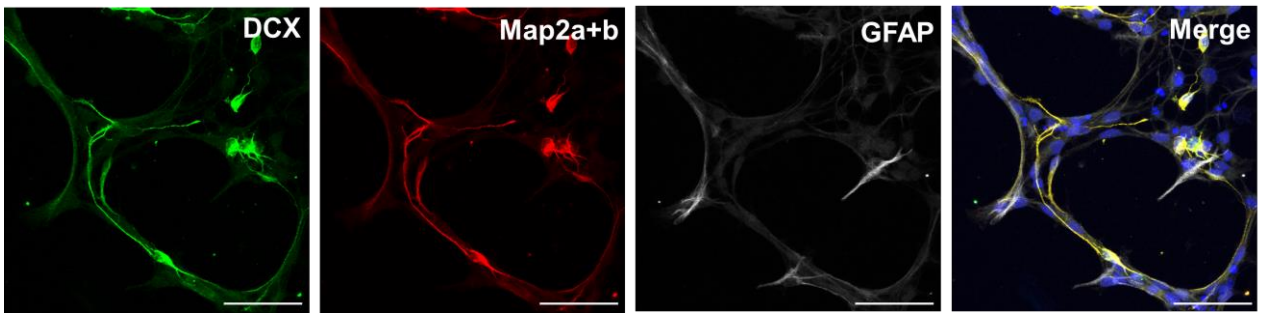

Figure 2-27 Neurospheres isolated from hippocampus and SVZ of cKO Sox4/11 animals have multipotent neural stem cell properties:

Immunocytochemistry of neuronal markers DCX and Map2a+b and the Glia marker GFAP indicate that isolated neurospheres are capable to differentiate into both neurons and astrocytes after 4 days differentiation.

In the present study, Sox4/11 KO in the NSC was induced by protein transduction of a HTN-Cre protein. The optimal concentration of the HTN-Cre that allows highly efficient recombination without toxic effects of the Cre protein has previously been determined (Doberauer, 2013). KO of Sox11 was confirmed by detection of mRNA levels via qPCR (Figure 2-28).

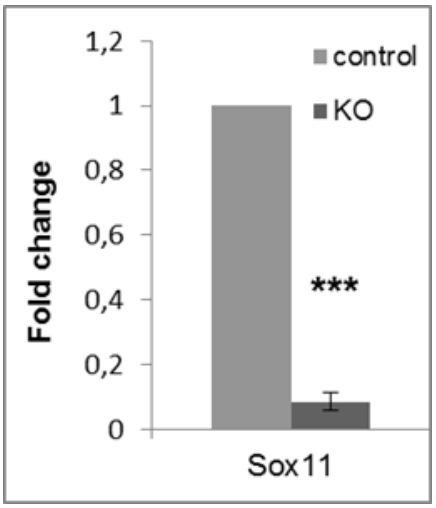

Figure 2-28 Confirmation of Sox11 knock out in HTN-Cre transduced NSC:
Normalized Sox11 transcription levels were significantly reduced (Relative fold change 0.09 ± 0.03) compared to control after double knock out.

The integrity of isolated mRNAs was determined via Bioanalyzer (RIN values of all samples were 8.4 or higher). Further quality checks proved the fulfillment of required standards, with regards to array metrics (signal distribution) and sample clustering according to the genotype (data not shown). The statistical analysis using the Student's T-test in combination with the Benjamini-Hochberg multiple testing correction (false discovery rate < 10%), revealed 1160 probe sets with expression values which were significantly altered with a relative fold change of > 1.5 - 296 of these were altered by a relative fold change of > 2, (see the heat map in Figure 2-29). The identity of the more than 2 fold regulated genes is listed in Table 6. Supporting information with respect to more detailed information and the values of all other probe sets is provided in the Appendix.

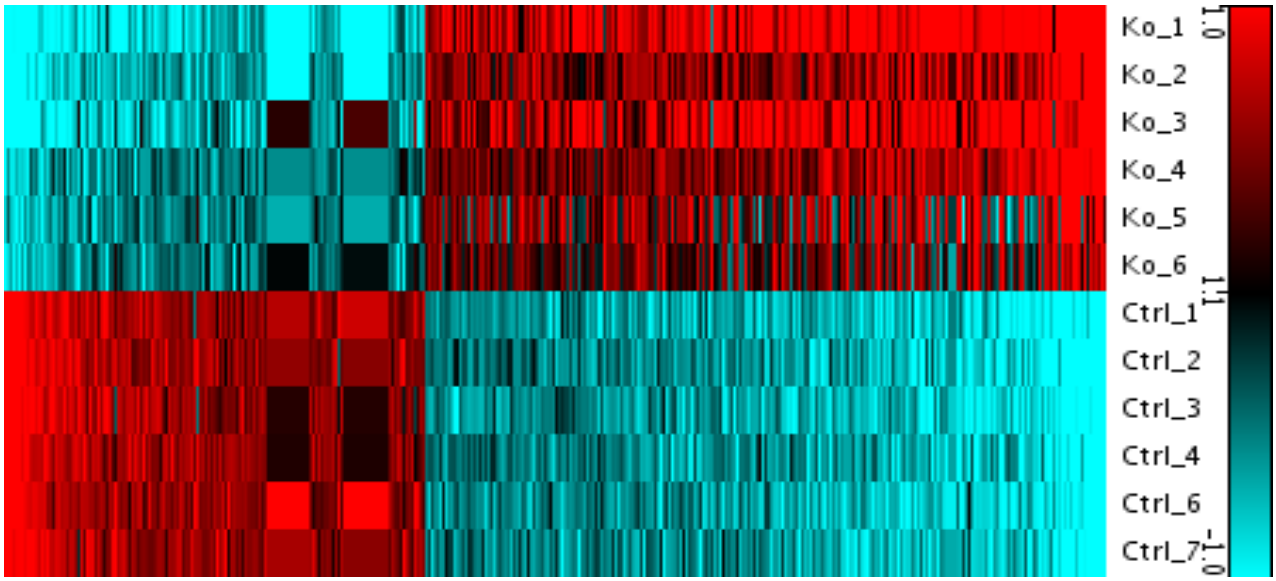

Figure 2-29 Heat map represents expression values:
296 significant probe sets with a FDR < 10% and fold changes > 2x; Red indicates higher, blue indicates lower expression.

Table 6 296 significant differentially regulated probe sets with FDR < 10% and fold changes > 2x

Gene symbol	Gene Description	FC, significant FDR<10%, FC>2x (296)
Kit	kit oncogene	-6,21
C1ql1	complement component 1, q subcomponent-like 1	-5,70
Dcx	doublecortin	-5,66
Tubb3	tubulin, beta 3 class III	-4,94
Tmeff1	transmembrane protein with EGF-like and two follistatin-like domains 1	-4,93
Gpr149	G protein-coupled receptor 149	-4,84
Pcdhb2	protocadherin beta 2	-4,57
Cd24a	CD24a antigen	-4,04
Pdgfra	platelet derived growth factor receptor, alpha polypeptide	-3,85
E130309F12Rik	RIKEN cDNA E130309F12 gene	-3,71
Pcdhb3	protocadherin beta 3	-3,53
Pcgf2	polycomb group ring finger 2	-3,35
3110035E14Rik	RIKEN cDNA 3110035E14 gene	-3,33
Mex3a	mex3 homolog A (C. elegans)	-3,31
Mex3b	mex3 homolog B (C. elegans)	-3,17
Stmn4	stathmin-like 4	-3,14
Sept3	septin 3	-3,12
Zfp804a	zinc finger protein 804A	-3,12
Cd24a	CD24a antigen	-3,08
Gabbr2	gamma-aminobutyric acid (GABA) B receptor, 2	-2,96
Tmeff1	transmembrane protein with EGF-like and two follistatin-like domains 1	-2,96
Gpr17	G protein-coupled receptor 17	-2,88
Dhrs3	dehydrogenase/reductase (SDR family) member 3	-2,85
Adamts5	a disintegrin-like and metallopeptidase (reprolysin type) with thrombospondin type 1 motif, 5 (aggrecanase-2)	-2,83
Fnbp1l	formin binding protein 1-like	-2,80
Zfp773	zinc finger protein 773	-2,80
Mir99a	microRNA 99a	-2,79
LOC100862467	uncharacterized LOC100862467	-2,75
Emp1	epithelial membrane protein 1	-2,69
Tub	tubby candidate gene	-2,66

Gene symbol	Gene Description	FC, significant FDR<10%, FC>2x (296)
Tmem100	transmembrane protein 100	-2,62
Zfp711	zinc finger protein 711	-2,56
Pcdhb10	protocadherin beta 10	-2,55
Samd14	sterile alpha motif domain containing 14	-2,52
Grik3	glutamate receptor, ionotropic, kainate 3	-2,51
Fxyd1	FXYD domain-containing ion transport regulator 1	-2,51
Fxyd6	FXYD domain-containing ion transport regulator 6	-2,49
D0H4S114	DNA segment, human D4S114	-2,48
Sparcl1	SPARC-like 1	-2,47
ENSMUST00000101859		-2,46
Panx1	pannexin 1	-2,41
Slc30a10	solute carrier family 30, member 10	-2,39
Crmp1	collapsin response mediator protein 1	-2,37
Sncaip	synuclein, alpha interacting protein (synphilin)	-2,37
Zfp68	zinc finger protein 68	-2,37
Mir9-2	microRNA 9-2	-2,37
Tubb4a	tubulin, beta 4A class IVA	-2,37
2610109H07Rik	RIKEN cDNA 2610109H07 gene	-2,36
ENSMUST00000174039		-2,36
Sh3gl3	SH3-domain GRB2-like 3	-2,35
Cxxc4	CXXC finger 4	-2,35
Sox11	SRY-box containing gene 11	-2,34
Zfp81	zinc finger protein 81	-2,31
Slc1a1	solute carrier family 1 (neuronal/epithelial high affinity glutamate transporter, system Xag), member 1	-2,31
Dcc	deleted in colorectal carcinoma	-2,31
Ina	internexin neuronal intermediate filament protein, alpha	-2,29
Pcdh11x	protocadherin 11 X-linked	-2,28
Pcdhb9	protocadherin beta 9	-2,28
Rph3a	rabphilin 3A	-2,27
Il17rd	interleukin 17 receptor D	-2,26
Epb4.1	erythrocyte protein band 4.1	-2,26
6330403K07Rik	RIKEN cDNA 6330403K07 gene	-2,26
Chd3	chromodomain helicase DNA binding protein 3	-2,24
Mllt11	myeloid/lymphoid or mixed-lineage leukemia (trithorax homolog, Drosophila); translocated to, 11	-2,24
Gjd2	gap junction protein, delta 2	-2,23
Ivns1abp	influenza virus NS1A binding protein	-2,23
Rbm15b	RNA binding motif protein 15B	-2,22
ENSMUST00000163719		-2,21
Zfp942	zinc finger protein 942	-2,21
Chd3	chromodomain helicase DNA binding protein 3	-2,19
Myo1b	myosin IB	-2,18
Hist3h2ba	histone cluster 3, H2ba	-2,18
Dennd5b	DENN/MADD domain containing 5B	-2,17
Helt	helt bHLH transcription factor	-2,17
Hes5	hairy and enhancer of split 5 (Drosophila)	-2,16
Mir1905	microRNA 1905	-2,16
Bcl11a	B cell CLL/lymphoma 11A (zinc finger protein)	-2,16
Rnf165	ring finger protein 165	-2,15
Eepd1	endonuclease/exonuclease/phosphatase family domain containing 1	-2,15
Gsx1	GS homeobox 1	-2,14
Dchs1	dachsous 1 (Drosophila)	-2,14
Apcdd1	adenomatosis polyposis coli down-regulated 1	-2,13
Nap1l2	nucleosome assembly protein 1-like 2	-2,13
Pygo1	pygopus 1	-2,11
ENSMUST00000134226		-2,11
Zfp566	zinc finger protein 566	-2,11

Gene symbol	Gene Description	FC, significant FDR<10%, FC>2x (296)
Shisa9	shisa homolog 9 (Xenopus laevis)	-2,11
Nsg1	neuron specific gene family member 1	-2,10
Ptbp2	polypyrimidine tract binding protein 2	-2,09
Fam60a	family with sequence similarity 60, member A	-2,09
Vps72	vacuolar protein sorting 72 (yeast)	-2,09
Rnf138	ring finger protein 138	-2,09
Vcan	versican	-2,08
Snord116	small nucleolar RNA, C/D box 116	-2,08
D930015E06Rik	RIKEN cDNA D930015E06 gene	-2,07
Atcay	ataxia, cerebellar, Cayman type homolog (human)	-2,06
Cacng4	calcium channel, voltage-dependent, gamma subunit 4	-2,06
D18Ertd653e	DNA segment, Chr 18, ERATO Doi 653, expressed	-2,06
Nkx2-2	NK2 transcription factor related, locus 2 (Drosophila)	-2,06
ENSMUST00000129089		-2,06
Dpysl3	dihydropyrimidinase-like 3	-2,05
Sox4	SRY-box containing gene 4	-2,05
Zik1	zinc finger protein interacting with K protein 1	-2,04
Add2	adducin 2 (beta)	-2,04
Lims2	LIM and senescent cell antigen like domains 2	-2,04
Snord116	small nucleolar RNA, C/D box 116	-2,04
Usp49	ubiquitin specific peptidase 49	-2,04
Gm5124	nucleolar and coiled-body phosphoprotein 1 pseudogene	-2,03
Elovl2	elongation of very long chain fatty acids (FEN1/Elo2, SUR4/Elo3, yeast)-like 2	-2,03
Cacnb3	calcium channel, voltage-dependent, beta 3 subunit	-2,03
ENSMUST00000139835		-2,03
Snord61	small nucleolar RNA, C/D box 61	-2,02
Grin3a	glutamate receptor ionotropic, NMDA3A	-2,02
Ets1	E26 avian leukemia oncogene 1, 5' domain	-2,02
Ranbp6	RAN binding protein 6	-2,01
Slc7a11	solute carrier family 7 (cationic amino acid transporter, y+ system), member 11	-2,01
LOC100862065	uncharacterized LOC100862065	-2,01
Pcbp4	poly(rC) binding protein 4	-2,01
Tuba1c	tubulin, alpha 1C	9,03
Lgals1	lectin, galactose binding, soluble 1	7,57
Gm3417	predicted gene 3417	7,56
Car3	carbonic anhydrase 3	7,53
Tuba1c	tubulin, alpha 1C	7,03
Tmc3	transmembrane channel-like gene family 3	6,79
Ccnb2	cyclin B2	6,59
Ankrd34c	ankyrin repeat domain 34C	6,57
Pbk	PDZ binding kinase	5,55
Trf	transferrin	5,39
Matn2	matrilin 2	5,30
1500015O10Rik	RIKEN cDNA 1500015O10 gene	5,30
Tcte3	t-complex-associated testis expressed 3	5,18
Gas7	growth arrest specific 7	4,90
Tcte3	t-complex-associated testis expressed 3	4,86
Tmem176a	transmembrane protein 176A	4,82
Igfbp2	insulin-like growth factor binding protein 2	4,59
Cox8b	cytochrome c oxidase, subunit VIIIb	4,44
Car3	carbonic anhydrase 3	4,37
ENSMUST00000150239		4,24
Sulf1	sulfatase 1	4,16
Cryab	crystallin, alpha B	4,03
Mki67	antigen identified by monoclonal antibody Ki 67	4,02
ENSMUST00000050763		4,00

Gene symbol	Gene Description	FC, significant FDR<10%, FC>2x (296)
Serpina3n	serine (or cysteine) peptidase inhibitor, clade A, member 3N	3,94
Cdh19	cadherin 19, type 2	3,90
Top2a	topoisomerase (DNA) II alpha	3,89
1190002F15Rik	RIKEN cDNA 1190002F15 gene	3,89
Cdk1	cyclin-dependent kinase 1	3,81
Gfra2	glial cell line derived neurotrophic factor family receptor alpha 2	3,78
Shisa6	shisa homolog 6 (Xenopus laevis)	3,70
Cenpf	centromere protein F	3,67
Leprel1	leprecan-like 1	3,63
Chrdl1	chordin-like 1	3,52
Cryab	crystallin, alpha B	3,47
Ptgds	prostaglandin D2 synthase (brain)	3,46
Tubb6	tubulin, beta 6 class V	3,46
ENSMUST00000161614		3,46
Igfbp3	insulin-like growth factor binding protein 3	3,43
Ecm1	extracellular matrix protein 1	3,35
Ogn	osteoglycin	3,34
2210404J11Rik	RIKEN cDNA 2210404J11 gene	3,31
Gas2l3	growth arrest-specific 2 like 3	3,30
Cd109	CD109 antigen	3,28
Cacng5	calcium channel, voltage-dependent, gamma subunit 5	3,25
E2f8	E2F transcription factor 8	3,23
Adm	adrenomedullin	3,17
9030025P20Rik	RIKEN cDNA 9030025P20 gene	3,16
Rab3b	RAB3B, member RAS oncogene family	3,14
Itga4	integrin alpha 4	3,10
Angpt2	angiopoietin 2	3,09
Mmp19	matrix metallopeptidase 19	3,07
Lgi3	leucine-rich repeat LGI family, member 3	3,06
Gadd45b	growth arrest and DNA-damage-inducible 45 beta	3,04
Gpr126	G protein-coupled receptor 126	3,02
Ckap2	cytoskeleton associated protein 2	3,02
2210404J11Rik	RIKEN cDNA 2210404J11 gene	3,01
Igfbp7	insulin-like growth factor binding protein 7	2,97
Rtn4rl1	reticulon 4 receptor-like 1	2,96
Cybrd1	cytochrome b reductase 1	2,95
Hspb8	heat shock protein 8	2,94
Ccnd2	cyclin D2	2,89
Mctp1	multiple C2 domains, transmembrane 1	2,88
Hist2h3c2	histone cluster 2, H3c2	2,87
Arpc1b	actin related protein 2/3 complex, subunit 1B	2,86
1110008P14Rik	RIKEN cDNA 1110008P14 gene	2,85
Anln	anillin, actin binding protein	2,84
Mef2c	myocyte enhancer factor 2C	2,83
Hist2h3b	histone cluster 2, H3b	2,81
Gas7	growth arrest specific 7	2,80
Tle6	transducin-like enhancer of split 6, homolog of Drosophila E(spl)	2,79
Smpdl3b	sphingomyelin phosphodiesterase, acid-like 3B	2,79
Olfm2	olfactomedin 2	2,76
Rhoj	ras homolog gene family, member J	2,72
Apln	apelin	2,71
9030617O03Rik	RIKEN cDNA 9030617O03 gene	2,67
Ehd2	EH-domain containing 2	2,66
Pcolce	procollagen C-endopeptidase enhancer protein	2,66
Cpne8	copine VIII	2,63
B4galt5	UDP-Gal:betaGlcNAc beta 1,4-galactosyltransferase, polypeptide 5	2,62
Slc27a6	solute carrier family 27 (fatty acid transporter), member 6	2,62
Tacc3	transforming, acidic coiled-coil containing protein 3	2,61

Gene symbol	Gene Description	FC, significant FDR<10%, FC>2x (296)
Rab38	RAB38, member of RAS oncogene family	2,60
Clstn2	calsyntenin 2	2,59
Mad2l1	MAD2 mitotic arrest deficient-like 1	2,55
Vwa5b1	von Willebrand factor A domain containing 5B1	2,50
Igfbp4	insulin-like growth factor binding protein 4	2,47
Hist1h2bc	histone cluster 1, H2bc	2,47
Ccnd1	cyclin D1	2,47
Gfpt2	glutamine fructose-6-phosphate transaminase 2	2,46
Arsb	arylsulfatase B	2,44
Rasl11a	RAS-like, family 11, member A	2,44
Camk2b	calcium/calmodulin-dependent protein kinase II, beta	2,43
Sod3	superoxide dismutase 3, extracellular	2,42
Il1r1	interleukin 1 receptor, type I	2,39
Cdkn3	cyclin-dependent kinase inhibitor 3	2,39
Lpo	lactoperoxidase	2,37
Timp1	tissue inhibitor of metalloproteinase 1	2,37
Psmb9	proteasome (prosome, macropain) subunit, beta type 9 (large multifunctional peptidase 2)	2,36
Pttg1	pituitary tumor-transforming gene 1	2,35
Zfp36	zinc finger protein 36	2,34
Grb14	growth factor receptor bound protein 14	2,33
Mest	mesoderm specific transcript	2,33
Ctsc	cathepsin C	2,32
Mboat1	membrane bound O-acyltransferase domain containing 1	2,31
Tmem176b	transmembrane protein 176B	2,31
D2Ertd750e	DNA segment, Chr 2, ERATO Doi 750, expressed	2,31
Cebpd	CCAAT/enhancer binding protein (C/EBP), delta	2,29
Ncapd2	non-SMC condensin I complex, subunit D2	2,29
Pmp22	peripheral myelin protein 22	2,29
Gm19522	predicted gene, 19522	2,28
Gabra2	gamma-aminobutyric acid (GABA) A receptor, subunit alpha 2	2,28
Ddx39b	DEAD (Asp-Glu-Ala-Asp) box polypeptide 39B	2,28
Psrc1	proline/serine-rich coiled-coil 1	2,28
BC031470		2,27
Clybl	citrate lyase beta like	2,27
Nampt	nicotinamide phosphoribosyltransferase	2,26
Ptp4a3	protein tyrosine phosphatase 4a3	2,26
A430110N23Rik	RIKEN cDNA A430110N23 gene	2,25
Rpe65	retinal pigment epithelium 65	2,24
Plscr2	phospholipid scramblase 2	2,24
4922501L14Rik	RIKEN cDNA 4922501L14 gene	2,23
Net1	neuroepithelial cell transforming gene 1	2,23
Parp3	poly (ADP-ribose) polymerase family, member 3	2,22
Mns1	meiosis-specific nuclear structural protein 1	2,22
Tspan17	tetraspanin 17	2,21
Mxra7	matrix-remodelling associated 7	2,20
Pde3a	phosphodiesterase 3A, cGMP inhibited	2,20
Cobll1	Cobl-like 1	2,19
Kitl	kit ligand	2,16
Cacna2d3	calcium channel, voltage-dependent, alpha2/delta subunit 3	2,16
Barx2	BarH-like homeobox 2	2,15
Fos	FBJ osteosarcoma oncogene	2,15
Cenpp	centromere protein P	2,15
Gpd1	glycerol-3-phosphate dehydrogenase 1 (soluble)	2,14
Arsb	arylsulfatase B	2,14
Shisa3	shisa homolog 3 (Xenopus laevis)	2,13
Gem	GTP binding protein (gene overexpressed in skeletal muscle)	2,13
Neat1	nuclear paraspeckle assembly transcript 1 (non-protein coding)	2,12

Gene symbol	Gene Description	FC, significant FDR<10%, FC>2x (296)
Mcm2	minichromosome maintenance deficient 2 mitotin (S. cerevisiae)	2,12
Ctsh	cathepsin H	2,12
Fndc1	fibronectin type III domain containing 1	2,11
Gamt	guanidinoacetate methyltransferase	2,11
C1rb	complement component 1, r subcomponent B	2,11
Chrna4	cholinergic receptor, nicotinic, alpha polypeptide 4	2,10
Iqgap1	IQ motif containing GTPase activating protein 1	2,10
Igtp	interferon gamma induced GTPase	2,10
Lix1	limb expression 1 homolog (chicken)	2,10
Nrn1	neuritin 1	2,10
Cp	ceruloplasmin	2,10
Phyhd1	phytanoyl-CoA dioxygenase domain containing 1	2,10
Pex5l	peroxisomal biogenesis factor 5-like	2,10
H2-Q7	histocompatibility 2, Q region locus 7	2,09
Sfxn1	sideroflexin 1	2,09
Anxa5	annexin A5	2,08
Ephx1	epoxide hydrolase 1, microsomal	2,07
LOC100862515	TBC1 domain family member 1-like	2,07
Tle2	transducin-like enhancer of split 2, homolog of Drosophila E(spl)	2,07
Slc44a1	solute carrier family 44, member 1	2,06
Dgat2	diacylglycerol O-acyltransferase 2	2,06
Tlr4	toll-like receptor 4	2,05
Chst2	carbohydrate sulfotransferase 2	2,05
ENSMUST00000173249		2,05
Pllp	plasma membrane proteolipid	2,05
Acy3	aspartoacylase (aminoacylase) 3	2,05
Wee1	WEE 1 homolog 1 (S. pombe)	2,04
Mef2c	myocyte enhancer factor 2C	2,03
4632434I11Rik	RIKEN cDNA 4632434I11 gene	2,03
Cmpk2	cytidine monophosphate (UMP-CMP) kinase 2, mitochondrial	2,03
Junb	Jun-B oncogene	2,03
E130203B14Rik	RIKEN cDNA E130203B14 gene	2,02
Itga1	integrin alpha 1	2,02
Npl	N-acetylneuraminate pyruvate lyase	2,01
5031439G07Rik	RIKEN cDNA 5031439G07 gene	2,01
Grm5	glutamate receptor, metabotropic 5	2,01
S100a4	S100 calcium binding protein A4	2,01
Pros1	protein S (alpha)	2,01

With respect to the mitochondria none of the anticipated candidate proteins known to be involved in mitochondrial biogenesis, for instance PGC-1α or Tfam, or involved in mitochondrial distribution such as Drp1 or the mitochondrial trafficking protein Miro1 was among the significantly regulated probe sets. However transcription levels of PolG, the mitochondrial polymerase was significantly reduced (-1.41). Since PolG is conducting replication of mtDNA and hence contributes to mitochondrial biogenesis, this raises the question if Sox11 is involved in regulation of mitochondrial mass *in vivo*. Even more intriguing, a fair amount of cytoskeleton proteins, such as tubulin beta 5 class I (Tubb5, -1.76), tubulin beta 3 class III (Tubb3, -4.9), tubulin beta 6 class V (Tubb6, 3.5), tubulin beta 4A class IVA (Tubb4a, -2.4) and tubulin alpha 1C (Tuba1c, 9.03) appeared to be

significantly up or down regulated, with some of them being among those genes which transcription levels were modified most. The robustness of these changes could be confirmed by determination of the respective fold change of expression levels by quantitative PCR: PolG 0.6 fold, Tubb5 0.3 fold, Tubb3 0.3 fold, Tubb6 4.8 fold, Tubb4a 0.2 fold and Tuba1c 1.9 fold (Figure 2-30). Since mitochondrial transport is highly dependent on the microtubule network, alterations within this network might affect mitochondrial distribution *in vivo*.

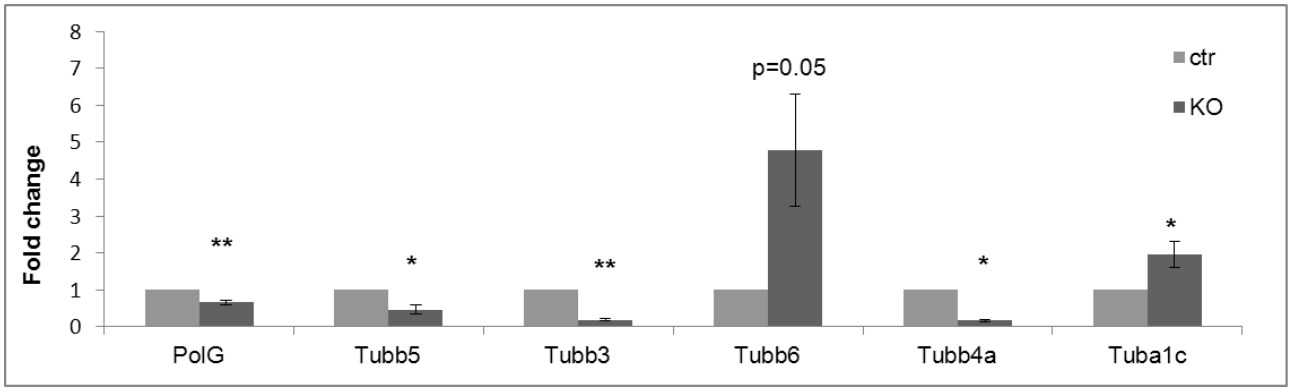

Figure 2-30 Confirmation of selected differentially regulated probe sets via qPCR:
The robustness of the results from the micro array for selected differentially regulated probe sets was confirmed via qPCR for PolG, Tubb5, Tubb3 Tubb6, Tubb4a and Tuba1c.

2.5.2. Loss-of-function of Sox4 and Sox11 impairs differentiation of dentate gyrus granule neurons and potentially affects the mitochondrial compartment

Next, I investigated the effects after loss-of-function of SoxC transcription factors on mitochondrial content and distribution *in vivo*. It has been demonstrated that Sox4 and Sox11, two members of the SoxC transcription factor family, exhibit a similar expression pattern in the dentate gyrus, which is restricted to neuronally committed immature newborn granule neurons (Mu et al., 2012). Thus, the mitochondria compartment was analyzed after double knock out of both transcription factors to exclude the possibility of compensatory effects due to redundant functions. Conditional KO mice, containing floxed alleles encoding for Sox4 and Sox11 were stereotactically injected with a mixture of GFP IRES Cre and mitoDsred viruses, to induce the KO specifically in transduced cells and to visualize mitochondria at the same time. Littermates, injected with GFP only and mitoDsred viruses were used as controls. At 5 dpi transduced highly amplifying neural precursor cells are characterized by a horizontal morphology with most of the cells composing of the soma. Analyses of mitochondria mass normalized to the volume of the soma revealed a significant reduction of mitochondrial content in Sox4/Sox11 KO cells (ctr 0.06 ± 0.004 $\mu m^3/\mu m^3$, KO ctr 0.04 ± 0.005 $\mu m^3/\mu m^3$; $p<0.05$) (Figure 2-31), suggesting that SoxC transcription factors are involved in the regulation of mitochondrial biogenesis.

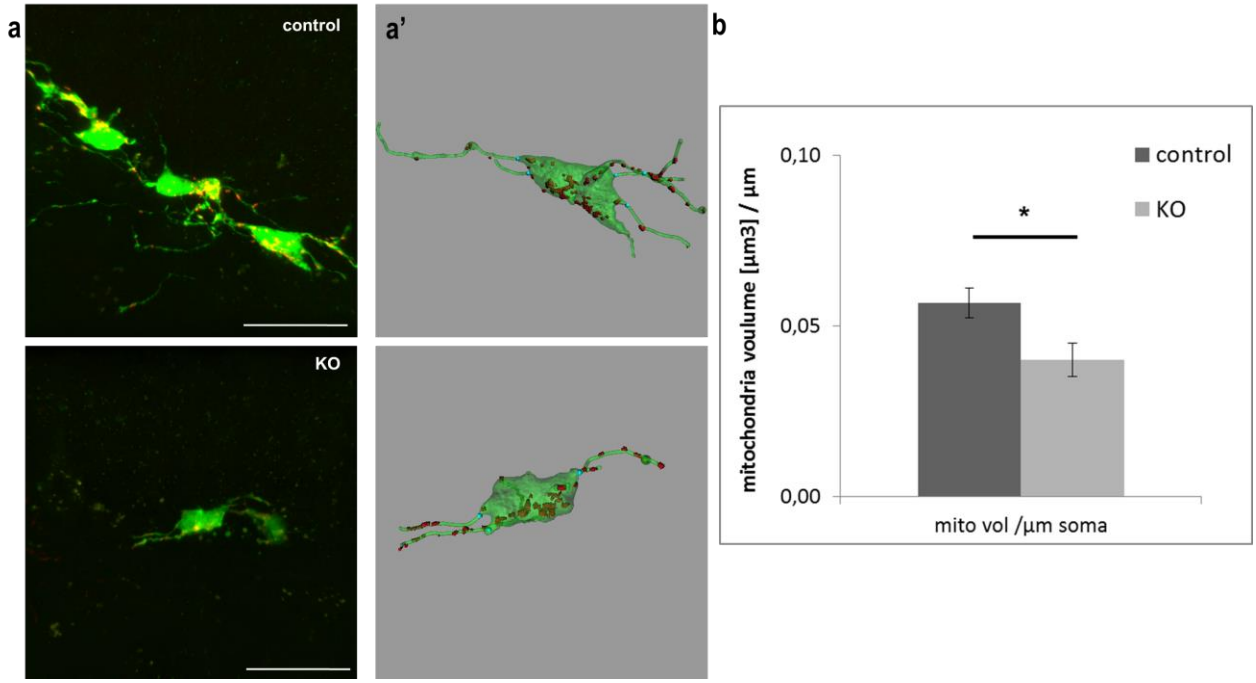

Figure 2-31 Sox4/Sox11 KO cells display a reduction of mitochondria content at 5 dpi
a Representative confocal images of a mitoDsred (red) and GFP (green) transduced cell in the mouse dentate gyrus at 5 dpi. Cre is bicistronically expressed with GFP in KO cells. Scale bar 25 µm. ***a'*** 3-D reconstructions of the cells depicted in a. ***b*** Quantification of mitochondrial mass normalized to the soma volume reveals a significant decrease of mitochondrial content after Sox4/11 KO. Scale bars 25 µm; n=12 transduced cells from 3 different animals; error bars represent ± SEM; Significance levels were assessed with Student's T-test with unpaired samples and unequal variances.

To evaluate this hypothesis further the time point 12 dpi was analyzed next. It was very obvious that cell morphology at this time point was completely different between control cells and KO cells. As expected, most of transduced control cells had committed to the neuronal lineage (79 ± 3%), identified by neuronal morphology with an apical dendritic tree towards the ML, and almost all remaining control cells developed a star-shaped morphology (20 ± 3%). In contrast, cells with neuronal morphology were largely absent among KO cells (3 ± 0%, $p<0.001$), and a significant higher proportion of star-shaped cells was detected among these cells (55 ± 1%; $p<0.01$). The most intriguing finding was the appearence of cells, being neither neuronal nor star-shaped (ctr 1 ± 1%, KO 42 ± 2%; $p<0.001$). These cells were termed amorphous cells. This population was almost exclusively located in the subgranular cell layer (SGZ) or adjacent to the SGZ in the hilus. In the following the phenotype of the Sox4/11 KO cells was determined. Among control (88 ± 8%) and KO (98 ± 2%) cells, most of the star-shaped cells were positive for the NSC and glial marker Sox2. Amorphous cells, which were almost exclusively found in the KO condition, were also Sox2 positive (97 ± 3%). Cells that displayed neuronal-like morphology among control cells were Sox2 negative without exception (100 ± 0%). Strikingly, the few neuronal-like KO cells, frequently expressed Sox2 (44 ± 29%), indicating that even in the cells with neuronal morphology Sox4/11 KO had interfered

with the neuronal differentiation program. To further characterize the phenotype of star-shaped and amorphous cells, the expression of specific glia markers was investigated. Star-shaped cells in control and KO conditions were almost all positive for the oligodendrocytic marker Sox10 (ctr 98 ± 2%, KO 96 ± 4%), but were negative for the astrocytic marker GFAP (ctr 0 ± 0%, KO 4 ± 4%). In contrast, a high proportion of cells displaying an amorphous morphology, both among control and KO cells, were astrocytes indicated by the expression of GFAP (ctr 100% n=1, KO 78 ± 14%) (Figure 2-33). These findings strongly suggest that Sox4/11 KO induces a fate switch towards an astrocyte-like phenotype. Since cell morphology of control and KO cells was very heterogeneous, a quantitative assessment of the mitochondrial compartment at 12 dpi was not appropriate. Mitochondria morphology turned out to be heavily dependent on the cell type. For instance, mitochondrial appearance in Sox10 positive oligodendrocytes was very fragmented and dispersed within the subtle cellular extensions. In contrast, amorphous cells were characterized by mitochondria that seemed to be more fused and agglomerated (Figure 2-32). Neurons, consistent to what was shown before (Figure 2-2) had clustered mitochondria in and close to the soma, but smaller and dispersed mitochondria in the peripheral dendrites.

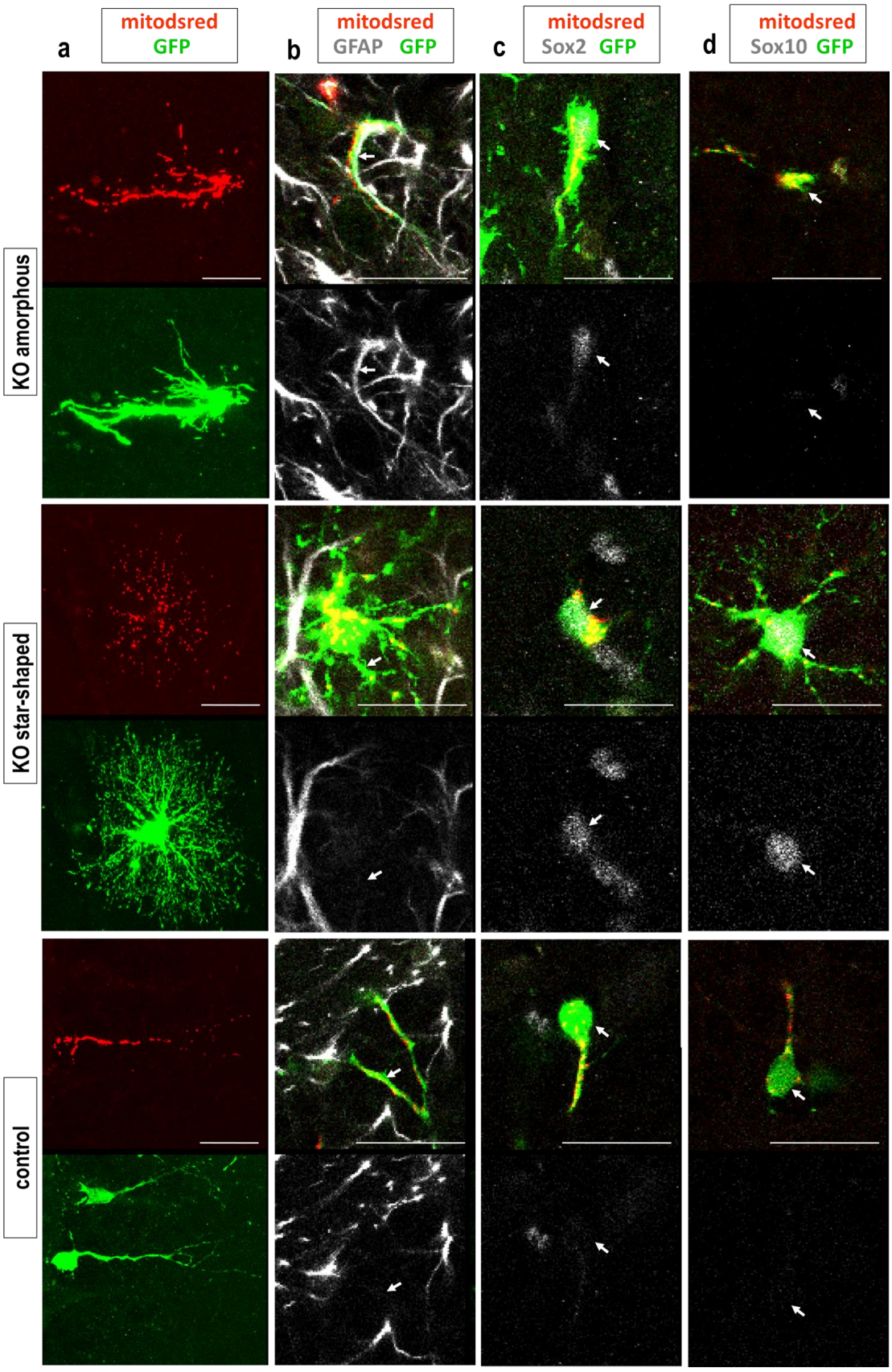

Figure 2-32 Sox4/Sox11 KO induces fate switch at 12 dpi and the mitochondrial compartment appears heavily dependent on cell type:
a Representative confocal images of mitoDsred (red) and GFP (green) transduced cells in the mouse dentate gyrus at 12 dpi, indicating various cell morphologies and differences in mitochondrial appearance. Cre is bicistronically expressed with GFP in KO cells. Scale bar 25 µm. ***b-d*** Single layer confocal images of double transduced cells showing GFAP (*b*), Sox2 (*c*) and Sox10 (*d*) expression in control cells (neurons) and KO cells (star-shaped and amorphous). Scale bars 25 µm.

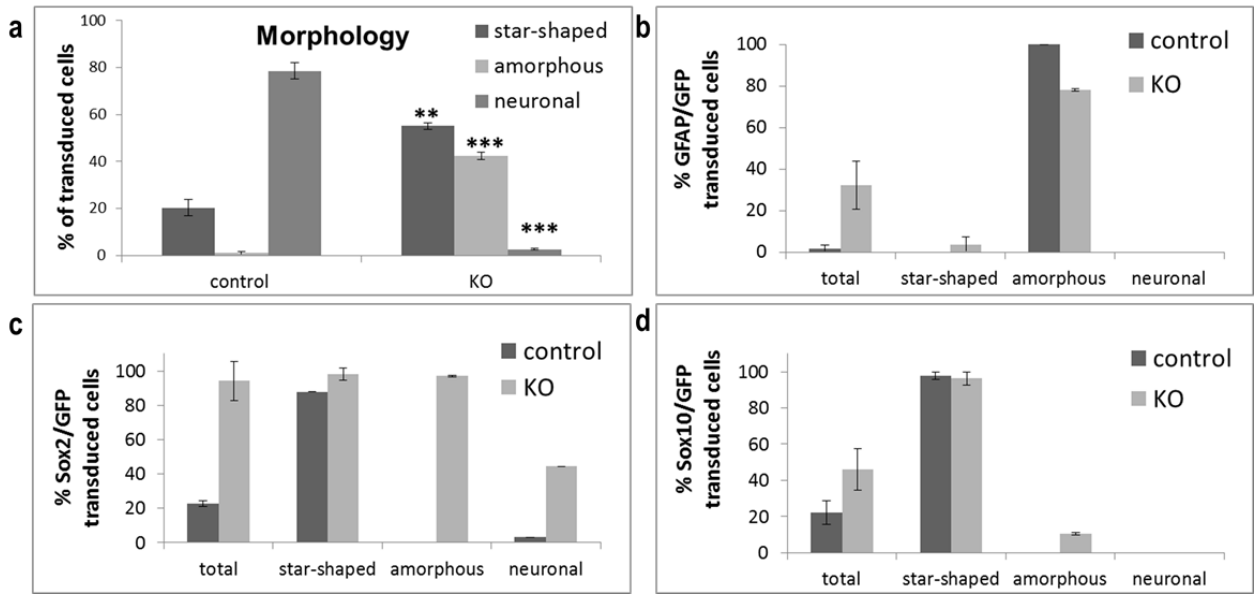

Figure 2-33 Sox4/Sox11 KO induces fate switch at 12 dpi and the mitochondrial compartment appears heavily dependent on cell type:
a Quantitative assessment of different cell morphologies among ctr and KO cells. ***b-d*** Quantitative evaluation of marker expression among different cell types for GFAP (*b*), Sox2 (*c*) and Sox10 (*d*). At least n=25 transduced cells from 3 different animals; error bars represent ± SEM; Significance levels were assessed with Student's T-test with unpaired samples and unequal variances.

2.5.3. Sox11 overexpression impairs mitochondrial distribution concomitantly with defects in maturation of adult newborn hippocampal neurons

In the next set of experiments mitochondria were assessed in developing neurons after gain-of-function of Sox11 mediated by viral transduction. This was performed via stereotactic injection of a combination of one retrovirus encoding for GFP bicistronically expressed with the Sox11 transgene and a second retrovirus encoding for mitoDsred to visualize mitochondria. Controls were injected with a combination of the empty GFP virus and mitoDsred virus. Animals were housed with unlimited access to running wheels, to maximize the amount of analyzable cells. First, the 21 dpi time point was analyzed, which is characterized by a gradual switch from the immature to the mature stage and down regulation of Sox11 in newborn neurons (Haslinger et al., 2009). Analysis of the morphology of double-transduced newborn neurons revealed that cellular growth is significantly delayed among Sox11 overexpressing neurons at 21 dpi (ctr 1110 ± 63 µm, Sox11 437 ± 59 µm; $p<0.001$). Consistently, number of branching points (ctr 11 ± 1; Sox11 8 ± 1; $p<0.05$) and cellular complexity, represented by a decreased of number of Sholl intersections, were also reduced (Figures 2-34 and Figure 2-35).

Next, I studied the effects of Sox11 overexpression on mitochondrial content and distribution. The total mitochondrial content per cell was decreased in Sox11 overexpressing cells (Table 7). Given that Sox11 overexpressing neurons displayed greatly reduced cell size, mitochondrial volume and number were related to the cell size. This analysis revealed that the mitochondrial density in Sox11 overexpressing neurons was indeed higher compared to control neurons (Table 7). The density of mitochondria within more distal dendritic segments however appeared to be decreased. Overall these results indicate that coordination of mitochondrial biogenesis and distribution with morphological development is perturbed by Sox11 overexpression (Table 7, Figure 2-34 and Figure 2-35).

Table 7 Quantitative assessment of the effects after Sox11 overexpression on the mitochondrial compartment at 21 dpi

absolute mitochondrial volume [µm^3]	**control**	**Sox11**	**p-value**
whole cell	202 ± 32	125 ± 13	p<0.05
dendritic tree	143 ± 30	31 ± 5	p<0.01
0-50 µm	59 ± 6	94 ± 9	p<0.01
50-100 µm	70 ± 28	27 ± 4	p=0.1
> 100 µm	73 ± 13	5 ± 2	p<0.001
relative mitochondrial volume [µm^3/µm length]	**control**	**Sox11**	**p-value**
whole cell	0.17 ± 0.02	0.31 ± 0.03	p<0.01
dendritic tree	0.13 ± 0.02	0.10 ± 0.02	p=0.33
0-50 µm	0.75 ± 0.07	1.11 ± 0.13	p<0.05
50-100 µm	0.19 ± 0.06	0.11 ± 0.02	p=0.26
> 100 µm	0.10 ± 0.01	0.06 ± 0.01	p<0.05
% of mitochondrial located per section	**control**	**Sox11**	**p-value**
dendritic tree	65 ± 4	23 ± 2	p<0.001
0-50 µm	35 ± 4	77 ± 2	p<0.001
50-100 µm	29 ± 5	20 ± 2	p=0.1
> 100 µm	37 ± 4	4 ± 1	p>0.001
mitochondrial density [mitochondria / µm length]	**control**	**Sox11**	**p-value**
whole cell	0.26 ± 0.02	0.33 ± 0.02	p>0.05
dendritic tree	0.19 ± 0.02	0.12 ± 0.01	p>0.06
0-50 µm	1.18 ± 0.07	1.19 ± 0.12	p=0.9
50-100 µm	0.18 ± 0.02	0.13 ± 0.01	p>0.05
> 100 µm	0.19 ± 0.02	0.12 ± 0.02	p>0.06

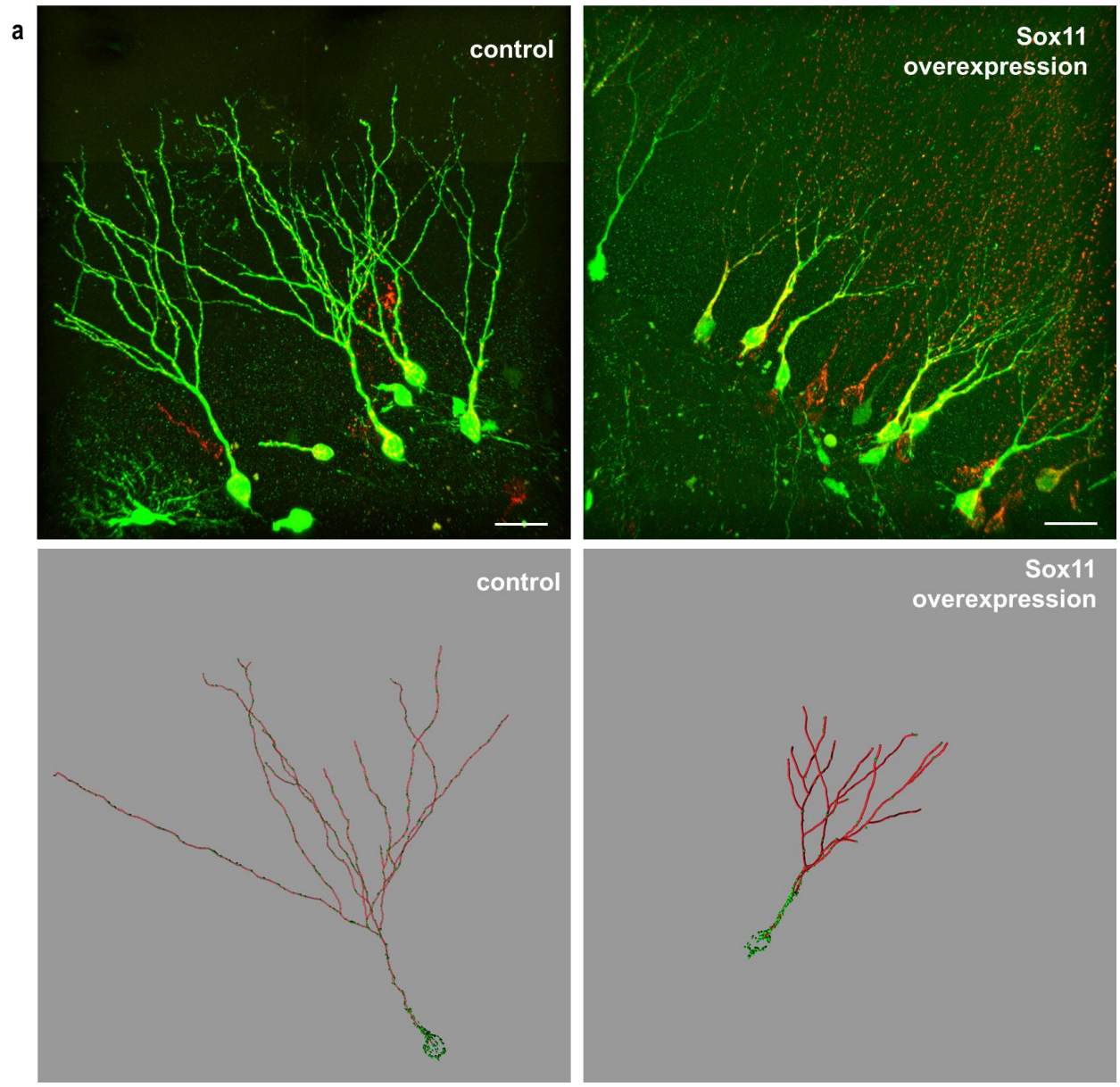

Figure 2-34 Sox11 overexpression delays morphological development but increases relative mitochondrial content at 21 dpi:
a Representative confocal images of a mitoDsred (red) and GFP (green) transduced cell in the mouse dentate gyrus at 21 dpi. Sox11 is bicistronically expressed with GFP. Scale bar 25 µm. ***a'*** 3-D reconstructions of the cells depicted in **a**.

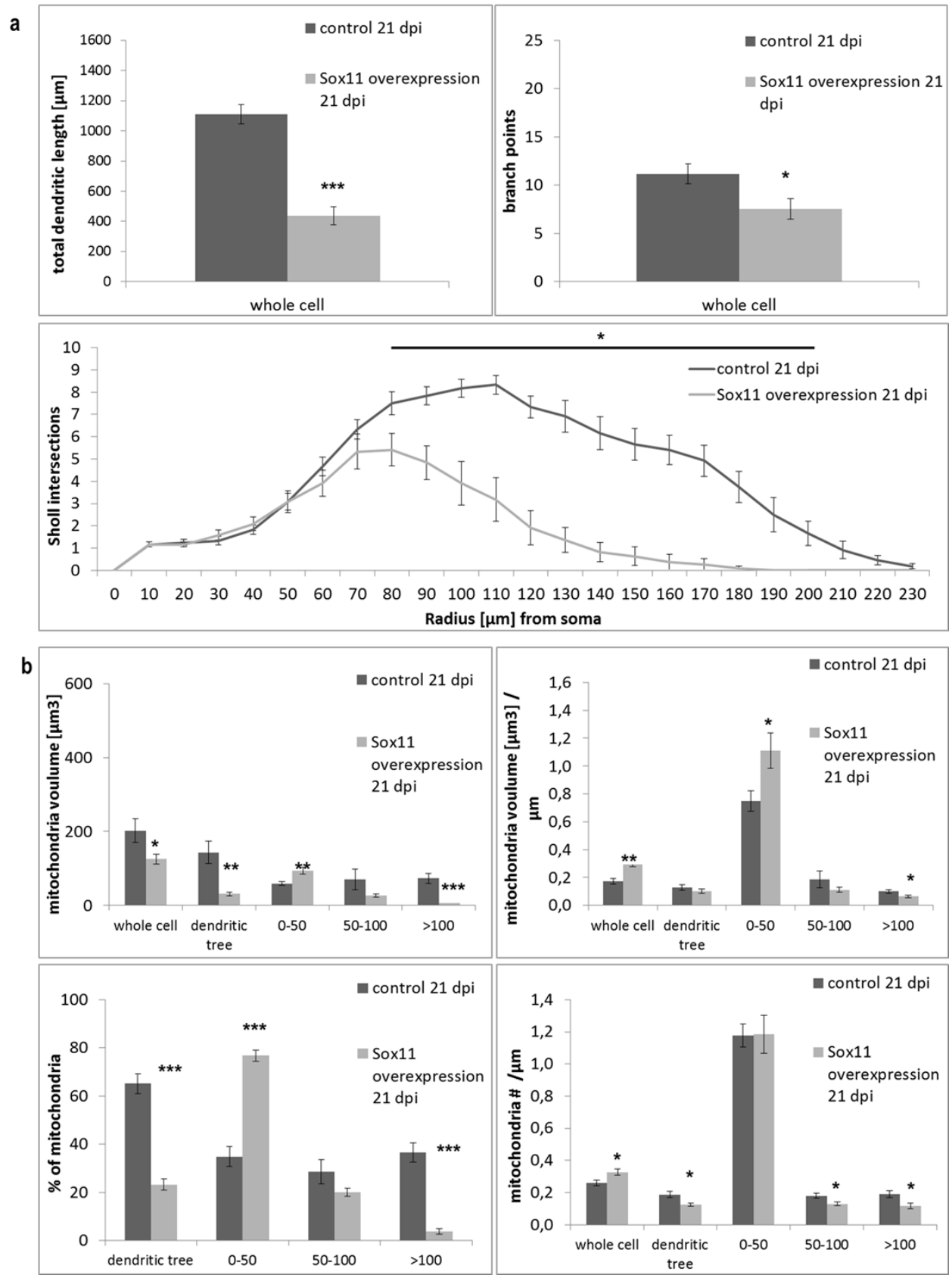

Figure 2-35 Sox11 overexpression delays morphological development but increases relative mitochondrial content at 21 dpi:
a Quantification of total dendritic length and number of dendritic branch points revealed a significant delay in Sox11 overexpressing animals. Sholl analyses (Sholl 1953) showed a significant decrease of number of intersections of Sox11 transduced cells with and without running. ***b*** Quantification of mitochondria mass, density and distribution demonstrated that absolute mitochondrial content and distribution are accordant to the developmental stage of the cells, but relative mitochondrial volume and density are increased in Sox11

overexpressing newborn neurons. Scale bars 25 µm; n=12 neurons from 3 different animals; error bars represent ± SEM; Significance levels were assessed with Student's T-test with unpaired samples and unequal variances.

The effect of Sox11 overexpression on newborn neurons was also investigated at a later time point (42 dpi). Analysis of the morphology indicated at first glance no significant differences between Sox11 transduced neurons and control neurons, as reflected in total dendritic length (ctr 1472 ± 67 µm, Sox11 1438 ± 106 µm) and number of branching points (ctr 10 ± 1; Sox11 9 ± 1). However, analysis of the cellular complexity with the Sholl analysis disclosed significant differences regarding the number of Sholl intersections in different areas: Sox11 overexpressing neurons develop the first branches very close to or even right at the soma, whereas control cells start branching in a greater distance from the soma. This finding may be explained by the fact, that Sox11 overexpressing neurons at 42 dpi are also characterized by wrong positioning in the outer part of the granular cell layer, compared to the positioning of control cells close to the sub granular zone (SGZ) of the dentate gyrus (Doberauer, 2013). Evaluation of the mitochondrial compartment revealed that absolute as well as relative mitochondrial content, and mitochondrial density were reduced among Sox11 transduced neurons. Comparable to the finding about mitochondrial distribution at 21 dpi, at 42 dpi Sox11 overexpressing cells do not accomplish to transport mitochondria at the same level into the dendrites, as observed in control cells. Therefore, a prolonged expression of Sox11 in mature neurons inhibits mitochondrial distribution to dendrites, which under physiological conditions accompanies the maturation process of newborn granule neurons (Table 8, Figure 2-36 and Figure 2-37).

Table 8 Quantitative assessment of the effects after Sox11 overexpression on the mitochondrial compartment at 42 dpi.

absolute mitochondrial volume [µm^3]	**control**	**Sox11**	**p-value**
whole cell	535 ± 48	364 ± 40	p<0.05
dendritic tree	438 ± 42	259 ± 34	p<0.01
0-50 µm	98 ± 11	105 ± 15	p=0.7
50-100 µm	80 ± 8	88 ± 13	p=0.6
> 100 µm	357 ± 39	171 ± 26	p<0.001
relative mitochondrial volume [µm^3/µm length]	**control**	**Sox11**	**p-value**
whole cell	0.36 ± 0.02	0.27 ± 0.04	p=0.07
dendritic tree	0.31 ± 0.02	0.21 ± 0.03	p<0.01
0-50 µm	1.37 ± 0.21	0.57 ± 0.08	p<0.01
50-100 µm	0.27 ± 0.02	0.20 ± 0.03	p<0.05
> 100 µm	0.32 ± 0.02	0.22 ± 0.03	p<0.01
% of mitochondrial located per section	**control**	**Sox11**	**p-value**
dendritic tree	81 ± 1	70 ± 4	p<0.05
0-50 µm	19 ± 1	31 ± 4	p<0.01
50-100 µm	15 ± 1	29 ± 5	p<0.05
> 100 µm	66 ± 2	57 ± 14	p=0.5
mitochondrial density [mitochondria/µm length]	**control**	**Sox11**	**p-value**
whole cell	0.34 ± 0.01	0.32 ± 0.02	p=0.1
dendritic tree	0.30 ± 0.01	0.26 ± 0.01	p<0.001
0-50 µm	1.17 ± 0.15	0.66 ± 0.11	p<0.05
50-100 µm	0.28 ± 0.01	0.24 ± 0.01	p<0.01
> 100 µm	0.31 ± 0.01	0.28 ± 0.01	p<0.05

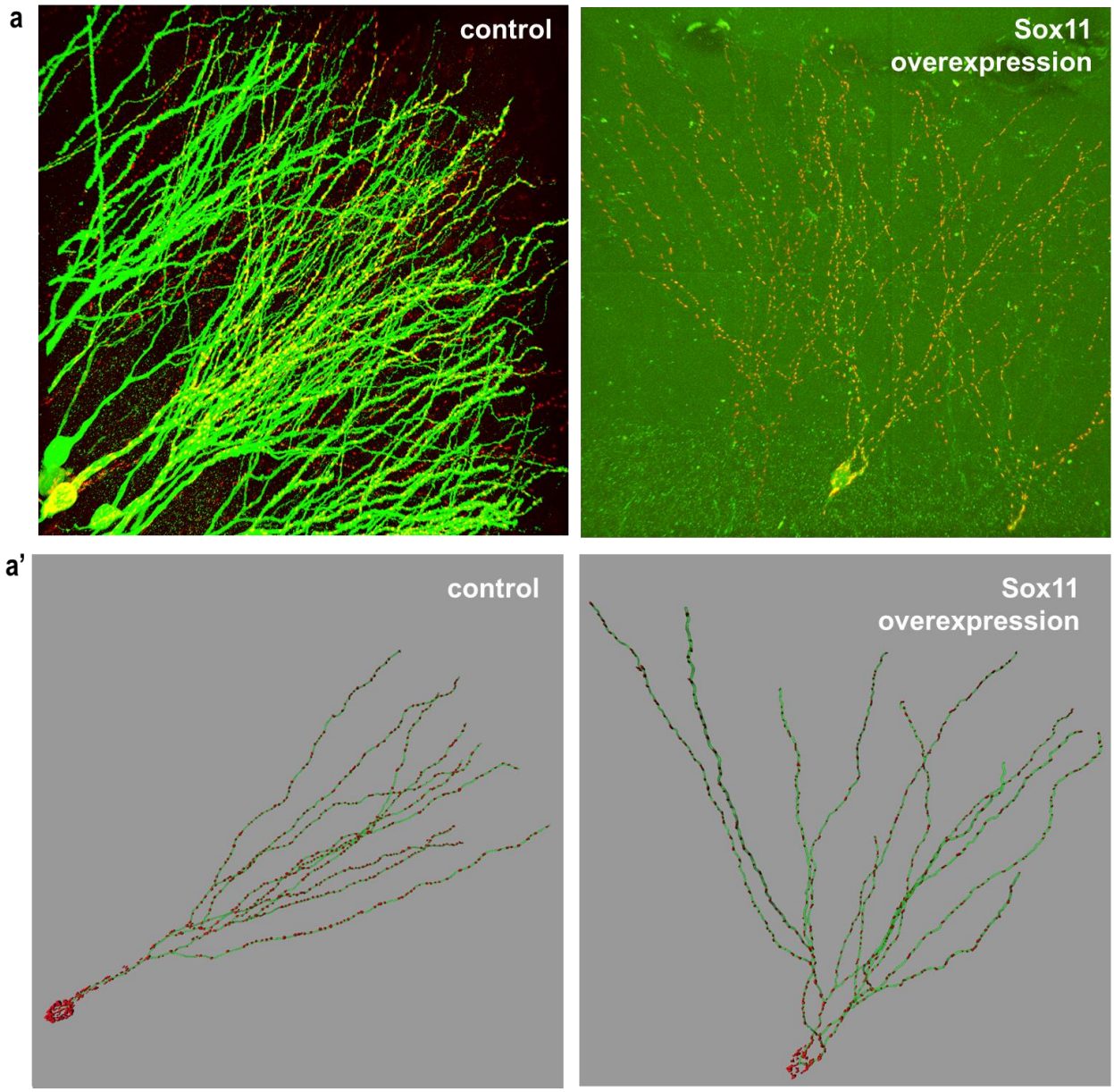

Figure 2-36 Neurons with prolonged Sox11 expression are characterized by deficits in morphology and in the mitochondrial compartment:
a Representative confocal images of a mitoDsred (red) and GFP (green) transduced cell in the mouse dentate gyrus at 42 dpi. Sox11 is bicistronically expressed with GFP. Scale bar 25 µm. ***a'*** 3-D reconstructions of the cells depicted in a.

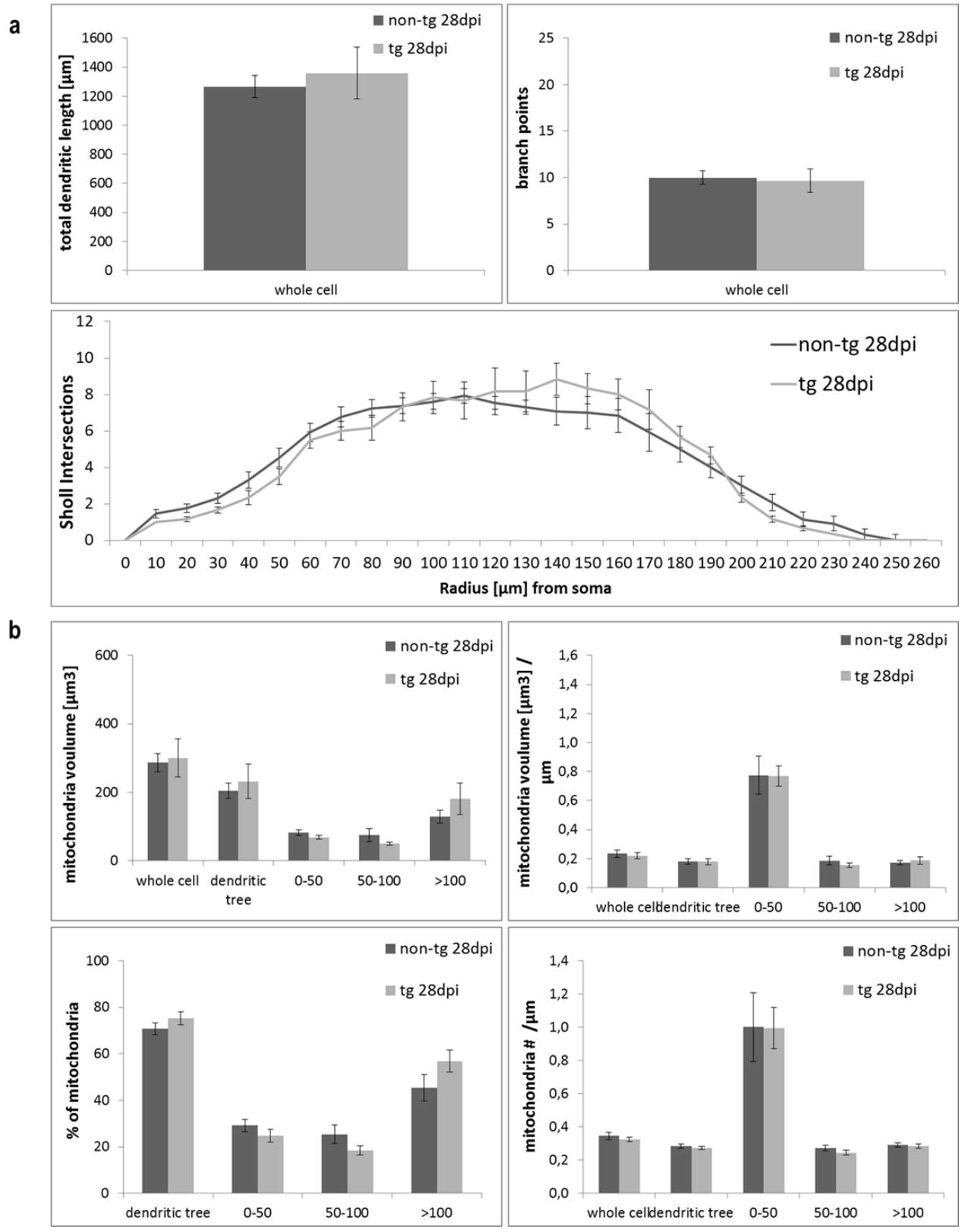

Figure 2-37 Neurons with prolonged Sox11 expression are characterized by deficits in morphology and in the mitochondrial compartment:
a Quantification of total dendritic length and number of dendritic branch points showed no significant differences between Sox11 transduced and control cells, but Sholl analyses (Sholl 1953) disclosed a differential complexity of Sox11 overexpressing neurons. ***b*** Quantification of mitochondria mass, density and distribution demonstrated that Sox11 transduced neurons display a reduction in absolute and relative mitochondrial content, as well as defects in mitochondrial distribution. Scale bars 25 µm; n=12 neurons from 3 different animals; error bars represent ± SEM; Significance levels were assessed with Student's T-test with unpaired samples and unequal variances.

2.6. Analysis of mitochondria in α-synuclein-dependent impairment of adult hippocampal neurogenesis

Various neurodegenerative diseases, such as Parkinson's or Alzheimer's disease are correlated to changes in mitochondrial dynamics and morphology [reviewed in (Lin and Beal, 2006; Exner et al., 2012; Leuner et al., 2012)]. In a mouse model for Parkinson's disease, in which α-synuclein is overexpressed under the control of the PDGF-promoter, severe defects in adult hippocampal neurogenesis reflected in compromised dendritic morphology and modified synaptic integration, were observed (Winner et al., 2012). This raised the question if alterations of the mitochondrial compartment are associated with these developmental defects.

2.6.1. PDGF driven α-synuclein overexpression does not affect neurogenesis or mitochondria content and distribution in young animals

This question was addressed by stereotactically injecting 8 weeks old heterozygous wildtype α-synuclein overexpressing mice with a combination of mitoGFP and RFP retroviruses, to label newborn neurons and to evaluate cell morphology and mitochondria in the transduced neurons. Wildtype littermates were injected with the same mixture and used as controls. Quantitative assessment of the morphological development of the newborn neurons at 28 dpi, did not disclose any defects among analyzed cells from transgenic animals compared to controls with regards to total dendritic length (ctr 1267 ± 77 µm, tg 1360 ± 177 µm) and number of branching points (ctr 10 ± 1; tg 10 ± 1), as well as no significant differences in the cellular complexity (Sholl analysis) were observed. In line with that, no changes within the mitochondrial compartment were detectable. Both absolute mitochondrial quantification and relative assessment of mitochondria volume and density were comparable between transgenic and control animals, as well as mitochondrial localization was similar (Table 9, Figure 2-38 and Figure 2-39). These results of not affected neurogenesis in wildtype α-synuclein overexpressing mice are contrasting the findings that have been previously reported (Winner et al., 2012). However, Winner and colleagues conducted the experiments with aged transgenic animals, which could be a sound explanation for the observed differences, since Parkinson's disease is an age-related disorder.

Table 9 Quantitative assessment of the effect on the mitochondrial compartment in young transgenic α-synuclein overexpression mice at 28 dpi

absolute mitochondrial volume [µm^3]	**control**	**tg**	**p-value**
whole cell	287 ± 27	301 ± 55	p=0.83
dendritic tree	204 ± 22	232 ± 50	p=0.63
0-50 µm	83 ± 9	68 ± 6	p=0.19
50-100 µm	75 ± 18	51 ± 5	p=0.25
> 100 µm	129 ± 19	181 ± 46	p=0.33
relative mitochondrial volume [µm^3/µm length]	**control**	**tg**	**p-value**
whole cell	0.23 ± 0.02	0.22 ± 0.02	p=0.70
dendritic tree	0.18 ± 0.02	0.18 ± 0.02	p=0.99
0-50 µm	0.77 ± 0.13	0.77 ± 0.07	p=0.98
50-100 µm	0.19 ± 0.03	0.16 ± 0.01	p=0.38
> 100 µm	0.17 ± 0.02	0.19 ± 0.02	p=0.64
% of mitochondrial located per section	**control**	**tg**	**p-value**
dendritic tree	71 ± 3	75 ± 3	p=0.26
0-50 µm	29 ± 3	25 ± 3	p=0.26
50-100 µm	25 ± 4	18 ± 2	p=0.16
> 100 µm	45 ± 6	57 ± 5	p=0.16
mitochondrial density [mitochondria/µm length]	**control**	**tg**	**p-value**
whole cell	0.35 ± 0.02	0.32 ± 0.01	p=0.42
dendritic tree	0.28 ± 0.01	0.27 ± 0.01	p=0.54
0-50 µm	1.00 ± 0.21	1.00 ± 0.12	p=0.98
50-100 µm	0.27 ± 0.02	0.24 ± 0.01	p=0.21
> 100 µm	0.29 ± 0.01	0.28 ± 0.01	p=0.65

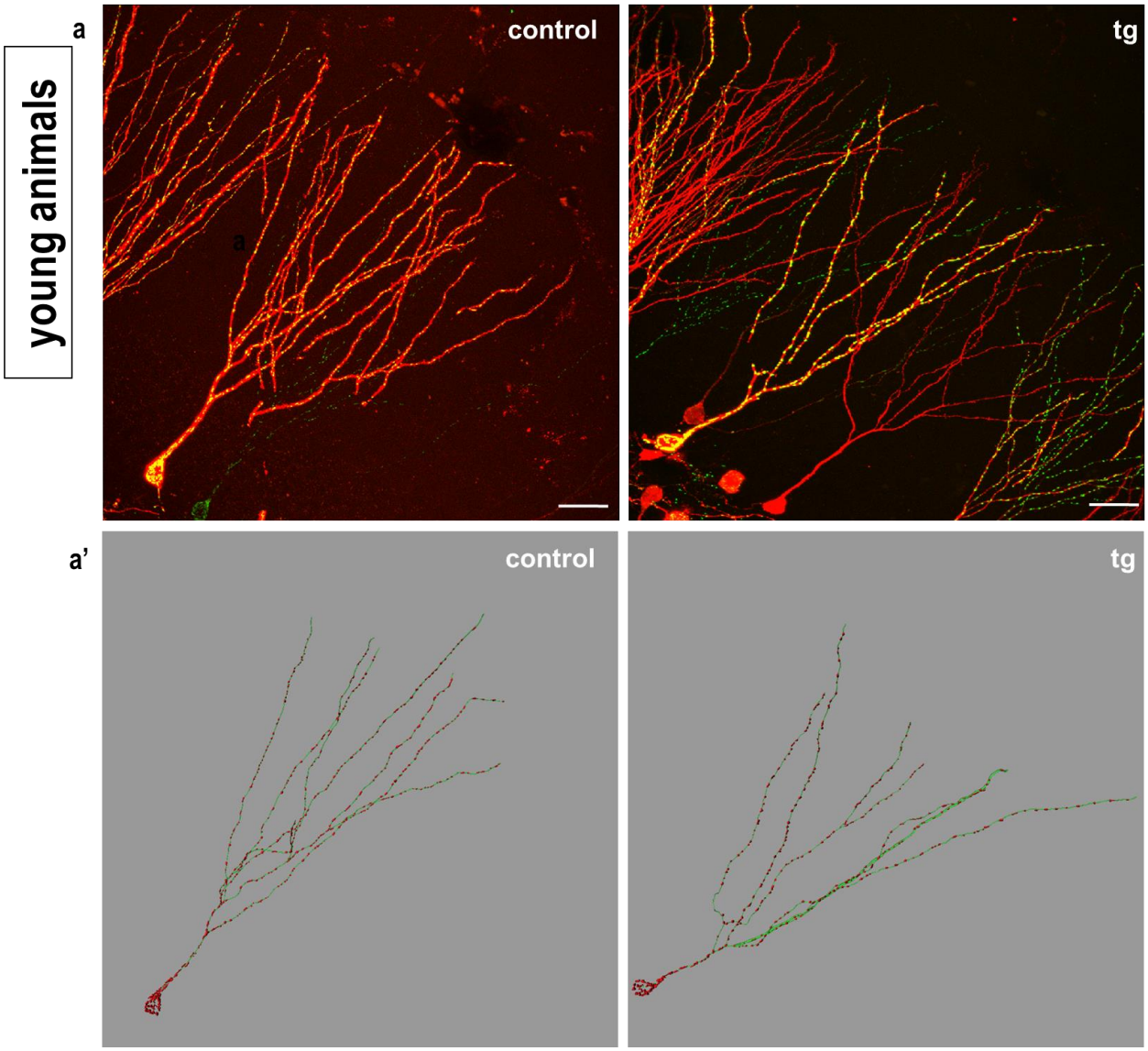

Figure 2-38 The effects of wildtype α-synuclein overexpression on morphology and mitochondria during adult neurogenesis in young animals:
a Representative confocal images of a RFP (red) and mitoGFP (green) transduced cell in the mouse dentate gyrus at 28 dpi in young transgenic and control animals. Scale bar 25 µm. ***a'*** 3-D reconstructions of the cells depicted in a.

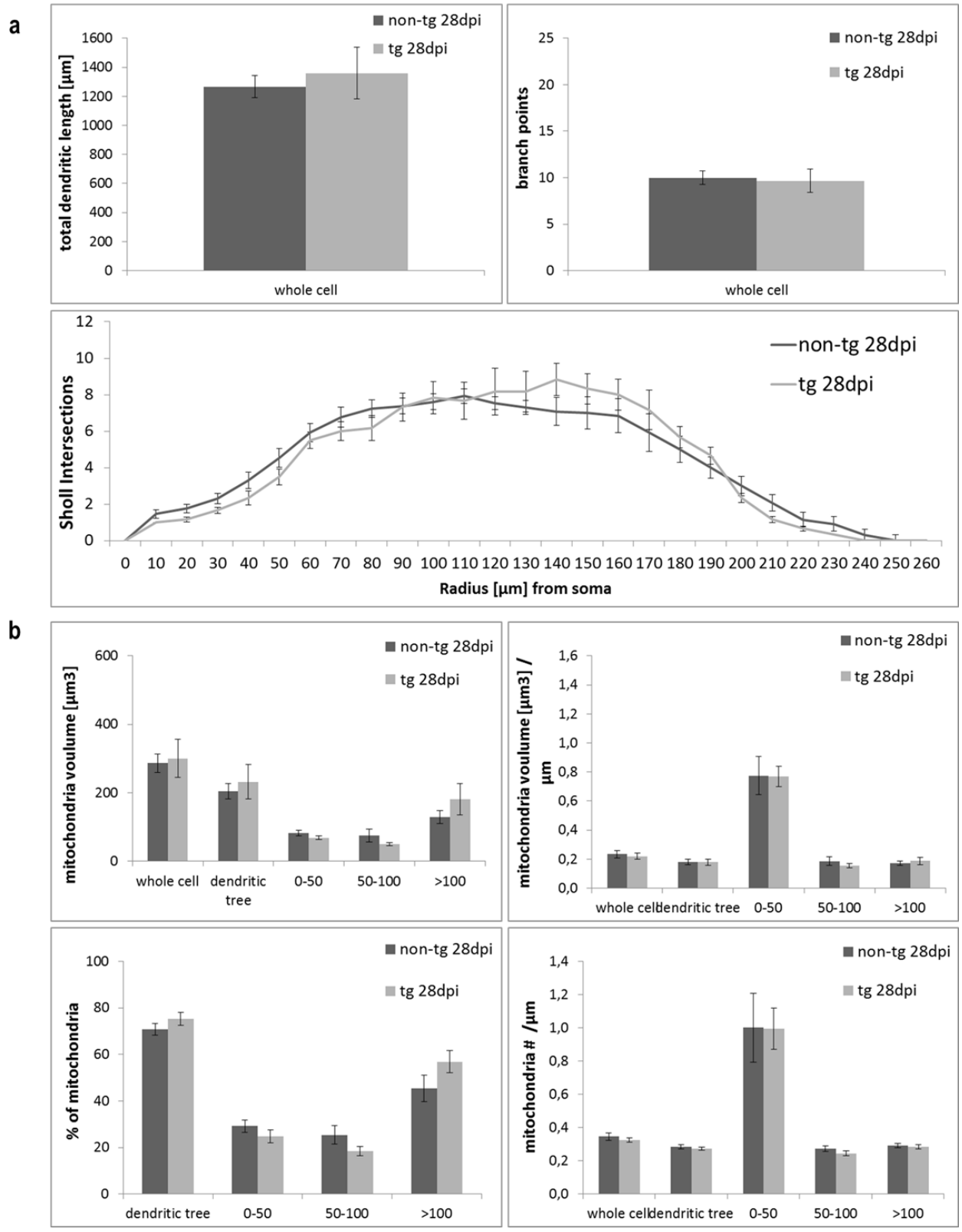

Figure 2-39 The effects of wildtype α-synuclein overexpression on morphology and mitochondria during adult neurogenesis in young animals:
a Quantification of total dendritic length and number of dendritic branch points revealed no significant differences. Sholl analyses (Sholl 1953) did not reveal significant differences in the complexity of the cells. ***b*** Quantitative analysis showed no significant differences within the mitochondrial compartment. n=12 neurons from 3 different animals; error bars represent ± SEM; Significance levels were assessed with Student's T-test with unpaired samples and unequal variances

2.6.2. Hippocampal neurogenesis and mitochondrial morphology might be affected in aged PDGF-α-synuclein mice

To further approach this hypothesis, the set of experiments has been repeated, but instead of 8 weeks old mice, 16 weeks old aged mice were injected this time. However, since hippocampal neurogenesis dramatically drops with aging (Morgenstern et al., 2008; Ben Abdallah et al., 2010), only very few cells in control and even less in heterozygous animals were present that could be analyzed. The challenge to find enough cells for quantitative evaluation was even hampered, as double-transduced cells were almost absent. Eventually, the transduced cells that were retrievable displayed very heterogeneous morphologies. While some of the newborn neurons from transgenic animals were completely normal with respect to their appearance, others displayed an aberrant dendritic morphology. Interestingly, these cells often displayed compromised spine formation (ctr 1.29 spines/µm; tg 0.57 spines/µm) and featured elongated mitochondria and a reduction of mitochondrial number (control 0.39 mitochondria/µm; tg 0.18 mitochondria/µm) (Figure 2-40). With the caveat that due to the described technical reasons only a low number of newborn neurons could be analyzed, these findings suggest that impairments of adult hippocampal neurogenesis are paralled by alterations of the mitochondrial compartment and that mitochondrial dysfunction may contribute to the hippocampal neurogenesis phenotype in preclinical models for α-synucleinopathies.

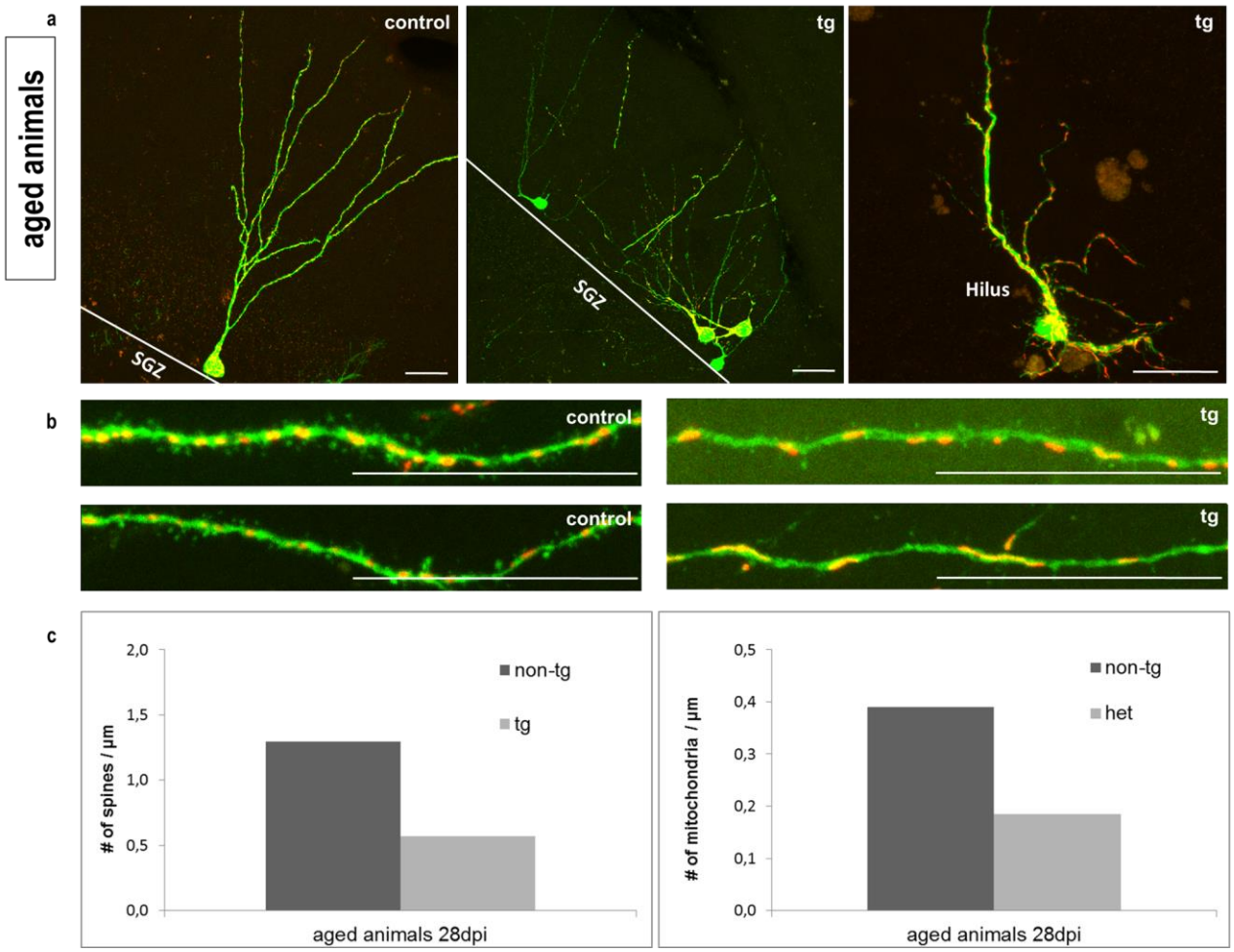

Figure 2-40 The effects of wildtype α-synuclein overexpression on morphology and mitochondria during adult neurogenesis in aged animals:
a-c Example images of double-transduced (mitoDsred and GFP) cells (**a**) and dendrites (**b**) detected in in the dentate gyrus of aged transgenic and control animals at 28 dpi. ***c*** Exemplary but not significantly relevant (n=2) quantitative analysis of dendrites from affected transgenic cells, indicating a reduction of spine and mitochondrial density. All scale bars 25 µm.

3. Discussion

3.1. Mitochondria and their role during the maturation of newborn neurons

Mitochondrial function is crucial for neuronal health, as reflected in numerous studies providing links between dysfunctional mitochondria and disorders of the central nervous system. Hence, it is surprising that little attention has been paid to mitochondria in neuronal development in the adult hippocampus so far. This study demonstrated that profound changes in the mitochondrial compartment, including increase of mitochondrial content, distribution and trafficking, are associated with distinct developmental stages. This observation suggests that mitochondria play a strategic role during adult neurogenesis. Work from Zhao and collaborators has convincingly demonstrated that exercise, such as voluntary wheel running accelerates the maturation of newborn neurons, as reflected in the earlier onset of spine development (Zhao et al., 2006). Here, I provide additional evidence for exercise induced maturation by revealing a significant increase in total dendritic length, branching points and cellular complexity in animals housed with running wheels. At later time points when dendritic growth goes down (28 dpi and 104 dpi), there are no morphological differences with regard to dendrite complexity. This suggest that the maturation process is probably accelerated by running rather than leading to permanent morphological alterations. In comparision in the study by Zhao, spine formation was still significantly enhanced at 56 dpi. However, at 126 dpi there was no difference in the number of mushroom spines, supporting the assumption that exercise does not alter the mature morphology but accelerates the maturation process (Zhao et al., 2006). Interestingly, the acceleration of maturation observed in the running paradigm are accompanied by a faster increase in mitochondrial content and dispersion into dendrites. Running did not affect the morphology or mitochondrial distribution in mature neurons, suggesting a developmental stage specific link between remodeling of the mitochondrial compartment and development/modulation of neuronal morphology. The correlation between accelerated maturation and accelerated adaptations of the mitochondrial compartment emphasizes a potential role of and requirement for mitochondria during adult neurogenesis. However, the underlying mechanisms linking these two distinct processes remain to be established.

The mitochondrial fission factor Drp1 has been proven to be crucial for the development, function and health of the central nervous system, both in mice and humans (Waterham et al., 2007; Ishihara et al., 2009; Uo et al., 2009; Wakabayashi et al., 2009; Kageyama et al., 2012). In addition, there is correlative evidence that a decrease of Drp1 activity contributes to the pathology of Alzheimer's disease (Wang et al., 2008; Wang et al., 2009). Compared to other cell types, neurons seem to be particularly dependent on Drp1 function, and there even exists a transcript variant that has been found to be exclusively expressed in mature neurons, strongly indicating Drp1's importance for brain homeostasis (Yoon et al., 2003; Uo et al., 2009). Loss of function of Drp1 by overexpressing a dominant-negative Drp1 pointed clearly out, that Drp1 is indispensable for the generation of new neurons in the adult dentate gyrus, since transduced cells were characterized by a compromised dendritic tree and expression of the pre-neuronal-commitment marker Sox2. Mitochondria of these cells were obviously agglomerated and hyperfused in the soma and mitochondrial transport into the dendritic tree was completely absent. In contrast, increase of Drp1-dependend mitochondrial fragmentation raised the density of this organelle within dendrites. This supports the notion that Drp1, besides conducting mitochondrial division, is involved in the distribution of mitochondria in neurons, although the mechanism has not been elucidated so far. Moreover, considerable work from Sheng and colleagues demonstrated that overexpression of Drp1 not only directs mitochondria into dendrites but at the same time increases synaptogenesis in primary hippocampal cultures (Li et al., 2004).

I previously demonstrated that increasing Drp1 levels stimulates the differentiation of isolated adult NPCs *in vitro*, since the percentages of astrocytes (GFAP), oligodendrocytes (RIP) and immature neurons (ß-tubulinIII) were elevated (Steib, 2009). In consistency, in ß-amyloid overexpressing neuroblastoma cells impairments of neuron-like differentiation can be rescued by restoring Drp1 wt levels (Wang et al., 2008). Moreover, I demonstrated that proliferation rates *in vitro* go down with wtDrp1 overexpression, even when cells were cultivated with growth factors, which correlates with the strong induction of differentiation by wtDrp1 (Steib, 2009).

While Drp1 overexpression was sufficient to promote the differentiation into all three neural lineages, from NPCs *in vitro*, there was no significant enhancement of neurogenesis among wtDrp1 cells under basal conditions *in vivo*. Therefore, I concluded that the differentiation of precursor cells in the adult brain is not limited by mitochondria fission/trafficking. Upon acceleration of neurogenesis by exercise, Drp1 overexpression had no impact on the rate of neurogenesis. However, I surprisingly found that wtDrp1

was further enhancing the maturation speed of newborn neurons. I discovered that the expression of the mature neuronal marker Calbindin was prematurely present at 16 dpi (Steib, 2009), and that the overall dendritic growth and spine formation were significantly enforced. From this finding I hypothesize that when physiological stimuli, such as running promote the generation of new neurons, mitochondrial distribution, to fulfill growing energy demands in the dendrites, might indeed be the limiting factor, determining the tempo of maturation. These findings suggest that the cell biological and genetic programs regulating neurogenesis need to be closely coordinated with adaptations of the mitochondrial compartment. The benefit for the individual newborn neuron that arises from acceleration of maturation is not understood. Considering that during adult neurogenesis most newly generated neurons die (Biebl et al., 2000; Kempermann et al., 2003; Sierra et al., 2010), that the strongest survival factor is functional integration which is highly competitive (Bergami and Berninger, 2012), and that newborn neurons appear to compete for synaptic input, an earlier onset of spines could be beneficial to increase the number of surviving newborn neurons. It is worth to note that it has been reported that the anti-apoptotic protein Bcl-XL interacts with Drp1 in promoting synaptogenesis (Li et al., 2008). This strengthens the assumption that Drp1 overexpression promotes integration and provides an interesting molecular link between synaptogenesis and survival.

The fact that various splicing forms of Drp1 exist, and only the longer ones are actually expressed in neurons raised the question, whether the neuron-specific variants are even more potential in promoting integration compared to variant 3. However, comparing the effects of different transcript forms during activity-dependent neurogenesis indicated that their potent to direct mitochondria into dendrites and to promote maturation is similar. This suggests that at least for the mobilization of Drp1 during exercise-dependent acceleration of development, post-translational modifications within the regions encoded by Exon 16 and 17, or protein-interactions with the 13 amino acids loop encoded by Exon 3 are not pivotal.

Furthermore, not only Drp1 has been shown to be particularly crucial for neuronal health, but also mitochondrial dynamics in general is associated with impaired mitochondrial function and distribution in various neurodegenerative diseases. In this context, it will be also worth investigating the impact of shifting the balance of fusion and fission by specific manipulation of other proteins. For instance, overexpression of the mitochondrial fusion proteins Mfn2 and Opa1 would result in elongated mitochondria similar to dnDrp1, but in contrast fission would be still functional, thus allowing Drp1-dependent quality control of

mitochondria. Interestingly, it has been published recently that Mfn2 is necessary for the transport of axonal mitochondria (Misko et al., 2010). As the membrane potential and the function of the respiratory chain complexes and thus neuronal survival are critical dependent on mitochondrial fusion (Chen et al., 2005; Chen et al., 2007), it will be worth to elucidate in this gain of function experiment whether the developing neurons could profit from increased fusion and how it affects synaptogenesis. Addressing the specific question of mitochondrial transport and synaptic integration, another protein is of particular interest: the mitochondrial Rho GTPase Miro1 controls anterograde mitochondrial trafficking via binding to the microtubule associated motor protein Kinesin1 (Kif5) (Fransson et al., 2006; Saotome et al., 2008; Macaskill et al., 2009; Wang and Schwarz, 2009). Increased expression of Miro1 stimulates mitochondrial trafficking in primary hippocampal neurons. Although I have preliminary results indicating that too high Miro1 levels might be potentially toxic for newborn neurons, I believe that a fine tuning of Miro1 overexpression by choosing adequate tools will allow to selectively evaluate the effects of mitochondrial transport/distribution on the development of newborn neurons, since Miro1 does not increase mitochondrial fission, but rather leads to the presence of more elongated mitochondria (Saotome et al., 2008). In this context, live imaging of the mitochondrial compartment during neuronal development rather than static histological analysis will provide greater insight into the role of mitochondrial trafficking and activity-dependent accumulation during spine formation. Either imaging after specific stimulation of acute organotypic hippocampal slice cultures or 2-photon-deep-brain imaging *in vivo* using the cranial window technique (Holtmaat et al., 2005; Fuhrmann et al., 2007; Mizrahi, 2007) can be used to elucidate specifically the impact of mitochondrial positioning and transport on spine motility, which is a correlate to synaptic plasticity (Bonhoeffer and Yuste, 2002; Zhao et al., 2006).

Like mitochondria, other intracellular organelles play essential roles in various cell-biological processes, and neurons turned out to be dependent in particular. Endosomes, which are conducting endocytosis to degrade and recycle proteins, have been described to be involved in dendritic branching and endosome trafficking has been shown to be essential for the plasticity of dendritic spines (Park et al., 2006; Sweeney et al., 2006). The secretory pathway, which is consisting of the ER for protein processing and the Golgi apparatus for protein packaging and transport, is spatially organized within neurons. Especially for the morphogenesis and dynamics of dendrites, this pathway has a pivotal function (Horton and Ehlers, 2003), and Golgi outposts may serve for local protein translation and modifications (Steward and Schuman, 2003). It will be interesting

to elucidate the role of these membrane delimited compartments during the maturation of newborn hippocampal neurons. Since the ER has in addition crucial function in regulating cellular calcium levels via close mitochondria-ER communication sites, it will be in particular compelling to address in future experiments how the ER is structured in these developing neurons and how ER dynamics are affected by exercise.

3.2. How is mitochondrial biogenesis and distribution regulated during adult hippocampal neurogenesis?

This study encouraged the hypothesis that Drp1-mediated mitochondrial fragmentation is involved in mitochondrial transport during activity-dependent neurogenesis. Multiple posttranslational modifications, which regulate Drp1 activity have been described, that can differentially activate or inhibit Drp1 (Frank et al., 2001; Uo et al., 2009). The kinase CamK1-α has been reported to phosphorylate Drp1 at serine 637, which induces mitochondrial fragmentation in primary hippocampal neurons. Interestingly, the activation of CamK1-α is triggered by depolarization, suggesting that this protein represents a promising candidate to mediate Drp1-dependent fission upon neuronal activation (Han et al., 2008a). Since a spatiotemporal expression study demonstrated that CamK1-α is indeed present at high levels in the adult dentate gyrus predominantly in the SGZ (Kamata et al., 2007), it might be worthwhile to assess the role of this kinase in Drp1-mediated mitochondrial distribution during hippocampal neurogenesis via gain- and loss-of-function studies. Contrary to the study by Han and colleagues, work from other laboratories proposed that not phosphorylation but dephosphorylation of Drp1 at S637 induces mitochondrial fission. In these studies, a sustained increase of intracellular Ca^{2+} levels was found to induce dephosphorylation by the phosphatase Calcineurin that resulted in translocation of Drp1 to the mitochondria and subsequent fragmentation of the organelle (Cribbs and Strack, 2007; Cereghetti et al., 2008). On the other hand, physiologically evoked Ca^{2+} signaling was observed to activate the protein kinase PKA which in turn phosphorylated Drp1 at S637, that in contrast to the study by Han and collaborators inhibited Drp1-dependent fission (Chang and Blackstone, 2007). Although all the opposing effects of post-translational modifications by different proteins at this serine residue leaves many questions and much room for speculation of how different Ca^{2+} signals are integrated into a response in alterations of mitochondrial morphology, it is beyond controversy that S637 plays an important role to regulate Drp1 activity upon neuronal depolarization. Interestingly, this specific phosphorylation site is not encoded by Exon 16 or 17 and therefore also present in the transcript variant 3, which suggests that

it might be involved in the regulation of Drp1-dependent mitochondrial distribution in the developing newborn neurons that overexpress Drp1 variant 3. In this context, a recent study tried to unravel the effects of opposing dephosphorylation/phosphorylation in the morphogenesis of primary hippocampal neurons. Consistent with what I found and what was also reported by others before (Li et al., 2004; Li et al., 2008), mitochondrial fission, here induced by PP2A/Bβ2-mediated dephosphorylation of Drp1 at S637, turned out to be an important player in synaptogenesis (Dickey and Strack, 2011). In contrast to the present study, Dickey and Strack reported a reduced mitochondria number in dendrites upon Drp1 activation, associated with compromised neurite outgrowth, while inhibition of Drp1 induced by PKA/AKAP1 phosphorylation, promoted dendritogenesis in primary hippocampal cultures (Dickey and Strack, 2011). With regard to mitochondrial distribution my data is more consistent with the report by Li and collegues who found that Drp1 overexpression induced mitochondrial trafficking into dendrites (Li et al., 2004). The reasons for the discrepancies between my findings and the findings by Dickey and Strack regarding the influence of Drp1 on dendritic development remains unknown. One likely cause might be the differences between the situation *in vitro* and *in vivo*, since it is known that adult neurogenesis is strongly modulated by extrinsic regulators in the hippocampal neurogenic niche.

In this work, I did not only observe alterations of mitochondrial distribution as a response to neuronal activation by exercise during hippocampal neurogenesis, but also profound effects on mitochondrial content. A central role of regulating mitochondrial biogenesis during adult neurogenesis might be granted to the activity-dependent transcription factor cAMP response element-binding protein (CREB) which we have found to be constitutively active during the differentiation of newborn dentate gyrus neurons (Jagasia et al., 2009). We demonstrated in this study that the phosphorylation of CREB in immature neurons is depending on synaptic activity induced by GABA-depolarization, which is known to raise intracellular Ca^{2+} levels. Besides neuronal activity, another mode that can specifically activate CREB signaling is mediated by growth factors, such as VEGF (Shaywitz and Greenberg, 1999; Ferrara et al., 2003; Fournier et al., 2012). Interestingly, it has been proposed that VEGF is directly involved in the regulation of exercise-induced neurogenesis (Palmer et al., 2000; Fabel et al., 2003). CREB in turn together with TORC regulates the transcription of the nuclear mitochondrial gene master activator PGC-1α that controls the expression of nuclear encoded mitochondrial proteins which are required for mitochondrial biogenesis (Herzig et al., 2001; De Rasmo et al., 2010; Fernandez-Marcos and Auwerx, 2011). Since it has recently been demonstrated

that the kinase Akt3 which is downstream of VEGF signaling and upstream of pCREB is essential for VEGF-stimulated mitochondrial biogenesis, the hypothesis that the CREB pathway is involved in activity-dependent biogenesis during neuronal maturation is furthermore supported (Wright et al., 2008). Transcription factors that are most likely involved in biogenesis downstream of CREB and PGC1-α include NRF1/2 and Tfam. They coordinate transcriptional programs regulating the expression of mitochondrial genes encoded by the nucleus and the mitochondrial genome, respectively (Scarpulla, 2008; Viña et al., 2009). Further studies will be required, to elucidate the specific function and contribution of the individual proteins in this signaling cascade to control mitochondrial biogenesis in newly generated hippocampal neurons. In this context, Birgit Ebert, a PhD student in our laboratory approached the question of the role for Tfam in this process in her thesis (Ebert, 2013). Interestingly, she found that acute TFAM-depletion did significantly affect dendritic growth. Even more intriguing, Tfam-depleted newborn neurons were not capable to react to the running stimulus comparable to control cells. This is in line with the finding that Drp1 requires exercise to promote maturation, and emphasizes the hypothesis that mitochondria function contributes significantly to exercise-induced acceleration of neuronal development.

Besides CREB, another transcription factor that should be taken in account with respect to coordination of processes related to neuronal differentiation and maturation is Sox11. Interestingly, a recently performed genome-wide binding study revealed an enrichment of Sox11 on promoters of genes associated with mitochondrial metabolism and function (Bergsland et al., 2011). In the present study, I identified Sox11 as a potential key contributor to both mitochondrial biogenesis and distribution during activity-dependent neurogenesis. Overexpression and prolonged expression of Sox11 increased relative mitochondrial mass although the morphological maturation of newly generated neurons was significantly delayed among transgenic cells three weeks after birth. Hence, this finding brought the hypothesis forth that Sox11 contributes to mitochondrial biogenesis during neurogenesis and thereby uncouples dendritic growth and increase of mitochondrial mass. Consistent with this finding, depletion of Sox4/11 resulted in a reduction of relative mitochondrial content at 3 dpi, strengthening the hypothesis that Sox11 is involved in mitochondrial biogenesis. Expression profiling of NPCs after induction of Sox4/11 KO revealed that though levels of the transcription factors directly associated with biogenesis such as PGC1-α, TFAM or NRF1/2 were not affected, the expression of the mitochondrial polymerase PolG was significantly reduced. This suggests that this enzyme, which is essential for the replication of the mitochondrial

genome, may be limiting for mtDNA content in developing neurons, and reduces mitochondrial mass in Sox11 KO cells. On the other hand PolG levels might be upregulated when Sox11 is overexpressed in newly generated neurons *in vivo* and thereby provide the basis for generation of a higher mitochondrial mass. However, other factors are required to coordinate mitochondrial transcriptional programs and interact with Sox11, which need to be identified in future experiments. In contrast to mitochondrial mass, the distribution of mitochondria at 21 dpi was as anticipated according to the developmental stage of Sox11 overexpressing cells. However, assessing the effect of Sox11 overexpression on mitochondrial localization six weeks after birth of the neurons, the relative number of dendritic mitochondria was drastically lowered. Mitochondrial transport is known to involve association of mitochondria to the microtubule network via adaptor proteins, although not much is known so far about the role of different cytoskeleton proteins in this context. Intriguingly, downstream targets of Sox11 that have been identified include several microtubule related proteins, which are specific for the immature neuronal stage (Mu et al., 2012; Doberauer, 2013). Moreover, loss of function of Sox4/11 in NPCs resulted in profound alterations of the expression levels of multiple cytoskeleton proteins, including several α- and β-tubulins. Hence, I hypothesize that the mode of mitochondrial trafficking, with respect to the proteins that are involved, changes when newborn neurons switch from the immature to the mature stage that is controlled by Sox11. In contrast, prolonged expression of Sox11 up to six weeks after birth, most likely results in the presence of cytoskeleton proteins specific for immature neurons, which might not be compatible with the protein machinery controlling mitochondrial transport in mature neurons. This may eventually lead to a decrease of mitochondrial density in dendrites and a reduction of relative mitochondrial content in general at 42 dpi in transgenic neurons. A lot progress is currently made in unraveling the underlying mechanisms controlling mitochondrial trafficking in neurons, and it will be very compelling to understand the interplay between Sox11 in coordinating the microtubule network in developing neurons and the machinery controlling mitochondrial transport.

Analysis of Sox4/11 cKO at 12 dpi *in vivo* revealed that depleted cells are not capable to differentiate into neurons but perform a fate switch towards glia phenotypes, such as astrocytes and oligodendrocytes, both characterized by the expression of Sox2. Since Sox10 positive oligodendrocytes can also be found in control animals and are most likely originating not from dentate gyrus NSCs, but from proliferating oligodendrocyte precursors residing in the hippocampus, the presence of those star-shaped cells expressing oligodendrocytic markers is probably not causally linked to the loss of

Sox4/11. Contrary, a high percentage of depleted cells displayed an astrocytic phenotype identified by the expression of GFAP and amorphous morphology, which is not present among control cells. As those cells are not present among retrovirally labeled cells under physiological conditions, one can only speculate about their actual phenotype. Being located in the SGZ or close to it in the hilus, the known population that corresponds closest to this appearance is the horizontal NSC pool, which is just as the Sox4/11 KO cells characterized by GFAP and Sox2 expression (Lugert et al., 2010). However, since the depleted cells are found rather scattered than accumulated in cell clusters, it is unlikely that they make a contribution to the active stem cell population which is highly proliferating and giving rise to new neurons. Future experiments are required to bring forward the final fate of Sox4/11 KO cells and unravel their long-term characteristics and survival. The mitochondria compartment in both glia phenotypes that were found among Sox4/11 depleted cells was comparable to control cells. Star-shaped oligodendrocytes among both control and KO cells have small fragmented mitochondria that are well dispersed, probably due to their very thin cellular extensions. In contrast, astrocytes are usually featured by highly interconnected mitochondrial networks composed of elongated mitochondria (Uo et al., 2009). Comparably, the astroyctic amorphous cells present among Sox4/11 KO cells had mitochondria that appeared to be more fused and agglomerated. Taken together, these results suggest that neurons require proper Sox11 function and timing for accurate development of the mitochondrial compartment during their maturation, whereas in glia cells, such as astrocytes and oligodendrocytes which do not express Sox11 in the first place, other proteins must account for coordination of cell-type speficfic mitochondrial biogenesis, distribution and morphology.

3.3. Mitochondria in stem cells and during differentiation

Mitochondria are increasingly in focus as important players in regulating stemness and cellular differentiation. Thus, it is not surprising that adaptations of the mitochondrial compartment occur during the differentiation of neural stem cells *in vivo*. Recent reports have convincingly demonstrated that the cellular energy metabolism of various types of pluripotent stem cells, as well as multipotent adult neural stem cells mainly depends on glycolysis (Kondoh et al., 2007; Chung et al., 2010; Mandal et al., 2011; Shyh-Chang et al., 2013). In contrast, the initiation of cellular differentiation requires the switch to oxidative phosphorylation as main metabolic pathway to provide energy (St. John et al., 2005; Cho et al., 2006; Chung et al., 2007; Zhang et al., 2011). Interestingly, it has been shown that the changes of mitochondrial metabolism during the transition from

proliferation to differentiation are accompanied by changes of mitochondrial morphology, content and subcellular localization (St. John et al., 2005; Chung et al., 2010; Prigione et al., 2010; Suhr et al., 2010; Zhang et al., 2011). In line with these observations, I found that developing adult born neural precursor cells in the hippocampus are characterized by a significant increase in mitochondrial mass and mitochondrial dispersion. Contrary to previous literature reports, in the context of adult neurogenesis the described elongation of the mitochondria as a result of mitochondrial activation was not evident, but the mitochondrial morphology appeared rather fragmented upon neuronal differentiation. However, since it was demonstrated that mitochondrial morphology and network structure is cell-type specific (Uo et al., 2009), the observed smaller appearance of mitochondria in neurons is explainable by the unique morphology of neurons and the need to distribute mitochondria efficiently over long distances through dendrites. This hypothesis is further supported by the finding that inhibition of neuronal differentiation by knock-out of the neuronal transcription factors Sox4/11, did actually result in a glia phenotype with a different mitochondrial morphology and network. The present study provided first insights on how mitochondria morphology, content and dispersion occur in order to meet the metabolic needs that have to be fulfilled for the development of a neural stem cell derived newborn neuron. However, further studies will be required to investigate the actual changes in metabolic pathways that accompany the obvious changes of the mitochondrial compartment. This new knowledge will not only help to understand the cell biological mechanisms regulating adult neurogenesis, but will also provide new potential pharmacological targets to govern the development of neurons in new stem-cell based therapies.

3.4. Creatine and neurogenesis

The natural bioenergetic compound creatine is known to have beneficial effects on neuronal health during aging and interestingly induced the expression of neurogenesis related genes (Bender et al., 2008). In the present study, creatine was assessed as a potential diet supplementation to promote adult hippocampal neurogenesis via modulating mitochondrial function and cellular energy homeostasis. However, analyzing the generation of newborn neurons at the level of proliferation, neuronal fate commitment and survival, revealed that none of these processes was improved by creatine, and proliferation seemed to be even slightly reduced. Besides that, the only change that was observed with creatine was an increase of mitoDsred positive newborn neurons, which is difficult to interpret. While one cannot definitely exclude, that differences within the

retroviral mixture which was injected account for the alteration in the number of mitoDsred cells, one could also speculate that a higher number of mitoDsred cells might be detectable since creatine is known to increase mitochondrial membrane potential and hence promotes the accumulation of mitoDsred protein in the mitochondrial membrane. Further experiments will be required to solve this question. Another issue refers to the bioavailability of higher creatine levels in the brain during creatine-supplemented diet. Although, creatine can in principle cross the blood-brain barrier, its uptake is very limited and the six to eight weeks food-supplementation until analysis in the present study might have been simply too short to saturate cerebral creatine pools and to evoke beneficial effects. The limited penetration of the blood-brain-barrier is explainable by the expression profile of the creatine transporter (CrT). Since astrocytes, which cover most of the surface of microcappilaries do not express the CrT, creatine has to be excreted through the remaining surface that is not covered and needs to be actively taken up by neurons from the extracellular brain fluid (Ohtsuki et al., 2002). Hence, it will take an extended period of time to charge neurons with higher creatine amounts.

However, if one could bypass the obstacles arising with creatine uptake, for instance by longer creatine food supplementation and/or higher dosages, it might be undeniable a promising treatment candidate to stimulate adult neurogenesis. The overexpression of Drp1 resulted in accelerated neuronal maturation most likely due to ameliorated energy supply in dendrites via enhanced mitochondrial transport. Hence, it will be interesting to assess whether mimicking the impact of mitochondrial trafficking, by shuttling not the mitochondria as cellular power plants but the energy equivalent itself in the form of PCr, will comparably enhance neuronal maturation. In line with that, Drp1-dependent induction of synaptogenesis in primary hippocampal neurons was imitated by creatine supplementation in the media (Li et al., 2004). However, the present study revealed that Drp1 requires additional physiological stimuli, such as exercise, to exhibit beneficial effects during adult neurogenesis. Hence one should consider that creatine may also only ameliorate neuronal development when energy demands are raised and the supply of energy becomes a limiting factor.

3.5. Mitochondria and their implications in α-synuclein-dependent impairment of adult hippocampal neurogenesis

Mitochondrial dysfunction has long been implicated in the pathogenesis of Parkinson's disease. Recent studies provided evidence that α-synuclein, a gene that is associated with PD, is involved in mitochondrial function (Liu et al., 2009; Devi and Anandatheerthavarada, 2010; Zhu et al., 2011). The present study aimed to elucidate the impact on the mitochondrial compartment during α-synuclein-dependent impairment of adult hippocampal neurogenesis. To maximize the number of analyzable cells, young adult (8 weeks) transgenic mice overexpressing wildtype α-synuclein under the PDGF promoter were injected with retroviruses to assess the morphological development and mitochondria. No significant differences, neither in neuronal maturation nor in mitochondrial biogenesis or distribution were observed. Since Parkinson's disease is an age-related disease and transgenic PDGF-α-synuclein were found to develop first intracytoplasmic α-synuclein inclusions just 2 months after birth (Masliah et al., 2000), it is possible that injection and analysis at this age is too early to detect significant defects in adult neurogenesis.

Studying aged animals (4 months) for this experiment caused other obstacles. Since neurogenesis drastically goes down with aging (Morgenstern et al., 2008; Ben Abdallah et al., 2010), only a very low number of newborn neurons was retrievable. In addition, analyzable newborn neurons were very heterogenous with respect to their morphology, which might be due to significant differences in α-synuclein expression levels. To overcome this issue, attempts are currently made to back-cross the transgenic mouse line into a clean Bl6C57 background, to minimize the heterogeneity caused by the present mixed genetic background. Besides that, another strategy to assess the correlation between increased intracellular α-synuclein levels and alterations within the mitochondria would be a cell-autonomous approach using retrovirus-mediated overexpression on a single-cell level. Although non-cell-autonomous effects will not be detected, this approach would have advantages since the retroviral cag promoter is very strong and the impact of increased α-synuclein accumulation will be evident prompt (Winner et al., 2012).

The number of double-transduced newborn neurons in aged transgenic PDGF-α-synuclein mice was too low to draw final conclusions. However, it should be noted that

cells were present in tg animals, that were clearly characterized by compromised dendritic arborization and disturbed polarity, since the dendritic tree was not located apical and growing towards the hippocampal fissure. Interestingly, these newborn neurons additionally failed efficient synaptic integration as reflected in the reduced number of dendritic spines. Contrary to this finding, in the previous work by Winner and collaborators (Winner et al., 2012) newborn neurons in tg animals displayed an increased spine density. On the other hand, all other previous studies reported a negative impact of α-synuclein on both dendrite and spine number in *in vitro* experiments (Takenouchi et al., 2001; Crews et al., 2008) as well as in neurons from PD patients (McNeill et al., 1988; Patt et al., 1991; Zaja-Milatovic et al., 2005), and Winner and colleagues also found a negative impact on spine density following retrovirus mediated α-synuclein overexpression (Winner et al., 2012). In the newly generated neurons that did not accomplisch accurate neuronal development, defects in synaptic integration were accompanied by a strong reduction of dendritic mitochondria density and an elongated mitochondrial morphology. This is opposing the recently reported hypothesis that an increase of α-synuclein accumulation inhibits by mitochondrial fusion and hence shifts the balance towards more fragmented mitochondria (Kamp et al., 2010; Nakamura et al., 2011). Although the underlying reasons that might cause these discrepancies are not yet unraveled, one could hypothesizes that in contrast to the previous reported cell culture studies, additional mechanisms control mitochondrial distribution and shape *in vivo*. In line with this notion is the fact that for Drp1 function (see above) as well as for PINK1 function, another PD associated gene, multiple sometimes contradictory effects on mitochondrial morphology, including fragmentation, swelling, enlargement and hyperfusion have been observed, depending on the cellular context and the experimental system (*in vivo* versus *in vitro*) (Clark et al., 2006; Poole et al., 2008; Lutz et al., 2009).

To elucidate the impact of α-synuclein on the mitochondrial compartment during the maturation of newly generated neurons in the adult hippocampus, further experiments will be required. If it will turn out that α-synuclein overexpression indeed lowers mitochondrial density in dendrites, potentially because elongated mitochondria might be too long for efficient trafficking within processes, it might be worth to investigate if Drp1 overexpression is capable to rescue this defect. Given that developmental impairments could be a result of inefficient energy supply, Drp1 overexpression eventually might also rescue compromised dendritic arborization and synaptic integration. This hypothesis is further supported by the fact, that creatine treatment, which functions as an energy shuttle and thereby optimizes cellular energy homeostasis, contributes to improve

neuronal health in preclinical mouse models of PD (Matthews et al., 1999; Klivenyi et al., 2003; Yang et al., 2009).

3.6. Conclusions

In summary, the present study revealed that alterations within the mitochondrial compartment are accompanying stage specific processes during the development of adult newborn neurons in the hippocampus. These adaptations of mitochondrial content and distribution are coupled to the morphological maturation and accompany behaviorally-induced changes in the tempo of dendritic growth and synaptic integration. In addition, evidence was acquired indicating that mitochondrial distribution is not only crucial for the neuronal differentiation, but in addition mitochondrial transport, which ensures sufficient energy supply, might be limiting the tempo of activity-dependent maturation. Moreover, the transcription factor Sox11 which is indispensable for neuronal differentiation in the adult hippocampus, was identified as a candidate factor that coordinates mitochondrial biogenesis with neuronal development and modulates mitochondrial trafficking via regulation of the expression of developmental stage-specific microtubule associated proteins. Eventually, evidence was found that deficits in mitochondrial distribution and morphology may be a potential cause for the compromised neuronal maturation in a Parkinson's disease preclinical mouse model.

Taken together, the present study identified the control of mitochondrial dynamics and transport as an important player for synaptogenesis in adult neurogenesis. Such knowledge could support ongoing efforts in the neural repair field ultimately aiming to restore compromised neural networks using stem cell derived neurons.

4. Material and Methods

4.1. Material and Equipment

Chemicals, media and supplements

0.5% Trypsin-EDTA	InvitrogenLifeTechnologies Ltd, Paisley, UK
1 kb DNA ladder	Thermo Fisher Scientific Inc., MA, USA
6 x loading dye	Thermo Fisher Scientific Inc., MA, USA
Ampicillin	Sigma-Aldrich, MO, USA
Ampuwa	Fresenius Kabi, Bad Homburg, Germany
BSA	Sigma-Aldrich, MO, USA
D-Glucose Stock: 300 mg/mL	Sigma-Aldrich, MO, USA
Dapi, dilactate	Sigma-Aldrich, MO, USA
DMEM (1×) with sodium pyruvate	InvitrogenLifeTechnologies Ltd, Paisley, UK
DMEM/F-12 with GlutaMax	InvitrogenLifeTechnologies Ltd, Paisley, UK
DMEM with high glucose/GlutaMax/Hepes	InvitrogenLifeTechnologies Ltd, Paisley, UK
DMSO	Sigma-Aldrich, MO, USA
Doxycycline	Sigma-Aldrich, MO, USA
D-PBS (-$CaCl_2$, -$MgCl_2$)	InvitrogenLifeTechnologies Ltd, Paisley, UK
EBSS	InvitrogenLifeTechnologies Ltd, Paisley, UK
EDTA	Sigma-Aldrich, MO, USA
EGF	Pepro Tech, NJ, USA
EtBr (1 mg/mL)	CARL ROTH GMBH + CO. KG, Karlsruhe, Germany
Ethanol (96%)	Merck KGaA, Darmstadt, Germany
FBS (Ultra low Endotoxin)	PAA Laboratories GmbH, Pasching, Germany
FCS	InvitrogenLifeTechnologies Ltd, Paisley, UK
FGF-2	Pepro Tech, NJ, USA
Geneticin	InvitrogenLifeTechnologies Ltd, Paisley, UK
HBSS	InvitrogenLifeTechnologies Ltd, Paisley, UK
HCl (32%)	Merck KGaA, Darmstadt, Germany
HEPES 1M	InvitrogenLifeTechnologies Ltd, Paisley, UK
HTN-Cre (500 µM, dissolved in 50% glycerol, 500 mM NaCl, 20 mM HEPES)	provided by the lab
Hyaluronidase	Sigma-Aldrich, MO, USA
Isopropanol (96%)	Merck KGaA, Darmstadt, Germany
KCl	Merck KGaA, Darmstadt, Germany
L-Glutamine (200 mM)	InvitrogenLifeTechnologies Ltd, Paisley, UK
Lipofectamine 2000	InvitrogenLifeTechnologies Ltd, Paisley, UK
Methanol (100%)	Merck KGaA, Darmstadt, Germany
B27-supplement (100X)	InvitrogenLifeTechnologies Ltd, Paisley, UK
NaAc	Merck KGaA, Darmstadt, Germany
NaCl	Merck KGaA, Darmstadt, Germany
NaOH tablets	Merck KGaA, Darmstadt, Germany
Na-Pyruvate (100X)	InvitrogenLifeTechnologies Ltd, Paisley, UK
NEAA (100X)	InvitrogenLifeTechnologies Ltd, Paisley, UK
Normal donkey serum	Chemicon
Opti-MEM I Reduced serum medium	InvitrogenLifeTechnologies Ltd, Paisley, UK

PFA	CARL ROTH GMBH + CO. KG, Karlsruhe, Germany
Antibiotic-Antimycotic (100X)	InvitrogenLifeTechnologies Ltd, Paisley, UK
Puromycin	Sigma-Aldrich, MO, USA
Sucrose	
Tris-Base	Sigma-Aldrich, MO, SA
Triton X-100	CARL ROTH GMBH + CO. KG, Karlsruhe, Germany
Trypsin	Sigma-Aldrich, MO, USA
BrdU	Sigma-Aldrich, MO, USA
Poly-D-Lysine	Sigma-Aldrich, MO, USA
Laminin	InvitrogenLifeTechnologies Ltd, Paisley, UK
PMSF	AppliChem GmbH, Gatersleben, Germany
TEMED Electrophoresis Reagent	Sigma-Aldrich, MO, USA
Tween-20	CARL ROTH GMBH + CO. KG, Karlsruhe, Germany
APS	Sigma-Aldrich, MO, USA
SDS	CARL ROTH GMBH + CO. KG, Karlsruhe, Germany
DTT	Sigma-Aldrich, MO, USA
ß-Mercaptoethanol	Sigma-Aldrich, MO, USA
Acrylamid	Sigma-Aldrich, MO, USA
Complete Mini Protease Inhibitor Cocktail Mix	Hoffmann-La Roche, Basel, Switzerland
PhosSTOP Phosphatase Inhibitor Cocktail Tablets	Hoffmann-La Roche, Basel, Switzerland
Page Ruler Plus prestained protein ladder	Thermo Fisher Scientific Inc., MA, USA
Milk powder	Sigma-Aldrich, MO, USA

Pharmaceutical products

Midazolam (Dormicum®)	Hoffmann-La Roche, Basel, Switzerland
Medetomidine (Domitor®)	Pfizer Inc., New York, USA
Fentanyl (Fentanyl®)	Janssen-Cilag AG, New Brunswick, USA
Buprenorphine (Temgesic®)	Essex Pharma GmbH, Munich, Germany
Atipamezol (Antisedan®)	Pfizer Inc., New York, USA
Flumazenil (Anexate®)	Hexal AG, Holzkirchen, Germany

Enzymes and enzyme buffers

buffer neb2	New England Biolabs, MA, USA
buffer neb4	New England Biolabs, MA, USA
Ligase-buffer with ATP	New England Biolabs, MA, USA
NotI	New England Biolabs, MA, USA
PmeI	New England Biolabs, MA, USA
SfiI	New England Biolabs, MA, USA
T4-Ligase	New England Biolabs, MA, USA
iProof High-Fidelity DNA Polymerase	BioRad Laboratories, Inc, Munich, Germany
Brilliant II Fast SYBR Green qPCR Master Mix	Agilent, Boeblingen, Germany

Antibodies

Calbindin d28-K *α* mouse (1:1000)	Swant
DCX *α* goat (1:250)	Santa Cruz Biotechnology, CA, USA
Drp1 *α* rabbit (1:400)	Novus Biologicals, CO, USA
GFAP *α* rabbit (1:500)	DAKO cytomation, Hamburg, Germany
GFP *α* chicken (1:1000)	AVES Labs, Inc. Labs, Tigard, OR, USA
Map2a+b *α* mouse (1:250)	Sigma-Aldrich, MO, USA
Sox11 *α* goat (1:500)	Santa Cruz Biotechnology, CA, USA
Sox2 *α* goat (1:1000)	Santa Cruz Biotechnology, CA, USA
Sox2 *α* rabbit (1:1000)	Merck Millipore, Darmstadt, Germany
Sox10 *α* goat (1:200)	Santa Cruz Biotechnology, CA, USA
CytochromC *α* mouse (1:1000)	BD Pharmingen, NJ, USA
Complex2 *α* mouse (1:10000)	InvitrogenLifeTechnologies Ltd, Paisley, UK
GAPDH *α* mouse (1:1000)	Santa Cruz Biotechnology, CA, USA
Porin *α* mouse (1:1000)	InvitrogenLifeTechnologies Ltd, Paisley, UK
ß-actin *α* mouse (1:10000)	Abcam, Cambridge, UK
NeuroD *α* goat (1:200)	Santa Cruz Biotechnology, CA, USA
BrdU *α* rat (1:200)	Oxford Biotechnology Ltd., Oxford, UK
Prox1 *α* rabbit (1:2000)	CHEMICON International, Inc., Temecula, CA, USA
Ki67p *α* rabbit (1:1000)	Novocastra Ltd., Newcastle, UK
RFP *α* rat (1:50)	Prof. Dr. H. Leonhardt, LMU, Munich, Germany

Secondary antibodies coupled to the flourophores Cy3, Cy5, FITC, or Alexa 488 were obtained from Jackson Laboratory (ME, USA) and were used at a dilution of 1:250. Secondary antibodies conjugated to CF633 were obtained from Biotium, Inc (CA, USA) and used at a dilution of 1:1000.
Secondary antibodies conjugated to HRP (Horse reddish peroxidase) were obtained from Jackson Laboratory (ME, USA) and were used at a dilution of 1:10000.

Kits

NucleoSpin plasmid kit	Machery Nagel, Düren, Germany
NucleoSpin® Gel and PCR Clean-up	Machery Nagel, Düren, Germany
EndoFree Plasmid Maxi Kit	Qiagen, Hilden, Germany
RNeasy Mini-Kit	Qiagen, Hilden, Germany
Qiashredder	Qiagen, Hilden, Germany
RNAse-free DNAse-Set	Qiagen, Hilden, Germany
Fermentas RevertAid First Strand cDNA Synthesis Kit	Thermo Fisher Scientific Inc., MA-USA
Bradford Protein Assay	BioRad Laboratories, Inc, Munich, Germany
ECL solution for western blots	GE Healthcare, Munich, Germany

Other material

Aqua Poly/Mount	Polysciences Inc., Warrington, USA
Cellstar pipettes	Greiner bio-one, Frickenhausen, Germany
Cell strainer 70 µm	BD Falcon, NJ, USA
Cover slips	Menzel-Gläser, Braunschweig, Germany
Cryoblock	Medite Medizintechnik GmbH, Burgsdorf, Germany
glass cover slips	Menzel-Gläser, Braunschweig, Germany
Reaction tube 15 mL	BD Falcon, NJ, USA
Reaction tube 50 mL	BD Falcon, NJ, USA
Rotilabo 96 well Micro testplates, lids	CARL ROTH GMBH + CO. KG, Karlsruhe, Germany
Safe lock tube 1.5 mL	Eppendorf, Hamburg, Germany
Safe lock tube 2 mL	Eppendorf, Hamburg, Germany
SuperFrost microscope slides	Menzel-Gläser, Braunschweig, Germany
Surgical disposal scapels	Braun Melsungen AG, Melsungen, Germany
Tissue Culture ware 10 cm plates	BD Falcon, NJ, USA
Tissue Culture ware 24 well plate	BD Falcon, NJ, USA
Syringe (1 mL)	Braun Melsungen AG, Melsungen, Germany
20-gauge needle Sterican®	Braun Melsungen AG, Melsungen, Germany
ECL (Enhanced Chemilumiscence)	Amersham GE Healthcare, NJ, USA
PVDF-(Polyvinylidenfluorid) membrane	Pall Corporation, NY, USA

Organisms and cells

C57/Bl6J	Harlan Laboratories, Inc, IN-USA
DBA PDGF-α-synuclein	provided by Prof. J. Winkler, University Erlangen, Germany
C57/Bl6J cKOSox411/Sox11	provided by the lab
E. Coli Top10 (competent cells)	InvitrogenLifeTechnologies Ltd, Paisley, UK
1F8 (derived from HEK 293GPG cells)	provided by the lab
HEK 293T cells (human)	provided by the lab

Plasmids

pCAG GFP	(Zhao et al., 2006; Jagasia et al., 2009)
pCAG IRES-GFP	(Zhao et al., 2006; Jagasia et al., 2009)
pCAG GFP-IRES-CRE	(Mu et al., 2012)
pCAG Sox11-IRES-GFP	(Mu et al., 2012)
pCAG IRES-mitodsRed	InvitrogenLifeTechnologies Ltd, Paisley, UK
pCAG wtdrp1-IRES-mitodsRed	(Smirnova et al., 1998; Frank et al., 2001)
pCAG dndrp1-IRES-mitodsRed	(Smirnova et al., 1998; Frank et al., 2001)
pCAG msdrp1 (incl.Ex3)-IRES-mitodsRed	ENSMUST00000115749
pCAG msdrp1 (full length)-IRES-mitodsRed	ENSMUST00000096229

Primers for cloning

Target		**Sequence (5'-3' direction)**
		GA GGCCGCCTGGGCC
Drp1	forward	ATGGAGGCGCTAATTCCTG
Drp1	reverse	GA GTTTAAAC TCACCAAAGATGAGTCTCCC
Drp1 Exon 3	forward	GTGGGAAGAGCTCAGTGCTGGAAAGC
	reverse	TTCATTTTCAATTTCTTGTCGAAT
Drp1 Exon 16 17	forward	CTTAGTGGCAATTGAGCTAGCGTATATC
	reverse	TGATAAGTCTTTCAATAACCTCACAA

Primers for qPCR

Target		**Sequence (5'-3' direction)**
Srp14	forward	CAGCGTGTTCATCACCCTCAA
	reverse	GGCTCTCAACAGACACTTGTTTT
VDAC1 (Porin)	forward	GGGGATGCGAGAGTTGATAA
	reverse	GGAATGGGGTTTCTGCTGTA
Drp1 mus 3'UTR	forward	TTCCACGCCAACAGAATACA
	reverse	ACCCTAACCCCCTGAATGAA
Tubb3	forward	TAGACCCCAGCGGCAACTAT
	reverse	GTTCCAGGTTCCAAGTCCACC
Tubb4a	forward	GGAAAGCTGCGACTGTCTCC
	reverse	ATGATCCTGTCTGGAAACTCCT
Tubb6	forward	ACCCACTTACGGGGACCTC
	reverse	GCCAGGGAAACGCAGTGAT
Tuba1c	forward	GCCCTACAATTCCATCCTCA
	reverse	TAAGGCGGTTAAGGTTGGTG
Tubb5	forward	GATCGGTGCTAAGTTCTGGGA
	reverse	AGGGACATACTTGCCACCTGT
PolG	forward	TCAGAACCAGGACACCAACA
	reverse	CACAGCAGGACAGAGAACCA
Sox11	forward	CCCTGTCGCTGGTGGATAAG
	reverse	GGTCGGAGAAGTTCGCCTC
Tfam	forward	CCGAAGTGTTTTTCCAGCAT
	reverse	CAGGGCTGCAATTTTCCTAA
PGC1-alpha	forward	ATGTGTCGCCTTCTTGCTCT
	reverse	ATCTACTGCCTGGGGACCTT
DCX	forward	TGCTCAAGCCAGAGAGAACA
	reverse	CTGCTTTCCATCAAGGGTGT

Solutions for Immunohisto- and Immunocytochemistry

2 N HCl:

9.5 mL	H_2O
2.5 mL	HCl (conc.)

Blocking solution brainslices:
3% donkey serum
0.25% Triton-X-100
in TBS

Blocking solution cells:
1% donkey serum
1% Triton-X-100
in TBS

Cryoprotectant:
250 mL Glycine
250 mL Ethylene Glycol
500 mL 0.1 M Phosphate buffer

Phosphate-Buffer (0.2 M)
16.6 g Sodium phosphate monobasic monohydrate
65.7 g Sodium phosphate dibasic dehydrated
@ 3 L H_2O

PFA (4%):
40 g PFA
500 mL Dissolve in H_2O
Add one NaOH-tablet and warm until solution is clear
500 mL 0.2 M Phosphate buffer
Adjust pH 7.4 (Solution needs to be at RT)

PBS (10×):
80.0 g NaCl
2.0 g KCl
14.4 g Na_2HPO_4
2.4 g KH_2PO_4
Dissolve in 800 mL H_2O.
Adjust to pH 7.2 with HCl

TBS (10×):
80.0 g NaCl
2.0 g KCl
250 mL Tris/HCl pH 7.5 (1 M)
@ 1 L H_2O

Sucrose (30%):
150 g Sucrose
500 mL 0.1 M Phosphate buffer.
Store at 4 °C.

Molecular Biology solutions

Agar plates:
Ready made LB Agar + antibiotic:
100 µg/mL Ampicillin

TAE (50X):
242 g Tris Base
57.1 mL Glacial acetic acid
100 mL 0.5 M EDTA pH 8.0
@ 1 L H_2O

Solutions for Proteinbiochemistry

Buffer A for protein isolation:
10 mM Hepes
1 mM EDTA
1 mM EGTA
10 mM KCl
1.5 mM $MgCl_2$

TBST

0.1% Tween in TBS (1X)

SDS-Page Transfer buffer
25 mM Tris base
192 mM Glycine
20% Methanol

Tris-Running buffer (10×)

250 mM TrisBase
1.9 M Glycin
1% SDS

Laemmli buffer

20 mM SDS
480 mM Glycerine
300 mM Tris/HCl, pH 6.8
0.4 mM ß-Mercaptoethanol

Upper Tris

0.5 M Tris
0.4% SDS
pH 6.8

Lower Tris

1.5 M Tris
0.4% SDS
pH 8.8

Stacking gel:

0.625 mL	Upper Tris
1.563 mL	ddH_2O
0.312 mL	acrylamide (40%)
3 µL	TEMED
15 µL	APS (10%)

Resolving gel

1.25 mL	Lower Tris
2.5 mL	ddH_2O l
1.25 mL	acrylamide (40%)
5 µL	TEMED
20 µL	APS (10%)

Solutions for preparation and culturing of mouse neural stem cells

Solution #1

50 mL	HBSS
9.0 mL	D-Glucose (Stock: 300 mg/mL)
7.5 mL	HEPES (1 M)

ddH_2O Bring to final volume 500 mL
Adjust pH to 7.5

Solution #2

25 mL	HBSS
154 g	Sucrose

ddH_2O Bring to final volume 500 mL
Adjust pH to 7.5

Solution #3

20 g	BSA
10 mL	HEPES (1 M)

EBSS (Life Tech, 1x) Bring to final volume 500 mL.
Adjust pH to 7.5

Neurosphere Media

47 mL	DMEM/F12
1 mL	B 27 supplement
0.5 mL	Antibiotic-Antimycotic (100×)
0.4 mL	HEPES (1 M)
50 µL	EGF (stock 20 µg/mL)
100 µL	BFGF (stock 10 µg/mL)

Dissociation media

10 mL	Solution #1
13.3 mg	Trypsin
7.0 mg	Hyaluronidase

Equipment

Hardware

accu-jet pro	BRAND GMBH + CO KG, Würzburg, Germany
Neubauer counting chamber	BRAND GMBH + CO KG, Würzburg, Germany
StepOnePlus Real-Time PCR System	Applied Biosystems, Inc, CA, USA
Nanodrop	PEQLAB Biotechnologie GMBH, Erlangen, Germany
Centrifuge 5415 D	Eppendorf, Hamburg, Germany
Centrifuge 5417 R	Eppendorf, Hamburg, Germany
Fluorescence microscope DMI 6000B	Leica, Wetzlar, Germany
Gelsystem Mini	PEQLAB Biotechnologie GMBH, Erlangen, Germany
HeraCell 150 incubator	Kendro, Hanau, Germany
HeraCell Tissue Culture hood	Kendro, Hanau, Germany
Leica SP5 confocal microscope	Leica, Wetzlar, Germany
Power supply	BioRad Laboratories, Inc, Munich, Germany
RH-5 darkroom hood (with transilluminator)	Herolab, wiesloch, Germany
Rotamax 150	Heidolph Instruments GmbH & Co.KG, fürth, Germany
SM2000R sliding microtome	Leica, Wetzlar, Germany
Sorvall Evolution High Speed Centrifuge	Thermo Fisher Scientific Inc., MA, USA
Thermomixer comfort	Eppendorf, Hamburg, Germany
PCR-Cycler	Eppendorf, Hamburg, Germany
Nanoliter 2000	WPI Inc. FL, USA
Micro4 controller	WPI Inc. FL, USA
Stereotactic Instrument	WPI Inc. FL, USA
Mini Protean 3 System	BioRad Laboratories, Inc, Munich, Germany
Semidry blotting chamber	BioRad Laboratories, Inc, Munich, Germany
Fusion SL Chemiluminiscence System	PEQLAB Biotechnologie GMBH, Erlangen, Germany

Software

LAS AF 2.5	Leica, Wetzlar, Germany
Imaris 6.3	Bitplane, Zürich, Switzerland
Fusion (1.0)	PEQLAB Biotechnologie GMBH, Erlangen, Germany
Vector NTI	InvitrogenLifeTechnologies Ltd, Paisley, UK
StepOne 2.0	Applied Biosystems, Inc, CA, USA
Primer3	http://primer3.sourceforge.net
NetPrimer	http://www.premierbiosoft.com

4.2. Methods

4.2.1. Plasmid production

Plasmid transformation in bacteria

For a transformation 0.5 µL of plasmid DNA were added to 100 µL chemo-competent E. coli Top10 (Invitrogen Life Technologies Ltd, Paisley, UK). The mixture was incubated for 20 min on ice and heat-shocked at 42 °C for 30 sec. After adding 500 µL of LB-medium the bacteria were subsequently incubated at 37 °C and 400 rpm for 1 h. 50 µL of transformed bacteria were plated on agar plates containing 100 µg/µL of ampicillin and incubated at 37 °C overnight.

Cultivation of bacteria and plasmid isolation

Transformed bacteria (E. coli strain Top10), containing the Amp-resistance containing plasmid, were incubated in LB-Amp medium overnight at 37 °C on a shaker. Depending on the desired amount of DNA the culture volume was between 5 mL and 200 mL. For smaller amounts, NucleoSpin plasmid kit (Machery Nagel, Düren, Germany, according to the protocol) was used.

To purify up to 1500 µg Endotoxin free DNA, EndoFree Plasmid Maxi Kit (Qiagen, Hilden, Germany) was used according to the provided manual. The concentration as well as the purity of the isolated DNA was determined by measuring the absorption at λ = 260 nm and λ = 280 nm with a NanoDrop (Thermo Fisher Scientific Inc., Waltham, USA) UV-spectrometer.

4.2.2. Molecular Cloning

Cloning PCR reaction

Cloning of cDNA was performed by PCR reaction in Eppendorf ThermoCyclers using iProof proof reading Polymerase (BioRad, Munich, Germany) and PCR reaction was set up according to the manufacturer's instructions. Primers that were used contained the gene specific 5' and 3' sequences and Sfi1 (5') and Pme1 (3') overhangs to allow direct cloning into the retroviral backbones. Templates were either cDNA, generated from total RNA extracts from the mouse dentate gyrus, or plasmid DNA containing the specific cDNA sequence.

Restriction digest

For a restricion digest, 0.5 µg plasmid DNA was mixed with 1 µL of the appropriate enzymes (20 U/µL) (neb, Frankfurt am Main, Germany) and 2 µL of the matching buffer. The digest was adjusted to a total volume of 20 µL with water and incubated at 37 °C for 2 h.

Analysis of restriction digest by agarose gel electrophoresis and gel purification

To separate and analyze DNA, agarose gel electrophoresis was performed. 1% agarose/TAE-gel was prepared by heating the solution in a microwave oven. To visualize DNA gels were supplemented with 0.02 µL/mL EtBr which allows the detection of nuleic acids at λ = 254 nm. The DNA solution was mixed with 6× loading dye in order to load it on the gel and the DNA fragments were subsequently separated in a constant electric field. The size of the DNA fragments was determined by loading 10 µL of 1 kb DNA ladder (prepared according to the provided protocol) on the gel with the specified digested samples. To isolate the appropriate DNA fragment, the gel was analyzed under UV-light and the correct band was excised with a scalpel. To purify DNA from the gel, NucleoSpin® Gel and PCR Clean-up (Machery Nagel, Düren, Germany) was used according to the manufacturer's protocol and the DNA was eluted in 15 µL water. The concentration was measured as described above.

Ligation

To perform a ligation 2 µL T4-Ligase and 3 µL Ligase-buffer containing ATP were added to the appropriate mixture of digested backbone and insert. The proper ratio was calculated by the formula:

$$m_i = 5 * m_v * \ l_i \ / l_v$$

The reaction was adjusted to 30 µL with sterile water and incubated for 2 h at RT.

Transformation of bacteria with Ligation product

To transform the ligated products in bacteria the protocol described before was used, but 15 µL of the ligation were added to bacteria, the heatshock time was extended up to 60 sec and all bacteria were plated on a LB-Amp plate after short centrifugation (1000 rcf).

Identification of positive clones

To identify positive clones, single colonies were picked from the plate and were cultivated in 3 mL overnight at 37 °C. After plasmid isolation, DNA was digested and analyzed by agarose gel electrophoresis.

4.2.3. RNA Methods

RNA isolation and DNAse treatment

Total RNA was isolated from cells, micro-dissected dentate gyrus or whole hippocampus, by using RNeasy Mini-Kit (Qiagen, Hilden, Germany) according to the manufacturer's protocol. Tissue was homogenized by passing the lysate through a 20-gauge-needle fitted on a 1 mL RNAse-free syringe (Braun AG, Melsungen, Germany) until completely dissociated. For homogenization of cells Qiashredder colums (Qiagen, Hilden, Germany) were used. To eliminate genomic DNA contamination, on-colum DNAse treatment was performed by using RNAse-free DNAse-Set (Qiagen, Hilden, Germany) according to the manufacturer's protocol. Isolated RNA was eluted in 30 µL RNAse-free water and the concentration determined with a NanoDrop (Thermo Fisher Scientific Inc., Waltham, USA) UV-spectrometer. RNA was immediately used for cDNA synthesis or stored at −80 °C.

cDNA synthesis

For cDNA-synthesis 300 ng of total RNA were adjusted with RNAse-free water to a volume of 12.5 µL. Fermentas RevertAid First Strand cDNA Synthesis Kit (Thermo Fisher Scientific Inc., MA-USA) was used according to the manufacturer's protocol. If cDNA was synthesized for cloning, random hexamer primer were used, for quantitative real-time PCR (qPCR) cDNA synthesis was carried out using, oligo(dt)$_{18}$ primer. cDNA was stored at −20 °C.

Quantitative real-time-PCR (qPCR)

Quantitative RT-PCR was performed using StepOnePlus™ Real-Time PCR System (Applied Biosystems, Inc, CA-USA). Brilliant II Fast SYBR Green qPCR Master Mix (Agilent, Boeblingen, Germany) was used for PCR reactions according to the manufacturer's protocol. qPCR primers were designed using softwares Primer3 (http://primer3.sourceforge.net) and NetPrimer (http://www.premierbiosoft.com). Amplicon sizes ranged from 100-250 bp. Suitability of qPCR Primer was analyzed by evaluation of melting curves and by determination of the efficiency via a standard curve. For quantitative expression analysis, the comparative CT (ΔΔCT) method was applied to determine the relative quantity of target sequence using a reference sample (control) and an endogenous control target sequence.

4.2.4. Protein Methods

Isolation of proteins

Proteins were isolated from harvested cells, micro-dissected dentate gyrus or whole hippocampus. After incubation for 15 min on ice in Lysis buffer (Buffer A, containing Protease-Inhibitor (10×), Phospho-Stop (10X), PMSF (final conc. 200 mM) and DTT (final conc. 0.1%)), NP-40 was added to a final concentration of 0.1%. After further incubation on ice for 5 min, NaCl was added to the lysates to a final concentration of 400 mM followed by incubation on ice for 30 min. Lysates were centrifuged for 5 min at 16.000 g at 4 °C to remove insolubilized cell membranes and pellets. Protein concentration was determined with a Bradford Protein assay (BioRad) using BSA as a standard. Proteins were frozen in liquid nitrogen and stored at -80°C.

SDS-polyacrylamide gel electrophoresis (SDS-Page)

For protein separation according to the molecular weight, SDS-Page using a Mini Protean 3 System (BioRad) was applied. Proteins were denaturized in Laemmli buffer at 95 °C for 10 min. 30 µg proteins were loaded in separate wells on a 5% acrylamide gel (stacking gel) and separated in a 10% acrylamide gel (resolving gel) in TRIS-running buffer at 120 V. Protein size was determined using Page Ruler Plus prestained protein ladder (Thermo-Scientific).

Western blot analysis

For detection of specific proteins, separated proteins were transferred on a methanol-activated PVDF membrane using a semidry blotting chamber (BioRad). Blotting was performed with a constant current of 0.1 A for 1 h. After protein transfer, membrane was incubated in 5% milk powder in TBST for 1 h to avoid unspecific antibody binding, and followed by incubation with the primary antibodies overnight. Membranes were washed three times in TBST before incubation with peroxidase-conjugated secondary antibodies (in TBST; 1:10000) for 60 min. Protein bands were visualized using ECL-solution (Enhanced chemilumiscence, Amersham GE Healthcare) and camera detection (Peqlab). Relative protein amounts were quantified using the Fusion software (1.0).

4.2.5. Cell culture

Culturing of HEK 293T cells

HEK 293T-cells cells were cultured in DMEM 1× (GIBCO Life Technologies Ltd, Paisley, UK, 41966, 4.5 g/L Glucose, L-Glutamine and Pyruvate) supplemented with Antibiotic-Antimycotic (GIBCO Life Technologies Ltd, Paisley, UK, 100x) and FBS (PAA, 100x). Cells were incubated at 37 °C with 5% CO_2. 500 mL DMEM were supplemented with 5 mL PSF (GIBCO Life Technologies Ltd, Paisley, UK) and 55 mL FBS (PAA). For splitting the cells, trypsine with EDTA (0.05%) (GIBCO Life Technologies Ltd, Paisley, UK) was used.

Calciumchloride Transfection

To test functionality of virus plasmids, HEK 293-T-cells were transfected. 50000 cells/well were plated on an uncoated but sterilized 24-well plate with glass cover slips. Transfection was performed on the next day when cells reached 80% confluency. 1 µg of DNA was adjusted to a volume of 547.5 µL sterile water. Then 77.5 µL $CaCl_2$ were added

and mixed with a pipette. 625 µL of 2× HBS were added slowly and dropwise while shaking. After waiting for approximately 3 min. 100 µL of transfection mix was put slowly in each well. Cells were fixed 48 h after transfection.

Preparation of neural stem cells from mouse brains

Conditional Sox4/Sox11 knock out animals were sacrificed via cervical dislocation and brains were kept in ice cold PBS. SVZ and HC were dissected under a binocular microscope. The tissue was dissociated by incubation for in total 30 minutes in 5 mL dissociation media at 37 °C and occasionally mechanically resuspended. The dissociation reaction was stopped by adding 5 mL of solution #3. Cells were passed through a 70 µm strainer to remove the tissue debris. Centrifugation was carried out at 1300 rpm for 10 min and supernatant was discarded afterwards. Cells were resuspended in 10 mL ice cold solution #2, and centrifuged at 1500 rpm for 1 min. Supernatant was removed and cells were resuspended in 2 mL ice cold solution #3. The 2 mL cell solution was carefully added on 12 mL ice cold solution #3 and centrifuged at 1000 rpm for 10 min. Supernatant was removed and cells were resuspended in neurosphere media (DMEMF12 with B27 supplement, 1 M HEPES buffer and Antibiotic-Antimycotic (all GIBCO Life Technologies Ltd, Paisley, UK).

Passaging of mouse neurospheres

Neurospheres were collected in a 15 mL tube and centrifuged at 500 rpm for 5 min. Supernatant was discarded and cells were resuspended in 1 mL accutase and incubated for 5 min at 37 °C. Neurospheres were dissociated into single cells by pipetting up and down. After centrifugation at 1500 rpm for 5 min cells were washed two times with 5 mL PBS. Cells were resuspended in 1 mL neurosphere media and cell number was determined by using a Neubauer counting chamber. 200 000 cells were passaged in a 75 cm^2 in 20 mL neurosphere media. Fresh EGF and FGF-2 (20 µg/mL) was added to the cultures every 2 days. Neurospheres were passaged on approximately every seven days.

Differentiation of mouse neurospheres

For differentiation experiments 24-well plates with glass covers slips were coated by overnight incubation with 50 µg/mL poly-D-Lysine/water at RT, and subsequent incubation with 5 µg/mL Laminin/DPBS at 37 °C overnight.

Neurospheres were dissociated and 100 000 cells/well were seeded in a 24-well plate containing coated cover slips to obtain monolayer cultures. Cells were cultivated without EGF and FGF-2 and fixed with 4% PFA/PBS after 4 days of differentiation.

Immunocytochemistry

After 3 times washing in TBS, cells were blocked with 1% donkey serum and 0.1% Triton-X-100 in TBS for 2 h and following incubated with the respective primary antibodies diluted in blocking solution overnight at 4 °C. Cells were washed three times with TBS and blocked again with for 30 min, and subsequently incubated with secondary antibodies for 2 h at RT. After washing cells once with TBS, cells were put in TBS with Dapi (10 mg/mL) for 5 min and then washed a last time with TBS. Finally, glass cover slips with cells were mounted on slides using Aqua/PolyMount and stored at 4 °C till used for microscopy.

Expression profiling

For expression profiling, neurospheres isolated from cKO Sox4/Sox11 animals were plated on 12 poly-D-Lysine (here 10 µg/mL) and laminin coated 10 cm culture dishes in a density of 2 mio cells/plate and cultivated in neurosphere media under proliferating conditions with EGF and FGF-2. On the next day, Sox4/Sox11 knock out was introduced in half of the plates by protein transduction via adding 0.75 µM of HTN-Cre to the dish. Controls were treated with the solvent (50% glycerol, 500 mM NaCl, 20 mM Hepes, pH 7.4). Medium was exchanged after approximately 12 hours to avoid toxic effects by the Cre protein. Cells were harvested two days after transduction, and RNA isolation, cDNA synthesis and qPCR performed as described above (see 4.2.3) to confirm knock out of Sox11.

Expression profiling was carried out in collaboration by Dr. M. Irmler (Institute of Experimental Genetics, Helmholtz-Zentrum München, Germany). Briefly, RNA integrity from each 6 samples knock out and control cells was evaluated using 2100 Bioanalyzer (Agilent Technologies, Inc., CA, USA). Micro array hybridization was carried out as recommended by the manufacturer's protocol using Affymetrix mouse gene St 2.0 (Affymetrix, CA, USA). Data was analyzed with the software Ingenuity (Ingenuity Systems, CA, USA) and Genomatix Pathway System (GePS) (Genomatix Software GmbH, Munich, Germany). Selected, differentially regulated probe sets were validated by qPCR.

4.2.6. Virus preparation

The pCAG GFP, pCAG IRES-GFP, pCAG GFP-IRES-CRE and pCAG Sox11-IRES-GFP retrovirus have been previously described (Tashiro et al., 2006a; Jagasia et al., 2009; Mu et al., 2012). CAG IRES-mitodsRed was generated from the pCAG IRES-GFP vector by replacing the GFP coding sequence with cDNA for mitochondrially targeted Dsred (mitoDsred). For retrovirus mediated expression of human dynamin-related protein 1 transcript variant 3 (ENST00000266481) (wtdrp1) and dominant-negative $Drp1^{K38A}$ (dndrp1) (Smirnova et al., 1998; Frank et al., 2001), their respective cDNAs were cloned into the pCAG IRES-mitoDsred to generate pCAG wtdrp1-IRES-mitoDsRed and pCAG dndrp1-IRES-mitoDsred. cDNAs for mouse drp1 transcript variants 1 (ENSMUST00000115749) and 2 (ENSMUST00000096229) were synthesized from RNA isolated from the mouse dentate gyrus and cloned into pCAG IRES mitoDsred as described above to generate pCAG ms drp1 (incl.Ex3)-IRES-mitoDsred and pCAG ms drp1 (full length)-IRES-mitoDsred.

For retrovirus production HEK 293 GPG-1F8 cells were used (Ory et al., 1996). These cells constitutively express the gag and pol genes of MMLV. The VSVG gene is under the control of a tetracycline responsive promoter and can be induced upon withdrawal of tetracycline. The viral RNA is encoded by a transiently transfected retroviral expression plasmid, minimally containing the 3' and 5' LTRs of MMLV, the retroviral packaging signal psi, a primer binding site for the retroviral reverse transcriptase and the cDNA of interest.

The cells were maintained in basal medium (DMEM High Glucose/GlutaMax/Hepes containing FCS (100×), NEAA (100×) and Na-Pyruvate (100×)) under double-selection (Geneticin (100 mg/mL) and Puromycin (2 mg/mL)) and Tet-repression (Tetracycline (1 mg/mL)).

For retrovirus preparation per culture dish 25 µg of the plasmid DNA of interest diluted in 1.5 mL Opti-MEM medium were mixed with 60 µL Lipofectamine 2000 (Invitrogen) in 1.5 mL Opti-MEM medium added to the resuspended cells (2-3 confluent 175 cm^2 flasks for 6 culture dishes in 30 mL Opti-MEM with 10% FCS). Cells were seeded on 10 cm culture dishes. After one day medium was exchanged to packaging medium (basal medium without NEAA and Na-Pyruvate). Virus-containing supernatant was harvested four times, (2, 4, 6 and 8 days after transfection), and concentrated by two rounds of ultracentrifugation (Tashiro et al., 2006a).

Virus Titering

To determine titers of the produced viruses, HEK 293T cells were plated on a uncoated but sterilized 24-well plate with glass cover slips (30000 cells/well). Different wells with cells were transduced 1 h later with the following volumes of virus: 0.01 µL, 0.005 µL. 0.001 µL and 0.0005 µL. Cells were fixed 72 h after transduction and number of colony forming units (cfu) quantified to calculate virus titers. Viral titers ranged between 1.0×10^8 and 1.0×10^{10} cfu × mL^{-1}.

4.2.7. Animals and Stereotactic Injections

All experiments were carried out in accordance with the European Communities Council Directive (86/609/EEC). All mice were kept in a normal light dark-cycle (12 hours light/12 hours dark) and had free access to food and water. For α-synuclein studies, male and female mice overexpressing wildtype α-synuclein under a PDGF-Promoter (genetic background DBA) (Rockenstein et al., 2002) were compared to non-transgenic littermates. The age of the mice was 8 weeks or 16 weeks, respectively. For all Sox4/11 loss-of-function experiments, male and female mice (8 weeks) of mixed 129SvJ/C57Bl6J background carrying Sox4loxP and Sox11loxP alleles were used (Penzo-Mendez et al., 2007; Bhattaram et al., 2010; Mu et al., 2012). All other animal experiments were performed with 8 weeks old female C57BL/6J mice (Harlan Laboratories, Inc, IN-USA). For creatine-diet experiments, starting at the age of 4 weeks, mice were fed with a standard rodent diet containing 1% creatine (Bender et al., 2008). Mice had unlimited access to running wheels, when experiments were performed under running conditions.

For BrdU retention experiments, 50 mg/kg BrdU/0.9% NaCl was injected intra parenteral once per day for 3 consecutive days.

For stereotactic injections, mice were deeply anesthetized by injecting 350 µL of the following mixture: 0.05 mg/kg Fentanyl (Janssen-Cilag AG, New Brunswick, USA), 5 mg/kg Midazolam (Dormicum, Hoffmann-La Roche, Basel, Switzerland) and 0.5 mg/kg Medetomidine (Domitor, Pfizer Inc., New York, USA) dissolved in 0.9% NaCl. Mice were stereotactically injected at a speed of 250 nL/minute with 0.9 µL the retroviruses with a titer of 2×10^8 cfu × mL^{-1} into the left and right dentate gyrus (coordinates from bregma were -1.9 anterior/posterior, ±1.6 medial/lateral, -1.9 dorsal/ventral from dura). Anasthesia was antagonized after surgery by injecting 400 µL of the following mixture: 0.1 mg/kg Buprenorphine (Temgesic, Essex Pharma GmbH, Munich, Germany),

2.5 mg/kg Atipamezol (Antisedan, Pfizer Inc., New York, USA) and 0.5 mg/kg Flumazenil (Anexate, Hexal AG, Holzkirchen, Germany) dissolved in 0.9% NaCl.

4.2.8. Tissue Processing

Animals were sacrificed using CO_2. Animals were transcardially perfused with approximately 100 mL PBS (pH 7.4) for 5 min followed by approximately 100 mL 4% paraformaldehyde (PFA/PBS) at the respective time points. Post fixation was performed in 4% PFA/PBS for 12 h at 4 °C and brains were subsequently transferred to a 30% sucrose solution. 40 µm and 100 µm thick coronal brain sections were produced using a sliding microtome (Leica Microsystems, Wetzlar, Germany) for phenotyping and morphological analysis of retrovirally manipulated cells, respectively. Sections were stored in a cryoprotectant solution at −20 °C until processed further.

4.2.9. Histology procedures

Appropriate free floating sections for staining were collected in 0.1 M phosphate buffer and rinsed 3 times (each 15 min) in TBS. Sections were blocked in TBS supplemented with 3% donkey serum and 0.25% Triton-X-100 for 2 h and then incubated with primary antibodies dissolved in blocking solution at 4 °C for 24-48 h. Primary antibodies against the following antigens were used: Sox2 (goat, Santa Cruz, 1:1000), Sox2 (rabbit, Millipore, 1:1000), GFAP (rabbit, Dako, 1:500), DCX (goat, Santa Cruz Biotechnology, 1:250), Calbindin (rabbit, Swant, 1:1000), GFP (chicken, Aves Labs, 1:1000), RFP (rat, Prof. Dr. Heinrich Leonhardt, LMU Munich, 1:50), CytochromC (mouse, BD Pharmingen, 1:1000), BrdU (rat, Oxford Biotechnology Ltd., 1:200), Prox1 (rabbit, Chemicon, 1:2000). After washing 3 times in TBS (each 15 min) and blocking for 30 min, sections were incubated in blocking solution containing secondary antibodies conjugated to FITC, Alexa488, Cy3, Cy5 or CF633 for 2 h. Sections were rinsed again 3 times in TBS, one wash step containing Dapi (10 mg/mL). Sections were mounted using SuperFrost microscope slides (Menzel-Gläser, Braunschweig, Germany) and Aqua/PolyMount (Polysciences Inc., Warrington, USA) and stored at 4 °C.

For BrdU detection, sections were pretreated with 2 N HCl for 30 min at 37 °C followed by incubation in borate buffer (0.1 M, 10 min) and 90 min washing in TBS before staining.

4.2.10. Phenotyping of cells

To phenotype genetically manipulated cells, transduced cells were evaluated for the expression of stage specific markers (Sox2, DCX, Calbindin, Sox10, GFAP, Ki67). At least 50-100 cells from 4-6 sections of the same regions from at least 3 different animals were analyzed. For BrdU retention experiments, number of BrdU positive cells was quantified and the size of the dentate gyrus measured in 6 different sections from at least 3 animals.

4.2.11. Morphology analysis

Global morphology analysis

To analyze the overall size of a large number of cells, confocal images of the dentate gyrus from several sections were obtained with a 40× oil objective using a Leica TCS Sp5 confocal microscope (Leica Microsystems, Wetzlar, Germany) (step size 0.7 µm, resolution 1024×1024). 25-50 double-transduced cells expressing the fluorescent markers (GFP and mitoDsred) per animal from at least 3 different animals were analyzed by measuring the maximum extension of the cell (distance soma to end of longest dendrite) and the maximum possible extension (distance soma to hippocampal fissure), by this normalizing the analysis to the specific hippocampus position. The cumulative distribution of the measured ratios was compared.

Cell specific analysis of cell length and complexity

To analyze detailed cell morphology, confocal images of double-transduced cells expressing the fluorescent markers (GFP and mitoDsred) were obtained with a 63× glycerol objective using Leica TCS Sp5 confocal microscope (Leica Microsystems, Wetzlar, Germany) (step size 0.3 µm, resolution 1024×1024). 100 µm sections from the same hippocampal position were used to avoid differences due to truncated cells and different positioning, respectively. 10-12 cells per group from at least 3 different animals were analyzed. 3D reconstructions were obtained by using the Filament Tracer tool in Imaris (Bitplane AG, Zürich, Switzerland), and values for total dendritic length, number of branch points and number of sholl intersections (Sholl, 1953) compared.

Morphological analysis of synaptic integration

To analyze morphological synaptic integration of transduced cells, confocal images of at least 10 dendrites in the mid-third of the molecular layer from 10 different double-transduced cells expressing a fluorescent marker (GFP and mitoDsred) were obtained

with a 63× glycerol objective using Leica TCS Sp5 confocal microscope (Leica Microsystems, Wetzlar, Germany) (step size system optimized, resolution 1024×1024, 5× zoom). Length of dendrites was measured using LAS AF software (Leica Microsystems, Wetzlar, Germany) and number of dendritic spines quantified. Spine number was normalized to dendritic length and compared. To analyze maturation of spines, number of mushroom spines (spine head > 0.6 µm) was quantified and percentage of total spine number calculated.

Analysis of mitochondrial volume, number and distribution

Mitochondria volumes were analyzed by reconstruction of mitochondria using the surface tool in Imaris (Bitplane AG, Zürich, Switzerland) in the same confocal images that were used for the morphology analyses. Mitochondria number and volume was reconstructed from the mitoDsred fluorescence. Laser intensity was set to the same signal saturation.

Mitochondria density was also quantified in dendrites that were analyzed for spine density.

Mitochondria distribution was analyzed by dividing 3D-reconstructed cells into 3 parts (using Imaris Measurement Tool): 0-50 µm radius from soma, 50-100 µm radius from soma and above 100 µm radius from soma. Mitochondria volume and number was individually calculated per section.

4.2.12. Statistics

Significance levels for global morphology analysis were assessed with 2-way Anova. For all other data, I used the unpaired Student's T-test with unequal variances. Differences were considered statistically significant at *$p<0.05$, **$p<0.01$ and ***$p<0.001$. All data are presented as mean ± SEM (standard error of the mean).

5. References

Ables JL, Breunig JJ, Eisch AJ, Rakic P (2011) Not(ch) just development: Notch signalling in the adult brain. Nat Rev Neurosci 12:269-283.

Ahlqvist KJ, Hämäläinen RH, Yatsuga S, Uutela M, Terzioglu M, Götz A, Forsström S, Salven P, Angers-Loustau A, Kopra OH (2012) Somatic progenitor cell vulnerability to mitochondrial DNA mutagenesis underlies progeroid phenotypes in Polg mutator mice. Cell Metabolism 15:100-109.

Aimone JB, Wiles J, Gage FH (2009) Computational Influence of Adult Neurogenesis on Memory Encoding. Neuron 61:187-202.

Aimone James B, Deng W, Gage Fred H (2011) Resolving New Memories: A Critical Look at the Dentate Gyrus, Adult Neurogenesis, and Pattern Separation. Neuron 70:589-596.

Alfieri RR, Bonelli MA, Cavazzoni A, Brigotti M, Fumarola C, Sestili P, Mozzoni P, De Palma G, Mutti A, Carnicelli D, Vacondio F, Silva C, Borghetti AF, Wheeler KP, Petronini PG (2006) Creatine as a compatible osmolyte in muscle cells exposed to hypertonic stress. The Journal of Physiology 576:391-401.

Alme CB, Buzzetti RA, Marrone DF, Leutgeb JK, Chawla MK, Schaner MJ, Bohanick JD, Khoboko T, Leutgeb S, Moser EI, Moser MB, McNaughton BL, Barnes CA (2010) Hippocampal granule cells opt for early retirement. Hippocampus 20:1109-1123.

Altman J (1969) Autoradiographic and histological studies of postnatal neurogenesis. IV. Cell proliferation and migration in the anterior forebrain, with special reference to persisting neurogenesis in the olfactory bulb. The Journal of Comparative Neurology 137:433-457.

Alvarez-Buylla A, García-Verdugo JM (2002) Neurogenesis in Adult Subventricular Zone. The Journal of Neuroscience 22:629-634.

Andreassen OA, Jenkins BG, Dedeoglu A, Ferrante KL, Bogdanov MB, Kaddurah-Daouk R, Beal MF (2001) Increases in cortical glutamate concentrations in transgenic amyotrophic lateral sclerosis mice are attenuated by creatine supplementation. Journal of Neurochemistry 77:383-390.

Andres RH, Ducray AD, Schlattner U, Wallimann T, Widmer HR (2008) Functions and effects of creatine in the central nervous system. Brain research bulletin 76:329-343.

Baar K, Wende AR, Jones TE, Marison M, Nolte LA, Chen MAY, Kelly DP, Holloszy JO (2002) Adaptations of skeletal muscle to exercise: rapid increase in the transcriptional coactivator PGC-1. The FASEB Journal 16:1879-1886.

Baba M, Nakajo S, Tu P-H, Tomita T, Nakaya K, Lee VM, Trojanowski JQ, Iwatsubo T (1998) Aggregation of alpha-synuclein in Lewy bodies of sporadic Parkinson's disease and dementia with Lewy bodies. The American journal of pathology 152:879.

Banerjee K, Sinha M, Pham CLL, Jana S, Chanda D, Cappai R, Chakrabarti S (2010) α-Synuclein induced membrane depolarization and loss of phosphorylation capacity of isolated rat brain mitochondria: Implications in Parkinson's disease. FEBS Letters 584:1571-1576.

Ben Abdallah NMB, Slomianka L, Vyssotski AL, Lipp H-P (2010) Early age-related changes in adult hippocampal neurogenesis in C57 mice. Neurobiol Aging 31:151-161.

Bender A, Beckers J, Schneider I, Holter SM, Haack T, Ruthsatz T, Vogt-Weisenhorn DM, Becker L, Genius J, Rujescu D, Irmler M, Mijalski T, Mader M, Quintanilla-Martinez L, Fuchs H,

Gailus-Durner V, de Angelis MH, Wurst W, Schmidt J, Klopstock T (2008) Creatine improves health and survival of mice. Neurobiol Aging 29:1404-1411.

Bergami M, Berninger B (2012) A fight for survival: The challenges faced by a newborn neuron integrating in the adult hippocampus. Developmental Neurobiology 72:1016-1031.

Bergsland M, Ramsköld D, Zaouter C, Klum S, Sandberg R, Muhr J (2011) Sequentially acting Sox transcription factors in neural lineage development. Genes & Development 25:2453-2464.

Berman SB, Pineda FJ, Hardwick JM (2008) Mitochondrial fission and fusion dynamics: the long and short of it. Cell Death Differ 15:1147-1152.

Berneburg M, Gremmel T, Kurten V, Schroeder P, Hertel I, von Mikecz A, Wild S, Chen M, Declercq L, Matsui M, Ruzicka T, Krutmann J (2005) Creatine Supplementation Normalizes Mutagenesis of Mitochondrial DNA as Well as Functional Consequences. J Investig Dermatol 125:213-220.

Bertholet AM, Millet AME, Guillermin O, Daloyau M, Davezac N, Miquel M-C, Belenguer P (2013) OPA1 loss of function affects in vitro neuronal maturation. Brain 136:1518-1533.

Bessman SP, Carpenter CL (1985) The Creatine-Creatine Phosphate Energy Shuttle. Annual Review of Biochemistry 54:831-862.

Bhattaram P, Penzo-Mendez A, Sock E, Colmenares C, Kaneko KJ, Vassilev A, DePamphilis ML, Wegner M, Lefebvre V (2010) Organogenesis relies on SoxC transcription factors for the survival of neural and mesenchymal progenitors. Nat Commun 1:9.

Bibb MJ, Van Etten RA, Wright CT, Walberg MW, Clayton DA (1981) Sequence and gene organization of mouse mitochondrial DNA. Cell 26:167-180.

Biebl M, Cooper CM, Winkler J, Kuhn HG (2000) Analysis of neurogenesis and programmed cell death reveals a self-renewing capacity in the adult rat brain. Neuroscience Letters 291:17-20.

Boldrini M, Underwood MD, Hen R, Rosoklija GB, Dwork AJ, John Mann J, Arango V (2009) Antidepressants increase neural progenitor cells in the human hippocampus. Neuropsychopharmacology 34:2376-2389.

Bonaguidi Michael A, Wheeler Michael A, Shapiro Jason S, Stadel Ryan P, Sun Gerald J, Ming G-l, Song H (2011) In Vivo Clonal Analysis Reveals Self-Renewing and Multipotent Adult Neural Stem Cell Characteristics. Cell 145:1142-1155.

Bonhoeffer T, Yuste R (2002) Spine motility. Phenomenology, mechanisms, and function. Neuron 35:1019-1027.

Bothwell JH, Rae C, Dixon RM, Styles P, Bhakoo KK (2001) Hypo-osmotic swelling-activated release of organic osmolytes in brain slices: implications for brain oedema in vivo. Journal of Neurochemistry 77:1632-1640.

Braissant O, Henry H, Loup M, Eilers B, Bachmann C (2001) Endogenous synthesis and transport of creatine in the rat brain: an in situ hybridization study. Molecular brain research 86:193-201.

Braissant O, Henry H, Villard A-M, Speer O, Wallimann T, Bachmann C (2005) Creatine synthesis and transport during rat embryogenesis: spatiotemporal expression of AGAT, GAMT and CT1. BMC Developmental Biology 5:9.

Brandt MD, Jessberger S, Steiner B, Kronenberg G, Reuter K, Bick-Sander A, Behrens Wvd, Kempermann G (2003) Transient calretinin expression defines early postmitotic step of neuronal differentiation in adult hippocampal neurogenesis of mice. Molecular and Cellular Neuroscience 24:603-613.

Breunig JJ, Silbereis J, Vaccarino FM, Šestan N, Rakic P (2007) Notch regulates cell fate and dendrite morphology of newborn neurons in the postnatal dentate gyrus. Proceedings of the National Academy of Sciences 104:20558-20563.

Brown J, Cooper-Kuhn CM, Kempermann G, Van Praag H, Winkler J, Gage FH, Kuhn HG (2003a) Enriched environment and physical activity stimulate hippocampal but not olfactory bulb neurogenesis. European Journal of Neuroscience 17:2042-2046.

Brown JP, Couillard-Després S, Cooper-Kuhn CM, Winkler J, Aigner L, Kuhn HG (2003b) Transient expression of doublecortin during adult neurogenesis. The Journal of Comparative Neurology 467:1-10.

Cameron HA, McEwen BS, Gould E (1995) Regulation of adult neurogenesis by excitatory input and NMDA receptor activation in the dentate gyrus. The Journal of Neuroscience 15:4687-4692.

Cameron HA, Woolley CS, McEwen BS, Gould E (1993) Differentiation of newly born neurons and glia in the dentate gyrus of the adult rat. Neuroscience 56:337-344.

Cereghetti GM, Stangherlin A, de Brito OM, Chang CR, Blackstone C, Bernardi P, Scorrano L (2008) Dephosphorylation by calcineurin regulates translocation of Drp1 to mitochondria. Proceedings of the National Academy of Sciences 105:15803-15808.

Chang C-R, Blackstone C (2007) Cyclic AMP-dependent Protein Kinase Phosphorylation of Drp1 Regulates Its GTPase Activity and Mitochondrial Morphology. Journal of Biological Chemistry 282:21583-21587.

Chang DTW, Honick AS, Reynolds IJ (2006) Mitochondrial Trafficking to Synapses in Cultured Primary Cortical Neurons. The Journal of Neuroscience 26:7035-7045.

Chen H, Chan DC (2006) Critical dependence of neurons on mitochondrial dynamics. Current Opinion in Cell Biology 18:453-459.

Chen H, Chomyn A, Chan DC (2005) Disruption of Fusion Results in Mitochondrial Heterogeneity and Dysfunction. Journal of Biological Chemistry 280:26185-26192.

Chen H, McCaffery JM, Chan DC (2007) Mitochondrial Fusion Protects against Neurodegeneration in the Cerebellum. Cell 130:548-562.

Chen H, Detmer SA, Ewald AJ, Griffin EE, Fraser SE, Chan DC (2003) Mitofusins Mfn1 and Mfn2 coordinately regulate mitochondrial fusion and are essential for embryonic development. J Cell Biol 160:189-200.

Cho D-H, Nakamura T, Fang J, Cieplak P, Godzik A, Gu Z, Lipton SA (2009) S-Nitrosylation of Drp1 Mediates β-Amyloid-Related Mitochondrial Fission and Neuronal Injury. Science 324:102-105.

Cho YM, Kwon S, Pak YK, Seol HW, Choi YM, Park DJ, Park KS, Lee HK (2006) Dynamic changes in mitochondrial biogenesis and antioxidant enzymes during the spontaneous differentiation of human embryonic stem cells. Biochemical and biophysical research communications 348:1472-1478.

Chung S, Arrell DK, Faustino RS, Terzic A, Dzeja PP (2010) Glycolytic network restructuring integral to the energetics of embryonic stem cell cardiac differentiation. Journal of molecular and cellular cardiology 48:725-734.

Chung S, Dzeja PP, Faustino RS, Perez-Terzic C, Behfar A, Terzic A (2007) Mitochondrial oxidative metabolism is required for the cardiac differentiation of stem cells. Nature Clinical Practice Cardiovascular Medicine 4:S60-S67.

Clark IE, Dodson MW, Jiang C, Cao JH, Huh JR, Seol JH, Yoo SJ, Hay BA, Guo M (2006) Drosophila pink1 is required for mitochondrial function and interacts genetically with parkin. Nature 441:1162-1166.

Clayton DA (2013) DNA Replication, Mitochondrial. In: Encyclopedia of Biological Chemistry (Editors-in-Chief: William JL, Lane MD, eds), pp 126-129. Waltham: Academic Press.

Clelland CD, Choi M, Romberg C, Clemenson GD, Fragniere A, Tyers P, Jessberger S, Saksida LM, Barker RA, Gage FH, Bussey TJ (2009) A Functional Role for Adult Hippocampal Neurogenesis in Spatial Pattern Separation. Science 325:210-213.

Coppedè F (2012) Genetics and Epigenetics of Parkinson's Disease. The Scientific World Journal 2012:12.

Crews L, Mizuno H, Desplats P, Rockenstein E, Adame A, Patrick C, Winner B, Winkler J, Masliah E (2008) α-synuclein alters Notch-1 expression and neurogenesis in mouse embryonic stem cells and in the hippocampus of transgenic mice. The Journal of Neuroscience 28:4250-4260.

Cribbs JT, Strack S (2007) Reversible phosphorylation of Drp1 by cyclic AMP-dependent protein kinase and calcineurin regulates mitochondrial fission and cell death. EMBO Rep 8:939-944.

David DJ, Samuels BA, Rainer Q, Wang J-W, Marsteller D, Mendez I, Drew M, Craig DA, Guiard BP, Guilloux J-P, Artymyshyn RP, Gardier AM, Gerald C, Antonijevic IA, Leonardo ED, Hen R (2009) Neurogenesis-Dependent and -Independent Effects of Fluoxetine in an Animal Model of Anxiety/Depression. Neuron 62:479-493.

De Rasmo D, Signorile A, Papa F, Roca E, Papa S (2010) cAMP/Ca2+ response element-binding protein plays a central role in the biogenesis of respiratory chain proteins in mammalian cells. IUBMB Life 62:447-452.

Deisseroth K, Singla S, Toda H, Monje M, Palmer TD, Malenka RC (2004) Excitation-Neurogenesis Coupling in Adult Neural Stem/Progenitor Cells. Neuron 42:535-552.

Delettre C, Lenaers G, Griffoin J-M, Gigarel N, Lorenzo C, Belenguer P, Pelloquin L, Grosgeorge J, Turc-Carel C, Perret E, Astarie-Dequeker C, Lasquellec L, Arnaud B, Ducommun B, Kaplan J, Hamel CP (2000) Nuclear gene OPA1, encoding a mitochondrial dynamin-related protein, is mutated in dominant optic atrophy. Nat Genet 26:207-210.

Deng W, Aimone JB, Gage FH (2010) New neurons and new memories: how does adult hippocampal neurogenesis affect learning and memory? Nat Rev Neurosci 11:339-350.

Deng W, Saxe MD, Gallina IS, Gage FH (2009) Adult-Born Hippocampal Dentate Granule Cells Undergoing Maturation Modulate Learning and Memory in the Brain. The Journal of Neuroscience 29:13532-13542.

Devi L, Anandatheerthavarada HK (2010) Mitochondrial trafficking of APP and alpha synuclein: Relevance to mitochondrial dysfunction in Alzheimer's and Parkinson's diseases. Biochimica et Biophysica Acta (BBA) - Molecular Basis of Disease 1802:11-19.

Dickey AS, Strack S (2011) PKA/AKAP1 and PP2A/Bβ2 Regulate Neuronal Morphogenesis via Drp1 Phosphorylation and Mitochondrial Bioenergetics. The Journal of Neuroscience 31:15716-15726.

Doberauer K (2013) Sox11 as a regulator of neuronal maturation & integration of newborn neurons in the adult hippocampus. PhD Thesis, TU München.

Dolder M, Walzel B, Speer O, Schlattner U, Wallimann T (2003) Inhibition of the Mitochondrial Permeability Transition by Creatine Kinase Substrates: REQUIREMENT FOR MICROCOMPARTMENTATION. Journal of Biological Chemistry 278:17760-17766.

Drapeau E, Montaron M-F, Aguerre S, Abrous DN (2007) Learning-Induced Survival of New Neurons Depends on the Cognitive Status of Aged Rats. The Journal of Neuroscience 27:6037-6044.

Duan X, Chang JH, Ge S, Faulkner RL, Kim JY, Kitabatake Y, Liu X-b, Yang C-H, Jordan JD, Ma DK, Liu CY, Ganesan S, Cheng H-J, Ming G-l, Lu B, Song H (2007) Disrupted-In-Schizophrenia 1 Regulates Integration of Newly Generated Neurons in the Adult Brain. Cell 130:1146-1158.

Ducray AD, Schläppi J-A, Qualls R, Andres RH, Seiler RW, Schlattner U, Wallimann T, Widmer HR (2007) Creatine treatment promotes differentiation of GABA-ergic neuronal precursors in cultured fetal rat spinal cord. J Neurosci Res 85:1863-1875.

Dupret D, Revest J-M, Koehl M, Ichas F, De Giorgi F, Costet P, Abrous DN, Piazza PV (2008) Spatial Relational Memory Requires Hippocampal Adult Neurogenesis. PLoS ONE 3:e1959.

Dzeja PP, Terzic A (2003) Phosphotransfer networks and cellular energetics. Journal of Experimental Biology 206:2039-2047.

Ebert B (2013) The effect of mitochondrial dysfunction on astrocytes and radial glia like stem cells in the adult hippocampus. PhD Thesis, TU München.

Ehm O, Göritz C, Covic M, Schäffner I, Schwarz TJ, Karaca E, Kempkes B, Kremmer E, Pfrieger FW, Espinosa L, Bigas A, Giachino C, Taylor V, Frisén J, Lie DC (2010) RBPJκ-Dependent Signaling Is Essential for Long-Term Maintenance of Neural Stem Cells in the Adult Hippocampus. The Journal of Neuroscience 30:13794-13807.

Ehses S, Raschke I, Mancuso G, Bernacchia A, Geimer S, Tondera D, Martinou J-C, Westermann B, Rugarli EI, Langer T (2009) Regulation of OPA1 processing and mitochondrial fusion by m-AAA protease isoenzymes and OMA1. J Cell Biol 187:1023-1036.

Encinas JM, Vaahtokari A, Enikolopov G (2006) Fluoxetine targets early progenitor cells in the adult brain. Proceedings of the National Academy of Sciences 103:8233-8238.

Eriksson PS, Perfilieva E, Bjork-Eriksson T, Alborn A-M, Nordborg C, Peterson DA, Gage FH (1998) Neurogenesis in the adult human hippocampus. Nat Med 4:1313-1317.

Exner N, Lutz AK, Haass C, Winklhofer KF (2012) Mitochondrial dysfunction in Parkinson/'s disease: molecular mechanisms and pathophysiological consequences. EMBO J 31:3038-3062.

Fabel K, Fabel K, Tam B, Kaufer D, Baiker A, Simmons N, Kuo CJ, Palmer TD (2003) VEGF is necessary for exercise-induced adult hippocampal neurogenesis. European Journal of Neuroscience 18:2803-2812.

Facucho-Oliveira JM, John JCS (2009) The relationship between pluripotency and mitochondrial DNA proliferation during early embryo development and embryonic stem cell differentiation. Stem Cell Reviews and Reports 5:140-158.

Facucho-Oliveira JM, Alderson J, Spikings EC, Egginton S, John JCS (2007) Mitochondrial DNA replication during differentiation of murine embryonic stem cells. Journal of Cell Science 120:4025-4034.

Farrer MJ (2006) Genetics of Parkinson disease: paradigm shifts and future prospects. Nat Rev Genet 7:306-318.

Faulkner RL, Jang M-H, Liu X-B, Duan X, Sailor KA, Kim JY, Ge S, Jones EG, Ming G-l, Song H, Cheng H-J (2008) Development of hippocampal mossy fiber synaptic outputs by new neurons in the adult brain. Proceedings of the National Academy of Sciences 105:14157-14162.

Favaro R, Valotta M, Ferri ALM, Latorre E, Mariani J, Giachino C, Lancini C, Tosetti V, Ottolenghi S, Taylor V, Nicolis SK (2009) Hippocampal development and neural stem cell maintenance require Sox2-dependent regulation of Shh. Nat Neurosci 12:1248-1256.

Fernandez-Marcos PJ, Auwerx J (2011) Regulation of PGC-1α, a nodal regulator of mitochondrial biogenesis. The American Journal of Clinical Nutrition 93:884S-890S.

Ferrante RJ, Andreassen OA, Jenkins BG, Dedeoglu A, Kuemmerle S, Kubilus JK, Kaddurah-Daouk R, Hersch SM, Beal MF (2000) Neuroprotective effects of creatine in a transgenic mouse model of Huntington's disease. The Journal of Neuroscience 20:4389-4397.

Ferrara N, Gerber H-P, LeCouter J (2003) The biology of VEGF and its receptors. Nat Med 9:669-676.

Ferri ALM, Cavallaro M, Braida D, Di Cristofano A, Canta A, Vezzani A, Ottolenghi S, Pandolfi PP, Sala M, DeBiasi S, Nicolis SK (2004) Sox2 deficiency causes neurodegeneration and impaired neurogenesis in the adult mouse brain. Development 131:3805-3819.

Fournier NM, Lee B, Banasr M, Elsayed M, Duman RS (2012) Vascular endothelial growth factor regulates adult hippocampal cell proliferation through MEK/ERK- and PI3K/Akt-dependent signaling. Neuropharmacology 63:642-652.

Frank S, Gaume B, Bergmann-Leitner ES, Leitner WW, Robert EG, Catez F, Smith CL, Youle RJ (2001) The role of dynamin-related protein 1, a mediator of mitochondrial fission, in apoptosis. Dev Cell 1:515-525.

Fransson S, Ruusala A, Aspenstrom P (2006) The atypical Rho GTPases Miro-1 and Miro-2 have essential roles in mitochondrial trafficking. Biochem Biophys Res Commun 344:500-510.

Friedman JR, Lackner LL, West M, DiBenedetto JR, Nunnari J, Voeltz GK (2011) ER Tubules Mark Sites of Mitochondrial Division. Science 334:358-362.

Fuhrmann M, Mitteregger G, Kretzschmar H, Herms J (2007) Dendritic Pathology in Prion Disease Starts at the Synaptic Spine. The Journal of Neuroscience 27:6224-6233.

Fujioka T, Fujioka A, Duman RS (2004) Activation of cAMP Signaling Facilitates the Morphological Maturation of Newborn Neurons in Adult Hippocampus. The Journal of Neuroscience 24:319-328.

Gao Z, Ure K, Ables JL, Lagace DC, Nave K-A, Goebbels S, Eisch AJ, Hsieh J (2009) Neurod1 is essential for the survival and maturation of adult-born neurons. Nat Neurosci 12:1090-1092.

Gawlowski T, Suarez J, Scott B, Torres-Gonzalez M, Wang H, Schwappacher R, Han X, Yates JR, Hoshijima M, Dillmann W (2012) Modulation of Dynamin-related Protein 1 (DRP1) Function by Increased O-linked-β-N-acetylglucosamine Modification (O-GlcNAc) in Cardiac Myocytes. Journal of Biological Chemistry 287:30024-30034.

Ge S, Pradhan DA, Ming G-l, Song H (2007a) GABA sets the tempo for activity-dependent adult neurogenesis. Trends in neurosciences 30:1-8.

Ge S, Yang C-h, Hsu K-s, Ming G-l, Song H (2007b) A Critical Period for Enhanced Synaptic Plasticity in Newly Generated Neurons of the Adult Brain. Neuron 54:559-566.

Ge S, Goh ELK, Sailor KA, Kitabatake Y, Ming G-l, Song H (2006) GABA regulates synaptic integration of newly generated neurons in the adult brain. Nature 439:589-593.

Gomes LC, Benedetto GD, Scorrano L (2011) During autophagy mitochondria elongate, are spared from degradation and sustain cell viability. Nat Cell Biol 13:589-598.

Gould E, McEwen BS, Tanapat P, Galea LAM, Fuchs E (1997) Neurogenesis in the Dentate Gyrus of the Adult Tree Shrew Is Regulated by Psychosocial Stress and NMDA Receptor Activation. The Journal of Neuroscience 17:2492-2498.

Gould E, Tanapat P, McEwen BS, Flügge G, Fuchs E (1998) Proliferation of granule cell precursors in the dentate gyrus of adult monkeys is diminished by stress. Proceedings of the National Academy of Sciences 95:3168-3171.

Gould E, Beylin A, Tanapat P, Reeves A, Shors TJ (1999) Learning enhances adult neurogenesis in the hippocampal formation. Nat Neurosci 2:260-265.

Han X-J, Lu Y-F, Li S-A, Kaitsuka T, Sato Y, Tomizawa K, Nairn AC, Takei K, Matsui H, Matsushita M (2008a) CaM kinase Iα–induced phosphorylation of Drp1 regulates mitochondrial morphology. J Cell Biol 182:573-585.

Han Y-G, Spassky N, Romaguera-Ros M, Garcia-Verdugo J-M, Aguilar A, Schneider-Maunoury S, Alvarez-Buylla A (2008b) Hedgehog signaling and primary cilia are required for the formation of adult neural stem cells. Nat Neurosci 11:277-284.

Haslinger A, Schwarz TJ, Covic M, Chichung Lie D (2009) Expression of Sox11 in adult neurogenic niches suggests a stage-specific role in adult neurogenesis. European Journal of Neuroscience 29:2103-2114.

Hastings NB, Gould E (1999) Rapid extension of axons into the CA3 region by adult-generated granule cells. The Journal of Comparative Neurology 413:146-154.

Henchcliffe C, Beal MF (2008) Mitochondrial biology and oxidative stress in Parkinson disease pathogenesis. Nat Clin Pract Neuro 4:600-609.

Herzig S, Long F, Jhala U, Hedrick S, Quinn R, Bauer A, Rudolph D, Schutz G, Yoon C, Puigserver P, Spiegelman B, Montminy M (2001) CREB regulates hepatic gluconeogenesis through the coactivator PGC-1. Nature 413:179 - 183.

Hodge RD, Hevner RF (2011) Expression and actions of transcription factors in adult hippocampal neurogenesis. Developmental Neurobiology 71:680-689.

Hodge RD, Kowalczyk TD, Wolf SA, Encinas JM, Rippey C, Enikolopov G, Kempermann G, Hevner RF (2008) Intermediate Progenitors in Adult Hippocampal Neurogenesis: Tbr2 Expression and Coordinate Regulation of Neuronal Output. The Journal of Neuroscience 28:3707-3717.

Hollenbeck PJ, Saxton WM (2005) The axonal transport of mitochondria. Journal of Cell Science 118:5411-5419.

Holtmaat AJ, Trachtenberg JT, Wilbrecht L, Shepherd GM, Zhang X, Knott GW, Svoboda K (2005) Transient and persistent dendritic spines in the neocortex in vivo. Neuron 45:279-292.

Horton AC, Ehlers MD (2003) Dual Modes of Endoplasmic Reticulum-to-Golgi Transport in Dendrites Revealed by Live-Cell Imaging. The Journal of Neuroscience 23:6188-6199.

Hoser M, Potzner MR, Koch JMC, Bösl MR, Wegner M, Sock E (2008) Sox12 Deletion in the Mouse Reveals Nonreciprocal Redundancy with the Related Sox4 and Sox11 Transcription Factors. Molecular and Cellular Biology 28:4675-4687.

Howng S-L, Sy W-D, Cheng T-S, Lieu A-S, Wang C, Tzou W-S, Cho C-L, Hong Y-R (2004) Genomic organization, alternative splicing, and promoter analysis of human dynamin-like protein gene. Biochem Biophys Res Commun 314:766-772.

Ingerman E, Perkins EM, Marino M, Mears JA, McCaffery JM, Hinshaw JE, Nunnari J (2005) Dnm1 forms spirals that are structurally tailored to fit mitochondria. J Cell Biol 170:1021-1027.

Ishihara N, Nomura M, Jofuku A, Kato H, Suzuki SO, Masuda K, Otera H, Nakanishi Y, Nonaka I, Goto Y-i, Taguchi N, Morinaga H, Maeda M, Takayanagi R, Yokota S, Mihara K (2009) Mitochondrial fission factor Drp1 is essential for embryonic development and synapse formation in mice. Nat Cell Biol 11:958-966.

Jagasia R, Grote P, Westermann B, Conradt B (2005) DRP-1-mediated mitochondrial fragmentation during EGL-1-induced cell death in C. elegans. Nature 433:754-760.

Jagasia R, Steib K, Englberger E, Herold S, Faus-Kessler T, Saxe M, Gage FH, Song H, Lie DC (2009) GABA-cAMP response element-binding protein signaling regulates maturation and survival of newly generated neurons in the adult hippocampus. J Neurosci 29:7966-7977.

James DI, Parone PA, Mattenberger Y, Martinou J-C (2003) hFis1, a Novel Component of the Mammalian Mitochondrial Fission Machinery. Journal of Biological Chemistry 278:36373-36379.

Jessberger S, Römer B, Babu H, Kempermann G (2005) Seizures induce proliferation and dispersion of doublecortin-positive hippocampal progenitor cells. Experimental Neurology 196:342-351.

Jessberger S, Clark RE, Broadbent NJ, Clemenson GD, Consiglio A, Lie DC, Squire LR, Gage FH (2009) Dentate gyrus-specific knockdown of adult neurogenesis impairs spatial and object recognition memory in adult rats. Learning & Memory 16:147-154.

Kageyama Y, Zhang Z, Roda R, Fukaya M, Wakabayashi J, Wakabayashi N, Kensler TW, Reddy PH, Iijima M, Sesaki H (2012) Mitochondrial division ensures the survival of postmitotic neurons by suppressing oxidative damage. J Cell Biol 197:535-551.

Kaldis P, Kamp G, Piendl T, Wallimann T (1997) Functions of Creatine Kinase Isoenzymes in Spermatozoa. In: Advances in Developmental Biology (1992) (Paul MW, ed), pp 275-312: Academic Press.

Kamata A, Sakagami H, Tokumitsu H, Owada Y, Fukunaga K, Kondo H (2007) Spatiotemporal expression of four isoforms of Ca2+/calmodulin-dependent protein kinase I in brain and its possible roles in hippocampal dendritic growth. Neuroscience Research 57:86-97.

Kamp F, Exner N, Lutz AK, Wender N, Hegermann J, Brunner B, Nuscher B, Bartels T, Giese A, Beyer K, Eimer S, Winklhofer KF, Haass C (2010) Inhibition of mitochondrial fusion by [alpha]-synuclein is rescued by PINK1, Parkin and DJ-1. EMBO J 29:3571-3589.

Kaplan MS, Hinds JW (1977) Neurogenesis in the adult rat: electron microscopic analysis of light radioautographs. Science 197:1092-1094.

Karten YJG, Jones MA, Jeurling SI, Cameron HA (2006) GABAergic signaling in young granule cells in the adult rat and mouse dentate gyrus. Hippocampus 16:312-320.

Kee N, Teixeira CM, Wang AH, Frankland PW (2007) Preferential incorporation of adult-generated granule cells into spatial memory networks in the dentate gyrus. Nat Neurosci 10:355-362.

Kempermann G, Kuhn HG, Gage FH (1997) More hippocampal neurons in adult mice living in an enriched environment. Nature 386:493-495.

Kempermann G, Kuhn HG, Gage FH (1998) Experience-Induced Neurogenesis in the Senescent Dentate Gyrus. The Journal of Neuroscience 18:3206-3212.

Kempermann G, Gast D, Kronenberg G, Yamaguchi M, Gage FH (2003) Early determination and long-term persistence of adult-generated new neurons in the hippocampus of mice. Development 130:391-399.

Kim Ju Y, Liu Cindy Y, Zhang F, Duan X, Wen Z, Song J, Feighery E, Lu B, Rujescu D, St Clair D, Christian K, Callicott Joseph H, Weinberger Daniel R, Song H, Ming G-l (2012) Interplay between DISC1 and GABA Signaling Regulates Neurogenesis in Mice and Risk for Schizophrenia. Cell 148:1051-1064.

Klivenyi P, Gardian G, Calingasan N, Yang L, Beal MF (2003) Additive neuroprotective effects of creatine and a cyclooxygenase 2 inhibitor against dopamine depletion in the 1-methyl-4-phenyl-1,2,3,6-tetrahydropyridine (MPTP) mouse model of Parkinson's disease. Journal of Molecular Neuroscience 21:191-198.

Klivenyi P, Kiaei M, Gardian G, Calingasan NY, Beal MF (2004) Additive neuroprotective effects of creatine and cyclooxygenase 2 inhibitors in a transgenic mouse model of amyotrophic lateral sclerosis. Journal of Neurochemistry 88:576-582.

Klivenyi P, Ferrante RJ, Matthews RT, Bogdanov MB, Klein AM, Andreassen OA, Mueller G, Wermer M, Kaddurah-Daouk R, Beal MF (1999) Neuroprotective effects of creatine in a transgenic animal model of amyotrophic lateral sclerosis. Nat Med 5:347-350.

Koirala S, Guo Q, Kalia R, Bui HT, Eckert DM, Frost A, Shaw JM (2013) Interchangeable adaptors regulate mitochondrial dynamin assembly for membrane scission. Proceedings of the National Academy of Sciences 110:E1342-E1351.

Komitova M, Eriksson PS (2004) Sox-2 is expressed by neural progenitors and astroglia in the adult rat brain. Neuroscience Letters 369:24-27.

Kondoh H, Lleonart ME, Nakashima Y, Yokode M, Tanaka M, Bernard D, Gil J, Beach D (2007) A high glycolytic flux supports the proliferative potential of murine embryonic stem cells. Antioxidants & redox signaling 9:293-299.

Kriegstein A, Alvarez-Buylla A (2009) The Glial Nature of Embryonic and Adult Neural Stem Cells. Annual Review of Neuroscience 32:149-184.

Kronenberg G, Reuter K, Steiner B, Brandt MD, Jessberger S, Yamaguchi M, Kempermann G (2003) Subpopulations of proliferating cells of the adult hippocampus respond differently to physiologic neurogenic stimuli. The Journal of Comparative Neurology 467:455-463.

Kruman II, Mattson MP (1999) Pivotal Role of Mitochondrial Calcium Uptake in Neural Cell Apoptosis and Necrosis. Journal of Neurochemistry 72:529-540.

Krzisch M, Sultan S, Sandell J, Demeter K, Vutskits L, Toni N (2013) Propofol Anesthesia Impairs the Maturation and Survival of Adult-born Hippocampal Neurons. Anesthesiology 118.

Kuhn HG, Dickinson-Anson H, Gage FH (1996) Neurogenesis in the dentate gyrus of the adult rat: age-related decrease of neuronal progenitor proliferation. The Journal of Neuroscience 16:2027-2033.

Kuwabara T, Hsieh J, Muotri A, Yeo G, Warashina M, Lie DC, Moore L, Nakashima K, Asashima M, Gage FH (2009) Wnt-mediated activation of NeuroD1 and retro-elements during adult neurogenesis. Nat Neurosci 12:1097-1105.

Lapasset L, Milhavet O, Prieur A, Besnard E, Babled A, Aït-Hamou N, Leschik J, Pellestor F, Ramirez J-M, De Vos J (2011) Rejuvenating senescent and centenarian human cells by reprogramming through the pluripotent state. Genes & development 25:2248-2253.

Larsson N-G (2010) Somatic Mitochondrial DNA Mutations in Mammalian Aging. Annual Review of Biochemistry 79:683-706.

Lavado A, Oliver G (2007) Prox1 expression patterns in the developing and adult murine brain. Developmental Dynamics 236:518-524.

Lavado A, Lagutin OV, Chow LML, Baker SJ, Oliver G (2010) Prox1 Is Required for Granule Cell Maturation and Intermediate Progenitor Maintenance During Brain Neurogenesis. PloS Biol 8:e1000460.

Lawler JM, Barnes WS, Wu G, Song W, Demaree S (2002) Direct antioxidant properties of creatine. Biochem Biophys Res Commun 290:47-52.

Lehman JJ, Barger PM, Kovacs A, Saffitz JE, Medeiros DM, Kelly DP (2000) Peroxisome proliferator–activated receptor γ coactivator-1 promotes cardiac mitochondrial biogenesis. The Journal of Clinical Investigation 106:847-856.

Leuner K, Müller W, Reichert A (2012) From Mitochondrial Dysfunction to Amyloid Beta Formation: Novel Insights into the Pathogenesis of Alzheimer's Disease. Molecular Neurobiology 46:186-193.

Li H, Chen Y, Jones AF, Sanger RH, Collis LP, Flannery R, McNay EC, Yu T, Schwarzenbacher R, Bossy B, Bossy-Wetzel E, Bennett MVL, Pypaert M, Hickman JA, Smith PJS, Hardwick JM, Jonas EA (2008) Bcl-xL induces Drp1-dependent synapse formation in cultured hippocampal neurons. Proceedings of the National Academy of Sciences 105:2169-2174.

Li Z, Okamoto K-I, Hayashi Y, Sheng M (2004) The Importance of Dendritic Mitochondria in the Morphogenesis and Plasticity of Spines and Synapses. Cell 119:873-887.

Lie D-C, Colamarino SA, Song H-J, Desire L, Mira H, Consiglio A, Lein ES, Jessberger S, Lansford H, Dearie AR, Gage FH (2005) Wnt signalling regulates adult hippocampal neurogenesis. Nature 437:1370-1375.

Lie DC, Dziewczapolski G, Willhoite AR, Kaspar BK, Shults CW, Gage FH (2002) The Adult Substantia Nigra Contains Progenitor Cells with Neurogenic Potential. The Journal of Neuroscience 22:6639-6649.

Lin MT, Beal MF (2006) Mitochondrial dysfunction and oxidative stress in neurodegenerative diseases. Nature 443:787-795.

Little JP, Safdar A, Benton CR, Wright DC (2011) Skeletal muscle and beyond: the role of exercise as a mediator of systemic mitochondrial biogenesis. Applied Physiology, Nutrition, and Metabolism 36:598-607.

Liu G, Zhang C, Yin J, Li X, Cheng F, Li Y, Yang H, Uéda K, Chan P, Yu S (2009) α-Synuclein is differentially expressed in mitochondria from different rat brain regions and dose-dependently down-regulates complex I activity. Neuroscience Letters 454:187-192.

Lois C, Alvarez-Buylla A (1994) Long-distance neuronal migration in the adult mammalian brain. Science 264:1145-1148.

Lonergan T, Bavister B, Brenner C (2007) Mitochondria in stem cells. Mitochondrion 7:289-296.

Lugert S, Basak O, Knuckles P, Haussler U, Fabel K, Götz M, Haas CA, Kempermann G, Taylor V, Giachino C (2010) Quiescent and Active Hippocampal Neural Stem Cells with Distinct

Morphologies Respond Selectively to Physiological and Pathological Stimuli and Aging. Cell Stem Cell 6:445-456.

Lutz AK, Exner N, Fett ME, Schlehe JS, Kloos K, Lämmermann K, Brunner B, Kurz-Drexler A, Vogel F, Reichert AS, Bouman L, Vogt-Weisenhorn D, Wurst W, Tatzelt J, Haass C, Winklhofer KF (2009) Loss of Parkin or PINK1 Function Increases Drp1-dependent Mitochondrial Fragmentation. Journal of Biological Chemistry 284:22938-22951.

Ma DK, Jang M-H, Guo JU, Kitabatake Y, Chang M-l, Pow-anpongkul N, Flavell RA, Lu B, Ming G-l, Song H (2009) Neuronal Activity–Induced Gadd45b Promotes Epigenetic DNA Demethylation and Adult Neurogenesis. Science 323:1074-1077.

Macaskill AF, Rinholm JE, Twelvetrees AE, Arancibia-Carcamo IL, Muir J, Fransson A, Aspenstrom P, Attwell D, Kittler JT (2009) Miro1 is a calcium sensor for glutamate receptor-dependent localization of mitochondria at synapses. Neuron 61:541-555.

Madsen TM, Treschow A, Bengzon J, Bolwig TG, Lindvall O, Tingström A (2000) Increased neurogenesis in a model of electroconvulsive therapy. Biological Psychiatry 47:1043-1049.

Malberg JE, Eisch AJ, Nestler EJ, Duman RS (2000) Chronic Antidepressant Treatment Increases Neurogenesis in Adult Rat Hippocampus. The Journal of Neuroscience 20:9104-9110.

Mandal S, Lindgren AG, Srivastava AS, Clark AT, Banerjee U (2011) Mitochondrial function controls proliferation and early differentiation potential of embryonic stem cells. Stem cells 29:486-495.

Marchetti P, Castedo M, Susin SA, Zamzami N, Hirsch T, Macho A, Haeffner A, Hirsch F, Geuskens M, Kroemer G (1996) Mitochondrial permeability transition is a central coordinating event of apoptosis. The Journal of Experimental Medicine 184:1155-1160.

Marxreiter F, Regensburger M, Winkler J (2013) Adult neurogenesis in Parkinson's disease. Cellular and Molecular Life Sciences 70:459-473.

Masliah E, Rockenstein E, Veinbergs I, Mallory M, Hashimoto M, Takeda A, Sagara Y, Sisk A, Mucke L (2000) Dopaminergic Loss and Inclusion Body Formation in α-Synuclein Mice: Implications for Neurodegenerative Disorders. Science 287:1265-1269.

Matiello R, Fukui R, Silva M, Rocha D, Wajchenberg B, Azhar S, Santos R (2010) Differential regulation of PGC-1alpha expression in rat liver and skeletal muscle in response to voluntary running. Nutrition & Metabolism 7:36.

Matthews RT, Yang L, Jenkins BG, Ferrante RJ, Rosen BR, Kaddurah-Daouk R, Beal MF (1998) Neuroprotective Effects of Creatine and Cyclocreatine in Animal Models of Huntington's Disease. The Journal of Neuroscience 18:156-163.

Matthews RT, Ferrante RJ, Klivenyi P, Yang L, Klein AM, Mueller G, Kaddurah-Daouk R, Beal MF (1999) Creatine and Cyclocreatine Attenuate MPTP Neurotoxicity. Experimental Neurology 157:142-149.

McBride HM, Neuspiel M, Wasiak S (2006) Mitochondria: More Than Just a Powerhouse. Current biology : CB 16:R551-R560.

McNeill TH, Brown SA, Rafols JA, Shoulson I (1988) Atrophy of medium spiny I striatal dendrites in advanced Parkinson's disease. Brain Research 455:148-152.

Meyer LE, Machado LB, Santiago APSA, da-Silva WS, De Felice FG, Holub O, Oliveira MF, Galina A (2006) Mitochondrial Creatine Kinase Activity Prevents Reactive Oxygen Species Generation: ANTIOXIDANT ROLE OF MITOCHONDRIAL KINASE-DEPENDENT ADP RE-CYCLING ACTIVITY. Journal of Biological Chemistry 281:37361-37371.

Misko A, Jiang S, Wegorzewska I, Milbrandt J, Baloh RH (2010) Mitofusin 2 Is Necessary for Transport of Axonal Mitochondria and Interacts with the Miro/Milton Complex. The Journal of Neuroscience 30:4232-4240.

Mizrahi A (2007) Dendritic development and plasticity of adult-born neurons in the mouse olfactory bulb. Nat Neurosci 10:444-452.

Mohapel P, Ekdahl CT, Lindvall O (2004) Status epilepticus severity influences the long-term outcome of neurogenesis in the adult dentate gyrus. Neurobiology of Disease 15:196-205.

Morgenstern NA, Lombardi G, Schinder AF (2008) Newborn granule cells in the ageing dentate gyrus. The Journal of Physiology 586:3751-3757.

Mortiboys H, Johansen KK, Aasly JO, Bandmann O (2010) Mitochondrial impairment in patients with Parkinson disease with the G2019S mutation in LRRK2. Neurology 75:2017-2020.

Mozdy AD, McCaffery JM, Shaw JM (2000) Dnm1p Gtpase-Mediated Mitochondrial Fission Is a Multi-Step Process Requiring the Novel Integral Membrane Component Fis1p. J Cell Biol 151:367-380.

Mu L, Berti L, Masserdotti G, Covic M, Michaelidis TM, Doberauer K, Merz K, Rehfeld F, Haslinger A, Wegner M, Sock E, Lefebvre V, Couillard-Despres S, Aigner L, Berninger B, Lie DC (2012) SoxC transcription factors are required for neuronal differentiation in adult hippocampal neurogenesis. J Neurosci 32:3067-3080.

Mu Y, Gage F (2011) Adult hippocampal neurogenesis and its role in Alzheimer's disease. Molecular Neurodegeneration 6:85.

Nakagawa S, Kim J-E, Lee R, Malberg JE, Chen J, Steffen C, Zhang Y-J, Nestler EJ, Duman RS (2002) Regulation of Neurogenesis in Adult Mouse Hippocampus by cAMP and the cAMP Response Element-Binding Protein. The Journal of Neuroscience 22:3673-3682.

Nakamura K, Nemani VM, Azarbal F, Skibinski G, Levy JM, Egami K, Munishkina L, Zhang J, Gardner B, Wakabayashi J (2011) Direct membrane association drives mitochondrial fission by the Parkinson disease-associated protein α-synuclein. Journal of Biological Chemistry 286:20710-20726.

Niemann A, Berger P, Suter U (2006) Pathomechanisms of mutant proteins in Charcot-Marie-Tooth disease. NeuroMolecular Medicine 8:217-241.

Niemann A, Ruegg M, La Padula V, Schenone A, Suter U (2005) Ganglioside-induced differentiation associated protein 1 is a regulator of the mitochondrial network: new implications for Charcot-Marie-Tooth disease. J Cell Biol 170:1067-1078.

Niemann HH, Knetsch MLW, Scherer A, Manstein DJ, Kull FJ (2001) Crystal structure of a dynamin GTPase domain in both nucleotide-free and GDP-bound forms. EMBO J 20:5813-5821.

Nilsson M, Perfilieva E, Johansson U, Orwar O, Eriksson PS (1999) Enriched environment increases neurogenesis in the adult rat dentate gyrus and improves spatial memory. Journal of Neurobiology 39:569-578.

Nimchinsky EA, Sabatini BL, Svoboda K (2002) STRUCTURE AND FUNCTION OF DENDRITIC SPINES. Annual Review of Physiology 64:313-353.

O'Gorman E, Beutner G, Dolder M, Koretsky AP, Brdiczka D, Wallimann T (1997) The role of creatine kinase in inhibition of mitochondrial permeability transition. FEBS Letters 414:253-257.

Ohtsuki S, Tachikawa M, Takanaga H, Shimizu H, Watanabe M, Hosoya K-i, Terasaki T (2002) The Blood—Brain Barrier Creatine Transporter Is a Major Pathway for Supplying Creatine to the Brain. Journal of Cerebral Blood Flow & Metabolism 22:1327-1335.

Ory DS, Neugeboren BA, Mulligan RC (1996) A stable human-derived packaging cell line for production of high titer retrovirus/vesicular stomatitis virus G pseudotypes. Proc Natl Acad Sci U S A 93:11400-11406.

Otera H, Wang C, Cleland MM, Setoguchi K, Yokota S, Youle RJ, Mihara K (2010) Mff is an essential factor for mitochondrial recruitment of Drp1 during mitochondrial fission in mammalian cells. J Cell Biol 191:1141-1158.

Palau F, Estela A, Pla-Martín D, Sánchez-Piris M (2009) The Role of Mitochondrial Network Dynamics in the Pathogenesis of Charcot-Marie-Tooth Disease. In: Springer Netherlands, Inherited Neuromuscular Diseases (Espinós C, Felipo V, Palau F, eds), pp 129-137.

Palma V, Lim DA, Dahmane N, Sánchez P, Brionne TC, Herzberg CD, Gitton Y, Carleton A, Álvarez-Buylla A, Altaba ARi (2005) Sonic hedgehog controls stem cell behavior in the postnatal and adult brain. Development 132:335-344.

Palmer CS, Osellame LD, Laine D, Koutsopoulos OS, Frazier AE, Ryan MT (2011) MiD49 and MiD51, new components of the mitochondrial fission machinery. EMBO Rep 12:565-573.

Palmer TD, Willhoite AR, Gage FH (2000) Vascular niche for adult hippocampal neurogenesis. The Journal of Comparative Neurology 425:479-494.

Panopoulos AD, Yanes O, Ruiz S, Kida YS, Diep D, Tautenhahn R, Herrerías A, Batchelder EM, Plongthongkum N, Lutz M (2011) The metabolome of induced pluripotent stem cells reveals metabolic changes occurring in somatic cell reprogramming. Cell research 22:168-177.

Park M, Salgado JM, Ostroff L, Helton TD, Robinson CG, Harris KM, Ehlers MD (2006) Plasticity-induced growth of dendritic spines by exocytic trafficking from recycling endosomes. Neuron 52:817-830.

Pathak D, Sepp KJ, Hollenbeck PJ (2010) Evidence That Myosin Activity Opposes Microtubule-Based Axonal Transport of Mitochondria. The Journal of Neuroscience 30:8984-8992.

Patt S, Gertz H-J, Gerhard L, Cervos-Navarro J (1991) Pathological changes in dendrites of substantia nigra neurons in Parkinson's disease: a Golgi study.

Penzo-Mendez A, Dy P, Pallavi B, Lefebvre V (2007) Generation of mice harboring a Sox4 conditional null allele. Genesis 45:776-780.

Peral MJ, García-Delgado M, Calonge ML, Duran JM, Horra MC, Wallimann T, Speer O, Ilundáin AA (2002) Human, rat and chicken small intestinal Na+-Cl−-creatine transporter: functional, molecular characterization and localization. The Journal of Physiology 545:133-144.

Piatti VC, Espósito MS, Schinder AF (2006) The Timing of Neuronal Development in Adult Hippocampal Neurogenesis. The Neuroscientist 12:463-468.

Pilling AD, Horiuchi D, Lively CM, Saxton WM (2006) Kinesin-1 and Dynein Are the Primary Motors for Fast Transport of Mitochondria in Drosophila Motor Axons. Molecular Biology of the Cell 17:2057-2068.

Poole AC, Thomas RE, Andrews LA, McBride HM, Whitworth AJ, Pallanck LJ (2008) The PINK1/Parkin pathway regulates mitochondrial morphology. Proceedings of the National Academy of Sciences 105:1638-1643.

Prass K, Royl G, Lindauer U, Freyer D, Megow D, Dirnagl U, Stockler-Ipsiroglu G, Wallimann T, Priller J (2006) Improved reperfusion and neuroprotection by creatine in a mouse model of stroke. J Cereb Blood Flow Metab 27:452-459.

Prigione A, Fauler B, Lurz R, Lehrach H, Adjaye J (2010) The Senescence-Related Mitochondrial/Oxidative Stress Pathway is Repressed in Human Induced Pluripotent Stem Cells. Stem Cells 28:721-733.

Rambold AS, Kostelecky B, Elia N, Lippincott-Schwartz J (2011) Tubular network formation protects mitochondria from autophagosomal degradation during nutrient starvation. Proceedings of the National Academy of Sciences 108:10190-10195.

Ransome MI, Renoir T, Hannan AJ (2012) Hippocampal Neurogenesis, Cognitive Deficits and Affective Disorder in Huntington's Disease. Neural Plasticity 2012:1-7.

Rao MS, Shetty AK (2004) Efficacy of doublecortin as a marker to analyse the absolute number anddendritic growth of newly generated neurons in the adult dentate gyrus. European Journal of Neuroscience 19:234-246.

Reif A, Fritzen S, Finger M, Strobel A, Lauer M, Schmitt A, Lesch KP (2006) Neural stem cell proliferation is decreased in schizophrenia, but not in depression. Mol Psychiatry 11:514-522.

Renault VM, Rafalski VA, Morgan AA, Salih DAM, Brett JO, Webb AE, Villeda SA, Thekkat PU, Guillerey C, Denko NC (2009) FoxO3 regulates neural stem cell homeostasis. Cell stem cell 5:527-539.

Rockenstein E, Mallory M, Hashimoto M, Song D, Shults CW, Lang I, Masliah E (2002) Differential neuropathological alterations in transgenic mice expressing alpha-synuclein from the platelet-derived growth factor and Thy-1 promoters. J Neurosci Res 68:568-578.

Russo GJ, Louie K, Wellington A, Macleod GT, Hu F, Panchumarthi S, Zinsmaier KE (2009) Drosophila Miro Is Required for Both Anterograde and Retrograde Axonal Mitochondrial Transport. The Journal of Neuroscience 29:5443-5455.

Sahay A, Scobie KN, Hill AS, O'Carroll CM, Kheirbek MA, Burghardt NS, Fenton AA, Dranovsky A, Hen R (2011) Increasing adult hippocampal neurogenesis is sufficient to improve pattern separation. Nature 472:466-470.

Saks VA, Rosenshtraukh LV, Smirnov VN, Chazov EI (1978) Role of creatine phosphokinase in cellular function and metabolism. Canadian Journal of Physiology and Pharmacology 56:691-706.

Santarelli L, Saxe M, Gross C, Surget A, Battaglia F, Dulawa S, Weisstaub N, Lee J, Duman R, Arancio O, Belzung C, Hen R (2003) Requirement of Hippocampal Neurogenesis for the Behavioral Effects of Antidepressants. Science 301:805-809.

Saotome M, Safiulina D, Szabadkai G, Das S, Fransson Å, Aspenstrom P, Rizzuto R, Hajnóczky G (2008) Bidirectional Ca2+-dependent control of mitochondrial dynamics by the Miro GTPase. Proceedings of the National Academy of Sciences 105:20728-20733.

Sappey-Marinier D, Calabrese G, Fein G, Hugg JW, Biggins C, Weiner MW (1992) Effect of Photic Stimulation on Human Visual Cortex Lactate and Phosphates Using 1H and 31P Magnetic Resonance Spectroscopy. J Cereb Blood Flow Metab 12:584-592.

Saxe MD, Malleret G, Vronskaya S, Mendez I, Garcia AD, Sofroniew MV, Kandel ER, Hen R (2007) Paradoxical influence of hippocampal neurogenesis on working memory. Proceedings of the National Academy of Sciences 104:4642-4646.

Scarpulla RC (2008) Transcriptional Paradigms in Mammalian Mitochondrial Biogenesis and Function. Physiological Reviews 88:611-638.

Schänzer A, Wachs F-P, Wilhelm D, Acker T, Cooper-Kuhn C, Beck H, Winkler J, Aigner L, Plate KH, Kuhn HG (2004) Direct Stimulation of Adult Neural Stem Cells In Vitro and Neurogenesis In Vivo by Vascular Endothelial Growth Factor. Brain Pathology 14:237-248.

Schmidt-Hieber C, Jonas P, Bischofberger J (2004) Enhanced synaptic plasticity in newly generated granule cells of the adult hippocampus. Nature 429:184-187.

Schmidt O, Pfanner N, Meisinger C (2010) Mitochondrial protein import: from proteomics to functional mechanisms. Nat Rev Mol Cell Biol 11:655-667.

Seki T (2002) Expression patterns of immature neuronal markers PSA-NCAM, CRMP-4 and NeuroD in the hippocampus of young adult and aged rodents. J Neurosci Res 70:327-334.

Seki T, Arai Y (1993) Distribution and possible roles of the highly polysialylated neural cell adhesion molecule (NCAM-H) in the developing and adult central nervous system. Neuroscience Research 17:265-290.

Seri B, García-Verdugo JM, McEwen BS, Alvarez-Buylla A (2001) Astrocytes Give Rise to New Neurons in the Adult Mammalian Hippocampus. The Journal of Neuroscience 21:7153-7160.

Sestili P, Martinelli C, Bravi G, Piccoli G, Curci R, Battistelli M, Falcieri E, Agostini D, Gioacchini AM, Stocchi V (2006) Creatine supplementation affords cytoprotection in oxidatively injured cultured mammalian cells via direct antioxidant activity. Free Radical Biology and Medicine 40:837-849.

Shaywitz AJ, Greenberg ME (1999) CREB: A Stimulus-Induced Transcription Factor Activated by A Diverse Array of Extracellular Signals. Annual Review of Biochemistry 68:821-861.

Shield AJ, Murray TP, Board PG (2006) Functional characterisation of ganglioside-induced differentiation-associated protein 1 as a glutathione transferase. Biochem Biophys Res Commun 347:859-866.

Shihabuddin LS, Horner PJ, Ray J, Gage FH (2000) Adult Spinal Cord Stem Cells Generate Neurons after Transplantation in the Adult Dentate Gyrus. The Journal of Neuroscience 20:8727-8735.

Sholl DA (1953) Dendritic organization in the neurons of the visual and motor cortices of the cat. J Anat 87:387–406.381.

Shors TJ, Miesegaes G, Beylin A, Zhao M, Rydel T, Gould E (2001) Neurogenesis in the adult is involved in the formation of trace memories. Nature 410:372-376.

Shyh-Chang N, Daley GQ, Cantley LC (2013) Stem cell metabolism in tissue development and aging. Development 140:2535-2547.

Sierra A, Encinas JM, Deudero JJP, Chancey JH, Enikolopov G, Overstreet-Wadiche LS, Tsirka SE, Maletic-Savatic M (2010) Microglia Shape Adult Hippocampal Neurogenesis through Apoptosis-Coupled Phagocytosis. Cell Stem Cell 7:483-495.

Sisti HM, Glass AL, Shors TJ (2007) Neurogenesis and the spacing effect: Learning over time enhances memory and the survival of new neurons. Learning & Memory 14:368-375.

Smirnova E, Shurland DL, Ryazantsev SN, van der Bliek AM (1998) A human dynamin-related protein controls the distribution of mitochondria. J Cell Biol 143:351-358.

Smirnova E, Griparic L, Shurland D-L, van der Bliek AM (2001) Dynamin-related Protein Drp1 Is Required for Mitochondrial Division in Mammalian Cells. Molecular Biology of the Cell 12:2245-2256.

Snyder JS, Hong NS, McDonald RJ, Wojtowicz JM (2005) A role for adult neurogenesis in spatial long-term memory. Neuroscience 130:843-852.

Song H, Stevens CF, Gage FH (2002) Astroglia induce neurogenesis from adult neural stem cells. Nature 417:39-44.

Song Z, Chen H, Fiket M, Alexander C, Chan DC (2007) OPA1 processing controls mitochondrial fusion and is regulated by mRNA splicing, membrane potential, and Yme1L. J Cell Biol 178:749-755.

Spillantini MG, Schmidt ML, Lee VMY, Trojanowski JQ, Jakes R, Goedert M (1997) [alpha]-Synuclein in Lewy bodies. Nature 388:839-840.

Sportiche N, Suntsova N, Methippara M, Bashir T, Mitrani B, Szymusiak R, McGinty D (2010) Sustained sleep fragmentation results in delayed changes in hippocampal-dependent cognitive function associated with reduced dentate gyrus neurogenesis. Neuroscience 170:247-258.

St. John JC, Ramalho-Santos J, Gray HL, Petrosko P, Rawe VY, Navara CS, Simerly CR, Schatten GP (2005) The expression of mitochondrial DNA transcription factors during early cardiomyocyte in vitro differentiation from human embryonic stem cells. Cloning and stem cells 7:141-153.

Steib K (2007) Role of mitochondrial dynamics in adult hippocampal neurogenesis. Bachelor Thesis, TU München.

Steib K (2009) The importance of mitochondria in the maturation of newborn neurons in the adult brain. Master Thesis, TU München.

Steiner B, Zurborg S, Hörster H, Fabel K, Kempermann G (2008) Differential 24 h responsiveness of Prox1–expressing precursor cells in adult hippocampal neurogenesis to physical activity, environmental enrichment, and kainic acid–induced seizures. Neuroscience 154:521-529.

Steiner B, Klempin F, Wang L, Kott M, Kettenmann H, Kempermann G (2006) Type-2 cells as link between glial and neuronal lineage in adult hippocampal neurogenesis. Glia 54:805-814.

Steiner JL, Murphy EA, McClellan JL, Carmichael MD, Davis JM (2011) Exercise training increases mitochondrial biogenesis in the brain. Journal of Applied Physiology 111:1066-1071.

Steward O, Schuman EM (2003) Compartmentalized Synthesis and Degradation of Proteins in Neurons. Neuron 40:347-359.

Sugiura A, Yonashiro R, Fukuda T, Matsushita N, Nagashima S, Inatome R, Yanagi S (2011) A mitochondrial ubiquitin ligase MITOL controls cell toxicity of polyglutamine-expanded protein. Mitochondrion 11:139-146.

Suhonen JO, Peterson DA, Ray J, Gage FH (1996) Differentiation of adult hippocampus-derived progenitors into olfactory neurons in vivo. Nature 383:624-627.

Suhr ST, Chang EA, Tjong J, Alcasid N, Perkins GA, Goissis MD, Ellisman MH, Perez GI, Cibelli JB (2010) Mitochondrial rejuvenation after induced pluripotency. PLoS One 5:e14095.

Sutherland LN, Bomhof MR, Capozzi LC, Basaraba SAU, Wright DC (2009) Exercise and adrenaline increase PGC-1α mRNA expression in rat adipose tissue. The Journal of Physiology 587:1607-1617.

Sweeney NT, Brenman JE, Jan YN, Gao F-B (2006) The Coiled-Coil Protein Shrub Controls Neuronal Morphogenesis in Drosophila. Current biology 16:1006-1011.

Taanman J-W (1999) The mitochondrial genome: structure, transcription, translation and replication. Biochimica et Biophysica Acta (BBA) - Bioenergetics 1410:103-123.

Taguchi N, Ishihara N, Jofuku A, Oka T, Mihara K (2007) Mitotic Phosphorylation of Dynamin-related GTPase Drp1 Participates in Mitochondrial Fission. Journal of Biological Chemistry 282:11521-11529.

Takenouchi T, Hashimoto M, Hsu LJ, Mackowski B, Rockenstein E, Mallory M, Masliah E (2001) Reduced neuritic outgrowth and cell adhesion in neuronal cells transfected with human α-synuclein. Molecular and Cellular Neuroscience 17:141-150.

Tashiro A, Zhao C, Gage FH (2006a) Retrovirus-mediated single-cell gene knockout technique in adult newborn neurons in vivo. Nat Protoc 1:3049-3055.

Tashiro A, Makino H, Gage FH (2007) Experience-Specific Functional Modification of the Dentate Gyrus through Adult Neurogenesis: A Critical Period during an Immature Stage. The Journal of Neuroscience 27:3252-3259.

Tashiro A, Sandler VM, Toni N, Zhao C, Gage FH (2006b) NMDA-receptor-mediated, cell-specific integration of new neurons in adult dentate gyrus. Nature 442:929-933.

Tatsuta T, Langer T (2008) Quality control of mitochondria: protection against neurodegeneration and ageing. EMBO J 27:306-314.

Thein DC, Thalhammer JM, Hartwig AC, Bryan Crenshaw Iii E, Lefebvre V, Wegner M, Sock E (2010) The closely related transcription factors Sox4 and Sox11 function as survival factors during spinal cord development. Journal of Neurochemistry 115:131-141.

Thomas KJ, McCoy MK, Blackinton J, Beilina A, van der Brug M, Sandebring A, Miller D, Maric D, Cedazo-Minguez A, Cookson MR (2011) DJ-1 acts in parallel to the PINK1/parkin pathway to control mitochondrial function and autophagy. Human Molecular Genetics 20:40-50.

Todd LR, Damin MN, Gomathinayagam R, Horn SR, Means AR, Sankar U (2010) Growth Factor erv1-like Modulates Drp1 to Preserve Mitochondrial Dynamics and Function in Mouse Embryonic Stem Cells. Molecular Biology of the Cell 21:1225-1236.

Tolosa E, Poewe W (2009) Premotor Parkinson disease. Neurology 72:S1.

Toni N, Laplagne DA, Zhao C, Lombardi G, Ribak CE, Gage FH, Schinder AF (2008) Neurons born in the adult dentate gyrus form functional synapses with target cells. Nat Neurosci 11:901-907.

Toni N, Teng EM, Bushong EA, Aimone JB, Zhao C, Consiglio A, van Praag H, Martone ME, Ellisman MH, Gage FH (2007) Synapse formation on neurons born in the adult hippocampus. Nat Neurosci 10:727-734.

Tozuka Y, Fukuda S, Namba T, Seki T, Hisatsune T (2005) GABAergic excitation promotes neuronal differentiation in adult hippocampal progenitor cells. Neuron 47:803-815.

Tronel S, Belnoue L, Grosjean N, Revest J-M, Piazza P-V, Koehl M, Abrous DN (2012) Adult-born neurons are necessary for extended contextual discrimination. Hippocampus 22:292-298.

Twig G, Hyde B, Shirihai OS (2008) Mitochondrial fusion, fission and autophagy as a quality control axis: The bioenergetic view. Biochimica et Biophysica Acta (BBA) - Bioenergetics 1777:1092-1097.

Uo T, Dworzak J, Kinoshita C, Inman DM, Kinoshita Y, Horner PJ, Morrison RS (2009) Drp1 levels constitutively regulate mitochondrial dynamics and cell survival in cortical neurons. Experimental Neurology 218:274-285.

van Praag H, Kempermann G, Gage FH (1999a) Running increases cell proliferation and neurogenesis in the adult mouse dentate gyrus. Nat Neurosci 2:266-270.

van Praag H, Christie BR, Sejnowski TJ, Gage FH (1999b) Running enhances neurogenesis, learning, and long-term potentiation in mice. Proceedings of the National Academy of Sciences 96:13427-13431.

van Praag H, Shubert T, Zhao C, Gage FH (2005) Exercise Enhances Learning and Hippocampal Neurogenesis in Aged Mice. The Journal of Neuroscience 25:8680-8685.

Varum S, Rodrigues AS, Moura MB, Momcilovic O, Easley Iv CA, Ramalho-Santos J, Van Houten B, Schatten G (2011) Energy metabolism in human pluripotent stem cells and their differentiated counterparts. PloS one 6:e20914.

Veena J, Srikumar BN, Raju TR, Shankaranarayana Rao BS (2009) Exposure to enriched environment restores the survival and differentiation of new born cells in the hippocampus and ameliorates depressive symptoms in chronically stressed rats. Neuroscience Letters 455:178-182.

Verstreken P, Ly CV, Venken KJT, Koh T-W, Zhou Y, Bellen HJ (2005) Synaptic Mitochondria Are Critical for Mobilization of Reserve Pool Vesicles at Drosophila Neuromuscular Junctions. Neuron 47:365-378.

Viña J, Gomez-Cabrera MC, Borras C, Froio T, Sanchis-Gomar F, Martinez-Bello VE, Pallardo FV (2009) Mitochondrial biogenesis in exercise and in ageing. Advanced Drug Delivery Reviews 61:1369-1374.

Wagner KM, Rüegg M, Niemann A, Suter U (2009) Targeting and Function of the Mitochondrial Fission Factor GDAP1 Are Dependent on Its Tail-Anchor. PLoS ONE 4:e5160.

Wakabayashi J, Zhang Z, Wakabayashi N, Tamura Y, Fukaya M, Kensler TW, Iijima M, Sesaki H (2009) The dynamin-related GTPase Drp1 is required for embryonic and brain development in mice. J Cell Biol 186:805-816.

Wallimann T, Wyss M, Brdiczka D, Nicolay K, Eppenberger HM (1992) Intracellular compartmentation, structure and function of creatine kinase isoenzymes in tissues with high and fluctuating energy demands: the 'phosphocreatine circuit' for cellular energy homeostasis. Biochemical Journal 281:21-40.

Walter C, Murphy BL, Pun RYK, Spieles-Engemann AL, Danzer SC (2007) Pilocarpine-Induced Seizures Cause Selective Time-Dependent Changes to Adult-Generated Hippocampal Dentate Granule Cells. The Journal of Neuroscience 27:7541-7552.

Wang X, Schwarz TL (2009) The Mechanism of Ca2+-Dependent Regulation of Kinesin-Mediated Mitochondrial Motility. Cell 136:163-174.

Wang X, Su B, Lee H-g, Li X, Perry G, Smith MA, Zhu X (2009) Impaired Balance of Mitochondrial Fission and Fusion in Alzheimer's Disease. The Journal of Neuroscience 29:9090-9103.

Wang X, Su B, Siedlak SL, Moreira PI, Fujioka H, Wang Y, Casadesus G, Zhu X (2008) Amyloid-β overproduction causes abnormal mitochondrial dynamics via differential modulation of mitochondrial fission/fusion proteins. Proceedings of the National Academy of Sciences 105:19318-19323.

Wang X, Winter D, Ashrafi G, Schlehe J, Wong Yao L, Selkoe D, Rice S, Steen J, LaVoie Matthew J, Schwarz Thomas L (2011) PINK1 and Parkin Target Miro for Phosphorylation and Degradation to Arrest Mitochondrial Motility. Cell 147:893-906.

Wang Z, Jiang H, Chen S, Du F, Wang X (2012) The mitochondrial phosphatase PGAM5 functions at the convergence point of multiple necrotic death pathways. Cell 148(1-2):228-243.

Wasiak S, Zunino R, McBride HM (2007) Bax/Bak promote sumoylation of DRP1 and its stable association with mitochondria during apoptotic cell death. J Cell Biol 177:439-450.

Waterham HR, Koster J, van Roermund CWT, Mooyer PAW, Wanders RJA, Leonard JV (2007) A Lethal Defect of Mitochondrial and Peroxisomal Fission. New England Journal of Medicine 356:1736-1741.

Westermann B (2002) Merging mitochondria matters. EMBO Rep 3:527-531.

Wexler EM, Geschwind DH, Palmer TD (2007) Lithium regulates adult hippocampal progenitor development through canonical Wnt pathway activation. Mol Psychiatry 13:285-292.

Whitworth AJ, Pallanck LJ (2009) The PINK1/Parkin pathway: a mitochondrial quality control system? Journal of bioenergetics and biomembranes 41:499-503.

Winner B, Lie DC, Rockenstein E, Aigner R, Aigner L, Masliah E, Kuhn HG, Winkler J (2004) Human wild-Type alpha-synuclein impairs neurogenesis. Journal of Neuropathology & Experimental Neurology 63:1155-1166.

Winner B, Regensburger M, Schreglmann S, Boyer L, Prots I, Rockenstein E, Mante M, Zhao C, Winkler J, Masliah E, Gage FH (2012) Role of α-Synuclein in Adult Neurogenesis and Neuronal Maturation in the Dentate Gyrus. The Journal of Neuroscience 32:16906-16916.

Wolf SA, Melnik A, Kempermann G (2011) Physical exercise increases adult neurogenesis and telomerase activity, and improves behavioral deficits in a mouse model of schizophrenia. Brain, Behavior, and Immunity 25:971-980.

Wright GL, Maroulakou IG, Eldridge J, Liby TL, Sridharan V, Tsichlis PN, Muise-Helmericks RC (2008) VEGF stimulation of mitochondrial biogenesis: requirement of AKT3 kinase. The FASEB Journal 22:3264-3275.

Wu Z, Puigserver P, Andersson U, Zhang C, Adelmant G, Mootha V, Troy A, Cinti S, Lowell B, Scarpulla RC, Spiegelman BM (1999) Mechanisms Controlling Mitochondrial Biogenesis and Respiration through the Thermogenic Coactivator PGC-1. Cell 98:115-124.

Wyss M, Kaddurah-Daouk R (2000) Creatine and Creatinine Metabolism. Physiological Reviews 80:1107-1213.

Yang L, Calingasan NY, Wille EJ, Cormier K, Smith K, Ferrante RJ, Flint Beal M (2009) Combination therapy with Coenzyme Q10 and creatine produces additive neuroprotective effects in models of Parkinson's and Huntington's Diseases. Journal of Neurochemistry 109:1427-1439.

Yoon Y, Pitts KR, McNiven MA (2001) Mammalian Dynamin-like Protein DLP1 Tubulates Membranes. Molecular Biology of the Cell 12:2894-2905.

Yoon Y, Pitts KR, Dahan S, McNiven MA (1998) A Novel Dynamin-like Protein Associates with Cytoplasmic Vesicles and Tubules of the Endoplasmic Reticulum in Mammalian Cells. J Cell Biol 140:779-793.

Yoon Y, Krueger EW, Oswald BJ, McNiven MA (2003) The Mitochondrial Protein hFis1 Regulates Mitochondrial Fission in Mammalian Cells through an Interaction with the Dynamin-Like Protein DLP1. Molecular and Cellular Biology 23:5409-5420.

Zaja-Milatovic S, Milatovic D, Schantz A, Zhang J, Montine K, Samii A, Deutch A, Montine T (2005) Dendritic degeneration in neostriatal medium spiny neurons in Parkinson disease. Neurology 64:545-547.

Zhang C-L, Zou Y, He W, Gage FH, Evans RM (2008) A role for adult TLX-positive neural stem cells in learning and behaviour. Nature 451:1004-1007.

Zhang J, Khvorostov I, Hong JS, Oktay Y, Vergnes L, Nuebel E, Wahjudi PN, Setoguchi K, Wang G, Do A (2011) UCP2 regulates energy metabolism and differentiation potential of human pluripotent stem cells. The EMBO journal 30:4860-4873.

Zhang P, Hinshaw JE (2001) Three-dimensional reconstruction of dynamin in the constricted state. Nat Cell Biol 3:922-926.

Zhao C, Deng W, Gage FH (2008) Mechanisms and Functional Implications of Adult Neurogenesis. Cell 132:645-660.

Zhao C, Teng EM, Summers RG, Jr., Ming GL, Gage FH (2006) Distinct morphological stages of dentate granule neuron maturation in the adult mouse hippocampus. J Neurosci 26:3-11.

Zhu P-P, Patterson A, Stadler J, Seeburg DP, Sheng M, Blackstone C (2004) Intra- and Intermolecular Domain Interactions of the C-terminal GTPase Effector Domain of the Multimeric Dynamin-like GTPase Drp1. Journal of Biological Chemistry 279:35967-35974.

Zhu Y, Duan C, Lü L, Gao H, Zhao C, Yu S, Uéda K, Chan P, Yang H (2011) α-Synuclein overexpression impairs mitochondrial function by associating with adenylate translocator. The International Journal of Biochemistry & Cell Biology 43:732-741.

Zuchner S et al. (2004) Mutations in the mitochondrial GTPase mitofusin 2 cause Charcot-Marie-Tooth neuropathy type 2A. Nat Genet 36:449-451.

6. Appendix

An Excel sheet containing raw data and detailed information from the expression profiling assay after Sox4/11 knock-out (see 2.5.3) can be found in the attached CD.